DEUTSCHES ELEKTRONEN-SYNCHROTRON
Ein Forschungszentrum der Helmholtz-Gemeinschaft

DESY-THESIS-2024-010
July 2024

Analytic and Algebraic Studies of Feynman Integrals

by

F. Tellander

ISSN 1435-8085

NOTKESTRASSE 85 – 22607 HAMBURG

Analytic and Algebraic Studies of Feynman Integrals

vorgelegt von
Felix Tellander

Dissertation
zur Erlangung des Doktorgrades
an der Fakultät für
Mathematik, Informatik und Naturwissenschaften
Fachbereich Physik der Universität Hamburg

2024
Hamburg

Gutachter der Dissertation:	Dr. Georgios Papathanasiou Prof. Dr. Gleb Arutyunov
Zusammensetzung der Prüfungskommission:	Dr. Georgios Papathanasiou Prof. Dr. Gleb Arutyunov Prof. Dr. Volker Schomerus Prof. Dr. Christian Schwanenberger Prof. Dr. Sven-Olaf Moch
Vorsitzender der Prüfungskommission:	Prof. Dr. Sven-Olaf Moch
Datum der Disputation:	21.06.2024
Vorsitzender des Fach-Promotionsausschusses PHYSIK:	Prof. Dr. Markus Drescher
Leiter des Fachbereichs PHYSIK:	Prof. Dr. Wolfgang J. Parak
Dekan der Fakultät MIN:	Prof. Dr.-Ing. Norbert Ritter

Till min mormor.

Contents

List of publications

This thesis is based on the following publications, referred to by their Roman numerals:

I **Symbol alphabets from the Landau singular locus**

Chrisoph Dlapa, Martin Helmer, Georgios Papathanasiou and **Felix Tellander**
J. High Energ. Phys. **10** (2023) 161, [2304.02629]

II **Cohen-Macaulay Propert of Feynman Integrals**

Felix Tellander and Martin Helmer
Commun. Math. Phys. **399** (2023) 1021–1037, [2108.01410]

III **Landau Singularities from Whitney Stratifications**

Martin Helmer, Georgios Papathanasiou and **Felix Tellander**
Submitted to *Physical Review Letters*, [2402.14787]

IV **Tropical Feynman integration in the Minkowski regime**

Michael Borinsky, Henrik J. Munch and **Felix Tellander**
Comput. Phys. Commun., **292** (2023) 108874, [2302.08955]

V **Tropical Feynman integration in the physical region**

Michael Borinsky, Henrik J. Munch and **Felix Tellander**
PoS **EPS-HEP2023** (2024) 499, [2310.19890]

Acknowledgements

First I would like to thank my supervisors Georgios Papathanasiou and Volker Schomerus for their supervision and collaboration during these years. I would also like to thank my long-time collaborator and former teacher Martin Helmer for sticking with me for almost eight years. During my PhD I have also had the pleasure of working with Christoph Dlapa and my tropical collaborators Michael Borinsky and Henrik Munch. I am very proud of the great work we have done.

Finally I would like to thank my fellow PhD students and Postdocs at DESY, with a special shoutout to my phenomenological officemates and to Gabriele Dian for company during much hard work and many late nights (some which did not always only involve work).

Abstract

Feynman integrals are central to the calculation of scattering amplitudes both in particle and gravitational wave physics. This thesis presents advancements in both the analytical and algebraic structure of these integrals and shows how this can be used for efficient evaluation of these integrals.

Paper I. In this paper the focus is on one-loop integrals. The singularities of these integrals are fully described and used to derive the full symbol alphabet and canonical differential equation for any number of external particles. It is proven that a large family of one-loop integrals satisfy the Cohen-Macaulay property.

Paper II. Two infinite families of Feynman integrals satisfying the Cohen-Macaulay property are classified. This property implies that both the singularities and the number of master integrals is independent of space-time dimension and propagator powers.

Paper III. In this paper the singular locus of a Feynman integral is defined as the critical points of a Whitney stratified map. Explicit code and calculations are provided which show that this method captures singularities otherwise hard to detect.

Paper IV-V. The algebraic properties of the integrand, especially that of its Newton polytope being a generalized permutohedron, is leverage together with tropical sampling to provide efficient numerical evaluation of Feynman integrals with physical kinematics. The connection between the generalized permutohedron property and the Cohen-Macaulay property is also discussed.

Zusammenfassung

Feynman-Integrale sind von zentraler Bedeutung für die Berechnung von Streuamplituden sowohl in der Teilchen- als auch in der Gravitationswellenphysik. In dieser Arbeit werden Fortschritte sowohl in der analytischen, als auch in der algebraischen Struktur der Integrale vorgestellt und gezeigt, wie diese für eine effiziente Auswertung dieser Integrale genutzt werden können.

Paper I. In dieser Arbeit liegt der Schwerpunkt auf Ein-Schleifen-Integralen. Die Singularitäten dieser Integrale werden vollständig beschrieben und zur Herleitung des vollständigen Symbolalphabets und der kanonischen Differentialgleichung für eine beliebige Anzahl von externen Teilchen verwendet. Es wird bewiesen, dass eine große Familie von Ein-Schleifen-Integralen die Cohen-Macaulay-Eigenschaft erfüllt.

Paper II. Zwei unendliche Familien von Feynman-Integralen, die die Cohen-Macaulay- Eigenschaft erfüllen, werden klassifiziert. Diese Eigenschaft impliziert, dass sowohl die Singularitäten, als auch die Anzahl der Basisintegrale unabhängig von der Raumzeitdimension und den Propagatorpotenzen sind.

Paper III. In dieser Arbeit wird der singuläre Ort eines Feynman-Integrals als die kritischen Punkte einer Whitney-stratifizierten Abbildung definiert. Es werden explizite Codes und Berechnungen bereitgestellt, die zeigen, dass diese Methode Singularitäten erfasst, die sonst nur schwer zu erkennen sind.

Paper IV-V. Die algebraischen Eigenschaften des Integranden, insbesondere die Tatsache, dass sein Newton-Polytop ein verallgemeinertes Permutaeder ist, werden zusammen mit tropischem Sampling genutzt, um eine effiziente numerische Auswertung von Feynman-Integralen mit physikalischer Kinematik zu ermöglichen. Die Verbindung zwischen der Eigenschaft des verallgemeinerten Permutaeder und der Cohen-Macaulay-Eigenschaft wird ebenfalls diskutiert.

Eidesstattliche Versicherung / Declaration on oath

Hiermit versichere ich an Eides statt, die vorliegende Dissertationsschrift selbst verfasst und keine anderen als die angegebenen Hilfsmittel und Quellen benutzt zu haben.

Sofern im Zuge der Erstellung der vorliegenden Dissertationsschrift generative Künstliche Intelligenz (gKI) basierte elektronische Hilfsmittel verwendet wurden, versichere ich, dass meine eigene Leistung im Vordergrund stand und dass eine vollständige Dokumentation aller verwendeten Hilfsmittel gemäß der Guten wissenschaftlichen Praxis vorliegt. Ich trage die Verantwortung für eventuell durch die gKI generierte fehlerhafte oder verzerrte Inhalte, fehlerhafte Referenzen, Verstöße gegen das Datenschutz- und Urheberrecht oder Plagiate.

Hamburg, den 01/03/2024

Unterschrift der Doktorandin / des Doktoranden

Introduction

1 Background

As students of physics we learn early on that physical phenomena can be described by differential equations. In classical mechanics we use Newton's second law, a second order differential equation, to describe the evolution of systems. Similarly, electromagnetism is described by Maxwell's equations, fluid dynamics by the Navier-Stokes equations, general relativity by Einstein's equations and quantum mechanics by the Schrödinger equation [1]. The list goes on and on with too many equations to mention. However, the diligent student will eventually notice that there is no differential equation for quantum field theory, well at least not as neatly packaged as the other ones. Even though you can find the short "Standard Model formula" on both coffee mugs and T-shirts in CERN's gift shop, this formula is still a textbook of work away from providing real predictions. With no PDE to write down and solve, quantum field theory and particle physics needed another approach, this was provided by Richard Feynman in 1949 [2]:

"The main principle is to deal directly with the solutions of to the Hamiltonian differential equations rather than the equations themselves."

What this quote alludes to is the usage of perturbation theory and the introduction of what we now call *Feynman integrals*. It is ironic however, that one of the most powerful methods we have today to calculate these integrals is to derive a PDE for it and then solve that.

In Feynman's space-time approach to quantum theory [3, 4], the way to describe the time evolution of a system is to sum over all, infinitely many, possibilities. Most famously this can be applied to the double slit experiment where shooting a beam of particles, say electrons, towards two tightly spaced slits in an absorber, shows an interference patter as if the particle beam was a wave. By democratically summing over all possible ways the electron can go

$$\sum_{\text{every path}} e^{i(\text{phase})/\hbar} \tag{1}$$

the interference between the phases will recover the observed interference pattern! This is the basis of Feynman's *path integral*. The idea of summing over all possibilities does not only work for shooting electrons at a target but also for shooting electrons at each other in a particle collider. A generic scattering event with two particles entering and two particles exiting is depicted to the left in Figure 1, where the dashed circle represents the actual interaction. Now following Feynman's idea we write down all possible events where two particles enter and two particles leave. What "all possible" means in this context is dictated by the physics we want to model. Let's say we want to calculate the scattering of two electrons and assume they only interact via the electromagnetic field, i.e. the photon. This restricts us to only being able to draw two type of lines; electron and photon lines and only one type of vertex where two electron and one photon line meet. This framework is called quantum electrodynamics (QED) and the observed corrections to the magnetic moment of the electron [5, 6] and the explanation [7, 8, 2] provided by QED was the first major success of quantum field theory.

These diagrams are called *Feynman diagrams* or *Feynman graphs* and the rules of how to draw them and what exactly they correspond to are called the *Feynman rules*. One such rule is that four momentum is preserved at each vertex, just like Kirchhoff's current law, everything that enters must also exit. What this means when we have a closed loop is that there is a four momentum

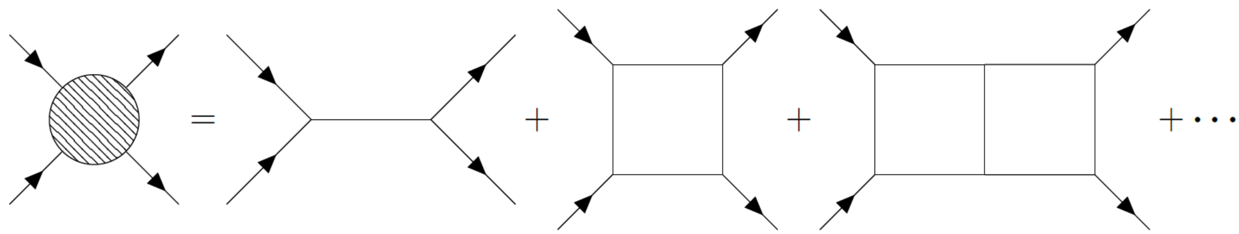

Figure 1: A generic $2 \to 2$ scattering process where the full matrix element on the left is expanded in a sum of Feynman graphs according to the Feynman rules.

that is not fixed by the external momenta, and there is one such un-fixed momentum for each loop. Following the idea of taking all possibilities into account, we have to integrate over this momentum, and to no ones surprise at this point, these integrals are called *Feynman integrals*.

Quantum field theory not only provides the tools for calculating observables in scattering experiments but is the language in which all microscopic interactions can be described, and it is truly one of physics greatest successes. Solving QFTs exactly is impossible for all realistic cases and we therefore have to rely on approximate perturbation theory. For over half a century the main method for these calculations have been to sum Feynman integrals. Recent developments like generalized unitarity [9], recursion relations [10], double copy [11] and the amplituhedron [12], show that there is much more to amplitudes than can be seen directly from the sum of Feynman integrals. However, this does in no way mean that Feynman integrals are outdated, for as deep as some of these concepts seem to pierce reality, when it comes to calculate actual observables at for example the Large Hadron Collider (LHC) [13] or gravitational-wave observables [14, 15], Feynman integrals stand supreme, at least for now.

From the mathematical side, Feynman integrals are a great vehicle for many different areas and especially unites analysis and algebra beautifully [16]. The following are the relations most relevant for my own research. Feynman integrals are solutions to linear systems of partial differential equations, these may for example be understood in the language of D-modules [17, 18, 19] or generalized hypergeometry in the sense of Gel'fand, Graev, Kapranov and Zelevinskiĭ (GKZ) [20, 21, 22]. This relates Feynman integrals to toric geometry [23], polytopes and also tropical geometry [24]. These integrals are defined from graphs, meaning that graph theory and matroids play a central role [25]. Certain families of Feynman integrals also evaluates to interesting type of numbers that are of interest from number theory [26, 27].

In this thesis I will show how to harness results from many of these different fields of mathematics and apply them to obtain concrete results about Feynman integrals and their physical applications. In Section 2, I will give background on Feynman integrals from both physics and mathematics and show how they are related to generalized hypergeometry. This is a large framework containing much more than needed for Feynman integrals, it is therefore natural to ask if these integrals have any special properties within this framework. I show in Section 3 that Feynman integrals are often *normal* or satisfy the *Cohen-Macaulay* property. This in particular implies that the dimension of the solution space of the associated GKZ system and its singularities are independent of the space-time dimension. Understanding the singularities of Feynman integrals is a longstanding problem and in Section 4 I provide two different way of obtaining these singularities. Knowing the singularities is a crucial ingredient in the modern canonical differential equation approach. Finally, in Section 5 I show how a very special geometric property of the integrand, the *generalized permutohedron*, can be used together with *tropical integration* can be used for very efficient direct evaluation of Feynman integrals.

2 Feynman integrals and GKZ systems

Let us consider a general scattering processes, such a process is described by the *S-matrix* taking the initial state $|i\rangle$ to the finial state $\langle f|$ with probability $\langle f| S |i\rangle$. Looking at the $2 \to 2$ process in the introduction, Figure 1, the circle of ignorance on the left hand side does not really correspond to the S-matrix, because there is the trivial scattering event when nothing happens, the particles just passes by each other. This is separated by $S = \mathbb{1} + i\mathcal{T}$ where $\mathcal{T}$ is the transfer matrix. Since four-momentum is conserved we can factor out a δ-distribution:

$$\langle f| \mathcal{T} |i\rangle = (2\pi)^4 \delta^4(\textstyle\sum p)\mathcal{M}. \tag{2}$$

This matrix $\mathcal{M}$ contains all the interactions of the theory and when particle physicists calculate or measure "matrix elements" this is what they mean. For the simple $2 \to 2$ process this is all you need to get the differential cross section:

$$\left(\frac{d\sigma}{d\Omega}\right)_{\text{CM}} (12 \to 34) = \frac{1}{64\pi^2 E_{\text{CM}}^2} \frac{|\boldsymbol{p}_f|}{|\boldsymbol{p}_i|} |\mathcal{M}|^2 H(E_{\text{CM}} - m_3 - m_4) \tag{3}$$

where H is the step function. This is something that can be measured in experiments [28].

The calculation of the matrix elements $\mathcal{M}$ is by perturbation theory, and it is here the Feynman integral comes into play. A fundamental assumption in scattering is that the interaction takes place during a finite time period $-T < t < T$ and that as $t \to \pm\infty$ the states are on-shell one-particle states with a given momenta, called *asymptotic states*. The S-matrix elements $\langle f| S |i\rangle$ for n asymptotic states can be expressed as a time-ordered product using the LSZ-formula [29]:

$$\langle f| S |i\rangle \sim \langle \Omega| T\{\phi(x_1) \cdots \phi(x_n)\} |\Omega\rangle \tag{4}$$

where $|\Omega\rangle$ is the vacuum ground state of the interacting theory. In order to calculate the the time-ordered product, let us start with the free theory where the field is:

$$\phi_0(t, \boldsymbol{x}) = \int \frac{d^3\boldsymbol{k}}{(2\pi)^3} \frac{1}{\sqrt{2\omega_{\boldsymbol{k}}}} \left(a_{\boldsymbol{k}} e^{-ikx} + a_{\boldsymbol{k}}^\dagger e^{ikx}\right). \tag{5}$$

with $\omega_{\boldsymbol{k}} = \sqrt{m^2 + |\boldsymbol{k}|^2}$. The time-ordered product for two of these fields is simply

$$\langle 0| T\{\phi_0(x_1)\phi_0(x_2)\} |0\rangle = \int \frac{d^3\boldsymbol{k}}{(2\pi)^3} \frac{e^{-i\omega_k |t_1 - t_2| + i\boldsymbol{k}\cdot(\boldsymbol{x}_1 - \boldsymbol{x}_2)}}{2\omega_{\boldsymbol{k}}}. \tag{6}$$

This object is the *Feynman propagator*, denoted $D_F(t_1 - t_2, \boldsymbol{x}_1 - \boldsymbol{x}_2) = D_F(x_1 - x_2)$, and can be written as the sum of two *oscillatory integrals*, as defined by Hörmander [30] cf. [31, Theorem 7.8.2]

$$H(t_1 - t_2) \int \frac{d^3\boldsymbol{k}}{(2\pi)^3} \frac{e^{-i\omega_k (t_1 - t_2) + i\boldsymbol{k}\cdot(\boldsymbol{x}_1 - \boldsymbol{x}_2)}}{2\omega_{\boldsymbol{k}}} + H(t_2 - t_1) \int \frac{d^3\boldsymbol{k}}{(2\pi)^3} \frac{e^{i\omega_k (t_1 - t_2) - i\boldsymbol{k}\cdot(\boldsymbol{x}_1 - \boldsymbol{x}_2)}}{2\omega_{\boldsymbol{k}}}. \tag{7}$$

Each term in this sum is the product of two distributions, a step function and the oscillatory integral, this product is well-defined by [31, Theorem 8.2.10] since the wave front sets do not collide.

The Feynman propagator is perfectly well-defined mathematically and below we list some of its most important properties

Theorem 2.1. *The Feynman propagator $D_F(t, \boldsymbol{x})$ defined in (6) satisfies:*

(i) *D_F is a fundamental solution to the Klein-Gordon equation: $(\partial_t^2 - \nabla_{\boldsymbol{x}}^2 + m^2)D_F = -i\delta$.*

(ii) *The full space-time Fourier transform of D_F is*

$$\widehat{D}_F(k) = \lim_{\varepsilon \to 0+} \frac{i}{k^2 - m^2 + i\varepsilon}, \tag{8}$$

where the limit is taken in the weak topology of tempered distributions.

(iii) *D_F is Lorentz invariant*

(iv) *D_F is a C^∞ function away from the light cone and its support is $\mathbb{R}^4$.*

(v) *The (smooth) wave front set of the Feynman propagator is given by*

$$WF(D_F(t,\boldsymbol{x})) = \{(0;k)|k \neq 0\} \cup \left\{(x;k) \mid t^2 - |\boldsymbol{x}|^2 = 0,\, t \neq 0,\, k_0 = \lambda t,\, \boldsymbol{k} = -\lambda \boldsymbol{x}\right\}, \tag{9}$$

where $\lambda > 0$.

The proof of this theorem is elementary, see e.g. [32, 33, 34, 35]. When people say "Feynman propagator", it is usually the momentum space representation $\widehat{D}_F$ in (8) that they refer to.

Before moving on with the calculation of matrix elements, I will describe another representation of the Feynman propagator $\widehat{D}_F$. Physicists often rely on a generalization of the definition of the Γ-function they refer to as the *Schwinger trick*. This writes the momentum space propagator as an integral over new parameters called *Schwinger parameters*:

$$\left(\frac{i}{q_e^2 - m_e^2 + i\varepsilon}\right)^{\nu_e} = \frac{1}{\Gamma(\nu_e)} \int_0^\infty \frac{dx_e}{x_e}\, x_e^{\nu_e} \exp\left(ix_e(q_e^2 - m_e^2 + i\varepsilon)\right) \tag{10}$$

which is absolutely convergent when $\varepsilon > 0$ and the real part of ν_e is positive, $\mathrm{Re}(\nu_e) > 0$, but can be analytically continued to all $\nu_e \in \mathbb{C}$. In the language of distributions, the limit $\varepsilon \to 0+$ can often be taken.

Let X be an open set in $\mathbb{R}^n$, $f \in C^\infty(X)$ and $\mathrm{Im}(f) \geq 0$. Assume that $df(x) \neq 0$ whenever $f(x) = 0$. Then the limit $\varepsilon \to 0$ with convergence in $\mathcal{D}'(X)$ for $\mathrm{Re}(\nu) > 0$ is:

$$\left(\frac{i}{f(x) + i0}\right)^{\nu} := \lim_{\varepsilon \to 0+} \left(\frac{i}{f(x) + i\varepsilon}\right)^{\nu} = \frac{1}{\Gamma(\nu)} \int_0^\infty \frac{d\tau}{\tau}\, \tau^{\nu} \exp\left(i\tau(f(x) + i\varepsilon)\right). \tag{11}$$

For this distribution we also know the wave front set:

$$WF\left(\frac{1}{(f(x) + i0)^{\nu}}\right) \subset \{(x, \lambda \cdot df(x)) \,:\, f(x) = 0, \lambda > 0\}, \qquad \mathrm{Re}(\nu) > 0. \tag{12}$$

After this mathematical interlude, let us continue our calculation of matrix elements. There are several ways to calculate the time ordered expectation for an interacting theory, one way is to use the Gell-Mann-Low formula [36]:

$$\langle\Omega|\, T\{\phi(x_1)\cdots\phi(x_n)\}\,|\Omega\rangle = \frac{\langle 0|\, T\left\{\phi_0(x_1)\cdots\phi_0(x_n) e^{i\int d^4x \mathcal{L}_{\mathrm{int}}[\phi_0]}\right\}|0\rangle}{\langle 0|\, T\left\{e^{i\int d^4x \mathcal{L}_{\mathrm{int}}[\phi_0]}\right\}|0\rangle}, \tag{13}$$

where $\mathcal{L}_{\mathrm{int}}$ is the interaction terms in the Lagrangian. Take for example $\mathcal{L}_{\mathrm{int}}[\phi] = \frac{g}{3!}\phi^3$ and expand the two-point function in the coupling constant g and only consider fully connected and amputated contributions [28, 35, 37]:

$$\langle\Omega|\, T\{\phi(x_1)\phi(x_2)\}\,|\Omega\rangle = D_F(x_1 - x_2) - g^2 \int d^4x \int d^4y \left(\frac{1}{2} D_F(x_1 - x) D_F(x-y)^2 D_F(y - x_2)\right) + \mathcal{O}(g^3)$$

Writing the propagators in Fourier space and using the LSZ formula to go back to the S-matrix contribution of the g^2 term we obtain

$$\langle f|\, S\, |i\rangle = -(2\pi)^4 \delta^4(p_i - p_f) \frac{g^2}{2} \lim_{\varepsilon \to 0+} \int \frac{d^4k}{(2\pi)^4} \frac{i}{(p_i - k)^2 - m^2 + i\varepsilon} \frac{i}{k^2 - m^2 + i\varepsilon}. \tag{14}$$

This identifies the order g^2 contribution to the matrix element as

$$i\mathcal{M} = -\frac{g^2}{2} \lim_{\varepsilon \to 0+} \int \frac{d^4k}{(2\pi)^4} \frac{i}{(p_i - k)^2 - m^2 + i\varepsilon} \frac{i}{k^2 - m^2 + i\varepsilon}. \tag{15}$$

This is what is called a scalar (momentum space) *Feynman integral* and is the main protagonist of this thesis. This particular integral can be considered as the convolution

$$(\widehat{D}_F * \widehat{D}_F)(p_i) = \int d^4k\, \widehat{D}_F(p_i - k) \widehat{D}_F(k). \tag{16}$$

Since a convolution in Fourier space corresponds to a product in spatial space, this is the same as asking for the product $D_F \cdot D_F$. Using Hörmander's product theorem, [31, Theorem 8.2.10], and the explicit wave front sets from (v) in Theorem 2.1 one sees immediately that this is **not** guaranteed to be a well-defined object. However, with detailed microlocal analysis of the integrand this seems to partially be resolved, especially within the D-module framework [38]. To get around this problem in general, physicists have developed an ingenious method of *renormalization* [39, 40, 41]. Making sense of this process is a challenging but fascinating task [42, 43, 44, 45].

We now proceed by giving different representations of the Feynman integral, each with its own features and draw-backs.

Schwinger parameterization

Consider one-particle irreducible Feynman graphs $G := (E, V)$ with edge set E, vertex set V and loop number $L = |E| - |V| + 1$. Every edge $e \in E$ is assigned an arbitrary direction with which we define the *incidence matrix* η_{ve} of G to satisfy $\eta_{ve} = 1$ if e ends at v, -1 if e starts at v, and 0 otherwise. The vertex set V has the disjoint partition $V = V_{\text{ext}} \sqcup V_{\text{int}}$ where each vertex $v \in V_{\text{ext}}$ is assigned an external incoming D_0-dimensional momentum $p_v \in \mathbb{R}^{1,D_0-1}$ and we put $p_v = 0$ for all $v \in V_{\text{int}}$. Using dimensional regularization with $D := D_0 - 2\epsilon$ and Feynman's causal $i\varepsilon$ prescription, scalar Feynman rules assigns the following integral to G[1]:

$$\mathcal{I} = \left(\frac{1}{i\pi^{D/2}}\right)^L \lim_{\varepsilon \to 0^+} \int \prod_{e \in E} d^D q_e \left(\frac{-1}{q_e^2 - m_e^2 + i\varepsilon}\right)^{\nu_e} \prod_{v \in V \setminus \{v_0\}} \delta^{(D)}\left(p_v + \sum_{e \in E} \eta_{ve} q_e\right) \tag{17}$$

where $\nu_e \in \mathbb{Z}$ are integers and q_e is the total momentum flowing through the edge e. Momentum is conserved at each vertex $v \in V$, but only $|V| - 1$ of these constraints are independent, we therefore remove an arbitrary vertex v_0 from V in (17) to avoid carrying through the overall momentum conservation $\delta^{(D)}\left(\sum_{v \in V} p_v\right)$ in every following expression.

To evaluate this integral we combine the propagators into an exponential function by introducing the Schwinger parameters (10). The δ-functions can also be lifted to an exponential using the mathematical physicists version of Fourier's inversion formula:

$$\delta^{(D)}(k) = \int \frac{d^D y}{(2\pi)^D} e^{iky}, \tag{18}$$

[1] Observe that the normalization is slightly different compared to (15).

which should be thought of as an oscillatory integral (c.f. [31, Equation (7.8.5)]).

We now have an integral over three sets of variables q_e, y_v and x_e. The q_e integrals are performed as Gaussian integrals after a shift of integration variables and Wick rotation to Euclidean space. The y_v integrals are performed in a similar manner. Denote by $\mathcal{L}$ the $|V|-1 \times |V|-1$ Laplacian matrix

$$\mathcal{L}_{vv'} := \sum_{e\in E} \frac{\eta_{ve}\eta_{v'e}}{x_e} \tag{19}$$

and define $\mathbf{p} = (p_1, \ldots, p_{|V|-1})^T$. The integral (17) can now be written as

$$\mathcal{I} = (i)^{\omega} \lim_{\varepsilon\to 0^+} \int_0^{\infty} \prod_{e\in E} \left(\frac{x^{\nu_e} dx_e}{x_e \Gamma(\nu_e)}\right) \frac{1}{\left((\prod_{e\in E} x_e) \det \mathcal{L}\right)^{D/2}} \exp\left(i\left[\mathbf{p}^T \mathcal{L}^{-1}\mathbf{p} - \sum_{e\in E}(m_e^2 - i\varepsilon)x_e\right]\right) \tag{20}$$

where ω is the superficial degree of divergence $\sum_{e\in E}\nu_e - LD/2$. We label the constituents of the integrand as

$$\mathcal{U} := \left(\prod_{e\in E} x_e\right) \det \mathcal{L}, \qquad \mathcal{F}_0 := -\mathcal{U}\cdot\left(\mathbf{p}^T\mathcal{L}^{-1}\mathbf{p}\right), \qquad \mathcal{F}_m := \mathcal{U}\cdot\sum_{e\in E} m_e^2 x_e$$
$$\mathcal{F} := \mathcal{F}_0 + \mathcal{F}_m \tag{21}$$

so the integral can now be written as

$$\mathcal{I} = (i)^{\omega} \lim_{\varepsilon\to 0^+} \int_0^{\infty} \prod_{e\in E} \left(\frac{x^{\nu_e} dx_e}{x_e\Gamma(\nu_e)}\right) \frac{1}{\mathcal{U}^{D/2}} \exp\left(i\left[\frac{-\mathcal{F}}{\mathcal{U}} + i\varepsilon\sum_{e\in E} x_e\right]\right). \tag{22}$$

The form (22) is called the *Schwinger parameterization* of the Feynman integral.

The two polynomials $\mathcal{U}$ and $\mathcal{F}$ are traditionally referred to as the first, respectivly, second *Symanzik polynomial*. This is most likely in reference to the paper [46] even though they were published one and a half year earlier in the same journal by Nakanishi [47]. These polynomials have a simple combinatorial description in terms of the underlying graph [48]:

$$\mathcal{U} = \sum_{\substack{T \text{ a spanning} \\ \text{tree of } G}} \prod_{e\notin T} x_e, \tag{23}$$

$$\mathcal{F} = \mathcal{F}_m + \mathcal{F}_0 = \mathcal{U}\sum_{e\in E} m_e^2 x_e - \sum_{\substack{F \text{ a spanning} \\ 2-\text{forest of } G}} p(F)^2 \prod_{e\notin F} x_e. \tag{24}$$

The matrix definition is more suitable for numerical evaluation, see Section 5, while the combinatorial description will be fruitful in proving algebraic properties of these polynomials, see Section 3.

Feynman parameterization

In order to derive the so called *Feynman parameterization*, we start from the Schwinger parameterization (22). Let $H(x)$ be a homogeneous function of degree one such that $H : \mathbb{R}^{|E|} \to \mathbb{R}_+$. Then we use $1 = \int_0^{\infty} \delta(t - H(x))dt$ and by rescaling the variables $x_e \to tx_e$, $t \in \mathbb{R}_+$ we get

$$\mathcal{I} = \Gamma(\omega) \lim_{\varepsilon\to 0^+} \int_0^{\infty} \prod_{e\in E}\left(\frac{x^{\nu_e}dx_e}{x_e\Gamma(\nu_e)}\right) \frac{\delta(1-H(x))}{\mathcal{U}^{D/2}} \left(\frac{1}{\mathcal{F}/\mathcal{U} - i\varepsilon\sum_{e\in E} x_e}\right)^{\omega}. \tag{25}$$

Projective representation

The δ-distribution in the integrand (25) can be thought of as specifying an affine chart of the projective space. In this sense the entire integral can be lifted to a projective one since the integrand is scale-invariant. The integral is now

$$\mathcal{I} = \Gamma(\omega) \int_{\mathbb{P}^E_+} \phi \quad \text{with} \quad \phi = \left(\prod_{e \in E} \frac{x_e^{\nu_e}}{\Gamma(\nu_e)} \right) \frac{1}{\mathcal{U}(\boldsymbol{x})^{D/2}} \left(\frac{1}{\mathcal{V}(\boldsymbol{x}) - i\varepsilon \sum_{e \in E} x_e} \right)^{\omega} \Omega \,. \tag{26}$$

Where the integration domain is over the *projective simplex* $\mathbb{P}^E_+ = \{\boldsymbol{x} = [x_1 : \cdots : x_{|E|}] \in \mathbb{RP}^{E-1} : x_e > 0\}$ with respect to its canonical Kronecker form

$$\Omega = \sum_{e=1}^{|E|} (-1)^{|E|-e} \frac{dx_1}{x_1} \wedge \cdots \wedge \widehat{\frac{dx_e}{x_e}} \wedge \cdots \wedge \frac{dx_{|E|}}{x_{|E|}} \,. \tag{27}$$

We write $\mathcal{V}(\boldsymbol{x})$ in (26) for the quotient of the two Symanzik polynomials, this will be the main form of the integral used in Section 5.

Lee-Pomeransky parameterization

The final representation of the Feynman integral (17) we will define here is the so called *Lee-Pomeransky parameterization* [49]. The easiest way to "derive" it is to just write it down as an ansatz and prove that we can recover the Feynman parameterization (25). The Lee-Pomeransky parameterization of the integral is

$$\mathcal{I} = \frac{\Gamma(D/2)}{\Gamma(D/2 - \omega)} \lim_{\varepsilon \to 0^+} \int_0^\infty \prod \frac{x^{\nu_e} dx_e}{x_e \Gamma(\nu_e)} \frac{1}{(\mathcal{U} + \mathcal{F} - i\varepsilon \cdot \mathcal{U} \sum_{e \in E} x_e)^{D/2}} \tag{28}$$

where it is common to introduce the Lee-Pomeransky polynomial $\mathcal{G} := \mathcal{U} + \mathcal{F}$.

The trick we use here is the same as when going from the Schwinger to Feynman parameterization; $1 = \int_0^\infty \delta(t - H(x)) dt$. Rescaling the variables $x_e \to t x_e$ with $t \in \mathbb{R}_+$ we get back the Feynman parameterization (25). The Lee-Pomeransky representation is central for the connection to generalized hypergeometry [50, 51] and therefore central in the sections that follow.

2.1 Generalized hypergeometry

Hypergeometric functions are classical and very well-studied objects in mathematics. The most recognized example is probably Gauss' ${}_2F_1(a, b, c; z)$ with series expansion

$${}_2F_1(a, b, c; y) = \sum_{n=0}^{\infty} \frac{(a)_n (b)_n}{(c)_n} \frac{y^n}{n!} \tag{29}$$

where $(a)_n := a(a+1) \cdots (a+n-1)$, this series is convergent for $|y| < 1$ and $c \notin \mathbb{Z}_-$. There are many different representations of this function, for example we have the Euler integral

$${}_2F_1(a, b, c; y) = \frac{\Gamma(c)}{\Gamma(a)\Gamma(b)} \int_0^1 s^{a-1} (1-s)^{c-a-1} (1-ys)^{-b} ds \tag{30}$$

convergent on $|\text{Arg}(1-y)| < \pi$. We can restore the symmetry in a and b by introducing a new variable

$${}_2F_1(a, b, c; y) = G(a, b, c) \int_0^1 \int_0^1 s^{a-1} t^{b-1} (1-s)^{c-a-1} (1-t)^{c-b-1} (1-zst)^{-c} ds\, dt \tag{31}$$

where $G(a,b,c) = \Gamma(c)^2/\Gamma(a)\Gamma(b)\Gamma(c-a)\Gamma(c-b)$. Introducing the new variables $x_1 = s/(1-s)$, $x_2 = t/(1-t)$ and $z = 1-y$ we can write the double integral as

$$\int_0^\infty \int_0^\infty \frac{x_1^a x_2^b}{(1+x_1+x_2+zx_1x_2)^c} \frac{dx_1\,dx_2}{x_1x_2}. \tag{32}$$

Ignoring the $i\varepsilon$ in (28), the Lee-Pomeransky representation is clearly the same type of integral as the above one. The authors of [52] and [53] introduced these integrals as *Euler-Mellin integrals*. Viewing Feynman integrals in the Lee-Pomeransky representation provides us with a rich and solid mathematical ground to stand on as we venture into the murky but exciting waters of physics. We start with a theorem showing when the integral is absolutely convergent.

Theorem 2.2 ([52, Theorem 1] and [53, Theorem 2.3]). *If the polynomial $\mathcal{G}$ is completely non-vanishing on the positive orthant $\mathbb{R}_+^{|E|}$, then the Euler-Mellin integral $\mathcal{I}$ in* (28) *converges and defines an analytic function on the tube domain*

$$\{(D,\nu) \in \mathbb{C}^{1+|E|} \mid \tau := \mathrm{Re}(D/2) \in \mathbb{R}_+,\ \sigma := \mathrm{Re}(\nu) \in \mathrm{int}(\tau\mathbf{N}[\mathcal{G}])\}. \tag{33}$$

A simple way of guaranteeing the the assumptions for this theorem are satisfied for a Feynman integral is to assume that the kinematics is in the Euclidean region, i.e. $-\left(\sum_{v\in V'} p_v\right)^2 > 0$ for all subsets $V' \subset V_{\mathrm{ext}}$. This implies that all coefficients of $\mathcal{G}$ are positive and thus neither $\mathcal{G}$ nor any of the restrictions can vanish on the positive orthant. As a function of D and ν, this function has a simple and explicit analytic continuation into all of $\mathbb{C}^{1+|E|}$ completely described by the Newton polytope $\mathbf{N}[\mathcal{G}]$. Expressing $\mathbf{N}[\mathcal{G}]$ in the half-space representation

$$\mathbf{N}[\mathcal{G}] = \bigcap_{i=1}^{N} \left\{ y \in \mathbb{R}^{|E|} \mid \langle \mu_i, y\rangle \le c_i \right\} \tag{34}$$

we can simply formulate the meromorphic continuation in terms of the normal vectors μ_i and bounds c_i.

Theorem 2.3 ([52, Theorem 2] and [53, Theorem 2.5]). *Suppose the polynomial $\mathcal{G}$ is completely non-vanishing on the positive orthant $\mathbb{R}_+^{|E|}$ and the Newton polytope $\mathbf{N}[\mathcal{G}]$ is of full dimension $|E|$. Then the Euler-Mellin integral* (28) *has the meromorphic continuation*

$$\mathcal{I}(D,\nu;\,z) = \Phi(D,\nu;\,z)\prod_{i=1}^{N}\Gamma(c_iD/2 - \langle\mu_i,\nu\rangle) \tag{35}$$

where Φ is an entire analytic function in D and ν.

This type of extension of domains of definition goes back to Hadamard (as cited in [31]) and Marcel Riesz [54, 55]. The modern algebraic approach was developed by Bernšteĭn and Sergei Gel'fand [56, 57]. A very general version of this, applicable to real analytic functions was proven by Atiyah [58].

Going back to the example of ${}_2F_1$ from the beginning of this section, assuming that $z > 0$ we can now write the double integral as

$$\int_0^\infty \int_0^\infty \frac{x_1^a x_2^b}{(1+x_1+x_2+zx_1x_2)^c} \frac{dx_1\,dx_2}{x_1x_2} = \Phi(a,b,c;\,z)\Gamma(a)\Gamma(b)\Gamma(c-a)\Gamma(c-b) \tag{36}$$

and by comparison we find

$$\Phi(a,b,c;z) = \frac{1}{\Gamma(c)^2}\,{}_2F_1(a,b,c;1-z). \tag{37}$$

We have now understood how Feynman integrals, or Euler-Mellin integrals, depend on the parameters D and $\nu_1,\ldots,\nu_{|E|}$, but how about the dependence on z, i.e. the kinematic dependence? It is easy to show that the function $z \mapsto \Phi(D,\nu;z)$ is an A-hypergeometric function in the sense of Gel'fand, Graev, Kapranov and Zelevinskiĭ.

Using multi-index notation we may write the Lee-Pomeransky polynomial as $\mathcal{G} = \sum_{i=1}^r z_i x^{\alpha_i}$ with $z_i \neq 0$ and $\alpha_i \in \mathbb{Z}_{\geq 0}^{|E|}$ for all $i = 1,\ldots,r$. We define the two matrices

$$A := \{1\} \times A_- = \begin{pmatrix} 1 & 1 & \cdots & 1, \\ \alpha_1 & \alpha_2 & \cdots & \alpha_r \end{pmatrix} \in \mathbb{Z}_{\geq 0}^{(|E|+1)\times r}, \text{ and} \tag{38}$$

$$\beta := \left(-D/2, \quad -\nu_1 \quad ,\ldots \quad ,-\nu_{|E|}\right)^T \in \mathbb{C}^{|E|+1}, \tag{39}$$

from which we construct the GKZ hypergeometric system $H_A(\beta)$ as the sum of two ideals:

$$I_A := \left\langle \partial^u - \partial^v \mid u,v \in \mathbb{Z}_{\geq 0}^r \text{ s.t. } Au = Av \right\rangle, \text{ and} \tag{40}$$

$$Z_A(\beta) := \left\langle \Theta_i(c,\partial) \mid \Theta = A \cdot \begin{pmatrix} c_1\partial_1 \\ \vdots \\ c_r\partial_r \end{pmatrix} - \beta \right\rangle. \tag{41}$$

The ideal I_A is actually an ideal in the *commutative* polynomial ring $\mathbb{Q}[\partial_1,\cdots,\partial_r]$, and as such has a finite generating set $I_A = \langle h_1,\ldots h_\ell\rangle$ with $h_i \in \mathbb{Q}[\partial_1,\cdots,\partial_r]$ being a binomial. This ideal I_A is a *toric ideal* and it gives the defining equations of the projective *toric variety*

$$X_A = \{z \in \mathbb{P}^{r-1} \mid h_1(z) = \cdots = h_\ell(z) = 0\}$$

associated to the matrix A, see e.g. [59] and [60, Chapter 5].

The ideal $H_A(\beta)$ is an ideal in the Weyl algebra $W := \mathbb{Q}(\beta)[z_1,\ldots,z_r]\,\langle\partial_1,\ldots,\partial_r\rangle$, this is a non-commutative algebra with $[\partial_i, z_i] = 1$, for a general introduction see e.g. [61] and [62]. In the general theory of Weyl algebras, $\mathbb{Q}(\beta)$ can be replaced with any commutative field k of characteristic zero. We say that an element $p \in W$ is *normal ordered* if all differential operators are to the right of the variables:

$$p = \sum_{(\alpha,\beta)\in E} c_{\alpha\beta} z^\alpha \partial^\beta, \qquad c_{\alpha\beta} \in k^*.^{2} \tag{42}$$

Moreover, the normal order is unique. This means that there is a natural k-vector space isomorphism between the polynomial ring $k[z,\zeta]$ of $2r$ variables and the Weyl algebra:

$$k[z_1,\ldots,z_r,\zeta_1,\ldots,\zeta_r] \to W: \quad z^\alpha\zeta^\beta \mapsto z^\alpha\partial^\beta. \tag{43}$$

We can now generalize the commutative Gröbner basis theory to the Weyl algebra. Generalizing the notion of initial ideal, we define the *principal symbol* of an element $p \in W$ as its initial ideal with all z_i having weight 0 and all ∂_i having weight 1:

$$\sigma(p) := \mathrm{in}_{(0,1)}(p) = \sum_{\substack{(\alpha,\beta)\in E \\ |v|=m}} z^\alpha\zeta^\beta \qquad \in k[z,\zeta]. \tag{44}$$

[2] This β is not the same as the homogenity parameter in the hypergeometric system, it is just a multi-index.

For any left-ideal I in a Weyl algebra we can similarly define the *initial ideal* as the ideal containing all initial forms of elements in I. The singularities of a system of PDEs are described by the zero locus of the *characteristic ideal* called the *characteristic variety*. For a left-ideal I in W this is the characteristic ideal is:

$$\mathrm{in}_{(0,1)}(I) := \{\sigma(p) \mid p \in I\} \subset k[z, \zeta] \tag{45}$$

and the characteristic variety is simply $\mathrm{Char}(I) := \mathbf{V}(\mathrm{in}_{(0,1)}(I))$. It is a theorem of Ōaku [63] that this definition coincides with the D-module definition.

The *singular locus* of an ideal in a Weyl algebra is given by removing the zero section from the characteristic variety and projecting onto the base variables z. This is done in practice by the saturation and elimination:

$$\left(\mathrm{in}_{(0,1)}(I) : \langle \zeta_1, \ldots, \zeta_r \rangle^{\infty}\right) \cap k[z_1, \ldots, z_r] \tag{46}$$

which is carried in the commutative ring $k[z, \zeta]$.

In the special case that I is a generalized hypergeometric system $H_A(\beta)$ the singular locus is given by the principal A-determinant E_A, see [64, 60] and especially Section 4. For Euler-Mellin integrals, the principal A-determinant precisely keeps track of when $z \mapsto \Phi(\beta; z)$ fails to be an analytic function:

Theorem 2.4 ([52, Theorem 5] and [53, Theorem 4.2]). *Let $z \in \mathbb{C}^r \setminus E_A(\mathcal{G})$, and let Σ be a connected component of $\mathbb{R}^{|E|} \setminus \overline{\mathcal{A}'_{\mathcal{G}}}$. Then for any $\sigma \in \Sigma$, the analytic germ $\Phi^{\Sigma}_{\mathcal{G}}(\beta; z)$ has a (potentially multivalued) analytic continuation to $\mathbb{C}^{1+|E|} \times (\mathbb{C}^r \setminus E_A(\mathcal{G}))$ that is everywhere A-hypergeometric in the variables z with homogenity parameter β.*

Where $\mathcal{A}'_{\mathcal{G}}$ is the *co-amoeba* (see [52, Section 2]) which keeps track of when $\mathcal{G} = 0$ and $E_A(\mathcal{G})$ is the principal A-determinant of the (Lee-Pomeransky) polynomial $\mathcal{G}$.

3 Cohen-Macaulay rings

It may well be said that the genesis of modern commutative algebra was David Hilbert's landmark papers in 1890 and 1893 [65, 66]. In these papers four cornerstones were proven:

(i) the polynomial behaviour of the Hilbert function,

(ii) the Nullstellensatz,

(iii) the basis theorem,

(iv) the syzygy theorem.

In any modern work on algebra, it is fair to say, that all four of these results play an important role, even if it may be in the background. The title of this section "Cohen-Macaulay rings" refers to result (iv), the syzygy theorem. Cohen-Macaulay rings have exceptionally simple syzigies, this propagates through the mathematical framework of GKZ systems, where it tells us that the characteristic ideal of a Feynman integral (i.e. the singularities) and the holonomic rank of the associated D-module are independent of β.

Let k be a field and $S = k[y_1, \ldots, y_n]$ a polynomial ring. By Hilbert's basis theorem, result (iii) above, any ideal $I \subset S$ has a finite number of generators. However, these generators need not be S-linearly independent. Meaning that if I is generated by $\{f_1, \ldots, f_n\}$, then if there exists elements

$g_i \in S$ such that $f_1 g_1 + \cdots + f_n g_n = 0$, the elements $\{g_i,\, i = 1, \ldots, n\}$ are called a syzygy relation. This process may be continued, for the list of polynomials $\{g_i\}$ there might exist polynomials $\{h_j\}$ providing a relation between the relations, etc. The point of Hilbert's syzygy theorem is that this process must terminate:

Theorem 3.1 (Hilbert's syzygy theorem)**.** *Let S be as above. Then every finitely generated S-module has a free resolution of length at most n.*

The free resolution is the sequence of maps given by the syzygies. If I is an ideal in S, then a *free resolution of S/I of length l* is a degree-preserving exact sequence of finitely generated S-modules:

$$0 \longleftarrow S/I \longleftarrow S = F_0 \longleftarrow F_1 \longleftarrow \cdots \longleftarrow F_l \longleftarrow 0 \tag{47}$$

such that every F_j is a free S-module. A free resolution is *minimal* when the ranks of F_j are taken to be as small as possible.

Example 3.2. Let $I \subset S = k[y_1, \ldots, y_4]$ be the toric ideal associated to the "twisted cubic":

$$A = \begin{pmatrix} 3 & 2 & 1 & 0 \\ 0 & 1 & 2 & 3 \end{pmatrix}, \qquad I_A = \left\langle y_2 y_3 - y_1 y_4,\; y_2^2 - y_1 y_3,\; y_3^2 - y_2 y_4 \right\rangle . \tag{48}$$

A simple syzygy is for example

$$-y_3(y_2^2 - y_1 y_3) + y_2(y_2 y_3 - y_1 y_4) - y_1(y_3^2 - y_2 y_4) = 0 \tag{49}$$

and the minimal free resolution is

$$0 \longleftarrow S/I_A \longleftarrow S \xleftarrow{\begin{pmatrix} y_2^2 - y_1 y_3 & y_2 y_3 - y_1 y_4 & y_3^2 - y_2 y_4 \end{pmatrix}} S^3 \xleftarrow{\begin{pmatrix} -y_3 & y_4 \\ y_2 & -y_3 \\ -y_1 & y_2 \end{pmatrix}} S^2 \longleftarrow 0 \tag{50}$$

For future notice, remark that the length of this resolution is the number of columns minus the number of rows of A, i.e. $4 - 2 = 2$. ◇

Just as the minimal free resolution cannot be arbitrarily long, the Auslander-Buchsbaum formula [67] restricts it from being arbitrarily short. Let A be an integer $d \times n$-matrix such that the row of ones is contained in its row span. We denote its toric ideal $I_A \subset k[y_1, \ldots, y_n]$ where the row-span condition guarantees that I_A is homogeneous. In this context the length l of the minimal free resolution of S/I_A satisfies

$$n - d \leq l \leq n. \tag{51}$$

When the lower bound is an equality, the ideal I_A is said to be *Cohen-Macaulay*:

Definition 3.3 (Cohen-Macaulay ideal)**.** An ideal I_A in S is said to be *Cohen-Macaulay* if the length of the minimal free resolution of S/I_A equals $n - d$.

From this definition we see that the previous example is Cohen-Macaulay. The important role of Cohen-Macaulay rings in connection to GKZ systems was realized by Adolphson in [64] leading to the correction [68]. In the hypergeometric case there is an equivalence between Cohen-Macaulayness and the rank of $H_A(\beta)$ being independent of β [69]:

$$\operatorname{rank}(H_A(\beta)) = \operatorname{vol}(\operatorname{conv}(A))\; \forall \beta \Longleftrightarrow I_A \text{ is Cohen} - \text{Macaulay}. \tag{52}$$

Another important effect of the Cohen-Macaulay property is on the structure of the characteristic ideal, defined in Equation (45). If I_A is Cohen-Macaulay then

$$\mathrm{in}_{(0,1)}(H_A(\beta)) = \langle \zeta^u - \zeta^v \mid u, v \in \mathbb{Z}^r_{\geq 0} \text{ s.t. } Au = Av \rangle + \left\langle A \cdot \begin{pmatrix} z_1\zeta_1 \\ \vdots \\ z_r\zeta_r \end{pmatrix} \right\rangle. \tag{53}$$

Example 3.4. Let $H_A(\beta)$ be the GKZ system defined by:

$$A = \begin{pmatrix} 4 & 3 & 1 & 0 \\ 0 & 1 & 3 & 4 \end{pmatrix}, \qquad \beta = \begin{pmatrix} a \\ b \end{pmatrix}. \tag{54}$$

We have $\#(\text{rows}) - \#(\text{cols}) = 4 - 2 = 2$, while from explicit calculation the minimal free resolution has length three, meaning that I_A is indeed not Cohen-Macaulay. This means that the characteristic ideal is not just generated by (53) but has more generators. In total the characteristic ideal of $H_A(\beta)$ has seven generators:

$$\zeta_2^3 - \zeta_1^2\zeta_3,\ \zeta_2\zeta_3 - \zeta_1\zeta_4,\ -\zeta_1\zeta_3^2 + \zeta_2^2\zeta_4,\ \zeta_3^3 - \zeta_2\zeta_4^2 \tag{55}$$
$$z_1\zeta_1 + z_2\zeta_2 + z_3\zeta_3 + z_4\zeta_4,\ z_2\zeta_2 + 3z_3\zeta_3 + 4z_4\zeta_4 \tag{56}$$
$$(b-2)z_1\zeta_2^2 + (b-a-1)z_2\zeta_1\zeta_3 + (b-3a+1)z_3\zeta_2\zeta_4 + (b-4a+2)z_4\zeta_3^2 \tag{57}$$

The characteristic ideal therefore depends on a and b while the characteristic variety is still independent of a and b since the radical of the ideal generated by the above three sets of equations is the same ideal as the radical of just the first two.

For any choices of a and b such that $(a,b) \neq (1,2)$ the system $H_A(\beta)$ has holonomic rank 4 while for $(a,b) = (1,2)$ the rank jumps to 5. Preparing for things to come in Section 4, let $f(x_0,x_1) = c_1x_0^4 + c_2x_0^3x_1 + c_3x_0x_1^3 + c_4x_1^4$ and let X_h be the projective variety $X_h = \mathbf{V}(x_0x_1f(x_0,x_1))$. We can now calculate the Euler characteristic

$$|\chi(\mathbb{C}^* \setminus \mathbf{V}(f(1,x_1)))| = |2 - \chi(X_h)| = |2 - 6| = 4 \tag{58}$$

which is the same as the rank for generic β while also clearly being independent of β. ⋄

As presented here, proving that families of rings or ideals are Cohen-Macaulay is not always easy. It might therefore be useful to rely on stronger and more explicit combinatorial properties that imply Cohen-Macaulayness. One such property is *normality*, the semigroup ring $\mathbb{C}[\mathbb{N}A] \cong \mathbb{C}[\partial]/I_A$ is said to be normal if

$$\mathbb{N}A = \mathbb{Z}A \cap \mathbb{R}_+A. \tag{59}$$

By a result of Hochster [70], every normal semigroup ring is Cohen-Macaulay. In the context above, A should really be thought of as a collection of lattice points rather than a matrix, but throughout the text the two will not be distinguished. The geometric meaning of (59) is that the lattice $\mathbb{N}A$ contains no holes, take e.g. the A-matrix from Example 3.4, then $\mathbb{N}A$ is not normal since

$$\begin{pmatrix} 3 \\ 1 \end{pmatrix} - \begin{pmatrix} 1 \\ 3 \end{pmatrix} + \begin{pmatrix} 0 \\ 4 \end{pmatrix} = \begin{pmatrix} 2 \\ 2 \end{pmatrix} \notin \mathbb{N}A, \tag{60}$$

i.e. the lattice has a "hole" at $\begin{pmatrix} 2 \\ 2 \end{pmatrix}$. There are many properties of A and its polytope $\mathrm{conv}(A)$ that imply normality:

- $\mathrm{conv}(A)$ has a regular unimodular triangularization,
- there exists a monomial order $\prec$ such that the initial ideal $\mathrm{in}_\prec(I_A)$ is radical,
- $\mathrm{conv}(A)$ is a *matroid polytope*.

In Figure 5 of [P1] the relation between many algebraic and combinatorial properties is summarized.

Matroids are classical objects, first introduced by Whitney (a name that will come back later) in 1935 [71], defined to be a generalization of the notion of linear independence. As such they are ubiquitous in modern mathematics and have at least ten equivalent definitions, each appearing more naturally in different branches of mathematics [72]. A matroid is a pair of two sets, a finite set E called the *ground set* and a family of subsets of E called *independent sets*. With respect to inclusion we can define the family of maximally independent sets $\mathcal{B}$ whose elements are called *bases*.

Definition 3.5 (Matroid)**.** A matroid is a pair $(E, \mathcal{B})$, where E is a finite set and $\mathcal{B}$ a collection of subsets of E satisfying

(B1) $\mathcal{B}$ is non-empty,

(B2) if A and B are distinct elements of $\mathcal{B}$ and $a \in A \setminus B$, then there exists $b \in B \setminus A$ such that $(A \setminus a) \cup b \in \mathcal{B}$.

The last property, **(B2)**, is known as the *basis exchange property*. It follows that every element in $\mathcal{B}$ has the same cardinality. If we identify $E = \{\mathbf{e}_1, \ldots, \mathbf{e}_n\}$ as the vector space basis of $\mathbb{R}^n$, then each element of $\mathcal{B}$ corresponds to a lattice point in $\mathbb{R}^n$, and we can define the matroid polytops as the convex hull of these points, $P[\mathcal{B}] := \mathrm{conv}(\mathcal{B})$. Actually, any polytope with vertices in a hypersimplex and all edges being equal to $\mathbf{e}_i - \mathbf{e}_j$ for some $i \neq j$ is a matroid polytope and matroid polytopes are in bijective correspondence to their associated matroid [73, 74]. The latter definition will play an important role later as it shows that the matroid polytope is a *generalized permutohedron* [75], see Section 5. Both matroids and generalized permutohedra play an important role in the geometric view of amplitudes via the amplituhedron, a good introduction is [76] and more details can be found in [77, 78, 79].

Example 3.6 (Matroid polytope). It follows directly from the definition of the first Symanzik polynomial $\mathcal{U}$ that the Newton polytope $\mathbf{N}[\mathcal{U}]$ is a matroid polytope. For a mathematician this would be the matroid polytope of the co-graphical matroid associated to the Feynman graph. ⋄

The main result of the publication [P2] is the classification of two infinite families of Feynman integrals such that $\mathbb{N}A$ is normal. This may be summarized in the following theorem:

Theorem 3.7 ([P2, Theorem 1.1])**.** *Let $G = (V, E)$ be a Feynman diagram with associated Symanzik polynomials $\mathcal{U}$ and $\mathcal{F}$. Set $\mathcal{G} = \mathcal{U} + \mathcal{F}$, then the Newton polytope $P_G = \mathbf{N}[\mathcal{G}]$ is normal if either*

(i) $m_e \neq 0$ for all $e \in E$, or

(ii) $m_e = 0$ for all $e \in E$ and every vertex is connected to an external off-shell leg, i.e. $p_v^2 \neq 0$ for every $v \in V = V_{\mathrm{ext}}$.

At the writing of [P2] we were unaware of the existence and theory around generalized permutohedra. From the proof in [P2] we obtain the following corollary, with the same numbering as in Theorem 3.7:

Corollary 3.8 ([P1, Proposition 5.10])**.**

(i) Assume $m_e \neq 0$ for all $e \in E$, then $\mathbf{N}[\mathcal{F}]$ is a generalized permutohedron for all possible choices of external kinematics.

(ii) Assume that every two-forest of the Feynman graph G comes with a non-zero coefficient, that is, $V = V_{\text{ext}}$ and that $p(V')^2 \neq 0$ for all $V' \subset V$ where $p(V') = \sum_{v \in V'} p_v$. Then setup $\mathbf{N}[\mathcal{F}]$ is a matroid polytope and hence a generalized permutohedron.

These results were later generalized by Uli Walther in [80] where he showed that normality can be preserved in case (i) even when internal masses m_e are set to zero and that $V = V_{\text{ext}}$ can be relaxed in (ii).

From the point of GKZ, the one-loop case is special since very often the degrees of freedom of the Feynman integral coincides with the number of variables in the GKZ system $H_A(\beta)$ meaning that this system of PDEs is precisly the system describing the Feynman integral. For this special case it is possible to write down a necessary and sufficient statement for normality in terms of the kinematics:

Theorem 3.9 ([P1, Theorem 5.4])**.** *Let $\mathcal{G}_h = \mathcal{U}x_0 + \mathcal{F}$ be the Symanzik polynomial of a one-loop Feynman diagram G. Then $\mathbb{N}A$ with $A = \operatorname{supp}(\mathcal{G}_h)$ is normal if and only if*

$$p(F_{ij})^2 - m_i^2 - m_j^2 \neq 0 \tag{61}$$

*for all edges i, j where **both** $m_i \neq 0$ and $m_j \neq 0$.*

The proof of this theorem relies on the odd-cycle condition constructed by Ohsugi and Hibi [81]. For example, this theorem proves that the massless on-shell one-loop box is normal, a case that is not captured by [P2] nor [80]. At the time of writing, it seems very likely that every massless on-shell integral is not only Cohen-Macaulay but also normal, but this is left as a conjecture for the time being.

4 Landau singularities

As was seen in Section 2 the matrix element for cross section calculations can be expanded as a series in the coupling constant g:

$$i\mathcal{M} = \sum_{n=0}^{\infty} g^n \mathcal{M}_n = \sum_{n=0}^{\infty} g^n \sum_{G_n} \mathcal{I}_{G_n} \tag{62}$$

where G_n denotes all Feynman graphs with n vertices with coupling constant g. This series is hard to make rigorous, in QED the coupling is very small, around $1/137$, while for low-energy quantum chromodynamics (QCD) it might be of the order 10. Moreover, the number of graphs in G_n grows roughly as $\sim n!$ and as discussed before, the Feynman integrals $\mathcal{I}_{G_n}$ can be divergent before renormalization.

Much work has been spent on trying to understand the analytic structure of the S-matrix without using perturbation theory [82], one of the few truly non-perturbative results we have is the Källén-Lehmann [41, 83] representation of the two-point function

$$\langle\Omega| T\{\phi(x)\phi(y)\} |\Omega\rangle = \int \frac{d^4p}{(2\pi)^4} e^{ip(x-y)} i\Pi(p^2), \qquad \Pi(p^2) := \int_0^\infty \frac{\rho(k^2)}{p^2 - k^2 + i\varepsilon} dk^2 \tag{63}$$

where $\rho(k^2)$ is the spectral density (a polynomially bounded measure). This statement can also be made rigorous within the Gårding-Wightman axioms [84].

For practical purposes, the full structure of $\mathcal{M}$ is not of concern. Usually we only have access to the first few terms in the expansion in g and at that level, even the convergence of this expansion is irrelevant. As seen below, a divergent series can very well be used to approximate a finite number.

Example 4.1 (Approximation by divergent series). Consider the two infinite series

$$\sum_{n=0}^{\infty} \frac{(-100)^n}{n!} = e^{-100} \sim 10^{-44}, \qquad \sum_{n=0}^{\infty} \frac{n!}{(-100)^n} = \infty. \tag{64}$$

The first series has partial sums $1, -99, 4901, -485297/3, 4004901, \ldots$ which clearly does nothing to "approximate" the actual value e^{-100}. The second series diverges but the first five partial sums are $1, 0.99, 0.9902, 0.990194, 0.99019424, \ldots$ which approximates the integral

$$\int_0^\infty \frac{100e^{-t}}{100+t} dt$$

with increasing accuracy. In fact, summing the first 100 terms in this divergent series provides the value of this integral to about 42 significant digits! ◇

The only obstacle left, is the individual terms $\mathcal{I}$, i.e. the Feynman integrals, in the series expansion of $\mathcal{M}$. If these are divergent or have poles and branch cuts, this affects even a truncated perturbative calculation.

The pionering work in understanding the analytic structure of individual Feynman diagrams was done by Landau [85], Nakanishi [86] and Cutkosky [87]. We begin by the definition of singularity due to Landau. Let $Q_e = q_e^2 - m_e^2$ be the denominator of the Feynman propagator, then the Feynman integral (17) is said to satisfy the *Landau equations* if

$$\begin{cases} x_e Q_e = 0, & \forall\, e \in E, \\ \sum_{e \in E} x_e \partial Q_e / \partial k_l = 0, & \forall\, l \in L \end{cases} \tag{65}$$

where k_l is the loop-momenta in loop l. According to Landau, when these equations are satisfied, the Feynman integral is singular.

Looking at the simultaneous work of Nakanishi, let $\mathcal{V} = \mathcal{F}/\mathcal{U}$ then a **necessary** condition for the Feynman integral to have a Landau singularity is that for a subgraph $\gamma \subseteq G$:

$$\begin{cases} x_e = 0, & \forall\, e \in \gamma, \\ \partial \mathcal{V} / \partial x_e = 0, & \forall\, e \in G/\gamma. \end{cases} \tag{66}$$

Going back to the Euler-Mellin integrals in Section 2, it is clear from Theorem 2.4 that the principal A-determinant captures when the integral fails to be an analytic function, i.e. it should also describe when the Feynman integral (28) has a Landau singularity. The principal A-determinant for any polynomial $\mathcal{G}$ is defined as a product of discriminants:

Definition 4.2 (Theorem 1.2, Chapter 10 of [60]). Let $\mathcal{G}$ be a polynomial with support A and let $Q = \mathbf{N}[\mathcal{G}] = \operatorname{conv}(A)$. Then the principal A-determinant is the polynomial

$$E_A(\mathcal{G}) = \pm \prod_{\Gamma \subseteq Q} \Delta_{A \cap \Gamma}(\mathcal{G})^{\mu_\Gamma} \tag{67}$$

where μ_Γ is a positive integer and where $\Delta_{A\cap\Gamma}(\mathcal{G}) := \Delta_{A\cap\Gamma}(\mathcal{G}|_\Gamma)$ and $\mathcal{G}|_\Gamma$ is the coordinate restriction of $\mathcal{G}$ supported on Γ.

These descriminants are defined as the Zariski closure of the set where the polynomial $\mathcal{G}$ and all its partial derivatives simultaneously vanish in the algebraic torus.

For this object to give a complete description of the singularities of the Feynman integral, it is important that the coefficients of $\mathcal{G}$ are considered to be generic. This is clearly not the case for general Feynman integrals, see (23) and (24). For one-loop integrals however, the GKZ perspective can often be used since Gale duality can be used to reduce the number of GKZ variables to match the number of physical degrees of freedom. In the paper [P1] we used this perspective to not only study the singularities of one-loop integrals but also derive the *symbol alphabet* and *canonical differential equation* for one-loop graphs.

In physics a common way of generating the PDEs satisfied by the Feynman integral is by integration by part identities [88, 89, 90, 91]. These PDEs generate a regular holonomic D-module and can thus always be written as a system of first order PDEs. An exceptional case is when this system can be written in *canonical* form [92], i.e. the dimensional regulator ϵ factorizes in the equation

$$d\mathbf{f} = \epsilon\, d\mathbf{M}(z) \cdot \mathbf{f}, \qquad \mathbf{M} = \sum_j \mathbf{C}_j \log(W_j(z)). \tag{68}$$

Knowledge of the symbol letters $W_j(z)$ and the basis $\mathbf{f}$ reduces the cosntruction of the PDE to a numerical problem of finding the C_j. In the paper [P1] the symbol alphabet is derived from the principal A-determinant by relying on Jacobi identities and the full canonical differential equation is provided explicitly for all one-loop graphs with generic kinematics.

Going to two loops and beyond, Gale duality is not enough to reduce the number of variables and actual restrictions [93, 94] have to be used. The principal A-determinant is therefore no longer guaranteed to provide the correct set of singularities. And there are computational methods that might provide too many components, like the polynomial reduction due to Brown [27] and implemented in [95] or the recently defined "principal Landau variety" that misses certain singularities [96, 97]. A current trend in the community is to use the Euler characteristic of the torus complement of $\mathcal{G} = 0$ as an indicator for singularities as motivated by [19] and [98]. This means that one can define a hypersurface in kinematic space where this Euler characteristic changes from its generic value for points on this surface. This object is hard to calculate directly, so in the paper [P3] we define an object *Landau variety*, in accordance to Pham [99], which fully captures the change in Euler characteristics and is well defined for any kinematic setup at any loop order.

Landau variety

Taking a step back to the S-matrix, unitarity implies that

$$\langle f|\, \mathcal{T}^\dagger \mathcal{T}\, |i\rangle = \sum_X \int d\Pi_X \,\langle f|\, \mathcal{T}^\dagger\, |X\rangle \,\langle X|\, \mathcal{T}\, |i\rangle \tag{69}$$

where the X denotes a complete set of states. If at an energy E_0 a new real intermediate state becomes accessible, a new contribution appears on the right-hand side meaning that it is non-analytic for $E = E_0$ as the new term is 0 for $E < E_0$ and non-zero for $E > E_0$. This is a so called *normal threshold* and only exists for real particles. Digressing our studies to Feynman integrals with kinematics in the complex plane, new singularities might appear without this interpretation, but we still expect them to be characterized by the failure of analyticity. This is incredible "lucky" that nature seems to care more about analyticity than smoothness. For example, any closed set (Cantor sets, Koch snowflakes etc.) $E \subset \mathbb{R}^n$ admits a C^∞ function $f : \mathbb{R}^n \to \mathbb{R}$ such that $E = f^{-1}(0)$.

One way of proving that this type of behaviour is impossible for algebraic and analytic functions is by considering the *Whitney stratification* [100, 101]. For an algebraic variety X of dimension

d we say that a filtration $X_\bullet$ of varieties $X_0 \subset \cdots \subset X_d = X$ is a Whitney stratification of X if the connected components of the difference $X_i - X_{i-1}$ (called strata) are analytic manifolds of smaller dimension satisfying the so called *B condition*. We refrain from giving the exact description here, see e.g. the original papers by Whitney, Mather's notes [102] or [P3]. This stratification can be calculated in Macaulay 2 [103] using [104].

Consider an algebraic map $f : X \to Y$ between varieties X and Y. A *Whitney stratification of the map* f is a pair $(X_\bullet, Y_\bullet)$ where $X_\bullet$ is a Whitney stratification of X, $Y_\bullet$ is a Whitney stratification of Y and for each strata M of X there is a strata N of Y with $f(M) \subset N$ such that the map $f|_M : M \to N$ is a *submersion*, i.e. the differential $df|_M$ is surjective. Just as for a variety, there exists a unique minimal Whitney stratified map. Given the defining equations of varieties X, Y and of a map f between them, the stratification $(X_\bullet, Y_\bullet)$ may be obtained explicitly using the algorithm of [104, 105] as implemented in the `WhitneyStratifications` Macaulay2 package.

When the map f is proper then we have, by *Thom's First Isotopy Lemma* [102, Proposition 11.1], that the topology of the fiber $f^{-1}(q)$ is constant over **all** points $q \in N$ for any strata N of Y.

We now describe the *Landau variety*, which is the locus in the parameter space of kinematic variables $\mathbb{C}^m_z$ where the Feynman integral is singular; the following definition is (a minor rephrasing of) that of Pham [99, §IV.5] for Feynman integrals in Lee-Pomeransky form:

Definition 4.3 (Landau variety)**.** Consider a Feynman integral in Lee-Pomeransky form and let $\mathcal{G}_h$ be the x-homogeneous polynomial defining it. Set $X = \mathbf{V}(x_0 \cdots x_n \mathcal{G}_h) \subset \mathbb{P}^n_x \times \mathbb{C}^m_z$ and consider the projection map $\pi : X \to \mathbb{C}^m_z$, then the Landau variety is given by the variety Y_{m-1} appearing in the unique minimal Whitney stratification $(X_\bullet, Y_\bullet)$ of the map π.

A highlight of the usefulness of this definition is the two-loop slashed box with $p_1^2 = 0 = p_2^2$ and $p_3^2 \neq 0$, $p_4^2 \neq 0$ studied in [P3, Section V.A] This diagram has the singularity $p_4^2 - s - t = 0$ where the Euler characteristic drops and is an element of the Landau variety. However, not every method captures this singularity.

The final definition of what we should mean by "Landau singularity" is still open, but it seams reasonable that the Landau variety, Euler discriminant and singular locus of the associated D-module have the same codimension-one components. This would mean that either of these three objects can be promoted to being **the** Landau singularity. A proof of this is currently a very active area of research.

In the beginning of this discussion on Landau varieties, we noted that the study of analytic functions is in some aspects easier than the study of smooth functions. The wave front set that has made an appearance a few times in Section 2 describes when a distribution u fails to be a smooth function. This can be refined to the *analytic wave front set* $WF_A(u)$ which describes when u fails to be an analytic function. In general $WF(u) \subset WF_A(u)$, but by results of Andronikof [106, 107] these sets are equal (and also equal to the characteristic variety of the D-module they generate) for all regular holonomic distributions. By the explicit construction of (38) it follows from a theorem by Hotta [108] that $H_A(\beta)$ is regular holonomic for Feynman integrals and since this property is stable under restrictions this holds for every Feynman integral. Thus, for Feynman integrals, failing to be smooth should be the same as failing to be analytic. So maybe we were not "lucky" that nature chose analyticity over smoothness but rather lucky that nature chose functions where such distinctions do not matter.

5 Tropical integration

If we think of physics as a phenomenological science, the goal at the end of the day is to actually evaluate Feynman integrals so that we can obtain the matrix elements that appear in cross-sections that can then be measured by experimentalists. In this section we will show how *tropical integration* together with very special mathematical structures of Feynman integrals, especially the generalized permutohedron property, can be used for highly efficient numerical evaluation of Feynman integrals.

Many modern numerical methods use the canonical differential equation approach [92], see e.g. `AMFlow` [109], `DiffExp` [110] and `SeaSyde` [111]. Deriving the canonical differential equation is a potential bottleneck in these calculations which can be sidestepped using direct integration. Analytic integration can be performed for certain integrals in `HyperInt` [95] while numerical Monte Carlo techniques are for example implemented in `pySecDec` [112]. The software `feyntrop` was introduced in [113] and further developed in [P4]. For example, this software has been used to integrate Euclidean Feynman integrals with 17 loops. More recently, `feyntrop` has been used in [114] to numerically verify the canonical differential equation result for a four-point three-loop process with one massive leg. It has also been used in [115] to calculate Feynman integrals in ϕ^4-theory to 13 loops and beyond. The tropical way of thinking also sheds light on infrared singularities [116] and how to calculate entire amplitudes directly without using Feynman integrals at all [117].

The main thrust of [P4] was to extend the previous implementation to also include kinematics in the physical (or Minkowski) region. As been discussed at length in Section 4, Feynman integrals in the physical region have singularities, meaning that an deformation of the integration contour has to be employed. Using the parametric representation (26), we want a deformation that defines the integral on the correct analytic branch instead of using the $i\varepsilon$ perscription. This is done using a finite contour deformation respecting the projective invariance [118].

The deformation is given by the embedding $\iota_\lambda : \mathbb{P}^E_+ \hookrightarrow \mathbb{CP}^{|E|-1} : \, x_e \mapsto X_e := x_e \exp\left(-i\lambda \partial \frac{\mathcal{V}}{\partial x_e}(\boldsymbol{x})\right)$ so the deformed integral is given by the pull-back:

$$\mathcal{I} = \Gamma(\omega) \int_{\mathbb{P}^E_+} \iota^*_\lambda \phi = \Gamma(\omega) \int_{\mathbb{P}^E_+} \left(\prod_{e \in E} \frac{X_e^{\nu_e}}{\Gamma(\nu_e)} \right) \frac{\det \mathcal{J}_\lambda(\boldsymbol{x})}{\mathcal{U}\left(\mathbf{X}\right)^{D/2} \cdot \mathcal{V}\left(\mathbf{X}\right)^{\omega}} \, \Omega \tag{70}$$

where $\boldsymbol{X} = \iota_\lambda(\boldsymbol{x})$ and the Jacobian is given by

$$\mathcal{J}_\lambda(\boldsymbol{x})^{e,h} = \delta_{e,h} - i\lambda x_e \frac{\partial^2 \mathcal{V}}{\partial x_e \partial x_h}(\boldsymbol{x}) \text{ for all } e, h \in E. \tag{71}$$

In order to sample this integral efficiently we use *tropical sampling*. For any polynomial $p(\boldsymbol{x})$ in $|E|$ variables we define the *tropical approximation* p^{tr} as

$$p^{\text{tr}}(\boldsymbol{x}) = \max_{\alpha \in \text{supp}(p)} \prod_{e=1}^{|E|} x_e^{\alpha_e} \, . \tag{72}$$

This is connected to the more standard *tropicalization* (see e.g. [119]) via

$$p^{\text{tr}}(\boldsymbol{x}) = \exp\left(\max_{\mathbf{v} \in \mathbf{N}[p]} \mathbf{v}^T \mathbf{y} \right), \tag{73}$$

where $\mathbf{y} = (y_1, \ldots, y_{|E|})$ with $y_e = \log x_e$, $\mathbf{v}^T \mathbf{y} = \sum_{e \in E} v_e y_e$ and we maximize over the Newton polytope $\mathbf{N}[p]$ of p, which is the tropicalization of p. In this sense we can think of $p^{\text{tr}}(\boldsymbol{x})$ as a representative of $\mathbf{N}[p]$. The tropical approximation has the important property that it can be used to put bounds on the integrand. This can be made mathematically precise, see [113, Theorem 8], for deformed integrals it is at the time of writing just a conjecture:

Conjecture 5.1. There are λ dependent constants $C_1(\lambda), C_2(\lambda) > 0$ such that for small $\lambda > 0$,

$$C_1(\lambda) \leq \left| \left(\frac{\mathcal{U}^{\text{tr}}(\boldsymbol{x})}{\mathcal{U}(\boldsymbol{X})} \right)^{D_0/2} \left(\frac{\mathcal{V}^{\text{tr}}(\boldsymbol{x})}{\mathcal{V}(\boldsymbol{X})} \right)^{\omega_0} \right| \leq C_2(\lambda) \quad \text{for all} \quad \boldsymbol{x} \in \mathbb{P}^E_+, \tag{74}$$

where we recall that $\boldsymbol{X} = (X_1, \ldots, X_{|E|})$ and $X_e = x_e \exp\big(-i\lambda \frac{\partial \mathcal{V}}{\partial x_e}(\boldsymbol{x})\big)$.

Multiplying and dividing with the tropical approximation of $\mathcal{U}$ and $\mathcal{V}$ and expanding in the dimensional regulator gives at order ϵ^k the integral

$$\mathcal{I}_k = I^{\text{tr}} \int_{\mathbb{P}^E_+} \frac{\left(\prod_{e\in E}(X_e/x_e)^{\nu_e}\right) \det \mathcal{J}_\lambda(\boldsymbol{x})}{\left(\mathcal{U}\left(\boldsymbol{X}\right)/\mathcal{U}^{\text{tr}}\left(\boldsymbol{x}\right)\right)^{D_0/2} \cdot \left(\mathcal{V}\left(\boldsymbol{X}\right)/\mathcal{V}^{\text{tr}}\left(\boldsymbol{x}\right)\right)^{\omega_0}} \log^k \left(\frac{\mathcal{U}(\boldsymbol{X})}{\mathcal{V}(\boldsymbol{X})^L} \right) \mu^{\text{tr}} \tag{75}$$

where μ^{tr} is the *tropical probability measure*

$$\mu^{\text{tr}} = \frac{1}{I^{\text{tr}}} \frac{\prod_{e\in E} x_e^{\nu_e}}{\mathcal{U}^{\text{tr}}(\boldsymbol{x})^{D_0/2}\, \mathcal{V}^{\text{tr}}(\boldsymbol{x})^{\omega_0}}\, \Omega\,, \tag{76}$$

with I^{tr} being a normalization factor.

The final task is now to sample from μ^{tr}, in principal this amounts to triangulate the Newton polytopes of $\mathcal{U}$ and $\mathcal{F}$. Up to this point, the process described is in principal valid for any integral with a rational integrand, however, if the Newton polytope of the integrand is a generalizaed permutohedron this costly step may be bypassed. For details on the sampling procedure, see [113] and [P4]. Since $\mathbf{N}[\mathcal{U}]$ is a matroid polytope, it is always a generalized permutohedron according to the results in Section 3. In this section we also gave Corollary 3.8 which gives to kinematic situations when $\mathbf{N}[\mathcal{F}]$ is a generalized permutohedron. This is discussed in greater detail in [P5] and interestingly, even though many sufficient conditions for $\mathbf{N}[\mathcal{F}]$ to be a generalized permutohedron are known, there does not seem to be any necessary conditions know at this point.

Finally, the program `feyntrop` is a `C++` program with `Python` and `JSON` interface available at https://github.com/michibo/feyntrop.

Example 5.2 ([P4, Section 6.5]). The following 5-point process with three massive external legs and a massive loop

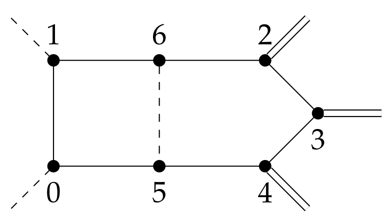

can be evaluated to percent precision to five orders in the dimensional regulator ϵ on a laptop in two seconds. ◇

6 Outlook

By now it is hopefully clear that theoretical physics and mathematics come together beautifully in the study of Feynman integrals. Yet one of the most basic questions is still studied: when is a Feynman integral singular? And what is the precise meaning of singular in this context? A satisfactory answer to this question would be if the following holds (at least for the codimension-one components):

$$\text{Landau variety} \overset{(?)}{\Longleftrightarrow} \text{Singular locus} \overset{(\text{Yes})}{\Longleftrightarrow} \text{Euler discriminant} \tag{77}$$

At the time of writing there seems to exist an unpublished proof of the second equivalence for codimension-one components. If all these objects are the same then the question is settled, at least for the time being.

These are questions of very analytical nature, and since the very beginning the *D*-module school has been studying these questions with their impressive set of tools. For whatever reason, the the parallel European microlocal analysis school does not seem to have shared these interests, neither historically nor today. I am looking forward for this to change in the future!

A branch of mathematics that does not lie idle when it comes to Feynman integrals, and especially amplitudes, is algebraic geometry. This is explored at conferences with hundreds of participants and new synergy grants will keep this interplay between mathematics and physics alive for years to come. We have seen in this thesis how the tropical approach to Feynman integrals can allow for very fast integration. As the understanding of the loop-amplituhedron and the overall tropical nature of amplitudes grow, an exciting future possibility is that these methods might allow us to integrate full amplitudes!

Analysis, algebra and physics are unified in the study of Feynman integrals and I urge the student of any of these subjects to also study the other, as the reward will be outstanding. We are down the rabbit hole now, and I think the best way out is to follow all these exciting threads to their end.

Publications

[P1] C. Dlapa, M. Helmer, G. Papathanasiou and F. Tellander, *Symbol Alphabets from the Landau Singular Locus*, *JHEP* **10** (2023) 161, [2304.02629].

[P2] F. Tellander and M. Helmer, *Cohen-Macaulay Property of Feynman Integrals*, *Commun. Math. Phys.* **399** (2023) 1021–1037, [2108.01410].

[P3] M. Helmer, G. Papathanasiou and F. Tellander, *Landau Singularities from Whitney Stratifications*, 2402.14787.

[P4] M. Borinsky, H. J. Munch and F. Tellander, *Tropical Feynman integration in the Minkowski regime*, *Comput. Phys. Commun.* **292** (2023) 108874, [2302.08955].

[P5] M. Borinsky, H. J. Munch and F. Tellander, *Tropical Feynman integration in the physical region*, *PoS* **EPS-HEP2023** (2024) 499, [2310.19890].

References

[1] R. P. Feynman, R. B. Leighton and M. L. Sands, *The Feynman lectures on physics.* Addison-Wesley, 1989.

[2] R. P. Feynman, *The Theory of positrons*, Phys. Rev. **76** (1949) 749–759.

[3] R. P. Feynman, *Space-time approach to nonrelativistic quantum mechanics*, Rev. Mod. Phys. **20** (1948) 367–387.

[4] R. P. Feynman, *Space-time approach to quantum electrodynamics*, Phys. Rev. **76** (1949) 769–789.

[5] J. E. Nafe, E. B. Nelson and I. I. Rabi, *The Hyperfine Structure of Atomic Hydrogen and Deuterium*, Phys. Rev. **71** (1947) 914–915.

[6] P. Kusch and H. M. Foley, *Precision measurement of the ratio of the atomic 'g values' in the $^2P_{\frac{3}{2}}$ and $^2P_{\frac{1}{2}}$ states of gallium*, Phys. Rev. **72** (1947) 1256–1257.

[7] S. Tomonaga, *On a relativistically invariant formulation of the quantum theory of wave fields*, Prog. Theor. Phys. **1** (1946) 27–42.

[8] J. S. Schwinger, *On Quantum electrodynamics and the magnetic moment of the electron*, Phys. Rev. **73** (1948) 416–417.

[9] Z. Bern, L. J. Dixon, D. C. Dunbar and D. A. Kosower, *One loop n point gauge theory amplitudes, unitarity and collinear limits*, Nucl. Phys. B **425** (1994) 217–260, [hep-ph/9403226].

[10] R. Britto, F. Cachazo, B. Feng and E. Witten, *Direct proof of tree-level recursion relation in Yang-Mills theory*, Phys. Rev. Lett. **94** (2005) 181602, [hep-th/0501052].

[11] Z. Bern, J. J. M. Carrasco and H. Johansson, *Perturbative Quantum Gravity as a Double Copy of Gauge Theory*, Phys. Rev. Lett. **105** (2010) 061602, [1004.0476].

[12] N. Arkani-Hamed and J. Trnka, *The Amplituhedron*, JHEP **10** (2014) 030, [1312.2007].

[13] G. Heinrich, *Collider physics at the precision frontier*, Phys. Rept. **922** (2021) 1–69, [2009.00516].

[14] Z. Bern, C. Cheung, R. Roiban, C.-H. Shen, M. P. Solon and M. Zeng, *Scattering Amplitudes and the Conservative Hamiltonian for Binary Systems at Third Post-Minkowskian Order*, Phys. Rev. Lett. **122** (2019) 201603, [1901.04424].

[15] C. Dlapa, G. Kälin, Z. Liu, J. Neef and R. A. Porto, *Radiation Reaction and Gravitational Waves at Fourth Post-Minkowskian Order*, Phys. Rev. Lett. **130** (2023) 101401, [2210.05541].

[16] S. Weinzierl, *Feynman Integrals*. 1, 2022, 10.1007/978-3-030-99558-4.

[17] M. Kashiwara and T. Kawai, *Holonomic systems of linear differential equations and Feynman integrals*, *Publ. Res. Inst. Math. Sci.* **12** (1976/77) 131–140.

[18] M. Kashiwara, T. Kawai and T. Ōshima, *A study of Feynman integrals by micro-differential equations*, *Comm. Math. Phys.* **60** (1978) 97–130.

[19] T. Bitoun, C. Bogner, R. P. Klausen and E. Panzer, *Feynman integral relations from parametric annihilators*, *Lett. Math. Phys.* **109** (2019) 497–564, [1712.09215].

[20] I. M. Gel'fand, M. I. Graev and A. V. Zelevinskiĭ, *Holonomic systems of equations and series of hypergeometric type*, *Dokl. Akad. Nauk SSSR* **295** (1987) 14–19.

[21] I. M. Gel'fand, A. V. Zelevinskiĭ and M. M. Kapranov, *Hypergeometric functions and toric varieties*, *Funktsional. Anal. i Prilozhen.* **23** (1989) 12–26.

[22] I. M. Gel'fand, M. M. Kapranov and A. V. Zelevinskiĭ, *Generalized Euler integrals and A-hypergeometric functions*, *Adv. Math.* **84** (1990) 255–271.

[23] K. Schultka, *Toric geometry and regularization of Feynman integrals*, 1806.01086.

[24] E. Panzer, *Hepp's bound for Feynman graphs and matroids*, *Ann. Inst. Henri Poincaré D* **10** (8, 2023) 31–119, [1908.09820].

[25] C. Bogner and S. Weinzierl, *Feynman graph polynomials*, *Int. J. Mod. Phys. A* **25** (2010) 2585–2618, [1002.3458].

[26] D. J. Broadhurst and D. Kreimer, *Knots and numbers in ϕ^4 theory to 7 loops and beyond*, *Int. J. Mod. Phys. C* **6** (1995) 519–524, [hep-ph/9504352].

[27] F. Brown, *On the periods of some Feynman integrals*, 0910.0114.

[28] M. D. Schwartz, *Quantum Field Theory and the Standard Model*. Cambridge University Press, 3, 2014.

[29] H. Lehmann, K. Symanzik and W. Zimmermann, *On the formulation of quantized field theories*, *Nuovo Cim.* **1** (1955) 205–225.

[30] L. Hörmander, *Fourier integral operators. I*, *Acta Math.* **127** (1971) 79–183.

[31] L. Hörmander, *The analysis of linear partial differential operators. I*. Classics in Mathematics. Springer-Verlag, Berlin, 2003.

[32] J. J. Duistermaat and L. Hörmander, *Fourier integral operators. II*, *Acta Math.* **128** (1972) 183–269.

[33] M. Reed and B. Simon, *Methods of modern mathematical physics. I. Functional analysis*. Academic Press, New York-London, 1972.

[34] G. B. Folland, *Fundamental solutions for the wave operator*, *Exposition. Math.* **15** (1997) 25–52.

[35] G. B. Folland, *Quantum field theory*, vol. 149 of *Mathematical Surveys and Monographs*. American Mathematical Society, Providence, RI, 2008, 10.1090/surv/149.

[36] M. Gell-Mann and F. Low, *Bound states in quantum field theory*, *Phys. Rev.* **84** (1951) 350–354.

[37] S. Weinberg, *The Quantum theory of fields. Vol. 1: Foundations*. Cambridge University Press, 6, 2005.

[38] M. Sato, *Recent development in hyperfunction theory and its application to physics (microlocal analysis of S-matrices and related quantities)*, in *International Symposium on Mathematical Problems in Theoretical Physics (Kyoto Univ., Kyoto, 1975)*, vol. 39 of *Lecture Notes in Phys.*, pp. 13–29. Springer, Berlin-New York, 1975.

[39] F. J. Dyson, *The renormalization method in quantum electrodynamics*, *Proc. Roy. Soc. Lond. A* **207** (1951) 395–401.

[40] F. J. Dyson, *Divergence of perturbation theory in quantum electrodynamics*, *Phys. Rev.* **85** (1952) 631–632.

[41] G. Källén, *On the definition of the Renormalization Constants in Quantum Electrodynamics*, *Helv. Phys. Acta* **25** (1952) 417.

[42] *Renormalization Theory. Proceedings, NATO Advanced Study Institute: Erice, 17-31 August, 1975*, vol. 23 of *NATO ASI, C - Mathematical and Physical Sciences*, (Dordrecht), Springer, 1976. 10.1007/978-94-010-1490-8.

[43] A. Connes and D. Kreimer, *Renormalization in quantum field theory and the Riemann-Hilbert problem. 1. The Hopf algebra structure of graphs and the main theorem*, *Commun. Math. Phys.* **210** (2000) 249–273, [hep-th/9912092].

[44] A. Connes and D. Kreimer, *Renormalization in quantum field theory and the Riemann-Hilbert problem. 2. The beta function, diffeomorphisms and the renormalization group*, *Commun. Math. Phys.* **216** (2001) 215–241, [hep-th/0003188].

[45] R. Brunetti and K. Fredenhagen, *Microlocal analysis and interacting quantum field theories: Renormalization on physical backgrounds*, *Commun. Math. Phys.* **208** (2000) 623–661, [math-ph/9903028].

[46] K. Symanzik, *Dispersion relations and vertex properties in perturbation theory*, *Progr. Theoret. Phys.* **20** (1958) 690–702.

[47] N. Nakanishi, *General integral formula of perturbation term in the quantized field theory*, *Progr. Theoret. Phys.* **17** (1957) 401–418.

[48] N. Nakanishi, *Graph theory and Feynman integrals.* Mathematics and its applications: 11. Gordon and Breach, 1971.

[49] R. N. Lee and A. A. Pomeransky, *Critical points and number of master integrals*, *JHEP* **11** (2013) 165, [1308.6676].

[50] L. de la Cruz, *Feynman integrals as A-hypergeometric functions*, *JHEP* **12** (2019) 123, [1907.00507].

[51] R. P. Klausen, *Hypergeometric Series Representations of Feynman Integrals by GKZ Hypergeometric Systems*, *JHEP* **04** (2020) 121, [1910.08651].

[52] L. Nilsson and M. Passare, *Mellin transforms of multivariate rational functions*, *J. Geom. Anal.* **23** (2013) 24–46, [1010.5060].

[53] C. Berkesch, J. Forsgård and M. Passare, *Euler-Mellin integrals and A-hypergeometric functions*, *Michigan Math. J.* **63** (2014) 101–123, [1103.6273].

[54] M. Riesz, *L'intégrale de Riemann-Liouville et le problème de Cauchy*, *Acta Math.* **81** (1949) 1–223.

[55] M. Riesz, *The analytic continuation of the Riemann-Liouville integral in the hyperbolic case*, *Canadian J. Math.* **13** (1961) 37–47.

[56] I. N. Bernšteĭn and S. I. Gel'fand, *Meromorphy of the function* P^{λ}, *Funkcional. Anal. i Priložen.* **3** (1969) 84–85.

[57] I. N. Bernšteĭn, *Analytic continuation of generalized functions with respect to a parameter*, *Funkcional. Anal. i Priložen.* **6** (1972) 26–40.

[58] M. F. Atiyah, *Resolution of singularities and division of distributions*, *Comm. Pure Appl. Math.* **23** (1970) 145–150.

[59] D. Eisenbud and B. Sturmfels, *Binomial ideals*, *Duke Math. J.* **84** (1996) 1–45.

[60] I. M. Gel'fand, M. Kapranov and A. Zelevinskĭ, *Discriminants, resultants, and multidimensional determinants*. Springer Science & Business Media, 2008.

[61] J.-E. Björk, *Rings of differential operators*, vol. 21 of *North-Holland Mathematical Library*. North-Holland Publishing Co., Amsterdam-New York, 1979.

[62] M. Saito, B. Sturmfels and N. Takayama, *Gröbner deformations of hypergeometric differential equations*, vol. 6 of *Algorithms and Computation in Mathematics*. Springer-Verlag, Berlin, 2000, 10.1007/978-3-662-04112-3.

[63] T. Ōaku, *Computation of the characteristic variety and the singular locus of a system of differential equations with polynomial coefficients*, *Japan J. Indust. Appl. Math.* **11** (1994) 485–497.

[64] A. Adolphson, *Hypergeometric functions and rings generated by monomials*, *Duke Math. J.* **73** (1994) 269–290.

[65] D. Hilbert, *Ueber die Theorie der algebraischen Formen*, *Math. Ann.* **36** (1890) 473–534.

[66] D. Hilbert, *Ueber die vollen Invariantensysteme*, *Math. Ann.* **42** (1893) 313–373.

[67] M. Auslander and D. A. Buchsbaum, *Homological dimension in local rings*, *Trans. Amer. Math. Soc.* **85** (1957) 390–405.

[68] I. M. Gel'fand, M. M. Kapranov and A. V. Zelevinskiĭ, *A correction to the paper "hypergeometric functions and toric varieties"*, *Funct. Anal. Appl.* **27** (1993) 295–295.

[69] L. F. Matusevich, E. Miller and U. Walther, *Homological methods for hypergeometric families*, *J. Amer. Math. Soc.* **18** (2005) 919–941, [math/0406383].

[70] M. Hochster, *Rings of invariants of tori, Cohen-Macaulay rings generated by monomials, and polytopes*, *Ann. of Math. (2)* **96** (1972) 318–337.

[71] H. Whitney, *On the Abstract Properties of Linear Dependence*, *Amer. J. Math.* **57** (1935) 509–533.

[72] J. Oxley, *Matroid theory*, vol. 21 of *Oxford Graduate Texts in Mathematics*. Oxford University Press, Oxford, second ed., 2011, 10.1093/acprof:oso/9780198566946.001.0001.

[73] I. M. Gel'fand and V. V. Serganova, *Combinatorial geometries and the strata of a torus on homogeneous compact manifolds*, *Uspekhi Mat. Nauk* **42** (1987) 107–134, 287.

[74] I. M. Gel'fand, R. M. Goresky, R. D. MacPherson and V. V. Serganova, *Combinatorial geometries, convex polyhedra, and Schubert cells*, *Adv. in Math.* **63** (1987) 301–316.

[75] A. Postnikov, *Permutohedra, associahedra, and beyond*, *Int. Math. Res. Not.* (2009) 1026–1106.

[76] L. K. Williams, *The positive Grassmannian, the amplituhedron, and cluster algebras*, in *International Congress of Mathematicians*, 10, 2021, 2110.10856.

[77] S. N. Karp and L. K. Williams, *The m=1 amplituhedron and cyclic hyperplane arrangements*, *Int. Math. Res. Not.* **5** (2019) 1401–1462, [1608.08288].

[78] T. Lukowski, M. Parisi and L. K. Williams, *The Positive Tropical Grassmannian, the Hypersimplex, and the $m = 2$ Amplituhedron*, *Int. Math. Res. Not.* **2023** (2023) 16778–16836, [2002.06164].

[79] M. Parisi, M. Sherman-Bennett and L. Williams, *The m=2 amplituhedron and the hypersimplex: signs, clusters, triangulations, Eulerian numbers*, 2104.08254.

[80] U. Walther, *On Feynman graphs, matroids, and GKZ-systems*, *Lett. Math. Phys.* **112** (2022) 120, [2206.05378].

[81] H. Ohsugi and T. Hibi, *Normal polytopes arising from finite graphs*, *J. Algebra* **207** (1998) 409–426.

[82] R. J. Eden, P. V. Landshoff, D. I. Olive and J. C. Polkinghorne, *The analytic S-matrix*. Cambridge Univ. Press, Cambridge, 1966.

[83] H. Lehmann, *On the Properties of propagation functions and renormalization contants of quantized fields*, *Nuovo Cim.* **11** (1954) 342–357.

[84] A. S. Wightman and L. Gårding, *Fields as Operator-Valued Distributions in Relativistic Quantum Theory*, *Arkiv Fys.* **28** (1965) 149–189.

[85] L. D. Landau, *On analytic properties of vertex parts in quantum field theory*, *Nucl. Phys.* **13** (1959) 181–192.

[86] N. Nakanishi, *Ordinary and anomalous thresholds in perturbation theory*, *Progr. Theoret. Phys.* **22** (1959) 128–144.

[87] R. E. Cutkosky, *Singularities and discontinuities of Feynman amplitudes*, *J. Math. Phys.* **1** (1960) 429–433.

[88] K. G. Chetyrkin and F. V. Tkachov, *Integration by parts: The algorithm to calculate β-functions in 4 loops*, *Nucl. Phys. B* **192** (1981) 159–204.

[89] A. V. Kotikov, *Differential equations method: New technique for massive Feynman diagrams calculation*, *Phys. Lett. B* **254** (1991) 158–164.

[90] E. Remiddi, *Differential equations for Feynman graph amplitudes*, *Nuovo Cim. A* **110** (1997) 1435–1452, [hep-th/9711188].

[91] T. Gehrmann and E. Remiddi, *Differential equations for two loop four point functions*, Nucl. Phys. B **580** (2000) 485–518, [hep-ph/9912329].

[92] J. M. Henn, *Multiloop integrals in dimensional regularization made simple*, Phys. Rev. Lett. **110** (2013) 251601, [1304.1806].

[93] T. Ōaku and N. Takayama, *Algorithms for D-modules—restriction, tensor product, localization, and local cohomology groups*, J. Pure Appl. Algebra **156** (2001) 267–308, [math.AG/9805006].

[94] V. Chestnov, S. J. Matsubara-Heo, H. J. Munch and N. Takayama, *Restrictions of Pfaffian systems for Feynman integrals*, JHEP **11** (2023) 202, [2305.01585].

[95] E. Panzer, *Algorithms for the symbolic integration of hyperlogarithms with applications to Feynman integrals*, Comput. Phys. Commun. **188** (2015) 148–166, [1403.3385].

[96] C. Fevola, S. Mizera and S. Telen, *Landau Singularities Revisited*, 2311.14669.

[97] C. Fevola, S. Mizera and S. Telen, *Principal Landau Determinants*, 2311.16219.

[98] C. Améndola, N. Bliss, I. Burke, C. R. Gibbons, M. Helmer, S. Hoşten et al., *The maximum likelihood degree of toric varieties*, J. Symb. Comput. **92** (2019) 222–242, [1703.02251].

[99] F. Pham, *Singularities of integrals*. Universitext. Springer, London; EDP Sciences, Les Ulis, 2011, 10.1007/978-0-85729-603-0.

[100] H. Whitney, *Local properties of analytic varieties*, in *Differential and Combinatorial Topology (A Symposium in Honor of Marston Morse)*, pp. 205–244. Princeton Univ. Press, Princeton, NJ, 1965.

[101] H. Whitney, *Tangents to an analytic variety*, Ann. of Math. (2) **81** (1965) 496–549.

[102] J. Mather, *Notes on topological stability*, Bull. Amer. Math. Soc. **49** (2012) 475–506.

[103] D. R. Grayson and M. E. Stillman, "Macaulay2, a software system for research in algebraic geometry." Available at http://www.math.uiuc.edu/Macaulay2.

[104] M. Helmer and V. Nanda, *Conormal spaces and Whitney stratifications*, Found. Comput. Math. **23** (2023) 1745–1780, [2106.14555].

[105] M. Helmer and V. Nanda, *Effective Whitney Stratification of Real Algebraic varieties*, 2307.05427.

[106] E. Andronikof, *On the $\mathscr{C}^\infty$-singularities of regular holonomic distributions*, *Ann. Inst. Fourier (Grenoble)* **42** (1992) 695–705.

[107] E. Andronikof, *The Kashiwara conjugation and wave-front sets of regular holonomic distributions on a complex manifold*, Invent. Math. **111** (1993) 35–49.

[108] R. Hotta, *Equivariant d-modules*, math/9805021.

[109] X. Liu and Y.-Q. Ma, *AMFlow: A Mathematica package for Feynman integrals computation via auxiliary mass flow*, Comput. Phys. Commun. **283** (2023) 108565, [2201.11669].

[110] M. Hidding, *DiffExp, a Mathematica package for computing Feynman integrals in terms of one-dimensional series expansions*, Comput. Phys. Commun. **269** (2021) 108125, [2006.05510].

[111] T. Armadillo, R. Bonciani, S. Devoto, N. Rana and A. Vicini, *Evaluation of Feynman integrals with arbitrary complex masses via series expansions*, Comput. Phys. Commun. **282** (2023) 108545, [2205.03345].

[112] S. Borowka, G. Heinrich, S. Jahn, S. P. Jones, M. Kerner, J. Schlenk et al., *pySecDec: a toolbox for the numerical evaluation of multi-scale integrals*, Comput. Phys. Commun. **222** (2018) 313–326, [1703.09692].

[113] M. Borinsky, *Tropical Monte Carlo quadrature for Feynman integrals*, Ann. Inst. Henri Poincaré Comb. Phys. Interact. (8, 2023) , [2008.12310].

[114] J. M. Henn, J. Lim and W. J. Torres Bobadilla, *First look at the evaluation of three-loop non-planar Feynman diagrams for Higgs plus jet production*, JHEP **05** (2023) 026, [2302.12776].

[115] P.-H. Balduf, *Statistics of Feynman amplitudes in ϕ^4-theory*, 2305.13506.

[116] N. Arkani-Hamed, A. Hillman and S. Mizera, *Feynman polytopes and the tropical geometry of UV and IR divergences*, Phys. Rev. D **105** (2022) 125013, [2202.12296].

[117] N. Arkani-Hamed, H. Frost, G. Salvatori, P.-G. Plamondon and H. Thomas, *All Loop Scattering as a Counting Problem*, 2309.15913.

[118] H. S. Hannesdottir and S. Mizera, *What is the iε for the S-matrix?* SpringerBriefs in Physics. Springer, 1, 2023, 10.1007/978-3-031-18258-7.

[119] D. Maclagan and B. Sturmfels, *Introduction to tropical geometry*, vol. 161 of *Graduate Studies in Mathematics*. American Mathematical Society, Providence, RI, 2015, 10.1090/gsm/161.

Scientific publications

Author contributions

Paper I: Symbol alphabets from the Landau singular locus

I observed that symbol alphabets could be obtained by "re-factorizing" singularities and I played a large part in proving the theorems on normality. We participated equally in writing the manuscript.

Paper II: Cohen-Macaulay Propert of Feynman Integrals

I proposed the study in this paper and proved the main theorems after discussions with Martin Helmer. We participated equally in writing the manuscript.

Paper III: Landau Singularities from Whitney Stratifications

I suggested to use the newly developed software to calculate singularities of Feynman integrals. I also participated in doing the calculations. We participated equally in writing the manuscript.

Paper IV: Tropical Feynman integration in the Minkowski regime

After Henrik Munch and I had started working on extending Michael Borinsky's code independently we all joined forces after a workshop. I participated mainly in the theory development. We participated equally in writing the manuscript.

Paper V: Tropical Feynman integration in the physical region

I wrote the manuscript.

Paper I

Symbol alphabets from the Landau singular locus
Chrisoph Dlapa, Martin Helmer, Georgios Papathanasiou and **Felix Tellander**
J. High Energ. Phys. **10** (2023) 161, [2304.02629]

Published for SISSA by Springer

Received: May 4, 2023
Accepted: October 16, 2023
Published: October 25, 2023

Symbol alphabets from the Landau singular locus

Christoph Dlapa,[a] Martin Helmer,[b] Georgios Papathanasiou[a] and Felix Tellander[a]

[a] *Deutsches Elektronen-Synchrotron DESY,
Notkestr. 85, 22607 Hamburg, Germany*

[b] *Department of Mathematics,
North Carolina State University, Raleigh, U.S.A.*

E-mail: christoph.dlapa@desy.de, mhelmer@ncsu.edu, georgios.papathanasiou@desy.de, felix@tellander.se

Abstract: We provide evidence through two loops, that rational letters of polylogarithmic Feynman integrals are captured by the Landau equations, when the latter are recast as a polynomial of the kinematic variables of the integral, known as the principal A-determinant. Focusing on one loop, we further show that all square-root letters may also be obtained, by re-factorizing the principal A-determinant with the help of Jacobi identities. We verify our findings by explicitly constructing canonical differential equations for the one-loop integrals in both odd and even dimensions of loop momenta, also finding agreement with earlier results in the literature for the latter case. We provide a computer implementation of our results for the principal A-determinants, symbol alphabets and canonical differential equations in an accompanying `Mathematica` file. Finally, we study the question of when a one-loop integral satisfies the Cohen-Macaulay property and show that for almost all choices of kinematics the Cohen-Macaulay property holds. Throughout, in our approach to Feynman integrals, we make extensive use of the Gel'fand, Graev, Kapranov and Zelevinskiĭ theory on what are now commonly called GKZ-hypergeometric systems whose singularities are described by the principal A-determinant.

Keywords: Differential and Algebraic Geometry, Higher-Order Perturbative Calculations, Scattering Amplitudes

ArXiv ePrint: 2304.02629

https://doi.org/10.1007/JHEP10(2023)161

JHEP10(2023)161

Contents

JHEP10(2023)161

1 Introduction

Feynman integrals are central objects in theoretical physics, for example, their evaluation is central for the calculation of any scattering amplitude in high-energy physics [1]. This not only includes experiments using the Large Hadron Collider at CERN but also amplitudes in gravitational wave physics [2, 3] or the critical exponent in statistical field theory [4].

Evaluation of these integrals is a challenging problem which has fostered two main lines of development: advanced numerical schemes have been developed for fast and accurate direct evaluation (see e.g. [5, 6] or [7, 8]) and sophisticated analytical computer tools have been developed for either direct evaluation or for understanding the analytic structure, see for example [9–22]. Focusing on the latter, the topic is classical and dates back to the seminal work of Landau [23], Cutkosky [24] and the S-matrix program of the 1960's [25]. At that time it was understood by Regge that every Feynman integral is a solution to a system of partial differential equations (PDEs) of "hypergeometric type" [26], and a strong connection with the Japanese D-module school of Sato and Kashiwara was established [27, 28].

Later in the 1980's, a completely combinatorial description of a vast family of D-modules, to which all Feynman integrals belong, was given by Gel'fand and collaborators [29]. D-modules in this family are now commonly referred to as *GKZ-hypergeometric systems*. The singularities of these GKZ-hypergeometric systems are described by a polynomial known as the *principal A-determinant*. When the GKZ-hypergeometric system under consideration arises from a Feynman integral, the principal A-determinant then describes the kinematic singularities of the Feynman integral, namely the values of the kinematic parameters of the integral, for which it may become singular. The zero set of the principal A-determinant is commonly referred to in physics as the *Landau singular locus*, in other words it is the solution to the Landau equations [23], where the presence of kinematic singularities is formulated as a condition for the contour of integration to become trapped. One important property of GKZ-hypergeometric systems is the *Cohen-Macaulay property*; when a GKZ-hypergeometric system has this property its *rank* is given by a simple combinatorial formula and series solutions to the system may be obtained in a much more straightforward manner. In the context of Feynman integrals, the rank of the GKZ-hypergeometric system bounds the number of *master integrals*, to be defined below. These connections have been rediscovered in recent years attracting a lot of interest, see e.g. [30–33].

Parallel to this, analytic evaluation approaches using partial differential equations were also developed natively within the physics community [34–36], culminating in what is now called *canonical differential equations* [37]. When a Feynman integral can be represented like this it can be expressed as a Chen iterated integral [38] which, when the kernels are rational, further reduces to the well-studied class of multiple polylogarithms (MPLs) [39, 40].

More concretely, these approaches are based on the solution of integration by parts identities (IBPs) [41], namely linear relations between any set of Feynman integrals with integer propagator powers, for example those contributing to a given process. The master integrals alluded to before are precisely a finite basis $\vec{g}$ in this linear space, obtained by solving the identities in question. Derivatives of the master integrals may then be re-expressed in terms of this basis. Regularizing the infrared and ultraviolet divergences of the integrals by setting the dimension of the loop momenta to $D = D_0 - 2\epsilon$, the canonical transformation that greatly facilitates their solution is then a change of basis such that

$$d\vec{g} = \epsilon \, d\widetilde{M} \, \vec{g}, \tag{1.1}$$

where we have grouped all partial derivatives with respect to the independent kinematic variables of the integrals, v_i, into the total differential $d = \sum_i dv_i \partial_{v_i}$. The matrix $\widetilde{M}$ is independent of ϵ and takes the simple dlog-form,

$$\widetilde{M} \equiv \sum_i \tilde{a}_i \log W_i, \tag{1.2}$$

where the $\tilde{a}_i$ are constant matrices and the W_i carry all kinematic dependence and are called *letters*. The set of all letters is called the *alphabet*. Evidence suggests that a transformation to the first equality is always possible, however the particular form of the $\widetilde{M}$ matrix given by the second equality is expected to exist only when the master integrals live in the aforementioned class of MPLs. The latter class of integrals will be the focus of this paper.

The merit of the canonical differential equations (1.1)–(1.2) for the integrals $\vec{g}$ is that they can now be easily solved as an expansion[1] in ϵ

$$\vec{g} = \sum_{k=0}^{\infty} \epsilon^k \vec{g}^{(k)}, \tag{1.3}$$

where at each order $\vec{g}^{(k)}$ the *symbol* $\mathcal{S}$ [42], capturing the full answer up to transcendental constants, is given by

$$\mathcal{S}(\vec{g}^{(k)}) = \sum_{i_1,\ldots,i_k=1}^{n} \tilde{a}_{i_k} \cdot \tilde{a}_{i_{k-1}} \cdots \tilde{a}_{i_1} \cdot \vec{g}^{(0)}\ W_{i_1} \otimes \cdots \otimes W_{i_k}. \tag{1.4}$$

In practical applications, two major bottlenecks that one often encounters in the above procedure are solving the IBPs analytically so as to find a basis of master integrals, and finding the transformation that relates this to a new, canonical basis (1.2). However, with knowledge of the letters W_i it would be possible to avoid doing these two steps analytically by using the latter equation as an ansatz. The unknown coefficient matrices $\tilde{a}_i$ can then be fixed by matching the partial derivatives of the ansatz to multiple numerical evaluations of (1.1) derived through numeric IBP identities (over finite fields if necessary). Similar approaches have, for example, been used in [43].

Motivated by the great potential benefits of this alternative route, in this paper we will open a new door to obtaining the symbol alphabet from the Landau equations, when recast in the form of the aforementioned principal A-determinant, before attempting to analytically evaluate the integrals. Many crucial results in theoretical physics have been obtained by analyzing the Landau equations, whose study has recently received renewed interest, see for example [44–54] for an incomplete list. From eqs. (1.1)–(1.2) it is evident that values of the kinematic variables where the letters W_i vanish are potential branch points of Feynman integrals, and it is well known that these values are indeed captured by the Landau equations. However this information is in general not enough for fixing the entire functional form of the letters.

Quite remarkably, here we observe that the principal A-determinant of a Feynman integral, in the natural factorization it is endowed with as a function of its kinematic variables, coincides with the product of rational letters of the integral in question! We will provide precise definitions in the following sections, but let us give an idea of this identification for the one-loop 'two-mass easy' box with all internal masses being zero, and

[1]We assume that the integrals are normalized such that they have uniform transcendental weight zero.

additionally $p_2^2 = p_4^2 = 0$, $p_1^2, p_3^2 \neq 0$:

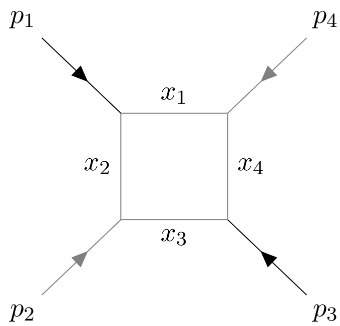

The principal A-determinant of this Feynman integral is

$$\widetilde{E_A} = \underbrace{(p_1^2 p_3^2 - st)}_{\text{type-I}} \underbrace{p_1^2 p_3^2 st(p_1^2 + p_3^2 - s - t)(p_3^2 - t)(p_3^2 - s)(p_1^2 - t)(p_1^2 - s)}_{\text{type-II}}. \tag{1.5}$$

where $s = (p_1 + p_2)^2$ and $t = (p_1 + p_4)^2$ are Mandelstam invariants. The 10 factors above in fact coincide with the 10 letters in the symbol alphabet of this diagram. In eq. (1.5) we have also indicated whether each factor describes a type-I and type-II Landau singularity, associated to the entrapment of the integration contour at finite or infinite values of the loop momentum, respectively (as also reviewed in section 2.2). In much of the relevant literature there has been a tendency to focus on type-I singularities, however here we wish to emphasize that for symbol alphabets the type-II singularities in general cannot be neglected.

We will also provide two-loop evidence of the connection between principal A-determinants and rational letters, but in this paper we will mainly focus on further extracting letters containing square roots from them, which is well known that already appear in one-loop integrals. For these integrals, we will also prove that the Cohen-Macaulay property holds.

The paper is organized as follows. In section 2 we provide the necessary background for Feynman integrals and generalized hypergeometric systems. In particular we connect the Landau singularities to the principal A-determinant. In section 3 we restrict our focus to one-loop graphs and provide the full principal A-determinant, symbol alphabet and canonical differential equations for all graphs with generic kinematics. The process of starting with the case of generic kinematics and taking limits to obtain non-generic kinematics, as well as the connection to previous work, are also discussed. Explicit examples are provided in section 4. In section 5 we prove that the Cohen-Macaulay property holds for one-loop graphs for almost all choices of kinematics (in fact we prove a stronger sufficient condition referred to as *normality*) and discuss the generalized permutohedron property. Finally in section 6 we provide conclusions and outlook. Our results on the principal A-determinant, symbol alphabet and differential equations have also been implemented in the `Mathematica` notebook `LandauAlphabetDE.nb` as Supplementary Material attached to our article.

Note added. While this project was in the process of writing up, we became aware of the recent preprint [55], which overlaps in part with the results presented in subsection 3.2.

2 Feynman integrals, Landau singularities and GKZ systems

In this section we establish our conventions on Feynman scalar integrals, and review how they can be interpreted as GKZ hypergeometric systems when expressed in the Lee-Pomeransky representation. We also recall how a natural object in this framework, the principal A-determinant, captures the Landau singularities of these integrals, mostly following [48].

2.1 Feynman integrals in the Lee-Pomeransky representation

In this paper we consider one-particle irreducible Feynman graphs $G := (E, V)$ with internal edge set E, vertex set V and loop number $L = |E| - |V| + 1$. Every edge $e \in E$ is assigned an arbitrary direction with which we define the *incidence matrix* η_{ve} of G to satisfy $\eta_{ve} = 1$ if e ends at v, -1 if e starts at v, and 0 otherwise. The vertex set V has the disjoint partition $V = V_{\text{ext}} \sqcup V_{\text{int}}$ where each vertex $v \in V_{\text{ext}}$ is assigned an external incoming d-dimensional momenta $p_v \in \mathbb{R}^{1,d-1}$ with the mostly minus convention $(p_v)^2 = (p_v^0)^2 - (p_v^1)^2 - \cdots$ and we put $p_v = 0$ for all $v \in V_{\text{int}}$. Using Feynman's causal $i\varepsilon$ prescription, scalar Feynman rules assigns the following integral to G:

$$\mathcal{I} = \left(\frac{e^{\gamma_E \epsilon}}{i\pi^{D/2}}\right)^L \lim_{\varepsilon \to 0^+} \int \prod_{e\in E} d^D q_e \left(\frac{-1}{q_e^2 - m_e^2 + i\varepsilon}\right)^{\nu_e} \prod_{v \in V \setminus \{v_0\}} \delta^{(D)}\left(p_v + \sum_{e\in E} \eta_{ve} q_e\right) \tag{2.1}$$

where $\gamma_E = -\Gamma'(1) \simeq 0.577$ is the Euler-Mascheroni constant, $\nu_e \in \mathbb{Z}$ are generalized propagator powers and q_e is the total internal momenta flowing through the edge e. We are also employing dimensional regularization with $D := D_0 - 2\epsilon$, and while the external and (integer part of) the internal momenta dimensions are usually taken to coincide, $D_0 = d$, here we will distinguish between the two. Physically this can be thought of as restricting one set of momenta to lie in a subspace of the other, and is further justified by the alternative parametric representations of Feynman integrals, which we will get to momentarily. Momentum is conserved at each vertex $v \in V$, but only $|V| - 1$ of these constraints are independent, we therefore remove an arbitrary vertex v_0 from V in (2.1) to avoid imposing $\delta^{(D)}\left(\sum_{v\in V} p_v\right)$ explicitly.

To evaluate the integrals we rewrite them in parametric form

$$\mathcal{I} = e^{L\gamma_E\epsilon}\Gamma(\omega) \lim_{\varepsilon\to 0^+} \int_0^\infty \prod_{e\in E}\left(\frac{x^{\nu_e} dx_e}{x_e \Gamma(\nu_e)}\right) \frac{\delta(1-H(x))}{\mathcal{U}^{D/2}} \left(\frac{1}{\mathcal{F}/\mathcal{U} - i\varepsilon \sum_{e\in E} x_e}\right)^{\omega} \tag{2.2}$$

where $\omega := \sum_{e\in E} \nu_e - LD/2$ is the superficial degree of divergence, $H : \mathbb{R}^{|E|} \to \mathbb{R}_+$ is a homogeneous function of degree one and x_e, $e \in E$, are the *Schwinger/Feynman parameters*. These are defined by the Γ-function identity

$$\left(\frac{i}{q_e^2 - m_e^2 + i\varepsilon}\right)^{\nu_e} = \frac{1}{\Gamma(\nu_e)} \int_0^\infty \frac{dx_e}{x_e}\, x_e^{\nu_e} \exp\left[ix_e(q_e^2 - m_e^2 + i\varepsilon)\right] \tag{2.3}$$

which is absolutely convergent when $\varepsilon > 0$ and the real part of ν_e is positive, $\Re(\nu_e) > 0$, but can be analytically continued to all $\nu_e \in \mathbb{C}$. In the representation (2.2) the information on the Feynman graph G has been encoded in two homogeneous *Symanzik polynomials* $\mathcal{U}$ and $\mathcal{F}$, of degree L and $L+1$ in the integration variables, respectively. As is reviewed in e.g. [56], by virtue of the matrix tree theorem these are equal to

$$\mathcal{U} = \sum_{\substack{T \text{ a spanning} \\ \text{tree of } G}} \prod_{e \notin T} x_e, \tag{2.4}$$

$$\mathcal{F} = \mathcal{F}_m + \mathcal{F}_0 = \mathcal{U} \sum_{e \in E} m_e^2 x_e - \sum_{\substack{F \text{ a spanning} \\ 2-\text{forest of } G}} p(F)^2 \prod_{e \notin F} x_e, \tag{2.5}$$

where a spanning tree is a connected subgraph of G which contains all of its vertices but no loops, and the spanning two-forest is defined similarly, but now has two connected components. For each spanning two-forest $F = (T, T')$ of G we let $p(F) = \sum_{v \in T \cap V_{\text{ext}}} p(v)$ denote the total momentum flowing through cut.

In this paper we will consistently think of the Feynman integral of a Feynman diagram G in their parametric representation due to Lee and Pomeransky [57], that is we consider integrals:

$$\mathcal{I} = e^{L\gamma_E \epsilon} \frac{\Gamma(D/2)}{\Gamma(D/2 - \omega)} \int_0^\infty \prod_{e \in E} \left(\frac{x_e^{\nu_e} dx_e}{x_e \Gamma(\nu_e)} \right) \frac{1}{\mathcal{G}^{D/2}} \tag{2.6}$$

where

$$\mathcal{G} = \mathcal{U} + \mathcal{F} \tag{2.7}$$

and the dependence on $i\varepsilon$ has been suppressed as it will not play a role in the rest of the paper. Going from (2.6) back to (2.2) is done by inserting $1 = \int_0^\infty \delta(t - H(x))dt$, re-scaling the variables $x_e \to t x_e,\ t > 0$ and performing the t-integral.

When a Feynman integral is written in Lee-Pomeransky form it is a generalized hypergeometric integral [30, 31] of the form studied by Passare and collaborators [58, 59]. As a consequence it is also a solution to a generalized hypergeometric system of partial differential equations in the sense of Gel'fand, Graev, Kapranov and Zelevinskiĭ (GGKZ, commonly shortened to GKZ) [29, 60–63]. The singularities of these hypergeometric systems are described by the *principal A-determinant*, see [64, §3] and [65, section 9] or [66, Theorem 1.36] or [48, §3]. We will define the principal A-determinant in section 2.2 below; in the context of Feynman integrals the zero set of the principal A-determinant contains all kinematic points where the Feynman integral fails to be an analytic function.

Using multi-index notation we may write the Lee-Pomeransky polynomial as $\mathcal{G} = \sum_{i=1}^r c_i x^{\alpha_i}$ with $c_i \neq 0$ and $\alpha_i \in \mathbb{Z}_{\geq 0}^{|E|}$ for all $i = 1, \ldots, r$. We define the two matrices

$$A := \{1\} \times A_- = \begin{pmatrix} 1 & 1 & \cdots & 1, \\ \alpha_1 & \alpha_2 & \cdots & \alpha_r \end{pmatrix} \in \mathbb{Z}_{\geq 0}^{(|E|+1) \times r}, \text{ and} \tag{2.8}$$

$$\beta := \left(-D/2,\ -\nu_1\ , \ldots\ , -\nu_{|E|} \right)^T \in \mathbb{R}^{|E|+1}, \tag{2.9}$$

where $A_- := \operatorname{Supp}(\mathcal{G})$ is the monomial *support* of $\mathcal{G}$, that is the matrix whose columns are the exponent vectors of the monomials appearing with non-zero coefficients in $\mathcal{G}$. From these two matrices the GKZ hypergeometric system can be defined as a left-ideal $H_A(\beta)$ in the Weyl algebra $W := \mathbb{Q}(\beta)[c_1,\ldots,c_r]\langle\partial_1,\ldots,\partial_r\rangle$ where ∂_i denotes the partial differential operator associated to c_i (cf. [67]). The hypergeometric ideal $H_A(\beta)$ can be written as the sum of the two ideals

$$I_A := \left\langle \partial^u - \partial^v \mid u,v \in \mathbb{Z}^r_{\geq 0} \text{ s.t. } Au = Av \right\rangle, \quad \text{and} \tag{2.10}$$

$$Z_A(\beta) := \left\langle \Theta_i(c,\partial) \mid \Theta = A \cdot \begin{pmatrix} c_1\partial_1 \\ \vdots \\ c_r\partial_r \end{pmatrix} - \beta \right\rangle, \tag{2.11}$$

where Θ is a vector containing $|E|+1$ polynomials. Note that a Feynman integral $\mathcal{I}$ is annihilated by all polynomials in the left-ideal $H_A(\beta) := I_A + Z_A(\beta)$, i.e. $H_A(\beta) \bullet \mathcal{I} = 0$, hence, from an analytic perspective, $H_A(\beta)$ is a system of partial differential equations. We also note that by definition the ideal I_A is in fact an ideal in the *commutative polynomial ring* $\mathbb{Q}[\partial_1,\cdots,\partial_r]$, (which we consider as a left ideal in the Weyl algebra) and has a finite generating set $I_A = \langle h_1,\ldots h_\ell\rangle$ with $h_i \in \mathbb{Q}[\partial_1,\cdots,\partial_r]$. This ideal I_A is a prime ideal whose finite generating set consists of binomials and is often referred to as a *toric ideal* as it gives the defining equations of the projective *toric variety*

$$X_A = \{z \in \mathbb{P}^{r-1} \mid h_1(z) = \cdots = h_\ell(z) = 0\}$$

associated to the matrix A, see e.g. [68], [65, II, section 5].

2.2 Landau singularities and the principal A-determinant

In going from the momentum space representation (2.1) to the parametric representation (2.2) one has the intermediate step

$$\mathcal{I} = \int \prod_{l=1}^{L} \frac{d^D k_l}{i\pi^{D/2}} \int_0^\infty \prod_{e\in E} dx_e \frac{\delta(1-H(x))}{\mathcal{Q}^{\sum_e \nu_e}} \tag{2.12}$$

where the momentum integrals is over the L independent loop momenta and

$$\mathcal{Q} = \sum_{e\in E} x_e(-q_e^2 + m_e^2). \tag{2.13}$$

The original Landau analysis [23] involves finding not only when $\mathcal{Q}$ is zero but when it has a stationary point so that the integration contour becomes pinched between poles of the integrand. These conditions are expressed in the *Landau equations*

$$\begin{cases} \mathcal{Q} = 0 \\ \frac{\partial}{\partial k_l}\mathcal{Q} = 0, \ \forall l = 1,\ldots,L. \end{cases} \tag{2.14}$$

If all loop momenta are kept finite the solutions are called type-I singularities while if all loop momenta are infinite it is referred to as a type-II singularity (first observed by Cutkosky [24]). In general some loop momenta can be finite while some pinch at infinity giving a *mixed* type-II singularity. However, at one-loop there are no such mixed singularities as there is only one loop momentum. The Landau equations have also been

JHEP10(2023)161

studied in the parametric representation (2.2), see for example [69, 70]. After introducing some machinery from the GKZ-formalism, we will see that solutions of the Landau equations in the Lee-Pomeransky formalism are associated with the vanishing of the principal A-determinant (cf. Definition 2.2).

Following the notation in [65] we let $A = \{a_1, \dots, a_n\} \subset \mathbb{Z}^{k-1}$ be a set of lattice points that generates $\mathbb{Z}^{k-1}$ and let $\mathbb{C}^A$ denote the finite dimensional $\mathbb{C}$-vector space of all Laurent polynomials with support A, meaning all Laurent polynomials which can be formed from the momomials $x^{a_1}, \dots, x^{a_n}$, i.e. $\mathbb{C}^A := \{\sum_{i=1}^n c_i x^{a_i} \mid c_i \in \mathbb{C}\}$.

Let $\mathcal{Z}_0(A) \subset (\mathbb{C}^A)^k$ be the set of polynomials $(f_1(x), \dots, f_k(x))$ for which there is x in the algebraic torus $(\mathbb{C}^*)^{k-1}$ satisfying $f_1(x) = \cdots f_k(x) = 0$, i.e.

$$\mathcal{Z}_0(A) := \left\{ (f_1, \dots, f_k) \in (\mathbb{C}^A)^k \,|\, \mathbf{V}\,(f_1, \dots, f_k) \neq \emptyset \text{ in } (\mathbb{C}^*)^{k-1} \right\}. \tag{2.15}$$

The closure $\mathcal{Z}(A)$ of $\mathcal{Z}_0(A)$ is an irreducible hypersurface in $(\mathbb{C}^A)^k$ over the rational numbers.

Definition 2.1 (***A***-resultant)**.** Since $\mathcal{Z}(A)$ is an irreducible hypersurface there is an irreducible polynomial R_A in the coefficients of $f_1, \dots, f_k$ with integer coefficients that is unique up to sign. This polynomial is called the *A-resultant*.

A special case of the A-resultant is when $f_k = f$ and $f_i = x_i \partial f / \partial x_i$ for $i = 1, \dots, k-1$:

Definition 2.2 (Principal ***A***-determinant)**.** The special A-resultant

$$E_A(f) := R_A \left(x_1 \frac{\partial f}{\partial x_1}, \dots, x_{k-1} \frac{\partial f}{\partial x_{k-1}}, f \right) \tag{2.16}$$

is called the *principal A-determinant*.

A major result in this field [65, section 10] is that the principal A-determinant can be written as a product of *A-discriminants*. Let $\nabla_0 \subset \mathbb{C}^A$ be the set defined as

$$\nabla_0 := \left\{ f \in \mathbb{C}^A \mid \mathbf{V} \left(f, \frac{\partial f}{\partial x_1}, \dots, \frac{\partial f}{\partial x_k} \right) \neq \emptyset \text{ for } x \in (\mathbb{C}^*)^k \right\} \tag{2.17}$$

and denote by ∇_A the Zariski closure of ∇_0.

Definition 2.3 (***A***-discriminant)**.** If $\nabla_A \subset \mathbb{C}^A$ has codimension 1, then the *A-discriminant* is the irreducible polynomial $\Delta_A(f)$ in the coefficients c_i of f that vanishes on ∇_A. If $\mathrm{codim}\nabla_A > 1$ we put $\Delta_A = 1$.

Again writing X_A for the toric variety associated to A, we have that the projectivization of ∇_A is the projective dual of X_A, see e.g. [65]. The faces $\Gamma \subset \mathrm{conv}(A)$ induce a stratification of X_A with strata $X(\Gamma)$ and projective duals $\nabla_{A\cap\Gamma}$; by $A \cap \Gamma$ we mean the matrix consisting of all columns of A which are also contained in the face Γ. For a variety $X(\Gamma) \subset X_A$ we denote the multiplicity of X_A along $X(\Gamma)$ as $\mathrm{mult}_{X(\Gamma)} X_A$, [65, Definition 3.15, section 5], and we have the following factorization theorem.

Theorem 2.4 (Prime factorization, Theorem 1.2, section 10 of [65])**.** *Let* $Q = \mathrm{conv}(A)$, *then the principal* A*-determinant is the polynomial*

$$E_A(f) = \pm \prod_{\Gamma \subseteq Q} \Delta_{A\cap\Gamma}(f)^{\mathrm{mult}_{X(\Gamma)} X_A} \tag{2.18}$$

where $\Delta_{A\cap\Gamma}(f) := \Delta_{A\cap\Gamma}(f|_\Gamma)$ *and* $f|_\Gamma$ *is the coordinate restriction of* f *supported on* Γ.

Calculating the principal A-determinant $E_A(f)$ now comes down to three steps: calculating all the faces Γ of $Q = \mathrm{conv}(A)$, calculating the multiplicities $\mathrm{mult}_{X(\Gamma)} X_A$, which are lattice indices [65, Theorem 3.16, section 5] and can be computed via integer linear algebra [71, Remark 2.2], and finally calculating the A-discriminants $\Delta_{A\cap\Gamma}(f)$ which can be obtained via elimination (which can be accomplished using Gröbner basis, see e.g. [72]).

In our discussion we are primarily interested in the zero set of the principal A-determinant $E_A(f)$, hence we may neglect the exponents appearing in (2.18), as these do not change the zero set. To this end we make the following definition of a *reduced principal* A*-determinant*, which is the unique polynomial (up to constant) that corresponds to the zero set of $E_A(f)$.[2]

Definition 2.5 (Reduced Principal $\boldsymbol{A}$-determinant)**.** Let $Q = \mathrm{conv}(A)$, then the reduced principal A-determinant is the polynomial

$$\widetilde{E_A}(f) = \prod_{\Gamma \subseteq Q} \Delta_{A\cap\Gamma}(f) \tag{2.19}$$

where $\Delta_{A\cap\Gamma}(f) := \Delta_{A\cap\Gamma}(f|_\Gamma)$ and $f|_\Gamma$ is the coordinate restriction of f supported on Γ.

Using the *homogenized* Lee-Pomeransky polynomial $\mathcal{G}_h := \mathcal{U}x_0 + \mathcal{F}$ and $A = \mathrm{Supp}(\mathcal{G}_h)$ [3] in the definition of $E_A(\mathcal{G}_h)$ we can understand $E_A(\mathcal{G}_h)$ as a polynomial in the coefficients c_i whose zeros correspond to coefficients such that

$$\mathcal{G}_h = 0, \text{ and either } x_i = 0 \text{ or } \frac{\partial \mathcal{G}_h}{\partial x_i} = 0 \;\forall\; i = 0, \ldots, |E| \text{ in } (\mathbb{C}^*)^{|E|+1}. \tag{2.20}$$

Written in this way this is the "third representation" of the Landau equations in [25, §2.2] with some important differences. In [25] they define the singularities only in terms of the $\mathcal{F}$-polynomial. Using the full Lee-Pomeransky polynomial, not only do we get all the Landau singularities from the $\mathcal{F}$-polynomial (the type-I singularities), but also the singularities only depending on external kinematics (type-II singularities) and the mixed type-II singularities. For a recent discussion on the relation between discriminants and Landau singularities see e.g. [48, 49]. In short we get all possible singularities by using the full Lee-Pomeransky polynomial.

[2]Mathematically speaking, the exponents in eq. (2.18) do contain important information; in the context of toric geometry this e.g. pertains to the local geometry in the neighbourhood of a singular point on the toric variety. The physical meaning of these exponents in the Feynman integral context is something that certainly merits further exploraton. As a first step in this direction, we have computed these exponents for several examples of generic 1-loop graphs, finding that they are always equal to 1. We defer a more detailed investigation to future work.

[3]This is equivalent to using $A = \{1\} \times \mathrm{Supp}(\mathcal{U} + \mathcal{F})$, see section 5.

Using the prime factorization theorem it is easy to associate each of the non-trivial discriminants appearing in the factorization to certain type of singularities, at least for generic kinematics at one-loop where contracting edges of the graph G is the equivalent to going to faces of $\mathrm{Newt}(\mathcal{G})$, as also discussed in [48]:

- $\Delta_A(\mathcal{G})$ is the type-II singularity for the full graph.
- $\Delta_{A\cap x_i=0}(\mathcal{G}|_{x_i=0})$ is the type-II singularity for the sub-graph with edge i contracted.
- $\Delta_{A\cap\mathrm{Newt}(\mathcal{F})}(\mathcal{F})$ is the type-I singularity for the full graph (i.e. the leading Landau singularity).
- $\Delta_{A\cap\mathrm{Newt}(\mathcal{F})\cap x_i=0}(\mathcal{F}|_{x_i=0})$ is the type-I singularity for the sub-graph with edge i contracted.
- $\Delta_{A\cap\Gamma}(\mathcal{G}|_\Gamma)$ with Γ having vertices both in $\mathrm{Supp}(\mathcal{U})$ and $\mathrm{Supp}(\mathcal{F})$ are mixed singularities.

Multiple edges can be contracted to get singularities for even smaller sub-graphs. Subtleties with these identifications can appear for specific kinematic configurations, as we will illustrate in subsection 4.3 in the concrete example of the box with three offshell external and all massless internal legs. Nevertheless, in subsection 3.4 we will also show that the principal A-determinant of a non-generic graph may be obtained as a limit of that of a generic graph, such that subtleties of this sort ultimately do not matter.

One of the main themes of this paper is to show how the principal A-determinant can be used to determine symbol letters. The argument for why this holds follows from the fact that every GKZ-hypergeometric system can be written as a system of first order differential equations, in this context this system is called the *Pfaffian system* and can be calculated using Gröbner basis methods [67]. The coefficients of this system depend rationally on the kinematic variables but polynomially on the parameters in the β-vector, and hence also on the dimensional regulator ϵ. The singular locus of the Pfaffian system is the product of its denominators, which may a priori be larger than the principal A-determinant. However if it is possible to find a transformation that brings it into an ϵ-factorized form (1.1), then the singular locus of the Pfaffian system coincides with the principal A-determinant. As shown in [73, 74], this is because the monodromy group has been normalized. Especially in the case when the denominators of the canonical differential equation factorize into linear factors, these factors correspond to the symbol letters and are also the factors of the principal A-determinant.

For our purposes the principal A-determinant is important since it describes the singularities of a GKZ system $H_\beta(A)$, but before concluding this section let us also mention its relation to the triangulations of the polytope $\mathrm{conv}(A) = \mathrm{Newt}(f)$ and the Chow form of the toric variety X_A. The relation between these three objects manifests as the following three polytopes coinciding

$$\mathrm{Newt}(E_A(f)) \simeq \Sigma(A) \simeq \mathrm{Ch}(X_A). \tag{2.21}$$

Here $\Sigma(A)$ denotes the *secondary polytope* of A, that is, the polytope that encodes the regular subdivisions of A, and whose vertices particularly correspond to the regular triangulations of A. Two vertices of $\Sigma(A)$ are connected by an edge if and only if the two triangulations are related by a modification along a circuit in A. The similarity between $\Sigma(A)$ and the exchange graph (more precisely, the cluster polytope) of a *cluster algebra* [75] is too striking to ignore. Specifically, if $A \subset \mathbb{R}^2$ is the set of vertices of a convex n-gon, then the secondary polytope $\Sigma(A)$ is the $n-$th associahedron, which is indeed isomorphic to the cluster polytope of the A_{n-3} cluster algebra. Since $\text{Newt}(E_A) \simeq \Sigma(A)$, our approach for extracting symbol alphabets from the principal A-determinant $E_A(\mathcal{G})$ offers promise for providing a first-principle derivation and extension of the intriguing cluster-algebraic structures observed in a wealth of different Feynman integrals [76–78], following similar observations in the context of scattering amplitudes in $\mathcal{N} = 4$ super Yang-Mills theory [79, 80], see also the recent review [81].

Finally, the third polytope in eq. (2.21), $\text{Ch}(X_A)$, is the Chow polytope. This is the weight polytope of the Chow form R_{X_A}, which describes all the $(n-k-1)-$dimensional projective subspaces in $\mathbb{P}^{n-1}$ that intersect X_A. Here X_A is a toric variety of dimension $k-1$ and degree d. Let $\mathcal{B} = \bigoplus \mathcal{B}_m$ be the homogeneous coordinate ring of $\mathbf{Gr}(n-k, n)$, then $R_{X_A} \in \mathcal{B}_d$. Again this seems to point towards cluster algebras since the homogeneous coordinate ring of a Grassmanian comes with a natural cluster algebra structure [82].

3 One-loop principal A-determinants and symbol letters

The goal of this section is to present a formula to compute the symbol alphabet of one-loop Feynman graphs from their principal A-determinant. At this loop order the relevant principal A-determinant is in turn computed via determinant calculations as described in subsection 3.1 below. The resulting formulas for the symbol letters of generic Feynman integrals, where all masses and momenta squared are nonzero and different from each other, are then given in subsection 3.2. These formulas are then verified by directly constructing the corresponding canonical differential equations in subsection 3.3, and by comparing with earlier results in the literature, whenever available. Finally, in subsection 3.4 we provide evidence that the principal A-determinant and symbol alphabets of non-generic graphs may be obtained from the generic ones by a limiting process.

3.1 Matrix representation of one-loop principal A-determinants

Let us start by further specializing the mostly general discussion of section 2.2 to one-loop graphs as shown and labeled in figure 1. In this case the number of external legs coincides with the number of internal legs and with the number of vertices, and for simplicity from this point onwards we will denote this number with

$$n = |E| = |V| \,. \tag{3.1}$$

For one-loop graphs $\mathcal{U}$ has degree one and $\mathcal{F}$ has degree two, so the homogenized Lee-Pomeransky polynomial $\mathcal{G}_h = \mathcal{U}x_0 + \mathcal{F}$ has degree two. For degree two polynomials

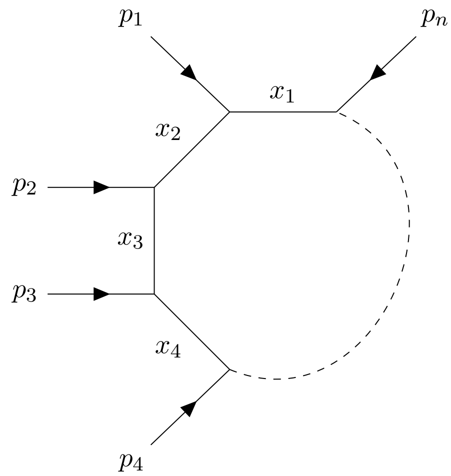

Figure 1. Generic one-loop Feynman diagram with n external legs.

the discriminant and hence also the principal A-determinant calculation, which we will consider in this section, can be made very simple.

Let f be a homogeneous polynomial of degree two. The homogeneity means that the vanishing of all partial derivatives implies the vanishing of f, i.e.

$$\frac{\partial f}{\partial x_1} = \cdots = \frac{\partial f}{\partial x_k} = 0 \Longrightarrow f = 0. \tag{3.2}$$

And since f has degree two, all partial derivatives are linear homogeneous functions. The definition of ∇_0 now reduces to requiring that the vanishing locus of the partial derivatives be non-empty with x in the torus $(\mathbb{C}^*)^k$.

Writing the zero set of the partial derivatives as

$$\begin{pmatrix} \frac{\partial f}{\partial x_1} \\ \vdots \\ \frac{\partial f}{\partial x_k} \end{pmatrix} =: \mathscr{J}(f) \begin{pmatrix} x_1 \\ \vdots \\ x_k \end{pmatrix} = \mathbf{0}, \tag{3.3}$$

where $\mathscr{J}(f)$ is the coefficient matrix associated to the Jacobian of f, we get that

$$\overline{\mathbf{V}\left(\frac{\partial f}{\partial x_1}, \ldots, \frac{\partial f}{\partial x_k}\right) \neq \emptyset \text{ for } x \in \mathbb{C}^k \setminus \{\mathbf{0}\}} \iff \det(\mathscr{J}(f)) = 0. \tag{3.4}$$

Note that this is an equivalence for x in the punctured affine space $\mathbb{C}^k \setminus \{\mathbf{0}\}$ and not for x in the torus $(\mathbb{C}^*)^k$, we will return to this important point shortly.

For the Lee-Pomeransky polynomial $\mathcal{G}$ the coefficient matrix $\mathscr{J}(\mathcal{G})$ coincides with the *modified Cayley matrix* as defined by Melrose in [83]. To begin with, we define the *Cayley matrix* Y to be the $n \times n$-matrix with elements

$$Y_{ii} = 2m_i^2\,, \qquad Y_{ij} = m_i^2 + m_j^2 - p(F_{ij})^2 \tag{3.5}$$

where

$$p(F_{ij})^2 = (p_i + \ldots + p_{j-1})^2 \equiv s_{ij-1} = s_{ji-1}\,, \tag{3.6}$$

is the total momenta flowing through the two-forest F_{ij} obtained from G by removing edges i and j. We have also expressed the latter in terms of the Mandelstam invariants in the labelling of figure 1, where cyclicity of the indices modulo n is implied. For concreteness, in what follows we will choose conventions where these $n(n-1)/2$ cyclic Mandelstam invariants do not contain p_n. In terms of the coefficient matrix of the Jacobian, $Y = \mathscr{J}(\mathcal{F})$. From the Cayley matrix the *modified Cayley matrix* $\mathcal{Y}$ is simply obtained by decorating it with a row and column in the following manner:[4]

$$\mathcal{Y} := \begin{pmatrix} 0 & 1 & 1 & \cdots & 1 \\ 1 & Y_{11} & Y_{12} & \cdots & Y_{1n} \\ 1 & Y_{12} & Y_{22} & \cdots & Y_{2n} \\ \vdots & \vdots & \vdots & & \vdots \\ 1 & Y_{1n} & Y_{2n} & \cdots & Y_{nn} \end{pmatrix} . \tag{3.7}$$

The determinant of both the Cayley and modified Cayley matrix can be understood as *Gram determinants*, defined in general as

$$G(k_1, \ldots, k_m; l_1, \ldots, l_m) \equiv \det(k_i \cdot l_j) = \det \begin{pmatrix} k_1 \cdot l_1 & k_1 \cdot l_2 & \cdots & k_1 \cdot l_m \\ k_1 \cdot l_2 & k_2 \cdot l_2 & \cdots & k_2 \cdot l_m \\ \vdots & \vdots & & \vdots \\ k_1 \cdot l_m & k_2 \cdot l_m & \cdots & k_m \cdot l_m \end{pmatrix} , \tag{3.8}$$

and further abbreviated as

$$G(k_1, \ldots, k_m) \equiv G(k_1, \ldots, k_m; k_1, \ldots, k_m) , \tag{3.9}$$

when the two sets of momenta coincide. The determinant of the Cayley matrix is up to a proportionality factor the Gram determinant of the internal momenta restricted to be on their mass shell $q_i^2 = m_i^2$,

$$\det(Y) = (-2)^n G(q_1, \ldots q_n) . \tag{3.10}$$

Similarly, the determinant of the modified Cayley matrix is proportional to the Gram determinant of any $n-1$ of the external momenta, for example

$$\det(\mathcal{Y}) = -2^{n-1} G(p_1, \ldots, p_{n-1}) , \tag{3.11}$$

namely it is independent of the internal masses. In what follows, we will call this particular determinant the Gram determinant of a Feynman graph/integral, and use the term general Gram determinant otherwise.

The relation between $\det(Y)$, $\det(\mathcal{Y})$ and general $m \times m$ Gram determinants is helpful since the latter can be written as certain $(m+2) \times (m+2)$ *Cayley-Menger* determinants

[4]The modified Cayley matrix also appears naturally in the embedding space formalism [84] as applied to one-loop integrals, see for example [85]. The compactification of the integration domain, which can be easily carried out in this formalism, also treats type I and II Landau singularities of one-loop integrals on the same footing.

according to

$$G(k_1,\ldots,k_m)=\frac{(-1)^{m+1}}{2^m}\det\begin{pmatrix}0 & 1 & 1 & 1 & \cdots & 1 & 1\\ 1 & 0 & (k_1-k_2)^2 & (k_1-k_3)^2 & \cdots & (k_1-k_m)^2 & k_1^2\\ 1 & (k_1-k_2)^2 & 0 & (k_2-k_3)^2 & \cdots & (k_2-k_m)^2 & k_2^2\\ 1 & (k_1-k_3)^2 & (k_2-k_3)^2 & 0 & \cdots & (k_3-k_m)^2 & k_3^2\\ \vdots & \vdots & \vdots & \vdots & & \vdots & \vdots\\ 1 & (k_1-k_m)^2 & (k_2-k_m)^2 & (k_3-k_m)^2 & \cdots & 0 & k_m^2\\ 1 & k_1^2 & k_2^2 & k_3^2 & \cdots & k_m^2 & 0\end{pmatrix}. \tag{3.12}$$

Cayley-Menger determinants have the important property that they are irreducible for $n \geq 3$, see [86]. This means that for a homogeneous polynomial f of degree two a sufficient condition for

$$\Delta_A(f)=\det(\mathscr{J}(f)) \tag{3.13}$$

is that $\det(\mathscr{J}(f))$ can be understood as a Cayley-Menger determinant with $n \geq 3$. The irreducibility of $\det(\mathscr{J})$ removes the need for the distinction between the algebraic torus and punctured affine space meaning that the determinant is equal to the discriminant; that is in this case we can replace $x \in \mathbb{C}^k \setminus \{\mathbf{0}\}$ with $x \in (\mathbb{C}^*)^k$ in (3.4). An example illustrating how this identification can fail when the determinant is reducible is given in Example 4.2.

For massive one-loop graphs with generic kinematics the result in [86] means that the Cayley determinant for $n \geq 3$ and the Gram determinant for $n \geq 4$ are all irreducible and thus coincide with the expected discriminant. For the few cases not covered by the theorem, explicit calculations confirm that the discriminant and determinant coincide.

We will not only be interested in the determinant of the modified Cayley matrix but also its minors. Let $1 \leq k < n+1$ be an integer, then the general minor of order $n+1-k$ is denoted as

$$\mathcal{Y}\begin{bmatrix} i_1 & i_2 & \cdots & i_k\\ j_1 & j_2 & \cdots & j_k\end{bmatrix}, \qquad 1 \leq i_1 < i_2 < \cdots i_k \leq n,\ 1 \leq j_1 < j_2 < \cdots j_k \leq n \tag{3.14}$$

where $I=\{i_1,i_2,\cdots,i_k\}$ and $J=\{j_1,j_2,\ldots,j_k\}$ denotes the rows resp, columns removed from $\mathcal{Y}$. If both I and J are empty we recover the full determinant $\det(\mathcal{Y})=\mathcal{Y}\begin{bmatrix}\cdot\\ \cdot\end{bmatrix}$. It will sometimes also be convenient to introduce the complementary notation where we index the rows and columns kept in the minor, this is signified by a parenthesis $(\cdot)$ instead of square brackets $[\cdot]$. Let $\mathcal{E}=\{1,2,\ldots,n+1\}$, then

$$\mathcal{Y}\begin{bmatrix} I\\ J\end{bmatrix}=\mathcal{Y}\begin{pmatrix}\mathcal{E}\setminus I\\ \mathcal{E}\setminus J\end{pmatrix}.$$

The identification between discriminants and subgraphs in section 2.2 can now be carried out for determinants as well:

- $\Delta_A(\mathcal{G})=\det(\mathcal{Y})$,
- $\Delta_{A\cap x_i=0}(\mathcal{G})=\mathcal{Y}\begin{bmatrix} i+1\\ i+1\end{bmatrix}$,

- $\Delta_{A\cap \mathrm{Newt}(\mathcal{F})}(\mathcal{F}) = \det(Y) = \mathcal{Y}\begin{bmatrix}1\\1\end{bmatrix}$,
- $\Delta_{A\cap \mathrm{Newt}(\mathcal{F})\cap x_i=0} = Y\begin{bmatrix}i\\i\end{bmatrix} = \mathcal{Y}\begin{bmatrix}1 & i+1\\1 & i+1\end{bmatrix}$,

For one-loop graphs with massive and generic kinematics this means that all non-trivial discriminants can be expressed as determinants, making the calculation much easier. Especially, the reduced principal A-determinant now has a simple expression as a product of minors of $\mathcal{Y}$:

$$\widetilde{E_A}(\mathcal{G}) = \mathcal{Y}\begin{bmatrix}\cdot\\\cdot\end{bmatrix}\prod_{i=1}^{n+1}\mathcal{Y}\begin{bmatrix}i\\i\end{bmatrix}\cdots\prod_{i_{n-1}>\ldots>i_1=1}^{n+1}\mathcal{Y}\begin{bmatrix}i_1\ldots i_{n-1}\\i_1\ldots i_{n-1}\end{bmatrix}\prod_{i=2}^{n+1}\mathcal{Y}_{ii}\,. \tag{3.15}$$

In other words, $\widetilde{E_A}$ is equal to the product of all diagonal k-dimensional minors of $\mathcal{Y}$ with $k = 1,\ldots,n+1$ (the largest one corresponding to the determinant of the entire matrix), except for the $\mathcal{Y}_{11}$ element, which is zero. Given that minors of $\mathcal{Y}$ where the first row and column has (not) been removed correspond to the Cayley (Gram) determinant of the Feynman graph, or its subgraphs where certain edges have been contracted, the above formula also has the following interpretation: The principal A-determinant of a generic 1-loop n-point graph is the product of the Cayley and Gram determinants of the graph and all of its subgraphs. From these considerations, we may also easily derive that the total number of factors in eq. (3.15), i.e. the total number of kinematic-dependent Cayley and Gram determinants of the Feynman graph and all of its subgraphs, is

$$2^{n+1} - n - 2\,, \tag{3.16}$$

namely 1, 4, 11, 26, 57 and 120 factors for $n = 1,\ldots,6$. In this counting we exclude not only the element $\mathcal{Y}_{11} = 0$ but also all two-dimensional minors including the first row and column, which always yield -1.

3.2 One-loop symbol alphabets

In this subsection we will show how to calculate the symbol alphabet of a one-loop graph by appropriately re-factorizing its principal A-determinant (3.15). Note that we are going to distinguish the two cases for the sum of loop integration dimension and number of external legs $D_0 + n$ being odd, respectively, even.

Jacobi identities. As has been seen in the example presented in the introduction, individual factors in the natural factorization of the principal A-determinant gives us all the rational letters for a Feynman graph. It is well known, however, that letters containing square roots quickly become unavoidable, even at one-loop. In order to construct the letters containing square roots we will use Jacobi determinant identities to re-factorize the factors of the principal A-determinant (3.15), namely of minors of the modified Cayley matrix $\mathcal{Y}$, in pairs. Jacobi determinant identities have played an important role in many areas of mathematics and physics, including the computation of volumes of spherical simplices [87], as well as the solution theory of integrable systems [88].

There will be two types of identities that we need; identities containing the full determinant $\mathcal{Y}\left[\begin{smallmatrix}\cdot\\\cdot\end{smallmatrix}\right]$ (of a given graph and of its subgraphs) and those containing the determinant of the Cayley sub-matrix $\mathcal{Y}\left[\begin{smallmatrix}1\\1\end{smallmatrix}\right]$. The identities containing the full determinant are

$$\begin{aligned}
\mathcal{Y}\begin{bmatrix}\cdot\\\cdot\end{bmatrix}\mathcal{Y}\begin{bmatrix}1&i\\1&i\end{bmatrix} &= \mathcal{Y}\begin{bmatrix}i\\i\end{bmatrix}\mathcal{Y}\begin{bmatrix}1\\1\end{bmatrix} - \mathcal{Y}\begin{bmatrix}i\\1\end{bmatrix}^2 , \\
\mathcal{Y}\begin{bmatrix}\cdot\\\cdot\end{bmatrix}\mathcal{Y}\begin{bmatrix}i&j\\i&j\end{bmatrix} &= \mathcal{Y}\begin{bmatrix}i\\i\end{bmatrix}\mathcal{Y}\begin{bmatrix}j\\j\end{bmatrix} - \mathcal{Y}\begin{bmatrix}i\\j\end{bmatrix}^2 , \quad i \geq 2 ,
\end{aligned} \tag{3.17}$$

where in the first line we have simply separated out the $i = 1$ case of the second line for later convenience. As we will get back to shortly, these identities are relevant in the case when $D_0 + n$ is odd as it is the modified Cayley determinant that contributes to the leading singularity, see also eq. (3.31) and the discussion around it in the next section.

The identities containing the determinant of the Cayley submatrix are

$$\begin{aligned}
\mathcal{Y}\begin{bmatrix}\cdot\\\cdot\end{bmatrix}\mathcal{Y}\begin{bmatrix}1&i\\1&i\end{bmatrix} &= \mathcal{Y}\begin{bmatrix}i\\i\end{bmatrix}\mathcal{Y}\begin{bmatrix}1\\1\end{bmatrix} - \mathcal{Y}\begin{bmatrix}i\\1\end{bmatrix}^2 , \\
\mathcal{Y}\begin{bmatrix}1\\1\end{bmatrix}\mathcal{Y}\begin{bmatrix}1&i&j\\1&i&j\end{bmatrix} &= \mathcal{Y}\begin{bmatrix}1&j\\1&j\end{bmatrix}\mathcal{Y}\begin{bmatrix}1&i\\1&i\end{bmatrix} - \mathcal{Y}\begin{bmatrix}1&j\\1&i\end{bmatrix}^2 ,
\end{aligned} \tag{3.18}$$

and these will in turn be relevant when $D_0 + n$ is even, as it is the Cayley determinant that yields the leading singularity. Note that the first identity in each case is the same.

Symbol letters. We now introduce a procedure for obtaining not only the rational but also the square-root letters of one-loop Feynman integrals as follows: We assume that the latter are produced by applying Jacobi determinant identities of the form

$$p \cdot q = f^2 - g = (f - \sqrt{g})(f + \sqrt{g}) , \tag{3.19}$$

where

1. p and q are both factors of the principal A-determinant, i.e. rational letters given by symmetric minors of the modified Cayley matrix.

2. The square-root letters $f \pm \sqrt{g}$ thus obtained contain the leading singularity of the Feynman integral considered in their second term.

This procedure is motivated by the interpretation of one-loop integrals as volumes of spherical simplices [89], and by the role Jacobi identities have played in their computation. Particularly the second assumption adopts a pattern that has been observed not only in one-, but also many two-loop computations. In the next subsection, we will validate the correctness of these assumptions by explicitly constructing the canonical differential equations of one-loop integrals, as well as compare with the existing results in the literature. While the precise identities and assumptions may differ beyond one loop, we expect that a similar re-factorization methodology should still apply.

Given that the rational letters at the very left of eq. (3.19) are already contained in the rational alphabet, the genuinely new square-root letter that will arise from the procedure we have described will be the ratio of the factors at the very right of the same equation,

$$\frac{f-\sqrt{g}}{f+\sqrt{g}}\,. \tag{3.20}$$

Furthermore, the subset of Jacobi identities chosen by the assumptions we have stated above will be precisely eqs. (3.17) and (3.18) for D_0+n odd and even, respectively. The first and second line of these equations then yields n letters of the first type,

$$W_{1,\dots,(i-1),\dots,n}=\begin{cases}\dfrac{\mathcal{Y}\begin{bmatrix}i\\1\end{bmatrix}-\sqrt{-\mathcal{Y}\begin{bmatrix}\cdot\\\cdot\end{bmatrix}\mathcal{Y}\begin{bmatrix}1\ i\\1\ i\end{bmatrix}}}{\mathcal{Y}\begin{bmatrix}i\\1\end{bmatrix}+\sqrt{-\mathcal{Y}\begin{bmatrix}\cdot\\\cdot\end{bmatrix}\mathcal{Y}\begin{bmatrix}1\ i\\1\ i\end{bmatrix}}}, & D_0+n \text{ odd},\\[4ex] \dfrac{\mathcal{Y}\begin{bmatrix}i\\1\end{bmatrix}-\sqrt{\mathcal{Y}\begin{bmatrix}i\\i\end{bmatrix}\mathcal{Y}\begin{bmatrix}1\\1\end{bmatrix}}}{\mathcal{Y}\begin{bmatrix}i\\1\end{bmatrix}+\sqrt{\mathcal{Y}\begin{bmatrix}i\\i\end{bmatrix}\mathcal{Y}\begin{bmatrix}1\\1\end{bmatrix}}}, & D_0+n \text{ even}.\end{cases} \tag{3.21}$$

and $n(n-1)/2$ letters of the second type,

$$W_{1,\dots,(i-1),\dots,(j-1),\dots,n}=\begin{cases}\dfrac{\mathcal{Y}\begin{bmatrix}i\\j\end{bmatrix}-\sqrt{-\mathcal{Y}\begin{bmatrix}\cdot\\\cdot\end{bmatrix}\mathcal{Y}\begin{bmatrix}i\ j\\i\ j\end{bmatrix}}}{\mathcal{Y}\begin{bmatrix}i\\j\end{bmatrix}+\sqrt{-\mathcal{Y}\begin{bmatrix}\cdot\\\cdot\end{bmatrix}\mathcal{Y}\begin{bmatrix}i\ j\\i\ j\end{bmatrix}}}, & D_0+n \text{ odd},\\[4ex] \dfrac{\mathcal{Y}\begin{bmatrix}1\ j\\1\ i\end{bmatrix}-\sqrt{-\mathcal{Y}\begin{bmatrix}1\\1\end{bmatrix}\mathcal{Y}\begin{bmatrix}1\ i\ j\\1\ i\ j\end{bmatrix}}}{\mathcal{Y}\begin{bmatrix}1\ j\\1\ i\end{bmatrix}+\sqrt{-\mathcal{Y}\begin{bmatrix}1\\1\end{bmatrix}\mathcal{Y}\begin{bmatrix}1\ i\ j\\1\ i\ j\end{bmatrix}}}, & D_0+n \text{ even},\end{cases} \tag{3.22}$$

respectively, where we remind the reader that $\mathcal{Y}$ denotes the modified Cayley matrix (3.7) of the n-point one-loop integral, and that minors of the latter, obtained by removing some of its rows and columns, have been defined in eq. (3.14).

Finally, the full determinant and the minor $\mathcal{Y}\begin{bmatrix}1\\1\end{bmatrix}$ should also in principle appear as rational letters of the n-point graph. However, as we will come back to in the next subsection, these in fact always come as a rational combination,

$$W_{1,2,\ldots,n} = \frac{\mathcal{Y}\begin{bmatrix}\cdot\\ \cdot\end{bmatrix}}{\mathcal{Y}\begin{bmatrix}1\\ 1\end{bmatrix}}\,. \tag{3.23}$$

Remark 3.1. It is interesting to note that this rational function has an intrinsic meaning in the GKZ approach to Feynman integrals: It is the value the Lee-Pomeransky polynomial attains on its critical point. If we solve $\partial\mathcal{G}/\partial x_i = 0$ for all $i = 1, \ldots, n$ and evaluate $\mathcal{G}$ at this unique point we get this fraction up to a numerical factor. This is a special case of a general property of the principal A-determinant [65, Theorem 1.17, section 10].

So far, we have obtained $1 + n(n+1)/2$ letters of the n-point graph for general n. To obtain the remaining letters, we apply the above expressions to each of the subgraphs of the n-point graph, obtained by contracting some of its edges. That is, we replace $\mathcal{Y}$ with the modified Cayley matrix of the subgraph in question on the right-hand side of eqs. (3.21)–(3.23), and we only keep the indices labeling its uncontracted edges on the left-hand side.[5] The correct $\mathcal{Y}$-matrix for a subgraph is obtained from the original one by removing the rows and columns corresponding to the contracted edges. This process terminates once the letters for the tadpoles have been calculated.

In the ancillary `Mathematica` file as Supplementary Material attached to our article, we provide code for generating the complete n-point alphabet in principle for any n. As a benchmark, the runtime for $n = 6$ is at the order of a minute on a laptop computer.

Remark 3.2. In the $n = 1$ case, or equivalently the tadpole graph, the modified Cayley matrix is too small to allow for any Jacobi identities, and hence only the rational letter of type (3.23) is present. Similarly, for $n = 2$ or the bubble graph there are no letters of the type $W_{(i),(j)}$.

Remark 3.3. For $n = 3$ or the triangle graph and even loop integration dimension D_0, one would expect $\binom{3}{2} = 3$ letters of the type $W_{(i),(j),k}$:

$$\frac{a-b+c-\sqrt{\lambda}}{a-b+c+\sqrt{\lambda}}, \qquad \frac{a+b-c-\sqrt{\lambda}}{a+b-c+\sqrt{\lambda}}, \qquad \frac{a-b-c-\sqrt{\lambda}}{a-b-c+\sqrt{\lambda}} \tag{3.24}$$

where $\lambda := \lambda(a,b,c)$ is the fully symmetric Källén function ,

$$\lambda(a,b,c) = a^2 + b^2 + c^2 - 2ab - 2bc - 2ac\,. \tag{3.25}$$

However, these have the multiplicative relation

$$\frac{a-b+c-\sqrt{\lambda}}{a-b+c+\sqrt{\lambda}} \cdot \frac{a+b-c-\sqrt{\lambda}}{a+b-c+\sqrt{\lambda}} = \frac{a-b-c-\sqrt{\lambda}}{a-b-c+\sqrt{\lambda}}\,. \tag{3.26}$$

[5] Our labeling conventions for the letters also reveal dihedral relations among them, e.g. $W_{1,2}$ and $W_{2,3}$ are related by a cyclic shift. Note however that due to our choice of conventions, these relations may come with additional minus signs or inversions.

Hence one need only include two out of the three so as to obtain a multiplicatively independent set, and here and in the attached ancillary file we will in particular choose them to be $W_{(i),(j),k}$ and $W_{i,(j),(k)}$. Note that the special cases of letters we have discussed pertain also to tadpole, bubble (and for D_0 even triangle) subgraphs of $n \geq 4$ graphs, hence the use of generic letter indices.

From the above formulas, we can also obtain a closed formula for the total number of letters of an n-point graph: the latter has $\binom{n}{m}$ m-point subgraphs, $m = 1, \dots n$, and each of them yields

$$\frac{m(m+1)}{2} + \delta_{m\geq 4} + \delta_{m,3}\delta_{D_0,\text{odd}}\,, \tag{3.27}$$

letters, where δ denotes the Kronecker delta function, with some abuse of notation to describe the cases where it equals 1 when its index is greater than a given integer value, or odd (and zero otherwise). Therefore in total the number of letters is

$$|W| = \begin{cases} 2^{n-3}\left(n^2+3n+8\right) - \frac{1}{6}\left(n^3+5n+6\right)\,, & D_0 \text{ even,} \\ \\ 2^{n-3}\left(n^2+3n+8\right) - \frac{1}{2}\left(n^2+n+2\right)\,, & D_0 \text{ odd,}\,, \end{cases} \tag{3.28}$$

that is, $|W| = 1, 5, 18, 57, 166, 454, 1184$ and $|W| = 1, 5, 19, 61, 176, 474, 1219$ for $n = 1, \dots, 7$ when D_0 even and odd, respectively. These counts correspond to the total number of multiplicatively independent letters of the generic n-point 1-loop integral shown in figure 1, provided that $n \leq d+1$, e.g. $n \leq 5$ when the external momenta live in $d = 4$ dimensions. This restriction ensures that all Mandelstam invariants appearing the letters may be treated as independent variables, given that no more than d vectors can be linearly independent in d dimensions.

For $n > d+1$, after choosing the first d momenta of the n-point integral as our basis in the space of external kinematics, expressing the remaining momenta in terms of them, and dotting these linear relations with the basis vectors, we may express them as polynomial relations between the Mandelstam invariants,

$$G(p_1, \dots, p_d, p_i) = 0\,, \quad i = d+1, \dots, n-1\,, \tag{3.29}$$

where G is the Gram determinant, defined in eq. (3.8). In subsection 3.4 we will provide evidence that the principal A-determinant and hence also the alphabet of any n-point 1-loop graph, obeying additional restrictions such as (3.29), or such that any of the masses and Mandelstam invariants become equal to each other or vanish, may be obtained as limits of the generic cases, eqs. (3.15) and (3.21)–(3.23), respectively. In these cases the limits will introduce additional multiplicative dependence among the letters, hence our generic formulas will provide a spanning set for the alphabet, and the counts (3.29) will correspond to upper bounds. As we will also see in the examples presented in section 4, a basis within this spanning set may be found immediately in any kinematic parametrization that rationalizes all resulting letters, or e.g. with the help of `SymBuild` [90] even in the presence of square roots.

3.3 Verification through differential equations and comparison with literature

In this section we show how the letters actually appear in the canonical differential equations. For our basis $\vec{g}$ of pure master integrals as defined in eq. (1.1), we use the fact that any integral in $D-2$ dimensions of loop momenta may be expressed as a linear combination of integrals in D dimensions and vice-versa, with the help of dimensional recurrence relations [91, 92]. As these relations are merely a change of basis, this implies that different cases of spaces of master integrals are simply distinguished by (the integer part of) D being even or odd, and that within each case we may choose our basis $\vec{g}$ to consist of integrals with different D. To be more concrete, we need to introduce some further notation: We write the integrals of (2.6) in $D = D_0 - 2\epsilon$ dimensions and for $a_i = 1$ as $\mathcal{I}_E^{(D_0)}$, where the set E indicates the edges of the corresponding graph. E.g. $\mathcal{I}_{134}^{(2)}$ denotes the triangle integral in $D = 2-2\epsilon$ dimensions that is obtained when the second propagator of the box integral $\mathcal{I}_{1234}^{(2)}$ is removed.

We then take the basis $\vec{g}$ to consist of the following canonical integrals:

$$\mathcal{J}_{i_1\ldots i_k} = \begin{cases} \dfrac{\epsilon^{\lfloor \frac{k}{2} \rfloor} \mathcal{I}^{(k)}_{i_1\ldots i_k}}{j_{i_1\ldots i_k}} & \text{for } k+D_0 \text{ even,} \\[2ex] \dfrac{\epsilon^{\lfloor \frac{k+1}{2} \rfloor} \mathcal{I}^{(k+1)}_{i_1\ldots i_k}}{j_{i_1\ldots i_k}} & \text{for } k+D_0 \text{ odd}\,, \end{cases} \tag{3.30}$$

where the leading singularities are

$$j_{i_1\cdots i_k} = \begin{cases} 2^{-\frac{k}{2}+1}\left[(-1)^{\lfloor \frac{k}{2}\rfloor}\mathcal{Y}\begin{pmatrix} i_1+1 & i_2+1 & \cdots & i_k+1 \\ i_1+1 & i_2+1 & \cdots & i_k+1 \end{pmatrix}\right]^{-1/2}, & \text{for } k+D_0 \text{ even}\,, \\ 2^{-\frac{k+1}{2}+1}\left[(-1)^{\lfloor \frac{k+1}{2}\rfloor}\mathcal{Y}\begin{pmatrix} 1 & i_1+1 & i_2+1 & \cdots & i_k+1 \\ 1 & i_1+1 & i_2+1 & \cdots & i_k+1 \end{pmatrix}\right]^{-1/2}, & \text{for } k+D_0 \text{ odd}\,. \end{cases} \tag{3.31}$$

These integrals have been observed to be pure integrals [93, 94] for D_0 even, see also [95–97] for earlier results with $\epsilon = 0$. Note that both the overall sign of the above equation, as well as the choice of branch for the square root, are a matter of choice of convention. As is discussed in e.g. [97], the former stems from the fact that as multidimensional residues, leading singularities are intrinsically dependent on the orientation of the integration contour; whereas the latter stems from the fact that while scalar Feynman integrals are positive definite in the Euclidean region, their pure counterparts need not be. In eq. (3.31), we have fixed this freedom, together with the overall kinematic independent normalization that we are also free to choose, such that the differential equations take a convenient form. This choice of pure basis also specifies how square roots of products of modified Cayley (sub)determinants should be replaced by the product of the square roots of the (sub)determinants in question in our basis of letters (3.21)–(3.23).

By explicit computation up to $n = 10$, we observe that the differential equations for the canonical integrals are then as follows: for even $n + D_0$ we have[6]

$$\begin{aligned} d\mathcal{J}_{1\ldots n} =& \epsilon \, d\log W_{1\ldots n} \, \mathcal{J}_{1\ldots n} \\ &+ \epsilon \sum_{1\leq i\leq n} (-1)^{i+\lfloor \frac{n}{2} \rfloor} d\log W_{1\ldots(i)\ldots n} \, \mathcal{J}_{1\ldots\widehat{i}\ldots n} \\ &+ \epsilon \sum_{1\leq i<j\leq n} (-1)^{i+j+\lfloor \frac{n}{2} \rfloor} d\log W_{1\ldots(i)\ldots(j)\ldots n} \, \mathcal{J}_{1\ldots\widehat{i}\ldots\widehat{j}\ldots n}, \end{aligned} \tag{3.32}$$

and for odd $n + D_0$,

$$\begin{aligned} d\mathcal{J}_{1\ldots n} =& \epsilon \, d\log W_{1\ldots n} \, \mathcal{J}_{1\ldots n} \\ &+ \epsilon \sum_{1\leq i\leq n} (-1)^{i+\lfloor \frac{n+1}{2} \rfloor} d\log W_{1\ldots(i)\ldots n} \, \mathcal{J}_{1\ldots\widehat{i}\ldots n} \\ &+ \epsilon \sum_{1\leq i<j\leq n} (-1)^{i+j+\lfloor \frac{n+1}{2} \rfloor} d\log W_{1\ldots(i)\ldots(j)\ldots n} \, \mathcal{J}_{1\ldots\widehat{i}\ldots\widehat{j}\ldots n}, \end{aligned} \tag{3.33}$$

where the hat indicates that the index is omitted, and $\lfloor x \rfloor$ is the floor function. Note that we chose to present our formulas in such a way that the latter is irrelevant for to case of even D_0. The matrix $\widetilde{M}$ encoding the above differential equations according to eq. (1.2), together with our choice of basis integrals (3.30) and associated leading singularities (3.31), may also be easily generated in principle for any n with the code provided in the attached ancillary file.

As mentioned in the introduction, the knowledge of the letters allows us to derive the differential equations without the need of any analytic computation. The formulas in (3.32) and (3.33) are based on following this procedure up to $n = 10$.[7] This confirms our prediction for the alphabet of one-loop integrals up to this number of external legs. The IBP reduction was done with a combination of FIRE6 [10] and LiteRed [9] by choosing values in a finite field for the v_i.

For generic kinematics and masses, it is also easy to determine the leading boundary vector $\vec{g}^{(0)}$ in eq. (1.4): The integrals in (3.30) are normalized by powers of ϵ to be of uniform transcendental weight zero. However, it is easy to see that all integrals except $\mathcal{I}_1^{(2)}$ are finite in integer dimensions. Therefore, only the tadpoles have vanishing weight zero contribution.[8] In summary, we find with our normalization

$$\vec{g}^{(0)} = (\underbrace{1, \ldots, 1}_{n}, \underbrace{0, \ldots, 0}_{2^n-1-n})^T. \tag{3.34}$$

This in principle allows us to compute the symbol at any order in ϵ from eq. (1.4).

[6]If we are interested in $D = D_0 - 2\epsilon$, with D_0 being an odd integer, the case of even and odd n is exchanged compared to the even-dimensional case. This can easily be seen in Baikov representation [98] where the integrals on the maximal cut are roughly equal to $I \sim G^{(n-D)/2} C^{(D-1-n)/2}$, where G is the Gram determinant, and C is the Cayley determinant which is obtained from setting all integration variables to zero in the Baikov polynomial [99].

[7]In practice, to derive the differential equations, one needs to use dimensional recurrence relations to translate all integrals of different dimensions into a common dimension. We stress however, that this choice does not affect the result for the differential equations.

[8]We thank the referee for pointing this out.

Finally, let us compare our findings with earlier results in the literature. For D_0 even, explicit expressions for the canonical differential equations and symbol alphabets of finite n-point one-loop graphs were first derived in [93], based on the diagrammatic coaction [100]. The latter decomposes any one-loop Feynman integral into simpler building blocks, mirroring the coaction of the multiple polylogarithmic functions, that these integrals evaluate to, but conjecturally holds to all orders in the dimensional regularization parameter ϵ. In this decomposition also cut integrals appear, where some of the propagators have been placed on their mass shell, and very interestingly it was found that these are restricted to a small subset where all, or all but one, or all but two propagators have been cut.

Based on the Baikov representation of Feynman integrals, a similar analysis of canonical differential equations and symbol alphabets, also working out the divergent cases in more detail, was carried out in [94]. The later and original analyses agree on the form of the letters associated to the maximal cut, and in order to avoid redundant letters coming from individual determinant factors of the principal A-determinant, for our rational letters (3.23) we have chosen those ratios that coincide with them (up to immaterial constant normalization factors). For the square-root letters, we will compare with [94], as the apparent presence of up to five different square roots in some of the letters of [93] renders this comparison more complicated. In the former reference, and in the orientation where the uncut propagators are those with momenta (p_{n-1} and) p_n for the letters associated to the (next-to-)next-to-maximal cut, their building blocks are the following general Gram determinants as defined in eqs. (3.8)–(3.9),

$$\begin{aligned}
\mathcal{K}_n &\equiv G(p_1,\ldots,p_{n-1})\,, \quad \tilde{G}_n \equiv G(l,p_1\ldots,p_{n-1})\,,\\
\tilde{B}_n &\equiv G(l,p_1,\ldots,p_{n-2};p_{n-1},p_1,\ldots,p_{n-2})\,,\\
C_n &\equiv G(p_1,\ldots p_{n-2};p_1,\ldots,p_{n-3},p_{n-2}+p_{n-1})\,,\\
D_n &\equiv G(l,p_1,\ldots p_{n-2};l,p_1,\ldots p_{n-3},p_{n-2}+p_{n-1})\,,
\end{aligned} \tag{3.35}$$

where the loop momentum

$$\begin{aligned}
l^2 &= m_1^2\,,\\
l\cdot p_i &= \frac{m_{i+1}^2-p_i^2-m_i^2}{2}-\sum_{j=1}^{i-1}p_i\cdot p_j\,,
\end{aligned} \tag{3.36}$$

is evaluated as a function of the Baikov variables when the latter are set to zero. As a consequence of (3.11),

$$\mathcal{Y}\begin{bmatrix}\cdot\\ \cdot\end{bmatrix} = -2^{n-1}\mathcal{K}_n\,, \tag{3.37}$$

whereas we find that the remaining determinants in (3.36) are related to minors of our modified Cayley matrix $\mathcal{Y}$ as follows,

$$\begin{aligned}
\mathcal{Y}\begin{bmatrix}1\\ 1\end{bmatrix} &= \det(Y) = 2^n\tilde{G}_n\,, \qquad \mathcal{Y}\begin{bmatrix}1\\ n+1\end{bmatrix} = -(-2)^{n-1}\tilde{B}_n\,,\\
\mathcal{Y}\begin{bmatrix}n\\ n+1\end{bmatrix} &= -2^{n-2}\tilde{C}_n\,, \qquad\quad \mathcal{Y}\begin{bmatrix}1 & n\\ 1 & n+1\end{bmatrix} = 2^{n-1}\tilde{D}_n\,.
\end{aligned} \tag{3.38}$$

From these identifications, it follows straightforwardly that up to immaterial overall signs and inversions, for D_0 even the next-to-maximal and next-to-next-to-maximal cut letters in question correspond to our $W_{1,\ldots,n-1,\ldots,(n)}$ and $W_{1,\ldots n-2,(n-1),\ldots,(n)}$, respectively, and similarly the differential equations (3.32)–(3.33) agree with those of [93, 94]. To the best of our knowledge, the odd D_0 case has not appeared before. In any case, we find it pleasing that our formulas are expressed in terms of a single quantity associated to each one-loop graph, its modified Cayley matrix, making it easy to keep track of both its Landau singularities and contributions of subgraphs from different minors of the matrix.

3.4 Limits of principal A-determinants and alphabets

So far, we have only considered the generic one-loop n-point Feynman integrals shown in figure 1, where all m_i^2, p_j^2 are nonvanishing and different from each other. In this subsection, we will provide strong evidence that the principal A-determinant and symbol alphabet of any one-loop integral, i.e. also including configurations where different scales are equal to each other or set to zero, may be obtained as limits of the generic ones, eqs. (3.15) and (3.21)–(3.23), respectively.

To this end, we will first prove that the principal A-determinant $\widetilde{E_A}$ has a well-defined limit when any $m_i^2, p_j^2 \to 0$, namely that this limit is unique regardless of the order or relative rate with which we send these parameters to zero. As is argued in [25], see also [48], this limit of $\widetilde{E_A}$ is defined by removing any of its factors that vanishes as its parameters approach their prescribed values. This reflects the fact that Feynman integrals converge in the Euclidean region for certain choices of propagator powers and dimension of loop integration, and hence they cannot be singular for all values of their kinematic parameters. In other words, assuming a single parameter x of $\widetilde{E_A}$ takes the limiting value a, the limit of the former is defined as

$$\lim_{x\to a} \widetilde{E_A} = \left.\frac{\partial^l \widetilde{E_A}}{\partial x^l}\right|_{x=a} \neq 0\,, \text{ with } \left.\frac{\partial^{l'} \widetilde{E_A}}{\partial x^{l'}}\right|_{x=a} = 0 \text{ for } l' = 0,\ldots,l-1\,, \tag{3.39}$$

also including the possibility $l = 0$, and with an obvious generalization to the multivariate case. However the fact that this limit is uniquely defined in multivariate limits is highly nontrivial, as can be seen in the following example of the triangle Cayley determinant with elements as shown in eq. (3.5) for $n = 3$, in the limit $p_1^2 \to 0, p_2^2 \to 0, s_{12} = p_3^2 \to 0$: Denoting this Cayley determinant as Y_3, its Taylor expansion in the limit is

$$Y_3 = 0 + 2\sum_{i=1}^{3} p_i^2 (m_i^2 - m_{i-1}^2)(m_{i+1}^2 - m_{i-1}^2) + \mathcal{O}(p_j^2 p_k^2)\,, \tag{3.40}$$

with $j, k = 1, 2, 3$, $m_{j+3} \equiv m_j$. Clearly, the value of Y_3 in the limit *does* depend on the order with which we set the three momenta-squared to zero. The upshot of our analysis will be that *while the limits of individual factors in $\widetilde{E_A}$ do depend on the rate of approach to the limit, the limit of $\widetilde{E_A}$ as a whole does not, since different rates of approach produce factors that are already contained in it.*

We start by noting that the only Gram (sub)determinant of a graph with $n \neq 3$ that vanishes as $p_i^2 \to 0$ is that of a bubble (sub)graph with momentum p_i, $G(p_i) = p_i^2$. By the above definition, the latter gives no nontrivial contribution in the limit. Particularly when $n = 3$ we also have a vanishing $G(p_1^2, p_2^2) \propto \lambda(p_1^2, p_2^2, p_3^2)$, where λ is the fully symmetric Källén function defined in eq. (3.25). In particular we have $\lambda(0, 0, p^2) = p^4$, and therefore this does not give any nontrivial contribution to the limit (3.39) either. For $n > 3$ we have sums of external momenta as arguments of the triangle subgraph, such that the corresponding Källén function does not vanish. Taking into account the fact that Gram determinants are independent of the masses, this exhausts the analysis of their potential ambiguities in the limit we are considering.

By the same token, it is possible to show that the only Cayley (sub)determinants of any graph that vanish as $m_i^2 \to 0$ are the diagonal m_i^2 elements of the matrix, also giving no contribution to the limit. Finally, we consider the behavior of the Cayley (sub)determinants when both m_i^2, p_i^2 vanish. The only vanishing (sub)determinants in this case are the Cayley determinants of bubble and triangle (sub)graphs. The former are proportional to $\lambda(m_i^2, m_{i+1}^2, p_i^2)$, and by the previous analysis we deduce that they do not affect the limit. For the triangle Cayley determinant Y_3, we have already shown in (3.40) that it vanishes as $p_1^2, p_2^2, p_3^3 \to 0$, and by examining all possibilities we similarly find that up to dihedral images, the only other minimum codimension limit for which the same is true is the limit $p_1^2, m_1^2, m_2^2 \to 0$. The Taylor expansion around the latter yields

$$Y_3 = 0+2p_1^2\prod_{i=1}^{2}(m_3^2-p_{i+1}^2)+2(p_2^2-p_3^2)\sum_{i=1}^{2}(-1)^i m_i^2(m_3^2-p_{i+1}^2)+\mathcal{O}(m_j^2 m_k^2)+\mathcal{O}(m_j^2 p_1^2)+\mathcal{O}(p_1^4)\,, \tag{3.41}$$

with $j, k = 1, 2$, respectively. We see that in both cases the three nonvanishing derivatives depend on the remaining variables and are not equal to each other, such that the value of Y_3 depends on the relative rate with which we approach the limit, and causing a potential ambiguity for the limit of the principal A-determinant as a whole. Very interestingly, however, the factor that Y_3 contributes in all different rates of approach is already contained in $\widetilde{E_A}$ in the limit. Specifically,

$$\lim_{p_1^2 \to 0} G(p_1, p_2) \to -\frac{1}{4}\lambda(p_2^2, p_3^2, 0) = -\frac{1}{4}\left(p_2^2 - p_3^2\right)^2\,, \tag{3.42}$$

accounts for one of the Taylor expansion coefficients in (3.41), and two-dimensional Cayley subdeterminants $\lambda(p_i^2, m_3^2, 0)$ of Y_3 account for the rest. Similarly, the Cayley subdeterminants $\lambda(m_i^2, m_j^2, 0)$ take care of all the Taylor expansion coefficients in (3.40).

Along the same lines, inspecting all higher-codimension $m_i^2, p_i^2 \to 0$ limits where Y_3 vanishes reveals that they are all contained in the two aforementioned codimension-3 limits. Thus they are covered by the previous analysis, and this concludes the proof that the principal A-determinant has a well-defined limit for any subset of $m_i^2, p_i^2 \to 0$.

The analysis we have carried out may of course also be repeated in any other multivariate limit, including restrictions on the dimension of external kinematics of the type (3.29). For example, $\widetilde{E_A}$ remains well-defined for any codimension-two limit where the Cayley determinant of any bubble subgraph of an n-point graph vanishes. As we will also discuss in the next section, in all cases we have considered this unambiguous limit of the principal A-determinant of the generic one-loop graph to any specific kinematic configuration also matches the direct computation of the principal A-determinant of the non-generic graph. These findings suggest that, quite remarkably, the space of solutions of the Landau equations for one-loop Feynman integrals smoothly interpolates between different kinematic configurations related by limits, even though the differential equations these integrals obey, be it of hypergeometric or canonical type, diverge and may not have well-defined such limits.

This in turn supports the expectation that also the symbol alphabet of non-generic Feynman integral may be correctly obtained as a limit of the generic one, based on the re-factorization we have exhibited, of the principal A-determinant in terms of the alphabet. In the next section we will explicitly confirm this expectation in several examples, further corroborating earlier observations made in [94]. These are also in line with the observation that the diagrammatic coaction [93, 100] reduces correctly in the limits of generic to non-generic and possibly divergent graphs. The conjectured equivalence of this coaction with the coaction on the polylogarithms these integrals evaluate to, is then also an implicit conjecture about the relation of their alphabets.

JHEP10(2023)161

4 Examples

In this section we present a series of examples illustrating the formulas for the principal A-determinant, symbol alphabet and canonical differential equations of a generic n-point one-loop Feynman integral presented in section 3, as well as the limiting procedure for obtaining the first two for any non-generic integral, for various values of n. We will consider several of these integrals around both even and odd dimensions of loop momenta D_0.

4.1 Bubble graph

Let us start with the $n = 2$ or bubble integral illustrated below.

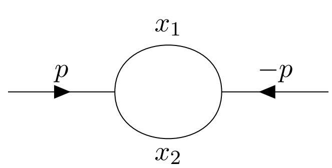

The Lee-Pomeransky polynomial for the latter in generic kinematics is

$$\mathcal{G} = x_1 + x_2 + (m_1^2 + m_2^2 - p^2)x_1x_2 + m_1^2x_1^2 + m_2^2x_2^2\,, \tag{4.1}$$

so the A-matrix is given by

$$A = \begin{pmatrix} 1 & 1 & 1 & 1 & 1 \\ 1 & 0 & 1 & 2 & 0 \\ 0 & 1 & 1 & 0 & 2 \end{pmatrix}. \tag{4.2}$$

As in section 2 we let α_i denote the exponents in the $\mathcal{G}$-polynomial. With this we can write the reduced principal A-determinant as

$$\begin{aligned}\widetilde{E_A}(\mathcal{G}) &= \Delta_{\alpha_4}\Delta_{\alpha_5}\Delta_{\alpha_4\alpha_5}\Delta_{\alpha_1\alpha_2\alpha_4\alpha_5} \\ &= m_1^2m_2^2(p^4 + m_1^4 + m_2^4 - 2p^2m_1^2 - 2p^2m_2^2 - 2m_1^2m_2^2)p^2\,,\end{aligned} \tag{4.3}$$

where we momentarily index the discriminants with the vertices in the corresponding face. The final expression as a polynomial of the variables m_1^2, m_2^2, p^2 indeed agrees with the general expression (3.15) in terms of the minors of the modified Cayley matrix,

$$\mathcal{Y} = \begin{pmatrix} 0 & 1 & 1 \\ 1 & 2m_1^2 & m_1^2+m_2^2-p^2 \\ 1 & m_1^2+m_2^2-p^2 & 2m_2^2 \end{pmatrix}. \tag{4.4}$$

Applying our general formulas for the alphabet, eqs. (3.21)–(3.23) to this case, we obtain five letters; one for each possible tadpole subgraph and three for the bubble itself. In even space-time dimension the letters are:

$$\begin{aligned}
W_1 &= \frac{\mathcal{Y}\begin{bmatrix}3\\3\end{bmatrix}}{\mathcal{Y}\begin{bmatrix}1&3\\1&3\end{bmatrix}} = \frac{-1}{2m_1^2}, \qquad W_2 = \frac{\mathcal{Y}\begin{bmatrix}2\\2\end{bmatrix}}{\mathcal{Y}\begin{bmatrix}1&2\\1&2\end{bmatrix}} = \frac{-1}{2m_2^2}, \qquad W_{12} = \frac{\mathcal{Y}\begin{bmatrix}\cdot\\\cdot\end{bmatrix}}{\mathcal{Y}\begin{bmatrix}1\\1\end{bmatrix}} = \frac{2p^2}{\lambda(p^2,m_1^2,m_2^2)},\\
W_{(1)2} &= \frac{\mathcal{Y}\begin{bmatrix}2\\1\end{bmatrix} - \sqrt{\mathcal{Y}\begin{bmatrix}2\\2\end{bmatrix}\mathcal{Y}\begin{bmatrix}1\\1\end{bmatrix}}}{\mathcal{Y}\begin{bmatrix}2\\1\end{bmatrix} + \sqrt{\mathcal{Y}\begin{bmatrix}2\\2\end{bmatrix}\mathcal{Y}\begin{bmatrix}1\\1\end{bmatrix}}} = \frac{-m_1^2+m_2^2+p^2-\sqrt{\lambda(p^2,m_1^2,m_2^2)}}{-m_1^2+m_2^2+p^2+\sqrt{\lambda(p^2,m_1^2,m_2^2)}},\\
W_{1(2)} &= \frac{\mathcal{Y}\begin{bmatrix}3\\1\end{bmatrix} - \sqrt{\mathcal{Y}\begin{bmatrix}3\\3\end{bmatrix}\mathcal{Y}\begin{bmatrix}1\\1\end{bmatrix}}}{\mathcal{Y}\begin{bmatrix}3\\1\end{bmatrix} + \sqrt{\mathcal{Y}\begin{bmatrix}3\\3\end{bmatrix}\mathcal{Y}\begin{bmatrix}1\\1\end{bmatrix}}} = \frac{-m_1^2+m_2^2-p^2-\sqrt{\lambda(p^2,m_1^2,m_2^2)}}{-m_1^2+m_2^2-p^2+\sqrt{\lambda(p^2,m_1^2,m_2^2)}},
\end{aligned} \tag{4.5}$$

where we recall that λ denotes the Källén function,

$$\lambda(p^2,m_1^2,m_2^2) = p^4 + m_1^4 + m_2^4 - 2p^2m_1^2 - 2p^2m_2^2 - 2m_1^2m_2^2. \tag{4.6}$$

While the dependence of the bubble on few kinematic variables does not leave much room for nontrivial limits, we have checked that in all codimension-1 limits where a momentum or mass squared vanishes, or two of them are set equal to each other, the above alphabet reduces to harmonic polylogarithms [101] as expected.

Apart from the bubble alphabet, let us also present the canonical differential equation for the corresponding master integrals. In this case, the choice of basis (3.30) specializes to

$$\mathcal{J}_1 = \frac{\epsilon\,\mathcal{I}_1^{(2)}}{j_1}, \quad \mathcal{J}_2 = \frac{\epsilon\,\mathcal{I}_2^{(2)}}{j_2}, \quad \mathcal{J}_{12} = \frac{\epsilon\,\mathcal{I}_{12}^{(2)}}{j_{12}}, \tag{4.7}$$

with the leading singularities being

$$j_1^{-1} = \sqrt{-\mathcal{Y}\begin{bmatrix}3\\3\end{bmatrix}} = 1, \quad j_2^{-1} = \sqrt{-\mathcal{Y}\begin{bmatrix}2\\2\end{bmatrix}} = 1, \quad j_{12}^{-1} = \sqrt{-\mathcal{Y}\begin{bmatrix}1\\1\end{bmatrix}} = \sqrt{\lambda(p^2,m_1^2,m_2^2)}. \tag{4.8}$$

Using the expression for the canonical differential equation in eq. (3.32), the matrix (1.2) is given by

$$\widetilde{M} = \begin{pmatrix} w_1 & 0 & 0 \\ 0 & w_2 & 0 \\ -w_{1(2)} & w_{(1)2} & w_{12} \end{pmatrix}, \tag{4.9}$$

where $w = \log W$.

At odd space-time dimension of loop momentum D_0, the rational letters W_1, W_2 and W_{12} are the same as in the even D_0 case, whereas the square-root letters become

$$W_{(1)2} = \frac{\mathcal{Y}\begin{bmatrix}2\\1\end{bmatrix} - \sqrt{-\mathcal{Y}\begin{bmatrix}\cdot\\\cdot\end{bmatrix}\mathcal{Y}\begin{bmatrix}1&2\\1&2\end{bmatrix}}}{\mathcal{Y}\begin{bmatrix}2\\1\end{bmatrix} + \sqrt{-\mathcal{Y}\begin{bmatrix}\cdot\\\cdot\end{bmatrix}\mathcal{Y}\begin{bmatrix}1&2\\1&2\end{bmatrix}}} = \frac{-m_1^2+m_2^2+p^2-\sqrt{4p^2m_2^2}}{-m_1^2+m_2^2+p^2+\sqrt{4p^2m_2^2}} \tag{4.10}$$

$$W_{1(2)} = \frac{\mathcal{Y}\begin{bmatrix}3\\1\end{bmatrix} - \sqrt{-\mathcal{Y}\begin{bmatrix}\cdot\\\cdot\end{bmatrix}\mathcal{Y}\begin{bmatrix}1&3\\1&3\end{bmatrix}}}{\mathcal{Y}\begin{bmatrix}3\\1\end{bmatrix} + \sqrt{-\mathcal{Y}\begin{bmatrix}\cdot\\\cdot\end{bmatrix}\mathcal{Y}\begin{bmatrix}1&3\\1&3\end{bmatrix}}} = \frac{-m_1^2+m_2^2-p^2-\sqrt{4p^2m_1^2}}{-m_1^2+m_2^2-p^2+\sqrt{4p^2m_1^2}} \tag{4.11}$$

For the basis of master integrals and leading singularities we obtain

$$\mathcal{J}_1 = \frac{\mathcal{I}_1^{(1)}}{j_1}, \qquad \mathcal{J}_2 = \frac{\mathcal{I}_2^{(1)}}{j_2}, \qquad \mathcal{J}_{12} = \frac{\epsilon\mathcal{I}_{12}^{(3)}}{j_{12}}, \tag{4.12}$$

$$j_1^{-1} = \sqrt{\frac{\mathcal{Y}\begin{bmatrix}1&3\\1&3\end{bmatrix}}{2}} = \sqrt{m_1^2}, \quad j_2^{-1} = \sqrt{\frac{\mathcal{Y}\begin{bmatrix}1&2\\1&2\end{bmatrix}}{2}} = \sqrt{m_2^2}, \quad j_{12}^{-1} = \sqrt{-2\mathcal{Y}\begin{bmatrix}\cdot\\\cdot\end{bmatrix}} = 2\sqrt{p_1^2}. \tag{4.13}$$

Putting this together in the differential equation matrix we get

$$\widetilde{M} = \begin{pmatrix} w_1 & 0 & 0 \\ 0 & w_2 & 0 \\ -w_{1(2)} & w_{(1)2} & w_{12} \end{pmatrix}. \tag{4.14}$$

Remark 4.1. The Newton polytope of $\mathcal{G}$ for the massive bubble is a trapezoid (see figure 2) with five regular triangulations, meaning that the secondary polytope is a pentagon, see figure 3. At the same time, the alphabet of the bubble graph may be expressed in terms of the variables of the A_2 cluster algebra, whose cluster polytope is also a pentagon. We find this match striking, even though the Newton polytope of $\mathcal{G}$ for the n-point graph is n-dimensional, and hence the correspondence with cluster algebras, which typically triangulate two-dimensional surfaces, it not as straightforward for $n > 2$.

JHEP10(2023)161

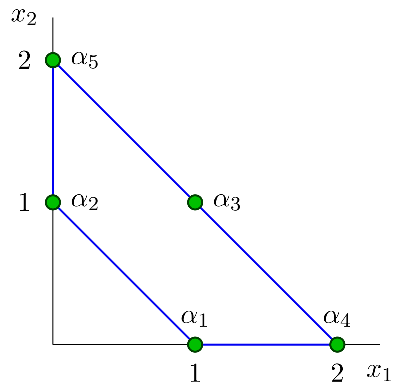

Figure 2. The Newton polytope of the Lee-Pomeransky polynomial $\mathcal{G}$ of the bubble. The edges $(a_1 a_4)$ and $(a_2 a_5)$ correspond to its tadpole or $n = 1$ subgraphs, and the edges $(a_1 a_2)$ and $(a_4 a_5)$ are the Newton polytopes of the first and second Symanzik polynomials $\mathcal{U}$ and $\mathcal{F}$, respectively. The former does not contribute to $\widetilde{E_A}$.

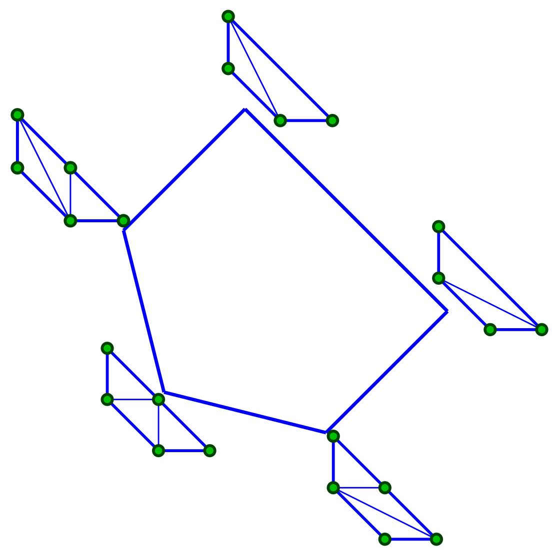

Figure 3. Secondary polytope and regular triangulations of Newt($\mathcal{G}$) for the 1-loop bubble graph, with $\mathcal{G}$ as in (4.1). It is isomorphic to the A_2 cluster polytope.

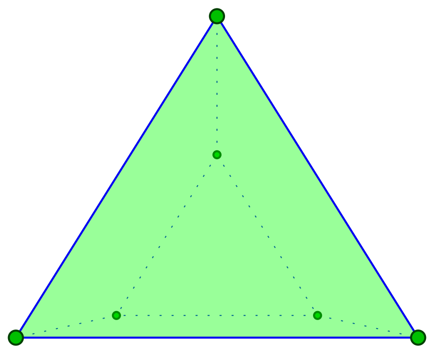

Figure 4. The Newton polytope of the Lee-Pomeransky polynomial $\mathcal{G}$ of the massive triangle, with two parallel triangular faces, and three trapezoidal faces from bubble subgraphs.

4.2 Triangle graphs

In our next example, we consider the $n = 3$ or triangle Feynman graph illustrated in the diagram below.

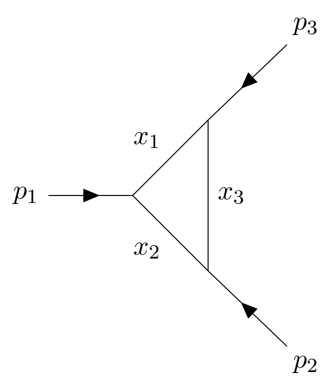

The two Symanzik polynomials of this graph with generic kinematics are

$$\begin{aligned}\mathcal{U} &= x_1 + x_2 + x_3,\\ \mathcal{F} &= (m_1^2 + m_2^2 - p_1^2)x_1x_2 + (m_1^2 + m_2^3 - p_3^2)x_1x_3 + (m_2^2 + m_3^2 - p_2^2)x_2x_3\\ &\quad + m_1^2x_1^2 + m_2^2x_2^2 + m_3^2x_3^2\end{aligned} \tag{4.15}$$

which with $\mathcal{G} = \mathcal{U} + \mathcal{F}$ gives the A-matrix:

$$A = \begin{pmatrix} 1 & 1 & 1 & 1 & 1 & 1 & 1 & 1 & 1\\ 1 & 0 & 0 & 1 & 1 & 0 & 2 & 0 & 0\\ 0 & 1 & 0 & 1 & 0 & 1 & 0 & 2 & 0\\ 0 & 0 & 1 & 0 & 1 & 1 & 0 & 0 & 2 \end{pmatrix}.$$

The Newton polytope of $\mathcal{G}$ is displayed in figure 4 where there are three facets looking like figure 2. These facets are obtained from $\mathrm{Newt}(\mathcal{G})$ by intersecting it with one of the coordinate hyperplanes $x_i = 0$. This of course corresponds to contracting edge i in the underlying Feynman graph, giving us a bubble graph. The discriminant factors making up

JHEP10(2023)161

the principal A-determinant E_A as described in (2.18) are:

$$
\begin{aligned}
\Delta_A &= p_1^4 + p_2^4 + p_3^4 - 2p_1^2p_2^2 - 2p_1^2p_3^2 - 2p_2^2p_3^2,\\
\Delta_{A\cap x_1=0} &= -p_2^2,\\
\Delta_{A\cap x_2=0} &= -p_3^2,\\
\Delta_{A\cap x_3=0} &= -p_1^2,\\
\Delta_{A\cap \mathrm{Newt}(\mathcal{F})} &= -m_1^2m_2^2p_1^2 + m_1^2m_3^2p_1^2 + m_2^2m_3^2p_1^2 - m_3^4p_1^2 - m_3^2p_1^4 - m_1^4p_2^2 + m_1^2m_2^2p_2^2\\
&\quad + m_1^2m_3^2p_2^2 - m_2^2m_3^2p_2^2 + m_1^2p_1^2p_2^2 + m_3^2p_1^2p_2^2 - m_1^2p_2^4 + m_1^2m_2^2p_3^2 - m_2^4p_3^2\\
&\quad - m_1^2m_3^2p_3^2 + m_2^2m_3^2p_3^2 + m_2^2p_1^2p_3^2 + m_3^2p_1^2p_3^2 + m_1^2p_2^2p_3^2 + m_2^2p_2^2p_3^2\\
&\quad - p_1^2p_2^2p_3^2 - m_2^2p_3^4,\\
\Delta_{A\cap \mathrm{Newt}(\mathcal{F})\cap x_1=0} &= p_2^4 + m_2^4 + m_3^2 - 2p_2^2m_2^2 - 2p_2^2m_3^2 - 2m_2^2m_3^2,\\
\Delta_{A\cap \mathrm{Newt}(\mathcal{F})\cap x_2=0} &= p_3^4 + m_1^4 + m_3^4 - 2p_3^2m_1^2 - 2p_3^2m_3^2 - 2m_1^2m_3^2,\\
\Delta_{A\cap \mathrm{Newt}(\mathcal{F})\cap x_3=0} &= p_1^4 + m_1^4 + m_2^4 - 2p_1^2m_1^2 - 2p_1^2m_2^2 - 2m_1^2m_2^2,\\
\prod_{\text{vertices}} \Delta_v &= m_1^2m_2^2m_3^2.
\end{aligned}
$$

Again, all these discriminants, calculated directly from the GKZ approach, correspond to minors of the modified Cayley matrix

$$
\mathcal{Y} = \begin{pmatrix} 0 & 1 & 1 & 1\\ 1 & 2m_1^2 & (m_1^2+m_2^2-p_1^2) & (m_1^2+m_2^3-p_3^2)\\ 1 & (m_1^2+m_2^2-p_1^2) & 2m_2^2 & (m_2^2+m_3^2-p_2^2)\\ 1 & (m_1^2+m_2^3-p_3^2) & (m_2^2+m_3^2-p_2^2) & 2m_3^2 \end{pmatrix}, \tag{4.16}
$$

and up to overall factors we have the identification

$$
\Delta_A \to \mathcal{Y}\begin{bmatrix} \cdot \\ \cdot \end{bmatrix}, \qquad \Delta_{A\cap x_i=0} \to \mathcal{Y}\begin{bmatrix} i+1 \\ i+1 \end{bmatrix}, \tag{4.17}
$$

$$
\Delta_{A\cap \mathrm{Newt}(\mathcal{F})} \to \mathcal{Y}\begin{bmatrix} 1 \\ 1 \end{bmatrix}, \qquad \Delta_{A\cap \mathrm{Newt}(\mathcal{F})\cap x_i=0} \to \mathcal{Y}\begin{bmatrix} 1 & i+1 \\ 1 & i+1 \end{bmatrix}, \tag{4.18}
$$

whereas the masses correspond the diagonal elements of $\mathcal{Y}$. As predicted by eq. (3.28), for D_0 even there are 18 multiplicatively independent letters, out of which 12 correspond to bubble subgraphs and are thus obtained by relabeling the formulas of the previous subsection. The remaining six letters are

$$W_{123} = \frac{\mathcal{Y}\begin{bmatrix} \cdot \\ \cdot \end{bmatrix}}{\begin{bmatrix} 1 \\ 1 \end{bmatrix}}, \tag{4.19}$$

$$W_{(1)23} = \frac{\mathcal{Y}\begin{bmatrix} 2 \\ 1 \end{bmatrix} - \sqrt{-\mathcal{Y}\begin{bmatrix} \cdot \\ \cdot \end{bmatrix}\mathcal{Y}\begin{bmatrix} 1 & 2 \\ 1 & 2 \end{bmatrix}}}{\mathcal{Y}\begin{bmatrix} 2 \\ 1 \end{bmatrix} + \sqrt{-\mathcal{Y}\begin{bmatrix} \cdot \\ \cdot \end{bmatrix}\mathcal{Y}\begin{bmatrix} 1 & 2 \\ 1 & 2 \end{bmatrix}}} \qquad \text{plus cyclic } (1) \to (2) \to (3)\,, \tag{4.20}$$

$$W_{(1)(2)3} = \frac{\mathcal{Y}\begin{bmatrix} 2 \\ 3 \end{bmatrix} - \sqrt{\mathcal{Y}\begin{bmatrix} \cdot \\ \cdot \end{bmatrix}}}{\mathcal{Y}\begin{bmatrix} 2 \\ 3 \end{bmatrix} + \sqrt{\mathcal{Y}\begin{bmatrix} \cdot \\ \cdot \end{bmatrix}}} \qquad \text{plus cyclic } (1)(2) \to (2)(3)\,. \tag{4.21}$$

In this case the basis integrals of eq. (3.30) read

$$\begin{aligned} \mathcal{J}_1 &= \frac{\epsilon\,\mathcal{I}_1^{(2)}}{j_1}, \quad \mathcal{J}_2 = \frac{\epsilon\,\mathcal{I}_2^{(2)}}{j_2}, \quad \mathcal{J}_3 = \frac{\epsilon\,\mathcal{I}_3^{(2)}}{j_3}, \\ \mathcal{J}_{12} &= \frac{\epsilon\,\mathcal{I}_{12}^{(2)}}{j_{12}}, \quad \mathcal{J}_{13} = \frac{\epsilon\,\mathcal{I}_{13}^{(2)}}{j_{13}}, \quad \mathcal{J}_{23} = \frac{\epsilon\,\mathcal{I}_{23}^{(2)}}{j_{23}}, \\ \mathcal{J}_{123} &= \frac{\epsilon^2\mathcal{I}_{123}^{(4)}}{j_{123}}, \end{aligned} \tag{4.22}$$

with leading singularities

$$\begin{aligned} j_1^{-1} &= \sqrt{-\mathcal{Y}\begin{bmatrix} 3 & 4 \\ 3 & 4 \end{bmatrix}} = 1, & j_2^{-1} &= \sqrt{-\mathcal{Y}\begin{bmatrix} 2 & 4 \\ 2 & 4 \end{bmatrix}} = 1, \\ j_3^{-1} &= \sqrt{-\mathcal{Y}\begin{bmatrix} 2 & 3 \\ 2 & 3 \end{bmatrix}} = 1, & j_{12}^{-1} &= \sqrt{-\mathcal{Y}\begin{bmatrix} 1 & 4 \\ 1 & 4 \end{bmatrix}} = \sqrt{\lambda(p_1^2, m_1^2, m_2^2)}, \\ j_{13}^{-1} &= \sqrt{-\mathcal{Y}\begin{bmatrix} 1 & 3 \\ 1 & 3 \end{bmatrix}} = \sqrt{\lambda(p_3^2, m_1^2, m_3^2)}, & j_{23}^{-1} &= \sqrt{-\mathcal{Y}\begin{bmatrix} 1 & 2 \\ 1 & 2 \end{bmatrix}} = \sqrt{\lambda(p_2^2, m_2^2, m_3^2)}, \\ j_{123}^{-1} &= 2\sqrt{\mathcal{Y}\begin{bmatrix} \cdot \\ \cdot \end{bmatrix}} = 2\sqrt{\lambda(p_1^2, p_2^2, p_3^2)}. \end{aligned} \tag{4.23}$$

Putting it all together we get the differential equation matrix

$$\widetilde{M} = \begin{pmatrix} w_1 & 0 & 0 & 0 & 0 & 0 & 0 \\ 0 & w_2 & 0 & 0 & 0 & 0 & 0 \\ 0 & 0 & w_3 & 0 & 0 & 0 & 0 \\ -w_{1(2)} & w_{(1)2} & 0 & w_{12} & 0 & 0 & 0 \\ -w_{1(3)} & 0 & w_{(1)3} & 0 & w_{13} & 0 & 0 \\ 0 & -w_{2(3)} & w_{(2)3} & 0 & 0 & w_{23} & 0 \\ -w_{1(2)(3)} & w_{(1)(2)3}+w_{1(2)(3)} & -w_{(1)(2)3} & -w_{12(3)} & w_{1(2)3} & -w_{(1)23} & w_{123} \end{pmatrix}. \tag{4.24}$$

For the case of odd D_0 there are now 19 letters, where again 12 of them are obtained from the odd D_0 bubble by relabeling. Out of the remaining seven, the rational letter W_{123} is the same as in the even D_0 case (4.19), and the rest are

$$W_{(1)23} = \frac{\mathcal{Y}\begin{bmatrix}2\\1\end{bmatrix} - \sqrt{\mathcal{Y}\begin{bmatrix}2\\2\end{bmatrix}\mathcal{Y}\begin{bmatrix}1\\1\end{bmatrix}}}{\mathcal{Y}\begin{bmatrix}2\\1\end{bmatrix} + \sqrt{\mathcal{Y}\begin{bmatrix}2\\2\end{bmatrix}\mathcal{Y}\begin{bmatrix}1\\1\end{bmatrix}}}, \qquad \text{plus cyclic } (1)\to(2)\to(3), \tag{4.25}$$

$$W_{(1)(2)3} = \frac{\mathcal{Y}\begin{bmatrix}1&2\\1&3\end{bmatrix} - \sqrt{-\mathcal{Y}\begin{bmatrix}1\\1\end{bmatrix}\mathcal{Y}\begin{bmatrix}1&2&3\\1&2&3\end{bmatrix}}}{\mathcal{Y}\begin{bmatrix}1&2\\1&3\end{bmatrix} + \sqrt{-\mathcal{Y}\begin{bmatrix}1\\1\end{bmatrix}\mathcal{Y}\begin{bmatrix}1&2&3\\1&2&3\end{bmatrix}}}, \qquad \text{plus cyclic } (1)(2)\to(1)(3)\to(2)(3). \tag{4.26}$$

The basis integrals now become,

$$\begin{aligned} \mathcal{J}_1 &= \frac{\mathcal{I}_1^{(1)}}{j_1}, \qquad \mathcal{J}_2 = \frac{\mathcal{I}_2^{(1)}}{j_2}, \qquad \mathcal{J}_3 = \frac{\mathcal{I}_3^{(1)}}{j_3}, \\ \mathcal{J}_{12} &= \frac{\epsilon\,\mathcal{I}_{12}^{(3)}}{j_{12}}, \quad \mathcal{J}_{13} = \frac{\epsilon\,\mathcal{I}_{13}^{(3)}}{j_{13}}, \quad \mathcal{J}_{23} = \frac{\epsilon\,\mathcal{I}_{23}^{(3)}}{j_{23}}, \\ \mathcal{J}_{123} &= \frac{\epsilon\,\mathcal{I}_{123}^{(3)}}{j_{123}}, \end{aligned} \tag{4.27}$$

where the leading singularities are explicitly given by

$$\begin{aligned}
j_1^{-1} &= \sqrt{\frac{\mathcal{Y}\begin{bmatrix}1\ 3\ 4\\1\ 3\ 4\end{bmatrix}}{2}} = \sqrt{m_1^2}, & j_2^{-1} &= \sqrt{\frac{\mathcal{Y}\begin{bmatrix}1\ 2\ 4\\1\ 2\ 4\end{bmatrix}}{2}} = \sqrt{m_2^2},\\
j_3^{-1} &= \sqrt{\frac{\mathcal{Y}\begin{bmatrix}1\ 2\ 3\\1\ 2\ 3\end{bmatrix}}{2}} = \sqrt{m_3^2}, & j_{12}^{-1} &= \sqrt{-2\mathcal{Y}\begin{bmatrix}4\\4\end{bmatrix}} = 2\sqrt{p_1^2},\\
j_{13}^{-1} &= \sqrt{-2\mathcal{Y}\begin{bmatrix}3\\3\end{bmatrix}} = 2\sqrt{p_2^2}, & j_{23}^{-1} &= \sqrt{-2\mathcal{Y}\begin{bmatrix}2\\2\end{bmatrix}} = 2\sqrt{p_3^2},\\
j_{123}^{-1} &= \sqrt{-2\mathcal{Y}\begin{bmatrix}1\\1\end{bmatrix}} = 2\sqrt{-\Delta_{A\cap\mathrm{Newt}(\mathcal{F})}},
\end{aligned} \tag{4.28}$$

and putting it all together we get the differential equation matrix

$$\widetilde{M} = \begin{pmatrix}
w_1 & 0 & 0 & 0 & 0 & 0 & 0\\
0 & w_2 & 0 & 0 & 0 & 0 & 0\\
0 & 0 & w_3 & 0 & 0 & 0 & 0\\
-w_{1(2)} & w_{(1)2} & 0 & w_{12} & 0 & 0 & 0\\
-w_{1(3)} & 0 & w_{(1)3} & 0 & w_{13} & 0 & 0\\
0 & -w_{2(3)} & w_{(2)3} & 0 & 0 & w_{23} & 0\\
w_{1(2)(3)} & -w_{(1)2(3)} & w_{(1)(2)3} & w_{12(3)} & -w_{1(2)3} & w_{(1)23} & w_{123}
\end{pmatrix}. \tag{4.29}$$

As an independent check of our results, we may also compare the finite part of the $D_0 = 3$ triangle integral $\mathcal{I}_{123}^{(3)}$, first computed in [102], with our prediction for its symbol based on eqs. (4.27)–(4.29), together with eq. (1.4). In particular, our prediction reads,

$$\mathcal{I}_{123}^{(3)} \propto \frac{1}{\sqrt{-Y_3}} \log \frac{W_{(1)(2)3} W_{1(2)(3)}}{W_{(1)2(3)}} + \mathcal{O}(\epsilon)\,, \tag{4.30}$$

where Y_3 denotes the triangle Cayley matrix with elements as shown in eq. (3.5), and $n = 3$. Taking into account that in [102] the Cayley matrix has been defined with an extra 1/2 overall factor, as well as rescaled to become dimensionless by dividing with the masses associated to each row and column, we indeed find agreement.

4.3 Box graphs

In our final example with full kinematic dependence, we present the alphabet for the box graph illustrated below.

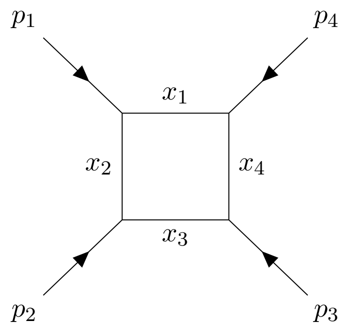

The two Symanzik polynomials of the box graph with generic massive kinematics are

$$\begin{aligned}
\mathcal{U} &= x_1 + x_2 + x_3 + x_4, \\
\mathcal{F} &= (m_1^2 + m_2^2 - p_1^2)x_1x_2 + (m_1^2 + m_3^2 - s)x_1x_3 + (m_1^2 + m_4^3 - p_4^2)x_1x_4 \\
&\quad + (m_2^2 + m_3^2 - p_2^2)x_2x_3 + (m_2^2 + m_4^2 - t)x_2x_4 + (m_3^2 + m_4^2 - p_3^2)x_3x_4 \\
&\quad + m_1^2x_1^2 + m_2^2x_2^2 + m_3^2x_3^2 + m_4^2x_4^2
\end{aligned}$$

and the modified Cayley matrix is given by

$$\mathcal{Y} = \begin{pmatrix} 0 & 1 & 1 & 1 & 1 \\ 1 & 2m_1^2 & m_1^2 + m_2^2 - p_1^2 & m_1^2 + m_3^2 - s & m_1^2 + m_4^2 - p_4^2 \\ 1 & m_1^2 + m_2^2 - p_1^2 & 2m_2^2 & m_2^2 + m_3^2 - p_2^2 & m_2^2 + m_4^2 - t \\ 1 & m_1^2 + m_3^2 - s & m_2^2 + m_3^2 - p_2^2 & 2m_3^2 & m_3^2 + m_4^2 - p_3^2 \\ 1 & m_1^2 + m_4^2 - p_4^2 & m_2^2 + m_4^2 - t & m_3^2 + m_4^2 - p_3^2 & 2m_4^2. \end{pmatrix} \tag{4.31}$$

The symbol alphabet with generic massive kinematics contains 57 letters for D_0 even and 61 for D_0 odd. These letters are to large to show here but are provided in the auxiliary `Mathematica` file.

The $\widetilde{M}$ matrices for the case of even and odd D_0 are given in (4.32) and (4.33), respectively. Compared to the bubble and triangle examples, the box is the first case where we see that a graph only depends on its subgraphs with at most two legs removed. This is evident in the vanishing of the box-tadpole elements of the differential equation matrices $\widetilde{M}_{15,1}, \ldots, \widetilde{M}_{15,4}$.

$$\begin{pmatrix}
w_1 & 0 & 0 & 0 & 0 & 0 & 0 & 0 & 0 & 0 & 0 & 0 & 0 & 0 & 0 \\
0 & w_2 & 0 & 0 & 0 & 0 & 0 & 0 & 0 & 0 & 0 & 0 & 0 & 0 & 0 \\
0 & 0 & w_3 & 0 & 0 & 0 & 0 & 0 & 0 & 0 & 0 & 0 & 0 & 0 & 0 \\
0 & 0 & 0 & w_4 & 0 & 0 & 0 & 0 & 0 & 0 & 0 & 0 & 0 & 0 & 0 \\
-w_{1(2)} & w_{(1)2} & 0 & 0 & w_{12} & 0 & 0 & 0 & 0 & 0 & 0 & 0 & 0 & 0 & 0 \\
-w_{1(3)} & 0 & w_{(1)3} & 0 & 0 & w_{13} & 0 & 0 & 0 & 0 & 0 & 0 & 0 & 0 & 0 \\
-w_{1(4)} & 0 & 0 & w_{(1)4} & 0 & 0 & w_{14} & 0 & 0 & 0 & 0 & 0 & 0 & 0 & 0 \\
0 & -w_{2(3)} & w_{(2)3} & 0 & 0 & 0 & 0 & w_{23} & 0 & 0 & 0 & 0 & 0 & 0 & 0 \\
0 & -w_{2(4)} & 0 & w_{(2)4} & 0 & 0 & 0 & 0 & w_{24} & 0 & 0 & 0 & 0 & 0 & 0 \\
0 & 0 & -w_{3(4)} & w_{(3)4} & 0 & 0 & 0 & 0 & 0 & w_{34} & 0 & 0 & 0 & 0 & 0 \\
-w_{1(2)(3)} & w_{(1)(2)3}+w_{1(2)(3)} & -w_{(1)(2)3} & 0 & -w_{12(3)} & w_{1(2)3} & 0 & -w_{(1)23} & 0 & 0 & w_{123} & 0 & 0 & 0 & 0 \\
-w_{1(2)(4)} & w_{(1)(2)4}+w_{1(2)(4)} & 0 & -w_{(1)(2)4} & -w_{12(4)} & 0 & w_{1(2)4} & 0 & -w_{(1)24} & 0 & 0 & w_{124} & 0 & 0 & 0 \\
-w_{1(3)(4)} & 0 & w_{(1)(3)4}+w_{1(3)(4)} & -w_{(1)(3)4} & 0 & -w_{13(4)} & w_{1(3)4} & 0 & 0 & -w_{(1)34} & 0 & 0 & w_{134} & 0 & 0 \\
0 & -w_{2(3)(4)} & w_{(2)(3)4}+w_{2(3)(4)} & -w_{(2)(3)4} & 0 & 0 & 0 & -w_{23(4)} & w_{2(3)4} & -w_{(2)34} & 0 & 0 & 0 & w_{234} & 0 \\
0 & 0 & 0 & 0 & -w_{12(3)(4)} & w_{1(2)3(4)} & -w_{1(2)(3)4} & -w_{(1)23(4)} & w_{(1)2(3)4} & -w_{(1)(2)34} & w_{123(4)} & -w_{12(3)4} & w_{1(2)34} & -w_{(1)234} & w_{1234}
\end{pmatrix} \qquad (4.32)$$

$$\begin{pmatrix}
w_1 & 0 & 0 & 0 & 0 & 0 & 0 & 0 & 0 & 0 & 0 & 0 & 0 & 0 & 0 \\
0 & w_2 & 0 & 0 & 0 & 0 & 0 & 0 & 0 & 0 & 0 & 0 & 0 & 0 & 0 \\
0 & 0 & w_3 & 0 & 0 & 0 & 0 & 0 & 0 & 0 & 0 & 0 & 0 & 0 & 0 \\
0 & 0 & 0 & w_4 & 0 & 0 & 0 & 0 & 0 & 0 & 0 & 0 & 0 & 0 & 0 \\
-w_{1(2)} & w_{(1)2} & 0 & 0 & w_{12} & 0 & 0 & 0 & 0 & 0 & 0 & 0 & 0 & 0 & 0 \\
-w_{1(3)} & 0 & w_{(1)3} & 0 & 0 & w_{13} & 0 & 0 & 0 & 0 & 0 & 0 & 0 & 0 & 0 \\
-w_{1(4)} & 0 & 0 & w_{(1)4} & 0 & 0 & w_{14} & 0 & 0 & 0 & 0 & 0 & 0 & 0 & 0 \\
0 & -w_{2(3)} & w_{(2)3} & 0 & 0 & 0 & 0 & w_{23} & 0 & 0 & 0 & 0 & 0 & 0 & 0 \\
0 & -w_{2(4)} & 0 & w_{(2)4} & 0 & 0 & 0 & 0 & w_{24} & 0 & 0 & 0 & 0 & 0 & 0 \\
0 & 0 & -w_{3(4)} & w_{(3)4} & 0 & 0 & 0 & 0 & 0 & w_{34} & 0 & 0 & 0 & 0 & 0 \\
w_{1(2)(3)} & -w_{(1)2(3)} & w_{(1)(2)3} & 0 & w_{12(3)} & -w_{1(2)3} & 0 & w_{(1)23} & 0 & 0 & w_{123} & 0 & 0 & 0 & 0 \\
w_{1(2)(4)} & -w_{(1)2(4)} & 0 & w_{(1)(2)4} & w_{12(4)} & 0 & -w_{1(2)4} & 0 & w_{(1)24} & 0 & 0 & w_{124} & 0 & 0 & 0 \\
w_{1(3)(4)} & 0 & -w_{(1)3(4)} & w_{(1)(3)4} & 0 & w_{13(4)} & -w_{1(3)4} & 0 & 0 & w_{(1)34} & 0 & 0 & w_{134} & 0 & 0 \\
0 & w_{2(3)(4)} & -w_{(2)3(4)} & w_{(2)(3)4} & 0 & 0 & 0 & w_{23(4)} & -w_{2(3)4} & w_{(2)34} & 0 & 0 & 0 & w_{234} & 0 \\
0 & 0 & 0 & 0 & -w_{12(3)(4)} & w_{1(2)3(4)} & -w_{1(2)(3)4} & -w_{(1)23(4)} & w_{(1)2(3)4} & -w_{(1)(2)34} & w_{123(4)} & -w_{12(3)4} & w_{1(2)34} & -w_{(1)234} & w_{1234}
\end{pmatrix} \qquad (4.33)$$

Massless off-shell box. In the limit $m_1, \ldots, m_4 \to 0$ the symbol alphabet simplifies from 57 letters to 25 letters for even D_0. We have obtained these letters both from our limiting procedure and from the canonical differential equation directly as an independent check. Our limiting procedure only generates a spanning set of letters, using the provided `Mathematica` code one obtains 30 letters. By the discussion in Remark 3.3 about letters containing the Källén function, these 30 letters can be reduced to 25 independent letters. The reduced principal A-determinant in this case contains 12 factors:

$$\begin{aligned}
\Delta_A &= p_1^4p_3^2 - p_1^2p_2^2p_3^2 + p_1^2p_3^4 - p_1^2p_2^2p_4^2 + p_2^4p_4^2 - p_1^2p_3^2p_4^2 - p_2^2p_3^2p_4^2 + p_2^2p_4^4 + p_1^2p_2^2s \\
&\quad - p_1^2p_3^2s - p_2^2p_4^2s + p_3^2p_4^2s - p_1^2p_3^2t + p_2^2p_3^2t + p_1^2p_4^2t - p_2^2p_4^2t - p_1^2st - p_2^2st \\
&\quad - p_3^2st - p_4^2st + s^2t + st^2, \\
\Delta_{A\cap\mathrm{Newt}(\mathcal{F})} &= p_1^4p_3^4 - 2p_1^2p_2^2p_3^2p_4^2 + p_2^4p_4^4 - 2p_1^2p_3^2st - 2p_2^2p_4^2st + s^2t^2, \\
\Delta_{A\cap x_1=0} &= p_2^4 - 2p_2^2p_3^2 + p_3^4 - 2p_2^2t - 2p_3^2t + t^2, \\
\Delta_{A\cap x_2=0} &= p_3^4 - 2p_3^2p_4^2 + p_4^4 - 2p_3^2s - 2p_4^2s + s^2, \\
\Delta_{A\cap x_3=0} &= p_1^4 - 2p_1^2p_4^2 + p_4^4 - 2p_1^2t - 2p_4^2t + t^2, \\
\Delta_{A\cap x_4=0} &= p_1^4 - 2p_1^2p_2^2 + p_2^4 - 2p_1^2s - 2p_2^2s + s^2, \\
\prod_{\text{vertices}} \Delta_v &= stp_1^2p_2^2p_3^2p_4^2.
\end{aligned}$$

Three off-shell legs. If we in addition to taking the masses to zero also impose $p_4^2 \to 0$ the symbol alphabet reduces to 18 letters for D_0 even. The reduced principal A-determinant contains eleven factors in this case

$$\begin{aligned}
\Delta_A &= p_1^2sp_2^2 - p_1^2st + s^2t - sp_2^2t + st^2 + p_1^4p_3^2 - p_1^2sp_3^2 - p_1^2p_2^2p_3^2 - p_1^2tp_3^2 - stp_3^2 + p_2^2tp_3^2 + p_1^2p_3^4, \\
\Delta_{A\cap x_1=0} &= p_2^4 + p_3^4 + t^2 - 2p_2^2p_3^2 - 2p_2^2t - 2p_3^2t, \\
\Delta_{A\cap x_4=0} &= p_1^4 + p_2^4 + s^2 - 2p_1^2p_2^2 - 2p_1^2s - 2p_2^2s, \\
\Delta_{A\cap x_2=0} &= p_3^2 - s, \\
\Delta_{A\cap x_3=0} &= p_1^2 - t, \\
\Delta_\Gamma &= p_1^2p_3^2 - st, \\
\prod_{\text{vertices}} \Delta_v &= stp_1^2p_2^2p_3^2.
\end{aligned}$$

We have now reached a level of reduced kinematics such that the identification between discriminants, determinants and subgraphs discussed in section 3.1 breaks down. The face Γ of $\mathrm{Newt}(\mathcal{G})$ is given by

$$\Gamma = \mathrm{conv}\begin{pmatrix} 1 & 0 & 1 & 0 \\ 0 & 1 & 1 & 0 \\ 1 & 0 & 0 & 1 \\ 0 & 1 & 0 & 1 \end{pmatrix}, \tag{4.34}$$

which should correspond to the box topology since all rows contain non-zero elements. This face actually corresponds to the box with only two off-shell external legs positioned at opposite corners, which also appeared as an example in the introduction. This is clearly not a subgraph of the box with three off-shell legs.

The mathematical origin of this subtlety is described in the following example.

Example 4.2. Let $\mathcal{F} = c_1x_1x_3 + c_2x_2x_4 + c_3x_1x_2 + c_4x_2x_3 + c_5x_3x_4$ where $(c_1, c_2, c_3, c_4, c_5) = (-s, -t, -p_1^2, -p_2^2, -p_3^2)$, this is the $\mathcal{F}$-polynomial of the box with all internal masses zero and three external massive legs. The coefficient matrix of the Jacobian, $\mathscr{J}(\mathcal{F})$, is just the Cayley matrix

$$Y = \begin{pmatrix} 0 & c_3 & c_1 & 0 \\ c_3 & 0 & c_4 & c_2 \\ c_1 & c_4 & 0 & c_5 \\ 0 & c_2 & c_5 & 0 \end{pmatrix}, \qquad \det(Y) = (c_1c_2 - c_3c_5)^2\,, \tag{4.35}$$

whose determinant is clearly reducible. This means that we expect the distinction between punctured affine space and algebraic torus to matter. To correctly calculate the disciminant we would work in the algebraic torus and compute

$$\overline{\left\{c \in \mathbb{C}^5 \mid \frac{\partial \mathcal{F}}{\partial x_1} = \cdots = \frac{\partial \mathcal{F}}{\partial x_4} = 0 \text{ has a solution for } x \in (\mathbb{C}^*)^4\right\}} = \{c \in \mathbb{C}^5 \mid c_4 = c_1c_2 - c_3c_5 = 0\}\,,$$

which has codimension two, meaning that $\Delta_{A\cap\mathrm{Newt}\mathcal{F}}(\mathcal{F}) = 1$ per definition. On the other hand, from linear algebra, we know that the determinant in (4.35) corresponds to working in the punctured affine space, where we obtain

$$\overline{\left\{c \in \mathbb{C}^5 \mid \frac{\partial \mathcal{F}}{\partial x_1} = \cdots = \frac{\partial \mathcal{F}}{\partial x_4} = 0 \text{ has a solution for } x \in \mathbb{C}^4 \setminus \{\mathbf{0}\}\right\}} = \{c \in \mathbb{C}^5 \mid (c_1c_2 - c_3c_5)^2 = 0\};$$

note that the defining polynomial $(c_1c_2 - c_3c_5)^2$ is **not** the desired discriminant. Hence working over the torus rather than the punctured affine space is essential in this example (precisely because $\det(Y)$ is reducible).

Despite these subtleties in the kinematic limits of individual discriminants, in section 3.4 we have provided strong evidence that the entire principal A-determinant does remain well-defined in these limits. In practice, therefore, they do not matter.

4.4 Pentagon graphs and beyond

The generic $n = 5$ or pentagon graph shown below depends on 15 dimensionfull variables, and as we have mentioned, its principal A-determinant consists of 57 different Cayley and Gram determinants, one of each associated to the graph itself (leading Landau singularities of type I and II), and the rest to its subgraphs. For simplicity we will restrict the discussion to the case of even dimension D_0 of loop momenta, but the entire analysis may of course be repeated also for the odd case. By the process of refactorizing these in pairs as described in subsection 3.2, we obtain a total of 166 letters, out of which 16 are genuinely new, and the rest may be obtained by relabeling the letters presented in the previous subsections, as they are associated to subgraphs with $n < 5$. As functions of the masses and Mandelstam invariants, these letters in total contain 26 square roots. Instead of presenting lengthy formulas, we refer the reader to the ancillary file for this new result.

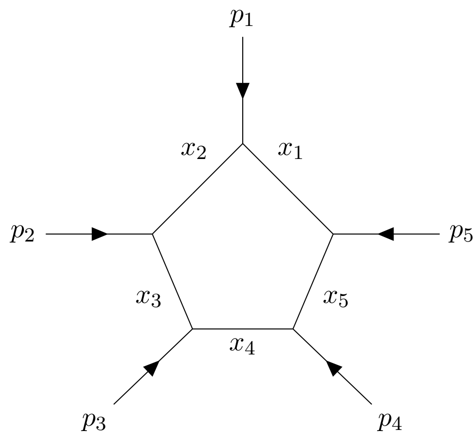

Based on the evidence presented in subsection 3.4, we expect that any other pentagon, where some of its masses or momenta have been identified or set to zero, may be obtained from the generic one by the limiting procedure we have described. In what follows, we will apply it to obtain further new results, as well as to check it against previously computed alphabets.

In particular, we will consider limits where all internal masses, as well as some of the external momenta have been set to zero. Let us start with the case of three offshell external legs, which thus now depends on 8 dimensionful variables. We distinguish two cases, based on whether the all three offshell legs are adjacent ('hard') or not ('easy'), and after taking the corresponding limits of the generic pentagon and eliminating multiplicative relations between letters, we arrive at 57 letters containing 7 square roots, and 54 letters containing 5 square roots, respectively. As far as we are aware of, these alphabets have not appeared in the literature before.

Next, we may continue the limiting process to similarly obtain pentagons where two external legs are offshell. Choosing for example the 'easy' configuration where the offshell legs are not adjacent, for this 7-variable alphabet we obtain 40 letters depending on 3 square roots, and we have checked that it is indeed equivalent to the one previously computed in [78]. Moving on to send another momentum-squared to zero, we land on the 6-variable alphabet of the massless pentagon with one offshell leg, which consists of 30 letters containing 2 square roots. We have also compared our alphabet to the result for the latter reported in [43], again finding perfect agreement.

Finally, let us also briefly discuss the $n = 6$ or hexagon case. As we have mentioned at the end of subsection 3.2, this integral requires us to be in $n > d = 5$ dimensions of external kinematics for all distinct Mandelstam invariants to be algebraically independent, and hence also for the symbol letters to be multiplicatively independent. We will in particular be restricting our attention to the limit where all masses and momenta squared are set to zero, and to the letters exclusively associated to the hexagon graph, and not to its subgraphs. In this limit, the 15 square-root letters of the second type, eq. (3.22) reduce to 3 multiplicatively ones, which now only depend on one square root, whereas all 6 square-root letters of the first type, eq. (3.22), remain multiplicatively independent. Together with the rational letter (3.23), we thus in total have 10 genuinely hexagon letters, and also here we establish their equivalence to their earlier determination in [103]. These checks further solidify the evidence provided in subsection 3.4 on the well-defined nature of the limiting process for principal A-determinants and symbol alphabets, and also support the correctness of the new limiting results we have obtained.

5 Normality, Cohen-Macaulay, and generalized permutohedra

In this section we study several mathematical properties of Feynman integrals. In subsection 5.1, we rigorously prove that the *Cohen-Macaulay* property holds for a larger collection of one-loop Feynman integrals[9] than was previously known; for one loop integrals this generalizes previous results of [104, 105]. As discussed in the introduction, and detailed further below, the physical meaning of the Cohen-Macaulay property is that the number of master integrals for a given topology is independent of the spacetime dimension and of the generalized propagator powers.

In subsection 5.2, we prove that the Newton polytope of the second Symanzik polynomial, as defined in section 2.1, is a *generalized permutohedron* (GP) for a new class of Feynman integrals of arbitrary loop order. The practical utility of this property, is that it facilitates new methods for fast Monte Carlo evaluation of Feynman integrals [7, 8].

The Cohen-Macaulay and GP property are also related to numerous other important properties in the context of toric geometry and the study of the polytopes associated to toric varieties. To better orient the reader, we summarize a selection of these properties and their relations in figure 5. Note that it is in particular the stronger property of *normality*, which implies Cohen-Macaulay, that we will prove in subsection 5.1. It would be very interesting to understand any additional physical implications these properties have for Feynman integrals, for example with respect to their ultraviolet or infrared divergences, however we will not attempt this here.

In the rest of this preamble, for the sake of completeness, we briefly recall the definitions of the properties summarized in figure 5, and further elaborate on the implications of the Cohen-Macaulay property for GKZ-hypergeometric systems and the associated Feynman integrals. Since, in this section, we are aiming for mathematical rigor, its content will inescapably be technical in nature. However, at the beginning of each subsection we will point the reader to the main results, and explain their physical significance.

Generalized hypergeometric systems $H_A(\beta)$, as defined by the matrix in (2.8) and vector in (2.9), have many nice combinatorial and analytic properties. The dimension of the solutions space of $H_A(\beta)$, also referred to as the rank of $H_A(\beta)$, is what physicists would call the number of master integrals. More precisely, for most one-loop integrals the number of master integrals and the rank of $H_A(\beta)$ are exactly the same, for higher loop orders or for special kinematics the rank of the hypergeometric system $H_A(\beta)$ only provides an upper bound on the number of master integrals. For generic β it is a classical result by GKZ

[9] More precisely, this is a property of the toric ideal associated to the Feynman integral, as defined in (2.10).

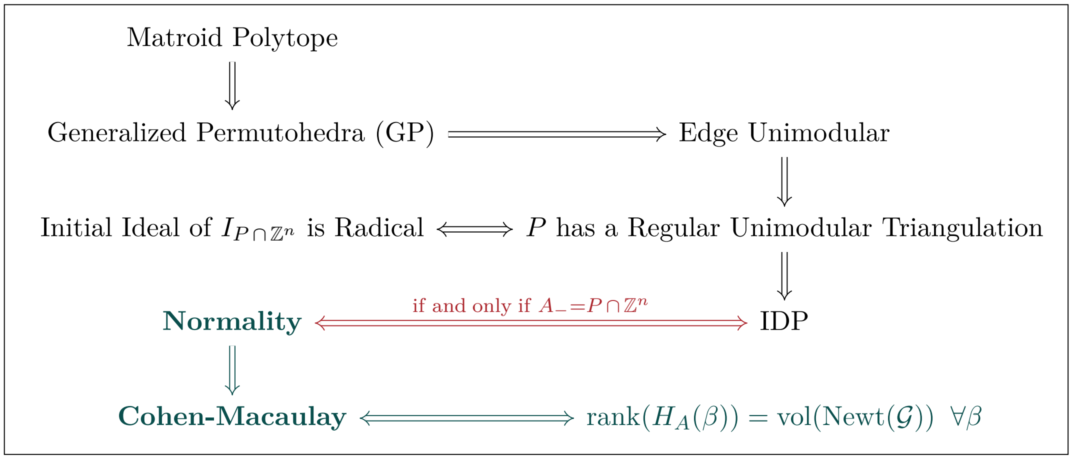

Figure 5. The diagram above considers the relationships between various properties of the hypergeometric system $H_A(\beta)$ arising from the Lee-Pomeransky polynomial $\mathcal{G}$ of a Feynman graph G, with associated semi-group $\mathbb{N}A$ and toric ideal I_A and the associated polytope $P = \text{conv}(A_-)$. The properties in **bold teal colored text** are properties of the toric ideal I_A, the semi-group ring $\mathbb{C}[\mathbb{N}A]$ and the hypergeometic system $H_A(\beta)$; the black plain text properties are properties of the associated polytope. Definitions of a matroid polytope, the Integer Decomposition Property (IDP), and edge unimodularity are given in subsection 5.2. Note that the equivalence (in red) between Normality and IDP holds if and only if $A_- = P \cap \mathbb{Z}^n$.

that the dimension of the solution space is given by the volume of the Newton polytope of $\mathcal{G}$, i.e. $\text{rank}(H_A(\beta)) = \text{vol}(\text{Newt}(\mathcal{G})) = \text{vol}(\text{conv}(A_-))$. However, for actual physical calculations the vector β is non-generic, for example the choice $\beta = (-D/2, -1, \ldots, -1)^T$ of space-time dimension and generalized propagator powers is often used. In order for the equality between the rank and volume of $\text{Newt}(\mathcal{G})$ to hold for every β we need I_A to be *Cohen-Macaulay*. Note that here, and in all other instances, by *volume* we mean *normalized volume*, that is we use the convention that the standard simplex in $\mathbb{R}^n$ has volume 1; that is our volume is $n!$ multiplied by the usual Euclidean volume in $\mathbb{R}^n$.

For our purposes we will define the Cohen-Macaulay property of toric ideals I_A in terms of hypergeometric systems; by doing so we are employing a deep result of [106]. For a definition of the Cohen-Macaulay property for arbitrary polynomial ideals we refer the reader to the book [107]. We say the ideal I_A in $\mathbb{C}[\partial]$ and the semigroup ring $\mathbb{C}[\mathbb{N}A] \cong \mathbb{C}[\partial]/I_A$ are *Cohen-Macaulay* if the associated hypergeometric system $H_A(\beta)$ is such that $\text{rank}(H_A(\beta)) = \text{vol}(\text{conv}(A_-))$ for all β. Hence in particular we have the following equivalence

$$\text{rank}(H_A(\beta)) = \text{vol}(\text{Newt}(\mathcal{G}))\ \forall\beta \Longleftrightarrow I_A \text{ is Cohen} - \text{Macaulay}. \tag{5.1}$$

In subsection 5.1 we prove that for one-loop graphs the semi-group $\mathbb{N}A$ is *normal* for almost every kinematic setup. We say the semi-group $\mathbb{N}A$, and the associated semi-group ring $\mathbb{C}[\mathbb{N}A]$, are *normal* if

$$\mathbb{N}A = \mathbb{Z}A \cap \mathbb{R}_{\geq 0}A.$$

Showing that $\mathbb{N}A$ is normal will in turn imply that the associated toric ideal I_A is Cohen-Macaulay by a result of [108]; hence in particular the relation (5.1) holds.

In the one loop case, with all internal and external masses non-zero and different we get the simple formula for the number of master integrals:

$$\#(\text{master integrals}) = \text{vol}(\text{Newt}(\mathcal{G})) = 2^n - 1. \tag{5.2}$$

This formula has been quoted before, see e.g. [49].

The properties above, namely normality and the Cohen-Macaulay property, are properties of the semi-group $\mathbb{N}A$ and the ring $\mathbb{C}[\mathbb{N}A]$, on the other hand the generalized permutohedra property is a property of a polytope P. A polytope $P \subset \mathbb{R}^n$ is a *generalized permutohedra (GP)* if and only if every edge is parallel to $\mathbf{e}_i - \mathbf{e}_j$ for some $i, j \in \{1, \dots, n\}$, where the $\mathbf{e}_\ell$ denotes the standard basis vectors in $\mathbb{R}^n$. When all lattice points in $P = \text{conv}(A_-)$ are contained in A_- then properties of the polytope, such as the GP property, have relations with those of the semi-group ring $\mathbb{C}[\mathbb{N}A]$; in particular in this case GP implies normality. Assuming $A_- = P \cap \mathbb{Z}^n$, another property which implies that $\mathbb{C}[\mathbb{N}A]$ is normal (and hence Cohen-Macaulay) is if there is some monomial order such that the *initial ideal* of I_{A_-} is radical; more precisely [109, Corollary 8.9] tells us that this is equivalent to P having a *regular unimodular triangulation*, which in turn implies normality. We now briefly recall some of these definitions. A regular triangulation of a polytope $P \subset \mathbb{R}^n$ is called unimodular if it consists only of simplices with volume 1 (recall our convention that a standard simplex has volume 1); for a definition of a regular triangulation see [110, §5.1]. For a polynomial ideal I with *Gröbner basis* $\{g_1, \dots, g_r\}$ in a polynomial ring with some monomial order $<$ the *initial ideal* is the ideal $in_<(I) := \langle in_<(g_1), \dots, in_<(g_r)\rangle$ where $in_<(f)$ is the monomial of a polynomial f which is largest with respect to the ordering $<$, [111, §1.2]. We say an ideal I in a polynomial ring R is *radical* if $I = \sqrt{I}$ where $\sqrt{I} := \{f \in R \mid f^\ell \in I \text{ for some } \ell \in \mathbb{N}\}$. We remind the reader that the key properties defined in the last several paragraphs, and their relations, may be found in figure 5.

5.1 Normality and Cohen-Macaulay for one-loop Feynman graphs

Throughout this subsection we assume that the Feynman graph G under consideration is a one-loop Feynman graph, and employ the notations introduced in section 2 with Symanzik polynomials $\mathcal{U}, \mathcal{F}$ giving $\mathcal{G} = \mathcal{U} + \mathcal{F}$ and $A = \{1\} \times A_- = \{1\} \times \text{Supp}(\mathcal{G})$ as above, see e.g. (2.8). Note that taking $\mathcal{G}_h = \mathcal{U}x_0 + \mathcal{F}$ we have that the matrix $\text{Supp}(\mathcal{G}_h)$ is obtained from A by elementary row operations; hence without loss of generality we may (and will) assume $\text{Supp}(\mathcal{G}_h) = A$.

The main result of this subsection is Theorem 5.4, which proves that the semi-group $\mathbb{N}A$ is normal if and only if we have that

$$p(F_{ij})^2 - m_i^2 - m_j^2 = (p_i + \cdots + p_{j-1})^2 - m_i^2 - m_j^2 \neq 0 \tag{5.3}$$

for all edges i, j where both $m_i \neq 0$ and $m_j \neq 0$; that is, the only cases where normality does not hold are when either all three terms on the right of the above equation are nonzero and the entire right-hand side vanishes, or when $p(F_{ij})^2 = 0$ and the two masses are equal to each other.[10] Hence this condition is sufficient for the Cohen-Macaulay property to hold, see figure 5. Note that if only one of the masses are non-zero, cancellation is allowed and the Cohen-Macaulay property (and even more strongly, normality) will hold. We also wish to highlight that all individual terms in (5.3) are allowed to be zero; this includes the case where all internal propagators are massless for any external kinematics, as illustrated in Corollary 5.6.

For Feynman graphs G of any loop order, but under the assumption of generic (i.e. non-zero) momenta, so that the momentum flow $p(F)$ between the two connected components of any two-forest F of G is nonzero, the Cohen-Macaulay property has been proven in the fully massive case by [105] and for generic (but some times zero) masses by [104].

Our proof in the one loop case is founded on a result of [112]; we begin with the relevant definitions. To a graph we may associate a matrix which catalogs which vertices in a graph are joined by an edge; note that in the discussion which follows this will be a *different* graph than the Feynman graph G.

Definition 5.1 (Edge Matrix)**.** Let $H = (E, V)$ be a finite connected graph with vertex set $V = \{0, \dots, d\}$. If $e = \{i, j\}$ is an edge of H joining vertices i and j we define $\rho(e) \in \mathbb{R}^{d+1}$ by $\rho(e) = \mathbf{e}_i + \mathbf{e}_j$ where $\mathbf{e}_i$ is the ith unit vector in $\mathbb{R}^{d+1}$. Let M be the matrix whose columns correspond to the finite set $\{\rho(e) : \ e \in E\}$, then M is called the *edge matrix* of H and the convex hull of M is called the *edge polytope*.

A result of [112] will tells us that if we can associate a certain graph H to A then the semi-group $\mathbb{N}A$ is normal, hence establishing the desired result. This result is based on verifying the following condition for a graph H.

Definition 5.2 (Odd cycle condition)**.** A cycle in a graph is called *minimal* if it has no chord and it is said to be *odd* if it is a cycle with odd length. A graph H satisfies the *odd cycle condition* if for two arbitrary minimal odd cycles C and C', either C and C' have a common vertex or there is an edge connecting a vertex of C with a vertex of C'.

We may now state a result of [112] which we will apply in Theorem 5.4 below.

Theorem 5.3 (Corollary 2.3, [112])**.** *Let B be the edge matrix of a graph H. The semi-group $\mathbb{N}B$ is normal if and only if the graph H satisfies the odd cycle condition.*

Using the above result we now prove the main result of this section, which gives a precise condition for when the semi-group $\mathbb{N}A$ is normal for the matrix A associated to a one loop Feynman graph; recall that normality of $\mathbb{N}A$ implies the Cohen-Macaulay property holds, see figure 5.

Theorem 5.4. *Let $\mathcal{G}_h = \mathcal{U}x_0 + \mathcal{F}$ be the Symanzik polynomial of a one-loop Feynman diagram G. Then the matrix $A = \mathrm{Supp}(\mathcal{G}_h)$ is the edge matrix of a graph H satisfying the odd cycle condition if and only if we have that*

$$p(F_{ij})^2 - m_i^2 - m_j^2 \neq 0 \tag{5.4}$$

[10] We do not currently have a physical justification for why this is the case, but it would be interesting to address this in the future.

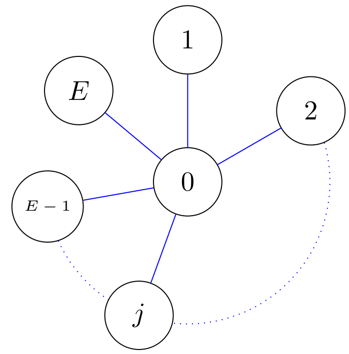

Figure 6. The part of H associated to $\mathcal{U}x_0$. The vertex labels in the graph denote the variable subscript.

for all edges i, j *where both* $m_i \neq 0$ *and* $m_j \neq 0$*. Hence, in particular, the semi-group* $\mathbb{N}A$ *is normal if and only if* (5.4) *holds for all edges* i, j *where both* $m_i \neq 0$ *and* $m_j \neq 0$*.*

Proof. First consider the structure of the matrix $A = \mathrm{Supp}(\mathcal{G}_h)$ for our one loop Feynman diagram G. Since we have exactly one loop in the diagram G then the exponent vectors of $\mathcal{U}$, which correspond to the spanning trees of G, are obtained by removing exactly one edge from the loop in G, and the exponent records this removed edge giving an identity matrix obtained from the monomials of $\mathcal{U}$. In other words, this means that the exponents of $\mathcal{U}$ are the indicator vectors of the bases of the co-graphic matroid of $M^*(G)$ of G. The matrix obtained from $\mathcal{U}x_0$ is then an identity matrix with a row of ones added on top:

$$\begin{pmatrix} 1 & \cdots & 1 \\ & \mathbf{1}_E & \end{pmatrix}$$

where $\mathbf{1}_E$ is the $E \times E$-identity matrix.

Hence the matrix A is the edge matrix (as in Definition 5.1) of a graph H. The part of A arising from $\mathcal{U}$ gives $E+1$ vertices of H and exactly one edge between the central vertex (corresponding to the exponent of x_0 in $\mathcal{U}x_0$). We now construct the graph H in three steps; the first step adds the vertices and edges arising from $\mathcal{U}x_0$, this step is illustrated in figure 6.

Now consider the columns of A arising from exponents of $\mathcal{F}_0$. The polynomial $\mathcal{F}_0$ has no monomials which contain x_0, hence the first entry of all columns of A arising from $\mathcal{F}_0$ is 0. In our one loop diagram, to obtain a 2-forest we remove 2 edges, and the monomials in $\mathcal{F}_0$ record these two edges which have been removed, it follows these columns contain exactly two 1s. Hence the columns of A arising from $\mathcal{F}_0$ contain two ones and a zero in the first entry. This will lead to connected edges between pairs of vertices on the circular arc. Each such connection will yield a new minimal odd three cycle, as illustrated in figure 7. It follows that the graph H obtained by this addition will satisfy the odd-cycle condition (Definition 5.2).

Now we consider the consequences of adding massive particles, that is edges with an associated mass in the Feynman graph G. In the polynomial $\mathcal{G}_h$ the addition of a massive

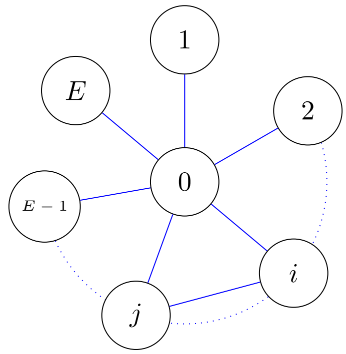

Figure 7. The part of H associated to $\mathcal{U}x_0$ with edges added corresponding to monomials of $\mathcal{F}_0$. One such edge is illustrated connected the vertices i and j below.

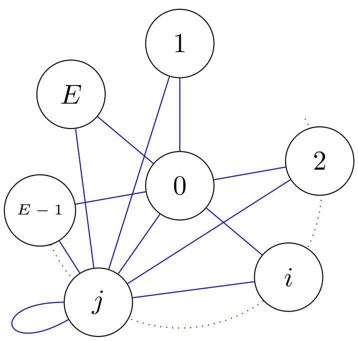

Figure 8. The part of H associated to $\mathcal{U}x_0$ with edges added from Equation (5.5). The term x_j^2 correspond to the self loop and the other terms connect j to every other vertex in H satisfying (5.4).

edge in G corresponds to the following product of polynomials

$$(x_1 + x_2 + \cdots + x_E) \cdot m_j^2 x_j; \tag{5.5}$$

this will contain the monomials $x_i x_j,\ i \neq j$ and x_j^2. The square term corresponds to adding a loop at vertex j of H. This odd-cycle is connected to vertex 0 by a simple edge and thus at most separated by one edge from every odd-cycle corresponding to terms $x_i x_j,\ i \neq j$. Assume now that we have two internal masses, $m_i \neq 0$ and $m_j \neq 0$, then the loops they create at vertex i resp. j have to be connected by an edge for the odd-cycle condition to hold. This is true if and only if (5.4) holds, i.e. if and only if the corresponding term in $\mathcal{F}_0 + \mathcal{F}_m$ is non-vanishing.

Since the graph H satisfies the odd-cycle condition it has edge matrix A, the algebra $\mathbb{N}A$ is normal by Theorem 5.3. □

We now illustrate this result on an example which is guaranteed to be normal, and hence Cohen-Macaulay, by the result of Theorem 5.4 but for which the earlier results of [105] and [104] do not apply.

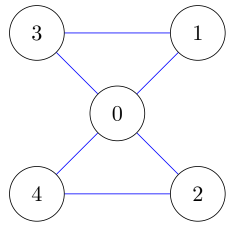

Figure 9. The edge graph in Example 5.5; as before the vertex labels denote variable subscripts.

Example 5.5. The arguments in [104, 105] rest on the assumption that for every proper subset $V' \subset V_{\text{ext}}$ we have $(\sum_{v\in V'} p_v)^2 \neq 0$. For on-shell massless diagrams this assumption fails, e.g. since $p_v^2 = 0$ for every $v \in V_{\text{ext}}$. This means for example that the on-shell massless box-diagram with homogeneous Lee-Pomeransky polynomial

$$\mathcal{G}_h = x_0(x_1 + x_2 + x_3 + x_4) - s x_1 x_3 - t x_2 x_4 \tag{5.6}$$

is not covered by any of the previous results but is still normal due to Theorem 5.4. The edge graph associated to $\mathcal{G}_h$ is shown in figure 9 which clearly satisfy the odd-cycle condition implying, by Theorem 5.4, that the semi-group $\mathbb{N}A$ is normal, and hence the Cohen-Macaulay property holds (see also figure 5). The number of master integrals can thus be calculated simply as $\text{vol}(\text{Newt}(\mathcal{G}_h)) = 3$ which corresponds to the box integral itself along with the s- and t-channel bubble integrals.

We especially note the following corollary of Theorem 5.4.

Corollary 5.6. *If G is a one-loop Feynman graph with $m_e = 0$ for all edges $e \in E$, i.e. $\mathcal{F}_m = 0$, or at most one edge has a non-zero mass. Then $\mathbb{N}A$ is normal for all possible external kinematics.*

Even though we have primarily discussed the Cohen-Macaulay property, the result above as well as the papers [104, 105] focus on proving normality of $\mathbb{N}A$ which is a stronger criteria, see figure 5. Going to special kinematics one may find Feynman integrals with the Cohen-Macaulay property but which are not normal as well as two-loop integrals where even the Cohen-Macaulay property fails [104].

5.2 Generalized permutohedra

We again employ the notations introduced in section 2 with Symanzik polynomials $\mathcal{U}, \mathcal{F}$ giving $\mathcal{G} = \mathcal{U} + \mathcal{F}$. The main contributions of this subsection are Proposition 5.10 and Theorem 5.11. Reinterpreting earlier results in the literature, in essence they demonstrate that the polytope $\text{Newt}(\mathcal{F})$[11] of a Feynman graph of arbitrary order is a generalized permutohedron (GP) if: 1) all internal propagators are massive for any external kinematics in the former case; 2) every vertex can be connected to an external vertex by a path of propagators that are all massive, and the graph is one-particle and one-vertex irreducible, with all external momenta offshell/massive in the latter case. This enlarges the class of integrals previously known to be GP [113], as we will also review in what follows.

[11] It is well-known that $\text{Newt}(\mathcal{U})$ is always GP, see the discussion after Proposition 5.9.

The *permutohedron* is a classical polytope with many special properties, for example, it is a simple zonotope, the monotone path polytope of a cube [110] and the secondary polytope of a triangular prism $\Delta(1,2)\times\Delta(1,n)$, see [65]. More recently the *generalized permutohedron* (GP) was introduced by Postnikov [114], and it was shown by Aguiar and Ardila that these polytopes are universal combinatorial representatives for a vast class of Hopf monoids [115]. In the physical context generalized permutohedra have facilitated new methods for fast Monte Carlo evaluation of Feynman integrals [7, 8].

Simply put, a generalized permutohedron is any polytope whose normal fan is a coarsening of a permutohedron's normal fan. In the context of establishing normality of a polytope or semi-group, the following classification is more useful.

Theorem 5.7 ([115, Theorem 12.3])**.** *A polytope $P\subset\mathbb{R}^n$ is a generalized permutohedra if and only if every edge is parallel to $\mathbf{e}_i-\mathbf{e}_j$ for some $i,j\in\{1,\dots,n\}$.*

A *matroid polytope* is the convex hull of the indicator vectors of all bases of matroid; note these vectors have entries 0 or 1 only. We will say that a polytope has the GP property if Theorem 5.7 is satisfied. This especially means that every matroid polytope [116, 117] has the GP property and that every polytope with the GP property is *edge-unimodular*, i.e., the matrix of edge-directions is unimodular.

As used in this paper, normality of a set of lattice points $A=\{1\}\times A_-\subset\mathbb{Z}^{n+1}$ is a property of the semi-group $\mathbb{N}A$ while the GP property is associated to a polytope. Even if $P=\operatorname{conv}(A_-)$, there is a priori no direct connection between the two properties, however, if A_- is the full set of lattice points in P, i.e.,

$$A_-=P\cap\mathbb{Z}^n \tag{5.7}$$

then GP implies normality. This is because every polytope with the GP property also has the *integer decomposition property* (IDP):

Definition 5.8 (Integer decomposition property)**.** A polytope $P\subset\mathbb{R}^n$ is said to have the *integer decomposition property* (IDP) if for every $k\in\mathbb{Z}_{>0}$ it satisfies

$$kP\cap\mathbb{Z}^n=P\cap\mathbb{Z}^n+(k-1)P\cap\mathbb{Z}^n. \tag{5.8}$$

By a result of Howard (see, [118], cf. [119]) every edge-unimodular polytope, and therefore especially every GP, has the IDP property. The significance of the IDP property in our setting is that it is equivalent to A being normal if $A_-=P\cap\mathbb{Z}^n$.

Proposition 5.9. *Let $P\subset\mathbb{R}^n$ be a polytope and $A_-=P\cap\mathbb{Z}^n$, then P has the IDP if and only if $A=\{1\}\times A_-$ is normal.*

Proof. Assume P has the IDP, then for every integer $k>0$ we have that $a\in kP\cap\mathbb{Z}^n$ implies there exists $a_1,\dots,a_k\in A_-$ such that $a=a_1+\dots+a_k$. By the construction of A we may choose a basis for $\mathbb{Z}A$ such that the first coordinate is 1 and the remaining entries are a basis for $\mathbb{Z}A_-$. An arbitrary point in $\mathbb{Z}A\cap\mathbb{R}_{\geq 0}A\subset\mathbb{Z}^{n+1}$ has the form (k,a) for some integer $k>0$ and where $a\in\mathbb{Z}A_-$, but $A_-=P\cap\mathbb{Z}^n$, so $a\in kP$ and the IDP implies that $a = a_1 + \cdots + a_k$ for some $a_1, \cdots, a_k \in A_-$ and thus $(k, a) = (1, a_1) + \cdots + (1, a_k)$. Therefore normality is proven.

Now, assume that $\mathbb{N}A$ is normal, that is, we can write every element $(k, a) \in \mathbb{R}_{\geq 0}A \cap \mathbb{Z}A$ as $(k, a) = (1, a_1) + \cdots + (1, a_k)$ for $a_1, \ldots, a_k \in A_-$; this directly implies the IDP. □

By definition $\mathrm{Newt}(\mathcal{U})$ is the matroid polytope of the dual matroid to the Feynman graph, meaning that not only does $\mathrm{Newt}(\mathcal{U})$ have the GP property but also $\mathrm{Supp}(\mathcal{U}) = \mathrm{Newt}(\mathcal{U}) \cap \mathbb{Z}^n$ so the semi-group generated by $\mathrm{Supp}(\mathcal{U})$ is normal.

Properties connected to the $\mathcal{F}$-polynomial are much more intricate as they are always dependent on the kinematic setup and not just on the underlying graph, however, some general statements are known. For example, Schultka proved in [113] that $\mathrm{Newt}(\mathcal{F})$ is a GP in the Euclidean regime with generic kinematics. Here we provide a slight generalization:

Proposition 5.10. *Assume $m_e \neq 0$ for all $e \in E$, then $\mathrm{Newt}(\mathcal{F})$ is a GP for all possible choices of external kinematics.*

The proof of this statement is contained in [105] but not in reference to the GP property. We state it here for completeness.

Proof. When all internal masses are non-zero all vertices of $\mathrm{Newt}(F)$ must always come from $\mathcal{U} \cdot \sum_{e\in E} m_e^2 x_e \subset \mathcal{F}$, i.e.

$$\mathrm{Newt}(\mathcal{F}) = \mathrm{Newt}\left(\mathcal{U} \cdot \sum_{e\in E} m_e^2 x_e\right) = \mathrm{Newt}\left(\mathcal{U}\right) + \mathrm{Newt}\left(\sum_{e\in E} m_e^2 x_e\right). \tag{5.9}$$

Since $\mathrm{Newt}\left(\sum_{e\in E} m_e^2 x_e\right)$ is just the standard simplex $\Delta(1, n)$, which is a GP, and $\mathrm{Newt}(\mathcal{U})$ is a GP, this means that $\mathrm{Newt}(\mathcal{F})$ is a GP since the GP property is closed under Minkowski addition [115]. □

Another case is contained in [105], assume all internal masses are zero, i.e. $m_e = 0$ for all $e \in E$, and that every two-forest of G comes with a non-zero coefficient. This last assumption means that $V = V_{\text{ext}}$ and that $p(V')^2 \neq 0$ for all $V' \subset V$ where $p(V') = \sum_{v\in V'} p_v$. For this setup $\mathrm{Newt}(\mathcal{F})$ is a matroid polytope and hence a GP.

This result was generalized by Walther in [104] where he managed to remove the assumption $V_{\text{ext}} = V$. He showed that $\mathrm{Newt}(\mathcal{F})$ is a matroid polytope, and hence GP, if $m_e = 0$ for all $e \in E$ and $p(V')^2 \neq 0$ for all $V' \subset V_{\text{ext}}$. The assumption placed on the external momenta essentially means that they behave as Euclidean vectors in the sense that (i) $p_v^2 \neq 0$ for all $v \in V_{\text{ext}}$ and (ii) $(p_v + p_u)^2 \neq 0$ for all $u, v \in V_{\text{ext}}$. Neither of these two assumptions are true in the general Minkowski setting.

As long as the equality

$$\mathrm{Newt}(\mathcal{F}) = \mathrm{Newt}\left(\mathcal{U} \cdot \sum_{e\in E} m_e^2 x_e\right) \tag{5.10}$$

holds for a Feynman graph (with at least one $m_e \neq 0$), it is clear that $\mathrm{Newt}(\mathcal{F})$ is a GP by the arguments in the proof of Proposition 5.10. This can be rephrased to the statement, that a sufficient condition for Newt($\mathcal{F}$) to be a GP is that $\mathrm{Supp}(\mathcal{F}_0) \subseteq \mathrm{Supp}(\mathcal{F}_m)$. Since the terms in $\mathcal{F}_0$ come from the two-forests of the graph, one way this can be true is if $\mathcal{F}_m$ contains terms from all two-forests. This is guaranteed if every vertex of G is connected to an external vertex by a massive path, i.e. a path of consecutive edges all with non-zero mass.

Theorem 5.11 (Theorem 4.5 in [104])**.** *Let G be a one-particle irreducible and one-vertex irreducible Feynman graph such that no cancellation between $\mathcal{F}_0$ and $\mathcal{F}_m$ occurs and $p(V') \neq 0$ for all $V' \subset V_{\mathrm{ext}}$. Then every term in $\mathcal{F}_0$ also appears in $\mathcal{F}_m$ (i.e. $\mathrm{Supp}(\mathcal{F}_0) \subseteq \mathrm{Supp}(\mathcal{F}_m)$) if and only if every $v \in V$ has a massive path to an external vertex $v' \in V_{\mathrm{ext}}$.*

A direct consequence is that Newt($\mathcal{F}$) is a GP for every Feynman graph satisfying Proposition 5.10 or Theorem 5.11. In addition to the GP property being a desirable property, see for example the discussion at the beginning of this section, GP also implies the Cohen-Macaulay property holds, see figure 5, and hence that the number of master integrals may be calculated from the volume of the associated polytope independent of generalized propagator powers and space time dimension.

6 Conclusions and outlook

In this paper we have recast the problem of determining the symbol alphabet of a polylogarithmic Feynman integral as the question of factorizing its principal A-determinant, which encodes its Landau singularities and may be obtained independently of the standard procedure of its analytic evaluation. We have primarily studied one-loop Feynman integrals. Our main results are the formulas for their symbol alphabet (3.21)–(3.23) and canonical differential equations (3.32)–(3.33) together with a `Mathematica` code for their automatic evaluation, as well as the proof that normality, and hence the Cohen-Macaulay property, holds in Theorem 5.4. These results are complimented with the limiting procedure for specialized kinematics in subsection 3.4, also implemented in `Mathematica`, and a discussion of the generalized permutohedron in subsection 5.2.

While the main focus of this paper is on one-loop graphs we are also optimistic that the approach to obtaining the symbol letters via the principal A-determinant described in this note will also apply in more generality. To this end we conclude with a simple example of a two-loop graph where the principal A-determinant gives the symbol alphabet. We consider the slashed box with two different choices for one off-shell leg.

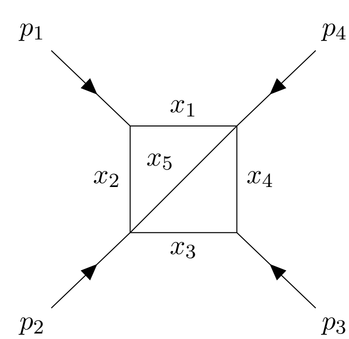

The first Symanzik polynomial is independent of the kinematics and is therefore the same in all the following different cases:

$$\mathcal{U} = x_1x_3 + x_1x_4 + x_1x_5 + x_2x_3 + x_2x_4 + x_2x_5 + x_3x_5 + x_4x_5. \tag{6.1}$$

The simplest one-mass case is the off-shell leg being connected to the internal diagonal, e.g. $p_2^2 \neq 0$ while $p_1^2 = p_3^2 = p_4^2 = 0$. This gives the $\mathcal{F}$-polynomial

$$\mathcal{F} = -sx_1x_3x_5 - tx_2x_4x_5 - p_2^2x_2x_3x_5. \tag{6.2}$$

The Newton polytope Newt($\mathcal{F}$) is not a generalized permutohedron (GP) and Newt($\mathcal{G}$) is not edge-unimodular, however, I_A has a radical initial ideal and therefore Newt($\mathcal{G}$) has a regular unimodular triangulation so $\mathbb{N}A$ is normal. At one-loop and with generic kinematics this means that the number of master integrals equals the volume of Newt($\mathcal{G}$). This is no longer true at two loops, since Gale duality is no longer enough to fix all coefficients in $\mathcal{U}$ to be one, as required for Feynman integrals. The physically interesting case now is a restriction ideal of $H_A(\beta)$. In physical variables (and with all coefficients in $\mathcal{U}$ one) we obtain that the reduced principal A-determinant is:

$$\widetilde{E_A}(\mathcal{G}) = (p_2^2 - s - t)(p_2^2 - s)(p_2^2 - t)stp_2^2.$$

With the three variables $z_1 = s/p_2^2,\ z_2 = t/p_2^2$ and z_3 satisfying $z_1 + z_2 + z_3 = 1$ we get

$$\widetilde{E_A}(\mathcal{G}) \propto z_3(1 - z_1)(1 - z_2)z_1z_2. \tag{6.3}$$

These five factors constitute all but one letter in the symbol alphabet for two-dimensional harmonic polylogarithms [120], known to be the appropriate class of functions for describing all four-point two-loop master integrals with one offshell leg, and hence also the slashed box integrals discussed here.

The other one-mass configuration has $\mathcal{F}$-polynomial

$$\mathcal{F} = -sx_1x_3x_5 - tx_2x_4x_5 - p_1^2x_1x_2(x_3 + x_4 + x_5).$$

Again Newt($\mathcal{F}$) is not GP and Newt($\mathcal{G}$) is not edge-unimodular, however, I_A has a radical initial ideal and therefore Newt($\mathcal{G}$) has a regular unimodular triangulation. So $\mathbb{N}A$ is normal, where A is the support of $\mathcal{G}$,

$$A = \begin{pmatrix} 1&1&1&1&1&1&1&1&1&1&1&1&1 \\ 1&1&1&0&0&0&0&0&1&0&1&1&1 \\ 0&0&0&1&1&1&0&0&0&1&1&1&1 \\ 1&0&0&1&0&0&1&0&1&0&1&0&0 \\ 0&1&0&0&1&0&0&1&0&1&0&1&0 \\ 0&0&1&0&0&1&1&1&1&1&0&0&1 \end{pmatrix}. \tag{6.4}$$

As before we use the physically relevant setup and work in physical variables. The reduced principal A-determinant is:

$$\widetilde{E_A}(\mathcal{G}) = (p_1^2 - t)(p_1^2 - s)(p_1^2 - s - t)(s + t)stp_1^2.$$

With the same change of variables as before (but with p_2 taking the role of p_1) we get

$$\widetilde{E_A}(\mathcal{G}) \propto (1-z_2)(1-z_1)z_3(1-z_3)z_1z_2, \tag{6.5}$$

which is the *full symbol alphabet for the two-dimensional harmonic polylogarithms*.

At this level the discriminants which needed to be calculated are quite sizeable. For example, not only does the full A-discriminant in this case have degree 14, but the discriminant corresponding to the face

$$A \cap \Gamma = \begin{pmatrix} 1&1&1&1&1&1&1&1&1&1 \\ 1&1&0&0&0&0&1&0&1&1 \\ 0&0&1&1&0&0&0&1&1&1 \\ 1&0&1&0&1&0&1&0&1&0 \\ 0&1&0&1&0&1&0&1&0&1 \\ 0&0&0&0&1&1&1&1&0&0 \end{pmatrix} \tag{6.6}$$

has degree 20. Even though computational complexity grows quickly at higher loops, and we have the fact that the physically interesting ideals will be restriction ideals of $H_A(\beta)$, this nontrivial two-loop example of the two-loop slashed box integral with one offshell leg not only shows that its principal A-determinant may still be computed directly; but also that it yields the full symbol alphabet of the integral in question.

Acknowledgments

We have benefited from stimulating discussions with Ekta Chaubey, Einan Gardi, Sebastian Mizera, Ben Page and Simone Zoia. GP and FT acknowledge support from the Deutsche Forschungsgemeinschaft under Germany's Excellence Strategy – EXC 2121 "Quantum Universe" – 390833306. While preparing this work Martin Helmer was partially supported by the Air Force Office of Scientific Research under award number FA9550-22-1-0462.

References

[1] S. Weinberg, *The quantum theory of fields. Vol. 1: Foundations*, Cambridge University Press (2005) [DOI:10.1017/CBO9781139644167] [INSPIRE].

[2] Z. Bern et al., *Scattering Amplitudes and the Conservative Hamiltonian for Binary Systems at Third Post-Minkowskian Order*, Phys. Rev. Lett. **122** (2019) 201603 [arXiv:1901.04424] [INSPIRE].

[3] C. Dlapa et al., *Radiation Reaction and Gravitational Waves at Fourth Post-Minkowskian Order*, Phys. Rev. Lett. **130** (2023) 101401 [arXiv:2210.05541] [INSPIRE].

[4] J. Zinn-Justin, *Quantum field theory and critical phenomena*, vol. 171, Oxford University Press (2021).

[5] S. Borowka et al., *pySecDec: a toolbox for the numerical evaluation of multi-scale integrals*, Comput. Phys. Commun. **222** (2018) 313 [arXiv:1703.09692] [inSPIRE].

[6] A.V. Smirnov, N.D. Shapurov and L.I. Vysotsky, *FIESTA5: Numerical high-performance Feynman integral evaluation*, Comput. Phys. Commun. **277** (2022) 108386 [arXiv:2110.11660] [inSPIRE].

[7] M. Borinsky, *Tropical Monte Carlo quadrature for Feynman integrals*, arXiv:2008.12310 [DOI:10.4171/AIHPD/158] [inSPIRE].

[8] M. Borinsky, H.J. Munch and F. Tellander, *Tropical Feynman integration in the Minkowski regime*, Comput. Phys. Commun. **292** (2023) 108874 [arXiv:2302.08955] [inSPIRE].

[9] R.N. Lee, *LiteRed 1.4: a powerful tool for reduction of multiloop integrals*, J. Phys. Conf. Ser. **523** (2014) 012059 [arXiv:1310.1145] [inSPIRE].

[10] A.V. Smirnov and F.S. Chuharev, *FIRE6: Feynman Integral REduction with Modular Arithmetic*, Comput. Phys. Commun. **247** (2020) 106877 [arXiv:1901.07808] [inSPIRE].

[11] A. von Manteuffel and C. Studerus, *Reduze 2 - Distributed Feynman Integral Reduction*, arXiv:1201.4330 [inSPIRE].

[12] P. Maierhöfer and J. Usovitsch, *Kira 1.2 Release Notes*, arXiv:1812.01491 [inSPIRE].

[13] E. Panzer, *Algorithms for the symbolic integration of hyperlogarithms with applications to Feynman integrals*, Comput. Phys. Commun. **188** (2015) 148 [arXiv:1403.3385] [inSPIRE].

[14] C. Duhr and F. Dulat, *PolyLogTools — polylogs for the masses*, JHEP **08** (2019) 135 [arXiv:1904.07279] [inSPIRE].

[15] M. Prausa, *epsilon: A tool to find a canonical basis of master integrals*, Comput. Phys. Commun. **219** (2017) 361 [arXiv:1701.00725] [inSPIRE].

[16] O. Gituliar and V. Magerya, *Fuchsia: a tool for reducing differential equations for Feynman master integrals to epsilon form*, Comput. Phys. Commun. **219** (2017) 329 [arXiv:1701.04269] [inSPIRE].

[17] C. Meyer, *Algorithmic transformation of multi-loop master integrals to a canonical basis with CANONICA*, Comput. Phys. Commun. **222** (2018) 295 [arXiv:1705.06252] [inSPIRE].

[18] C. Dlapa, J. Henn and K. Yan, *Deriving canonical differential equations for Feynman integrals from a single uniform weight integral*, JHEP **05** (2020) 025 [arXiv:2002.02340] [inSPIRE].

[19] R.N. Lee, *Libra: A package for transformation of differential systems for multiloop integrals*, Comput. Phys. Commun. **267** (2021) 108058 [arXiv:2012.00279] [inSPIRE].

[20] A.V. Belitsky, A.V. Smirnov and V.A. Smirnov, *MB tools reloaded*, Nucl. Phys. B **986** (2023) 116067 [arXiv:2211.00009] [inSPIRE].

[21] B. Jantzen, A.V. Smirnov and V.A. Smirnov, *Expansion by regions: revealing potential and Glauber regions automatically*, Eur. Phys. J. C **72** (2012) 2139 [arXiv:1206.0546] [inSPIRE].

[22] T. Peraro, *FiniteFlow: multivariate functional reconstruction using finite fields and dataflow graphs*, JHEP **07** (2019) 031 [arXiv:1905.08019] [inSPIRE].

[23] L.D. Landau, *On analytic properties of vertex parts in quantum field theory*, Nucl. Phys. **13** (1959) 181 [inSPIRE].

[24] R.E. Cutkosky, *Singularities and discontinuities of Feynman amplitudes*, *J. Math. Phys.* **1** (1960) 429 [INSPIRE].

[25] R.J. Eden, P.V. Landshoff, D.I. Olive and J.C. Polkinghorne, *The analytic S-matrix*, Cambridge University Press, Cambridge (1966) [INSPIRE].

[26] T. Regge, *Algebraic Topology Methods in the Theory of Feynman Relativistic Amplitudes*, in the proceedings of the *Battelle rencontres - 1967 lectures in mathematics and physics*, New York, NY (1968), pp. 433–458.

[27] M. Kashiwara and T. Kawai, *Holonomic Systems of Linear Differential Equations and Feynman Integrals*, *Publ. Res. Inst. Math. Sci. Kyoto* **12** (1977) 131 [INSPIRE].

[28] M. Kashiwara, T. Kawai and T. Ōshima, *A Study of Feynman Integrals by Micro Differential Equations*, *Commun. Math. Phys.* **60** (1978) 97 [INSPIRE].

[29] I.M. Gel'fand, A.V. Zelevinskii and M.M. Kapranov, *Hypergeometric functions and toral manifolds*, *Funct. Anal. Appl.* **23** (1989) 94.

[30] L. de la Cruz, *Feynman integrals as A-hypergeometric functions*, *JHEP* **12** (2019) 123 [arXiv:1907.00507] [INSPIRE].

[31] R.P. Klausen, *Hypergeometric Series Representations of Feynman Integrals by GKZ Hypergeometric Systems*, *JHEP* **04** (2020) 121 [arXiv:1910.08651] [INSPIRE].

[32] A. Klemm, C. Nega and R. Safari, *The l-loop Banana Amplitude from GKZ Systems and relative Calabi-Yau Periods*, *JHEP* **04** (2020) 088 [arXiv:1912.06201] [INSPIRE].

[33] B. Ananthanarayan, S. Banik, S. Bera and S. Datta, *FeynGKZ: A Mathematica package for solving Feynman integrals using GKZ hypergeometric systems*, *Comput. Phys. Commun.* **287** (2023) 108699 [arXiv:2211.01285] [INSPIRE].

[34] A.V. Kotikov, *Differential equations method: New technique for massive Feynman diagrams calculation*, *Phys. Lett. B* **254** (1991) 158 [INSPIRE].

[35] E. Remiddi, *Differential equations for Feynman graph amplitudes*, *Nuovo Cim. A* **110** (1997) 1435 [hep-th/9711188] [INSPIRE].

[36] T. Gehrmann and E. Remiddi, *Differential equations for two loop four point functions*, *Nucl. Phys. B* **580** (2000) 485 [hep-ph/9912329] [INSPIRE].

[37] J.M. Henn, *Multiloop integrals in dimensional regularization made simple*, *Phys. Rev. Lett.* **110** (2013) 251601 [arXiv:1304.1806] [INSPIRE].

[38] K.-T. Chen, *Iterated path integrals*, *Bull. Am. Math. Soc.* **83** (1977) 831 [INSPIRE].

[39] A.B. Goncharov, *Multiple polylogarithms and mixed Tate motives*, math/0103059 [INSPIRE].

[40] A.B. Goncharov, *Galois symmetries of fundamental groupoids and noncommutative geometry*, *Duke Math. J.* **128** (2005) 209 [math/0208144] [INSPIRE].

[41] K.G. Chetyrkin and F.V. Tkachov, *Integration by Parts: The Algorithm to Calculate beta Functions in 4 Loops*, *Nucl. Phys. B* **192** (1981) 159 [INSPIRE].

[42] A.B. Goncharov, M. Spradlin, C. Vergu and A. Volovich, *Classical Polylogarithms for Amplitudes and Wilson Loops*, *Phys. Rev. Lett.* **105** (2010) 151605 [arXiv:1006.5703] [INSPIRE].

[43] S. Abreu et al., *Two-Loop Integrals for Planar Five-Point One-Mass Processes*, *JHEP* **11** (2020) 117 [arXiv:2005.04195] [INSPIRE].

[44] T. Dennen, M. Spradlin and A. Volovich, *Landau Singularities and Symbology: One- and Two-loop MHV Amplitudes in SYM Theory*, *JHEP* **03** (2016) 069 [arXiv:1512.07909] [INSPIRE].

[45] I. Prlina, M. Spradlin and S. Stanojevic, *All-loop singularities of scattering amplitudes in massless planar theories*, *Phys. Rev. Lett.* **121** (2018) 081601 [arXiv:1805.11617] [INSPIRE].

[46] J. Collins, *A new and complete proof of the Landau condition for pinch singularities of Feynman graphs and other integrals*, arXiv:2007.04085 [INSPIRE].

[47] S. Mizera, *Crossing symmetry in the planar limit*, *Phys. Rev. D* **104** (2021) 045003 [arXiv:2104.12776] [INSPIRE].

[48] R.P. Klausen, *Kinematic singularities of Feynman integrals and principal A-determinants*, *JHEP* **02** (2022) 004 [arXiv:2109.07584] [INSPIRE].

[49] S. Mizera and S. Telen, *Landau discriminants*, *JHEP* **08** (2022) 200 [arXiv:2109.08036] [INSPIRE].

[50] H.S. Hannesdottir, A.J. McLeod, M.D. Schwartz and C. Vergu, *Implications of the Landau equations for iterated integrals*, *Phys. Rev. D* **105** (2022) L061701 [arXiv:2109.09744] [INSPIRE].

[51] M. Correia, A. Sever and A. Zhiboedov, *Probing multi-particle unitarity with the Landau equations*, *SciPost Phys.* **13** (2022) 062 [arXiv:2111.12100] [INSPIRE].

[52] H.S. Hannesdottir, A.J. McLeod, M.D. Schwartz and C. Vergu, *Constraints on sequential discontinuities from the geometry of on-shell spaces*, *JHEP* **07** (2023) 236 [arXiv:2211.07633] [INSPIRE].

[53] L. Lippstreu, M. Spradlin and A. Volovich, *Landau Singularities of the 7-Point Ziggurat I*, arXiv:2211.16425 [INSPIRE].

[54] M. Berghoff and E. Panzer, *Hierarchies in relative Picard-Lefschetz theory*, arXiv:2212.06661 [INSPIRE].

[55] X. Jiang and L.L. Yang, *Recursive structure of Baikov representations: Generics and application to symbology*, *Phys. Rev. D* **108** (2023) 076004 [arXiv:2303.11657] [INSPIRE].

[56] S. Weinzierl, *Feynman Integrals*, arXiv:2201.03593 [DOI:10.1007/978-3-030-99558-4] [INSPIRE].

[57] R.N. Lee and A.A. Pomeransky, *Critical points and number of master integrals*, *JHEP* **11** (2013) 165 [arXiv:1308.6676] [INSPIRE].

[58] L. Nilsson and M. Passare, *Mellin Transforms of Multivariate Rational Functions*, *J. Geom. Anal.* **23** (2011) 24.

[59] C. Berkesch, J. Forsgård and M. Passare, *Euler-Mellin integrals and A-hypergeometric functions*, *Michigan Math. J.* **63** (2014) 101.

[60] I.M. Gel'fand, *General theory of hypergeometric functions*, *Dokl. Akad. Nauk SSSR* **288** (1986) 14.

[61] I.M. Gel'fand, M.I. Graev and A.V. Zelevinskiĭ, *Holonomic systems of equations and series of hypergeometric type*, *Dokl. Akad. Nauk SSSR* **295** (1987) 14.

[62] I.M. Gelfand, M.M. Kapranov and A.V. Zelevinsky, *Generalized Euler integrals and A-hypergeometric functions*, *Adv. Math.* **84** (1990) 255.

JHEP10(2023)161

[63] I.M. Gelfand, M.M. Kapranov and A.V. Zelevinsky, *A correction to the paper "hypergeometric functions and toric varieties"*, Funct. Anal. Appl. **27** (1994) 295.

[64] A. Adolphson, *Hypergeometric functions and rings generated by monomials*, Duke Math. J. **73** (1994) 269.

[65] I.M. Gel'fand, M. Kapranov and A. Zelevinskĭ, *Discriminants, resultants, and multidimensional determinants*, Springer Science & Business Media (2008).

[66] E. Cattani, *Three lectures on hypergeometric functions*, https://people.math.umass.edu/~cattani/hypergeom_lectures.pdf.

[67] M. Saito, B. Sturmfels and N. Takayama, *Gröbner Deformations of Hypergeometric Differential Equations*, Springer Berlin Heidelberg (2000) [DOI:10.1007/978-3-662-04112-3].

[68] D. Eisenbud and B. Sturmfels, *Binomial ideals*, Duke Math. J. **84** (1996) 1.

[69] J.C. Polkinghorne and G.R. Screaton, *The analytic properties of perturbation theory — I*, Nuovo Cim. **15** (1960) 289 [INSPIRE].

[70] J.C. Polkinghorne and G.R. Screaton, *The analytic properties of perturbation theory — II*, Nuovo Cim. **15** (1960) 925 [INSPIRE].

[71] M. Helmer and B. Sturmfels, *Nearest points on toric varieties*, Math. Scand. **122** (2018) 213.

[72] D.A. Cox, J. Little and D. O'Shea, *Ideals, Varieties, and Algorithms*, Springer International Publishing (2015) [DOI:10.1007/978-3-319-16721-3].

[73] R.N. Lee, *Reducing differential equations for multiloop master integrals*, JHEP **04** (2015) 108 [arXiv:1411.0911] [INSPIRE].

[74] R.N. Lee and A.A. Pomeransky, *Normalized Fuchsian form on Riemann sphere and differential equations for multiloop integrals*, arXiv:1707.07856 [INSPIRE].

[75] S. Fomin and A. Zelevinsky, *Cluster algebras I: Foundations*, Journal of the American Mathematical Society **15** (2001) 497.

[76] D. Chicherin, J.M. Henn and G. Papathanasiou, *Cluster algebras for Feynman integrals*, Phys. Rev. Lett. **126** (2021) 091603 [arXiv:2012.12285] [INSPIRE].

[77] S. He, Z. Li and Q. Yang, *Kinematics, cluster algebras and Feynman integrals*, arXiv:2112.11842 [INSPIRE].

[78] S. He, J. Liu, Y. Tang and Q. Yang, *The symbology of Feynman integrals from twistor geometries*, arXiv:2207.13482 [INSPIRE].

[79] J. Golden et al., *Motivic Amplitudes and Cluster Coordinates*, JHEP **01** (2014) 091 [arXiv:1305.1617] [INSPIRE].

[80] J. Drummond, J. Foster and Ö. Gürdoğan, *Cluster Adjacency Properties of Scattering Amplitudes in $N = 4$ Supersymmetric Yang-Mills Theory*, Phys. Rev. Lett. **120** (2018) 161601 [arXiv:1710.10953] [INSPIRE].

[81] G. Papathanasiou, *The SAGEX review on scattering amplitudes Chapter 5: Analytic bootstraps for scattering amplitudes and beyond*, J. Phys. A **55** (2022) 443006 [arXiv:2203.13016] [INSPIRE].

[82] J.O.S.H.U.A.S. SCOTT, *Grassmannians and cluster algebras*, Proc. London Math. Soc. **92** (2006) 345.

[83] D.B. Melrose, *Reduction of Feynman diagrams*, Nuovo Cim. **40** (1965) 181 [INSPIRE].

[84] P.A.M. Dirac, *Wave equations in conformal space*, *Annals Math.* **37** (1936) 429 [INSPIRE].

[85] S. Abreu, R. Britto, C. Duhr and E. Gardi, *Cuts from residues: the one-loop case*, *JHEP* **06** (2017) 114 [arXiv:1702.03163] [INSPIRE].

[86] C. D'Andrea and M. Sombra, *The Cayley-Menger determinant is irreducible for $n \geq 3$*, *Sib. Math. J.* **46** (2005) 71.

[87] K. Aomoto, *Analytic structure of Schläfli function*, *Nagoya Math. J.* **68** (1977) 1.

[88] R. Hirota, *The Direct Method in Soliton Theory*, Cambridge University Press (2004) [DOI:10.1017/cbo9780511543043].

[89] A.I. Davydychev and R. Delbourgo, *Geometrical approach to the evaluation of multileg Feynman diagrams*, *Acta Phys. Polon. B* **29** (1998) 2891 [hep-th/9806248] [INSPIRE].

[90] V. Mitev and Y. Zhang, *SymBuild: a package for the computation of integrable symbols in scattering amplitudes*, arXiv:1809.05101 [INSPIRE].

[91] O.V. Tarasov, *Connection between Feynman integrals having different values of the space-time dimension*, *Phys. Rev. D* **54** (1996) 6479 [hep-th/9606018] [INSPIRE].

[92] R.N. Lee, *Space-time dimensionality D as complex variable: Calculating loop integrals using dimensional recurrence relation and analytical properties with respect to D*, *Nucl. Phys. B* **830** (2010) 474 [arXiv:0911.0252] [INSPIRE].

[93] S. Abreu, R. Britto, C. Duhr and E. Gardi, *Diagrammatic Hopf algebra of cut Feynman integrals: the one-loop case*, *JHEP* **12** (2017) 090 [arXiv:1704.07931] [INSPIRE].

[94] J. Chen, C. Ma and L.L. Yang, *Alphabet of one-loop Feynman integrals*, *Chin. Phys. C* **46** (2022) 093104 [arXiv:2201.12998] [INSPIRE].

[95] M. Spradlin and A. Volovich, *Symbols of One-Loop Integrals From Mixed Tate Motives*, *JHEP* **11** (2011) 084 [arXiv:1105.2024] [INSPIRE].

[96] N. Arkani-Hamed and E.Y. Yuan, *One-Loop Integrals from Spherical Projections of Planes and Quadrics*, arXiv:1712.09991 [INSPIRE].

[97] J.L. Bourjaily, E. Gardi, A.J. McLeod and C. Vergu, *All-mass n-gon integrals in n dimensions*, *JHEP* **08** (2020) 029 [arXiv:1912.11067] [INSPIRE].

[98] P.A. Baikov, *Explicit solutions of the multiloop integral recurrence relations and its application*, *Nucl. Instrum. Meth. A* **389** (1997) 347 [hep-ph/9611449] [INSPIRE].

[99] W. Flieger and W.J. Torres Bobadilla, *Landau and leading singularities in arbitrary space-time dimensions*, arXiv:2210.09872 [INSPIRE].

[100] S. Abreu, R. Britto, C. Duhr and E. Gardi, *Algebraic Structure of Cut Feynman Integrals and the Diagrammatic Coaction*, *Phys. Rev. Lett.* **119** (2017) 051601 [arXiv:1703.05064] [INSPIRE].

[101] E. Remiddi and J.A.M. Vermaseren, *Harmonic polylogarithms*, *Int. J. Mod. Phys. A* **15** (2000) 725 [hep-ph/9905237] [INSPIRE].

[102] B.G. Nickel, *Evaluation of Simple Feynman Graphs*, *J. Math. Phys.* **19** (1978) 542 [INSPIRE].

[103] J.M. Henn, A. Matijašić and J. Miczajka, *One-loop hexagon integral to higher orders in the dimensional regulator*, *JHEP* **01** (2023) 096 [arXiv:2210.13505] [INSPIRE].

[104] U. Walther, *On Feynman graphs, matroids, and GKZ-systems*, *Lett. Math. Phys.* **112** (2022) 120 [arXiv:2206.05378] [INSPIRE].

[105] F. Tellander and M. Helmer, *Cohen-Macaulay Property of Feynman Integrals*, *Commun. Math. Phys.* **399** (2023) 1021 [arXiv:2108.01410] [INSPIRE].

[106] L. Matusevich, E. Miller and U. Walther, *Homological methods for hypergeometric families*, *Journal of the American Mathematical Society* **18** (2005) 919.

[107] W. Bruns and H.J. Herzog, *Cohen-Macaulay Rings*, Cambridge University Press (1998) [DOI:10.1017/cbo9780511608681].

[108] M. Hochster, *Rings of Invariants of Tori, Cohen-Macaulay Rings Generated by Monomials, and Polytopes*, *Annals Math.* **96** (1972) 318.

[109] B. Sturmfels, *Gröbner Bases and Convex Polytopes*, American Mathematical Society (1995) [DOI:10.1090/ulect/008].

[110] G.M. Ziegler, *Lectures on polytopes*, vol. 152, Springer Science & Business Media (2012).

[111] M. Michałek and B. Sturmfels, *Invitation to nonlinear algebra*, *Graduate Studies in Mathematics* **211** (2021).

[112] H. Ohsugi and T. Hibi, *Normal Polytopes Arising from Finite Graphs*, *J. Algebra* **207** (1998) 409.

[113] K. Schultka, *Toric geometry and regularization of Feynman integrals*, arXiv:1806.01086 [INSPIRE].

[114] A. Postnikov, *Permutohedra, Associahedra, and Beyond*, *Int. Math. Res. Not.* **2009** (2009) 1026.

[115] M. Aguiar and F. Ardila, *Hopf monoids and generalized permutahedra*, arXiv:1709.07504.

[116] I.M. Gelfand, R.M. Goresky, R.D. MacPherson and V.V. Serganova, *Combinatorial geometries, convex polyhedra, and schubert cells*, *Adv. Math.* **63** (1987) 301.

[117] I.M. Gel'fand and V.V. Serganova, *Combinatorial geometries and the strata of a torus on homogeneous compact manifolds*, *Uspekhi Mat. Nauk* **42** (1987) 107.

[118] B.J. Howard, *Matroids and Geometric Invariant Theory of torus actions on flag spaces*, *J. Algebra* **312** (2007) 527.

[119] B.J. Howard, *Edge unimodular polytopes in mini-Workshop: Projective Normality of Smooth Toric Varieties*, vol. 4 (2007), pp. 2283–2319.

[120] T. Gehrmann and E. Remiddi, *Two loop master integrals for $\gamma* \to 3$ jets: The Planar topologies*, *Nucl. Phys. B* **601** (2001) 248 [hep-ph/0008287] [INSPIRE].

Paper II

Cohen-Macaulay Propert of Feynman Integrals
Felix Tellander and Martin Helmer
Commun. Math. Phys. **399** (2023) 1021–1037, [2108.01410]

Commun. Math. Phys. 399, 1021–1037 (2023)
Digital Object Identifier (DOI) https://doi.org/10.1007/s00220-022-04569-6

Communications in
Mathematical Physics

Cohen-Macaulay Property of Feynman Integrals

Felix Tellander[1], **Martin Helmer**[2]

[1] Deutsches Elektronen-Synchrotron DESY, Notkestr. 85, 22607 Hamburg, Germany.
E-mail: felix@tellander.se
[2] Mathematical Sciences Institute, The Australian National University, Canberra, Australia.
E-mail: mhelmer@ncsu.edu

Received: 19 August 2021 / Accepted: 8 November 2022
Published online: 10 December 2022 –

Abstract: The connection between Feynman integrals and GKZ A-hypergeometric systems has been a topic of recent interest with advances in mathematical techniques and computational tools opening new possibilities; in this paper we continue to explore this connection. To each such hypergeometric system there is an associated toric ideal, we prove that the latter has the Cohen-Macaulay property for two large families of Feynman integrals. This implies, for example, that both the number of independent solutions and dynamical singularities are independent of space-time dimension and generalized propagator powers. Furthermore, in particular, it means that the process of finding a series representation of these integrals is fully algorithmic.

1. Introduction

Much of our understanding of physical amplitudes in quantum field theory is tied to their perturbative expansion in terms of Feynman diagrams. This makes Feynman diagrams and their associated integrals central objects in quantum field theory [14,36,42]. The analytic view of Feynman integrals is as old as the integrals themselves, e.g. to guarantee causality they are often continued into the complex plane in a predetermined manner. An algebraic viewpoint is not as common in physics, even though it has been known for a some time [28], see also [16]. Recently the algebraic methods of Gelfand, Kapranov and Zelevinski [15–17,19], using what are now called GKZ A-hypergeometric systems, in tandem with the Lee-Pomeransky representation of Feynman integrals [31] have attracted interest (see e.g. [5,10,13,29,30] also [27]), partially due to the computational utility of this perspective. In this paper we focus on the study of Feynman integrals using this GKZ A-hypergeometric system point of view.

Throughout this paper we will assume that the underlying Feynman graph G is two-edge connected, or in common physics terminology, G is one particle irreducible (1PI). This means that at least two edges in the graph have to be cut for the graph to become disconnected. This is not a substantial restriction from a physical point of view as any connected amplitude can be factored into its 1PI components [3,11,14,35,36]. Moreover, all integrals are assumed to be dimensionally regularized with generalized dimension D.

More precisely we consider scalar Feynman integrals arising from a 1PI Feynman diagram, i.e. a graph $G = (V, E)$ where each edge is labeled with a mass m_e, momentum k_e, and propagator $1/(k_e^2 - m_e^2)$ and certain vertices are labeled with a momentum $p(v)$. This set of distinguished vertices are called external vertices, V_{ext}, and are required to satisfy momentum conservation $\sum_{v\in V_{\text{ext}}} p(v) = 0$. Such integrals can be converted to the *Lee-Pomeransky* form, which is the standard form we will use here. For a graph G we work over $\mathbb{R}^{|E|}$ where $|E|$ is the size of the edge set E of the graph G. We will also define the Symanzik polynomials $\mathcal{U}$ and $\mathcal{F}$ associated to G, cf. [4]. The polynomial $\mathcal{U}$ is obtained by summing over all spanning trees in G and for each such tree adding a monomial consisting of all variables whose edge is not in the spanning tree, to obtain $\mathcal{F}$ we sum a polynomial depending on $\mathcal{U}$ with one obtained by summing over spanning two-forests of G. Given a spanning two-forest $F = (T, T')$ of G set $p(F) = \sum_{v\in T\cap V_{\text{ext}}} p(v)$. In symbols the *Symanzik polynomials* are:

$$\mathcal{U} = \sum_{\substack{T \text{ a spanning} \\ \text{tree of } G}} \prod_{e\notin T} x_e, \tag{1}$$

$$\mathcal{F} = \mathcal{F}_m + \mathcal{F}_0 = \mathcal{U} \sum_{e\in E} m_e^2 x_e + \sum_{\substack{F \text{ a spanning} \\ 2-\text{forest of } G}} |p(F)|^2 \prod_{e\notin F} x_e, \tag{2}$$

where m_e is the mass associated to the edge e and $|p(F)|^2$ is obtained from the Wick rotation of the Lorentz form $p(F)^2 \to -|p(F)|^2$. If the Wick rotation is undone, we consider the Euclidean reagion s.t. $p(F)^2 < 0$ for every F.

Our main result is a theorem stating that in many cases the Newton polytope $P = \text{Newt}(\mathcal{U} + \mathcal{F})$ (cf. (4)) associated to a Feynman integral is normal. This proves a weaker version of the conjecture about existence of unimodular triangulations proposed in [29] for our considered classes of diagrams. When working with Feynman integrals from the GKZ A-hypergeometric system perspective we will also associate an ideal I_A to such a system. Our main result will directly imply that this ideal I_A is Cohen-Macaulay; this in turn has several important theoretical and computational consequences which are discussed in more depth in Section 1.1.

Theorem 1.1 *(Main Theorem). Let $G = (V, E)$ be a Feynman diagram with associated Symanzik polynomials $\mathcal{U}$ and $\mathcal{F}$. Set $\mathcal{G} = \mathcal{U}+\mathcal{F}$, then the Newton polytope $P_G = \text{Newt}(\mathcal{G})$ is normal if either*

- *$m_e \neq 0$ for all $e \in E$, or*
- *$m_e = 0$ for all $e \in E$ and every vertex is connected to an external off-shell leg, i.e. $p_v^2 \neq 0$ for every $v \in V = V_{\text{ext}}$.*

The second case especially includes all polygon diagrams like the triangle, box or pentagon.

We prove this theorem in two parts, the massive case is treated in Theorem 3.1 and the massless case in Theorem 3.5. In short, this result means that not only can we expect the hypergeometric systems associated to a Feynman diagram to have desirable mathematical properties, but additionally we can expect that the associated Gröbner deformation will be straightforward to compute, allowing us to obtain series solutions effectively in an algorithmic manner.

1.1. Feynman integrals and hypergeometric systems. Let $b \in \mathbb{Z}_{\geq 0}^{|E|}$ be an integral vector, and $D \in \mathbb{R}$; after conversion to Lee-Pomeransky form the Feynman integral associated to the graph G is the integral $\mathfrak{I}_G(D, b)$ given by

$$\mathfrak{I}_G(D, b) := \frac{\Gamma(D/2)}{\Gamma(D/2 - \varsigma)\Gamma(b_1)\cdots\Gamma(b_{|E|})} \int_{\mathbb{R}_{>0}^{|E|}} \frac{x_1^{b_1-1}\cdots x_{|E|}^{b_{|E|}-1}}{\mathcal{G}(x)^{D/2}} dx_1 \cdots dx_{|E|} \quad (3)$$

where $\mathcal{G} = \mathcal{U} + \mathcal{F}$, and $\varsigma := \sum_i b_i - L \cdot D/2$ with L the number of independent cycles in the graph G.

Suppose that for a given Feynman diagram G the polynomial $\mathcal{G}$ has the form $\mathcal{G} = \sum_{i=1}^r \tilde{c}_i x^{a_i}$. Note that the $\tilde{c}_i$ are explicitly given constants determined by the momenta, masses and graph structure. To consider this as an A-hypergoemtric system we will instead take the coefficients as undetermined parameters and consider $\mathcal{G} = \sum_{i=1}^r c_i x^{a_i}$ as a polynomial in the ring $\mathbb{Q}(D)[c_1, \ldots, c_r][x_1, \ldots, x_{|E|}]$, this recovers our original polynomial $\mathcal{U} + \mathcal{F}$ in $\mathbb{Q}(D)[x_1, \ldots, x_{|E|}]$ when we set $c_i = \tilde{c}_i$. We abuse notation and use $\mathcal{U}$, $\mathcal{F}$, and $\mathcal{G}$ to denote both the polynomials in $\mathbb{Q}(D)[c_1, \ldots, c_r][x_1, \ldots, x_{|E|}]$ and the resulting polynomial in $\mathbb{Q}(D)[x_1, \ldots, x_{|E|}]$ when we set $c_i = \tilde{c}_i$. The polynomial $\mathcal{G}$ determines an $(|E| + 1) \times r$ integer matrix A obtained by adding a row of ones above the matrix with column vectors the exponents a_i of $\mathcal{G}$:

$$A = A_- \times \{1\} := \begin{pmatrix} 1 & 1 & \cdots & 1 & 1 \\ a_1 & a_2 & \cdots & a_{r-1} & a_r \end{pmatrix} \in \mathbb{N}^{(|E|+1)\times r}, \quad (4)$$

where $A_- = \begin{pmatrix} a_1 & a_2 & \cdots & a_{r-1} & a_r \end{pmatrix} \in \mathbb{N}^{|E|\times r}$ is the matrix whose columns are the exponent vectors of $\mathcal{G}$. We will refer to the Newton polytope of $\mathcal{G}$, $\mathrm{Newt}(\mathcal{G}) = \mathrm{conv}(\{a_1, \ldots, a_r\})$, defined by the convex hull of the vectors as the *Symanzik polytope*. We suppose this polytope is given in half-space representation as

$$\mathrm{Newt}(\mathcal{G}) = \bigcap_{i=1}^{N} \left\{ \sigma \in \mathbb{R}^{|E|} \mid \langle \mu_i, \sigma \rangle \leq \nu_i \right\} \quad (5)$$

where $\mu_i \in \mathbb{R}^{|E|}$, $\nu \in \mathbb{R}^N$.

Now return to considering the Feynman integral $\mathfrak{I}_G(D, b; c)$, which we now take as a function of c since we consider $\mathcal{G}$ as a polynomial in $\mathbb{Q}(D)[c_1, \ldots, c_r][x_1, \ldots, x_{|E|}]$. The integral $\mathfrak{I}_G(D, b; c)$ is a special case of a so called *Euler-Mellin integral*; it is shown in [2] that such integrals admit a meromorphic continuation, giving

$$\mathfrak{I}_G(D, b; c) = \Phi(D, b; c) \prod_{i=1}^{N} \Gamma(\nu_i D/2 - \langle \mu_i, b \rangle) \quad (6)$$

for some function Φ entire in D and b; note ν, μ are as in (5). We will also define a vector β determined by the vector b and the value D appearing in the Feynman integral in Lee-Pomeransky form (3), that is

$$\beta = \begin{pmatrix} -D/2 \\ -b_1 \\ \vdots \\ -b_{|E|} \end{pmatrix}. \tag{7}$$

The function $\Phi(D, b; c)$ is a GKZ A-hypergeometric function of c and satisfies the GKZ A-hypergeometric system $H_A(\beta)$, which we now define. Let $W = \mathbb{Q}(D)[c_1, \ldots, c_r, \partial_1, \ldots, \partial_r]$ be a Weyl algebra with ∂_i denoting the differential operator association to c_i (i.e. ∂_i acts as differentiation by c_i on a polynomial in $\mathbb{Q}[c_1, \ldots, c_r]$) and let $I_A = \langle \partial^u - \partial^v \mid Au = Av \rangle$ be the *toric ideal* in $\mathbb{Q}[\partial_1, \ldots, \partial_r]$ defined by the matrix A as in (4) above; the toric ideal is a prime binomial ideal and such ideals define toric varieties, see [40, Chapter 4]. Writing $A = [a_{i,j}]$, the system $H_A(\beta)$ is a left ideal $H_A(\beta) := I_A + Z_A(\beta)$ in W where

$$Z_A(\beta) = \left\langle \sum_{j=1}^{r} a_{i,j} c_j \partial_j - \beta_i \mid i = 1, \ldots, |E| + 1 \right\rangle. \tag{8}$$

Finding a basis consisting of holomorphic functions for the space of solutions to the A-hypergeometric system $H_A(\beta)$ gives an expression for $\Phi(D, b; c)$, and hence an expression for the Feynman integral $\mathfrak{I}_G(D, b; c)$. By the Cauchy-Kowalevskii-Kashiwara Theorem (see also [38, Theorem 1.4.19]) the dimension of the complex vector space of solutions to the system $H_A(\beta)$ in a neighbourhood of a smooth point is equal to $\text{rank}(H_A(\beta))$, the *holonomic rank* of the ideal $H_A(\beta)$. Results of [1,16], see also [38, Theorem 4.3.8], tell us that if the toric ideal I_A is Cohen-Macaulay for a given A then $\text{rank}(H_A(\beta)) = (|E|!) \cdot \text{vol}(\text{conv}(A))$ and the singular points where solutions to the system $H_A(\beta)$ do not exist are independent of β. In fact an even stronger statement is shown in [32], in particular in [32, Theorem 1.1] it is shown that the toric ideal I_A being Cohen-Macaulay for a given A is *equivalent* to $\text{rank}(H_A(\beta))$ being constant and independent of β.

A basis for the solution space to the system $H_A(\beta)$ may be computed using techniques described in [38, Chapter 3]. An important step in this computation is finding the *Gröbner deformation* of $H_A(\beta)$ with respect to a generic *weight vector* $\omega \in \mathbb{R}^r$, denoted $\text{in}_{(-\omega,\omega)}(H_A(\beta))$. This is also greatly simplified in the case I_A is Cohen-Macaulay since in this case

$$\text{in}_{(-\omega,\omega)}(H_A(\beta)) = Z_A(\beta) + \text{in}_\omega(I_A), \tag{9}$$

[38, Theorem 4.3.8], where the later expression $\text{in}_\omega(I_A)$ is the *initial ideal* (or lead term ideal) of I_A. The initial ideal of I_A can be computed directly from a Gröbner basis of I_A, which is in turn straightforward to obtain using standard methods. We obtain the appropriate weight vectors ω by computing the Gröbner fan of I_A and choosing a (generic) representative vector ω from each cone in the Gröbner fan of I_A, an efficient procedure (and accompanying software implementation) for computing this Gröbner fan of such a toric ideal is detailed in [25]. Gröbner fans can also be computed using the package Gfan [26], we make use of this implementation via it's Macualay2 [20] interface in Section 1.2 below. Note we only need to take a generic weight vector in one Gröbner cone to obtain a series solution, however each cone in the fan will give a different series solution with a different domain of convergence meaning it may be advantageous to consider different cones for physical reasons related to the desired domain of convergence. We also note that solutions to the A-hypergeometric system $H_A(\beta)$ can take the form of logarithms, not just power series, see, for example, [37].

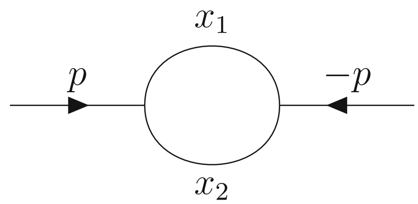

Fig. 1. Feynman diagram G for the massive bubble. There are two edges, with mass m_1 associated to the edge x_1, and m_2 associated to the edge x_2 and two vertices with (external) momenta p and $-p$, respectively

1.2. Example. We illustrate this process on the Feynman diagram G shown in Figure 1. For further reading on the techniques employed in our example we recommend the book [38].

In D dimensions the classical presentation for the Feynman integral for the diagram in Figure 1 is

$$\mathfrak{I} = \int \frac{d^D k}{\pi^{D/2}} \frac{1}{k^2 - m_1^2} \frac{1}{(k-p)^2 - m_2^2}. \tag{10}$$

After Wick-rotating, introducing Feynman parameters and integrating over the loop momenta, this integral can be written in the Lee-Pomeransky form (up to some factors of π and i), as in (3) with $b = (1, 1)$ as

$$\mathfrak{I}_G(D, b) = \mathfrak{I}_G(D, (1,1)) = \frac{\Gamma(D/2)}{\Gamma(D-2)} \int_{\mathbb{R}_+^2} (\mathcal{U}(x) + \mathcal{F}(x))^{-D/2} dx_1 dx_2, \tag{11}$$

$$\mathcal{U}(x) = x_1 + x_2,\ \mathcal{F}(x) = (m_1^2 + m_2^2 + |p|^2)x_1x_2 + m_1^2x_1^2 + m_2^2x_2^2 \tag{12}$$

where $|p|^2 > 0$ is the Euclidean norm obtained by Wick rotation: $p^2 \to -|p|^2$. This integral is a special case of the Euler-Mellin integral which admits the meromorphic continuation

$$\int_{\mathbb{R}_+^2} (\mathcal{U} + \mathcal{F})^{-D/2} dx_1 dx_2 = \Gamma(2 - D/2)\Gamma(D-2)\Phi(D) \tag{13}$$

where $\Phi(D)$ is an entire analytic function. Treating all the coefficients of the polynomial $\mathcal{U} + \mathcal{F}$ as arbitrary coefficients c_i, gives

$$\mathcal{G}(x, c) = \mathcal{U}(x, c) + \mathcal{F}(x, c) = c_1x_1 + c_2x_2 + c_3x_1x_2 + c_4x_1^2 + c_5x_2^2.$$

Then the function $\Phi(D; c)$ associated to the resulting integral

$$\mathfrak{I}_G(D, 1; c) = \int_{\mathbb{R}_+^2} \mathcal{G}(x, c)^{-D/2} dx_1 dx_2 = \Gamma(2 - D/2)\Gamma(D-2)\Phi(D; c) \tag{14}$$

is A-hypergeometric as a function of c and satisfies the A-hypergeometric system $H_A(\beta)$ with

$$A = \begin{pmatrix} 1 & 1 & 1 & 1 & 1 \\ 1 & 0 & 1 & 2 & 0 \\ 0 & 1 & 1 & 0 & 2 \end{pmatrix} = \{1\} \times \mathrm{Newt}(\mathcal{G}), \quad \beta = \begin{pmatrix} -D/2 \\ -1 \\ -1 \end{pmatrix}. \tag{15}$$

Now let W be the Weyl algebra

$$W = \mathbb{Q}(D)[c_1, \ldots, c_5, \partial_1, \ldots, \partial_5]. \tag{16}$$

Then the A-hypergemoetric system $H_A(\beta) = Z_A(\beta) + I_A$ is the left-ideal in W defined by

$$I_A = \left\langle \partial_3^2 - \partial_4\partial_5,\ \partial_2\partial_3 - \partial_1\partial_5,\ \partial_1\partial_3 - \partial_2\partial_4 \right\rangle \tag{17}$$

$$Z_A(\beta) = \begin{cases} c_1\partial_1 + c_2\partial_2 + c_3\partial_3 + c_4\partial_4 + c_5\partial_5 = \beta_1 \\ c_1\partial_1 + c_3\partial_3 + 2c_4\partial_4 = \beta_2 \\ c_2\partial_2 + c_3\partial_3 + 2c_5\partial_5 = \beta_3 \end{cases} \tag{18}$$

where I_A is the toric ideal in ∂_i defined by A. Since m_1 and m_2 are assumed to be non-zero, Theorem 1.1 guarantees that the polytope $\mathrm{conv}(A)$ is normal which in particular implies that I_A is Cohen-Macaulay. For $(-\omega, \omega) \in \mathbb{R}^{10}$ the Cohen-Macaulay property of I_A guarantees that the Gröbner deformation of $H_A(\beta)$ can be decomposed as

$$\mathrm{in}_{(-\omega,\omega)}(H_A(\beta)) = Z_A(\beta) + \mathrm{in}_\omega(I_A). \tag{19}$$

The procedure for constructing a series solutions to $H_A(\beta)$ consists of solving the system given by the Gröbner deformation $\mathrm{in}_{(-\omega,\omega)}(H_A(\beta))$ and lifting these solutions to $H_A(\beta)$ by attaching them to a Γ-series.

The solutions to $\mathrm{in}_{(-\omega,\omega)}(H_A(\beta))$ will be monomials $c^u = c_1^{u_1} \cdots c_5^{u_5}$, $u \in \mathbb{C}^5$. The toric ideal I_A has a Gröbner fan consisting of seven top-dimensional cones, meaning that there are seven distinct initial ideals $\mathrm{in}_\omega(I_A)$. If we choose weight vector $\omega = (0, 0, -2, 1, 1)$, then I_A has the reduced Gröbner basis

$$\{(\partial_2\partial_4) - \partial_1\partial_3,\ (\partial_1\partial_5) - \partial_2\partial_3,\ (\partial_4\partial_5) - \partial_3^2\} \tag{20}$$

where the monomials marked with parentheses generates $\mathrm{in}_\omega(I_A)$. If c^u is a solution of the initial system, then the exponent vectors must satisfy

$$u_2u_4 = u_1u_5 = u_4u_5 = 0, \tag{21}$$

$$\begin{pmatrix} 1 & 1 & 1 & 1 & 1 \\ 1 & 0 & 1 & 2 & 0 \\ 0 & 1 & 1 & 0 & 2 \end{pmatrix} \begin{pmatrix} u_1 \\ u_2 \\ u_3 \\ u_4 \\ u_5 \end{pmatrix} = \begin{pmatrix} -D/2 \\ -1 \\ -1 \end{pmatrix}. \tag{22}$$

The Cohen-Macaulay property of I_A guarantees that the number of solutions to these equations is the normalized volume of the polytope $\mathrm{conv}(A)$, i.e., these six equations have three solutions:

$$\begin{aligned} u^{(1)} &= \left(2 - D,\ 0,\ -1,\ D/2 - 1,\ 0\right) \\ u^{(2)} &= \left(0,\ 2 - D,\ -1,\ 0,\ D/2 - 1\right) \\ u^{(3)} &= \left(1 - D/2,\ 1 - D/2,\ D/2 - 2,\ 0,\ 0\right). \end{aligned} \tag{23}$$

The three monomials $c^{u^{(1)}}, c^{u^{(2)}}, c^{u^{(3)}}$ generate the solution space of $\mathrm{in}_{(-\omega,\omega)}(H_A(\beta))$ and can be lifted to solutions of $H_A(\beta)$ as

$$\phi^{(i)} = \sum_{v\in N^{(i)}} \frac{\Gamma(u^{(i)}+1)}{\Gamma(u^{(i)}+v+1)} c^{u^{(i)}+v}, \quad \text{with,} \tag{24}$$

$$\begin{aligned}N^{(1)} &= \{v = m(-1,1,1,0,-1) + n(2,-2,0,-1,1),\\ &\quad m,n\in\mathbb{Z} \mid m \geq 2n,\ m\leq 0,\ n\geq m\},\\ N^{(2)} &= \{v = m(-1,1,1,0,-1) + n(2,-2,0,-1,1),\\ &\quad m,n\in\mathbb{Z} \mid 2n \geq m,\ m\leq 0,\ n\leq 0\},\ \text{and}\\ N^{(3)} &= \{v = m(-1,1,1,0,-1) + n(2,-2,0,-1,1),\ m,n\in\mathbb{Z} \mid n\leq 0,\ n\geq m\},\end{aligned}$$

where $(-1,1,0,-1)$ and $(2,-2,0,-1,1)$ span the integral kernel of A and the inequalities guarantee that the quotients of Γ-functions are always well-defined. A solution $\Phi(D;c)$ to the hypergeometric system $H_A(\beta)$ can now be written as $\Phi(D;c) = K_1\phi^{(1)} + K_2\phi^{(2)} + K_3\phi^{(3)}$. The coefficients K_i must be such that the meromorphic continuation on the right hand side of (14) matches the left hand side on the domain of convergence of the integral. For example, K_1 can be determined by taking the limit $c_2, c_5 \to 0$ in (14) where c_2 and c_5 are picked because their respective exponents in $u^{(1)}$ are zero. The integral becomes

$$\int_{\mathbb{R}^2_+} \frac{dx_1dx_2}{(c_1x_1 + c_3x_1x_2 + c_4x_1^2)^{D/2}} = \frac{\Gamma(D-2)\Gamma(1-D/2)}{\Gamma(D/2)} c_1^{2-D}c_3^{-1}c_4^{D/2-1}, \tag{25}$$

note the limit is not well-defined for $\Phi(D;c)$ because c_2 and c_5 appear as denominators, or more precisely, they will have exponents with negative real part[1]. However, the limit is well-defined in the Weyl algebra as the restriction ideal:

$$H_A(\beta)|_{c_2,c_5=0} := (H_A(\beta) + c_2W + c_5W) \cap \mathbb{Q}(D)[c_1,c_3,c_4,\partial_1,\partial_3,\partial_4]. \tag{26}$$

The solution space to this ideal is one-dimensional and spanned by $c_1^{2-D}c_3^{-1}c_4^{D/2-1}$, we thus interpret the limit as $\Phi(D;c) \to K_1c_1^{2-D}c_3^{-1}c_4^{D/2-1}$. Equating this with the explicitly evaluated integral and substituting into (14) yields

$$K_1 = \frac{\Gamma(1-D/2)}{\Gamma(D/2)\Gamma(2-D/2)}. \tag{27}$$

Similarly we obtain

$$K_2 = K_1, \quad K_3 = \frac{\Gamma(D/2-1)\Gamma(D/2-1)}{\Gamma(D/2)\Gamma(D-2)}. \tag{28}$$

We have now obtained an explicit series representation for the Feynman integral in one of the seven Gröbner cones, the same procedure can be used to obtain an explicit representation in the other cones.

The paper is organized as follows; in Section 2 we review several definitions and results which will be needed to prove the main theorem, Theorem 1.1. The main theorem is proved in Section 3, this proof is separated into two cases, massive and massless. The massive case is treated in Section 3.1 and the massless case is treated in Section 3.2.

[1] Note that the form of $N^{(1)}$ guarantees that the limit is well-defined for $\phi^{(1)}$.

2. Background

In this section we briefly review several definitions and results from different areas of algebra which will be needed in Section 3. Readers wishing further details should consult books such as [7,12,19,33] on algebraic geometry and [34] on matroid theory. As was discussed in Section 1, in the context of computing series solutions to Feynman integrals, many things become much simpler when the toric ideal I_A associated to the matrix A in (4) has the *Cohen-Macaulay* property. Since the matrix A in (4) is always full rank with a row of ones the resulting toric ideal is *homogeneous*; recall an ideal I is called homogeneous if it has a homogeneous generating set (equivalently its Gröbner basis consists of homogeneous polynomials), i.e. $I = \langle g_1, \ldots, g_t \rangle$ where all monomials appearing in g_i have the same degree. Hence we will restrict our attention to the case of homogeneous ideals.

Let I be a homogeneous ideal in a polynomial ring $R = k[z_1, \ldots, z_r]$ over a field k of characteristic zero defining a projective variety $X = V(I) \subset \mathbb{P}^{r-1}$ with $d := \dim(I) = \dim(X) + 1$. Then d homogeneous polynomials $h_1, \ldots h_d$ in R/I are called a *homogeneous system of parameters* for R/I if $\dim_k(R/I + \langle h_1, \ldots, h_d \rangle) < \infty$. We say that a subsequence $h_1, \ldots, h_\nu$ is a (R/I)*-regular sequence of length r* if R/I is a free $k[h_1, \ldots, h_\nu]$ module, or equivalently if the Hilbert series of I, $H_I(z)$, is equal to the Hilbert series of $I + \langle h_1, \ldots, h_\nu \rangle$ divided by the polynomial $\prod_{i=1}^{\nu}(1 - z^{\deg(h_i)})$.

Definition 2.1 *(Cohen-Macaulay).* A homogeneous ideal I in a polynomial $R = k[z_1, \ldots, z_r]$ over a field k with $d = \dim(I)$ is *Cohen-Macaulay* if there exists a homogeneous system of parameters $h_1, \ldots h_d$ such that $h_1, \ldots h_d$ is also a (R/I)-regular sequence of length d.

Our interest is in homogeneous toric ideals. That is for a full rank $(|E|+1) \times r$ integer matrix with first row the all ones vector (e.g. as in (4)) we wish to consider the ideal $I_A = \langle z^u - z^v \mid Au = Av \rangle$ in the polynomial ring $k[z_1, \ldots, z_r]$; this ideal I_A is always a homogeneous prime ideal generated by a finite set of homogeneous binomials. The toric ideal I_A defines a projective toric variety $X_A = V(I_A) \subset \mathbb{P}^{r-1}$. We say the semi-group $\mathbb{N}A$ is *normal* if

$$\mathbb{N}A = \mathbb{Z}A \cap \mathbb{R}_{\geq 0}A.$$

For toric ideals a result of Hochster's [22], see also [39, Corollary 1.7.6], gives us a characterization of the Cohen-Macaulay property of the toric ideal I_A in terms of the normality of the semi-group $\mathbb{N}A$.

Theorem 2.2 *(Hochster). If the semi-group $\mathbb{N}A$ is normal then the toric ideal I_A is Cohen-Macaulay.*

Normality of a configuration of lattice points $A = A_- \times \{1\}$ can be characterised by a combinatorial property of the polytope $P = \text{conv}(A_-)$:

Definition 2.3 *(Normal Polytope).* A polytope P is called normal, or said to have the *integer decomposition property*[2] (IDP), if for any $k \in \mathbb{N}$

$$kP \cap \mathbb{Z}^d = (k-1)P \cap \mathbb{Z}^d + P \cap \mathbb{Z}^d. \tag{29}$$

Proposition 2.4 *(Remark 0.1 of [8]). A polytope P is IDP if and only if $\mathbb{N}(P \times \{1\} \cap \mathbb{Z}^{d+1}) = \mathbb{R}_{\geq 0}(P \times \{1\}) \cap \mathbb{Z}^{d+1}$.*

[2] This is sometimes called integrally closed.

This means especially that if all lattice points in $\mathrm{conv}(A_-)$ are column vectors in A_- (which correspond to exponents of monomials in $\mathcal{G}$), i.e. the set of column vectors of A_- is $\mathrm{conv}(A_-) \cap \mathbb{Z}^d$, the toric ideal I_A will be Cohen-Macaulay if the polytope $P = \mathrm{conv}(A_-)$ is IDP.

Hence when considering the question of if a toric ideal I_A is Cohen-Macaulay in Section 3 we will instead seek to prove the stronger sufficient condition that the polytope $P = \mathrm{conv}(A_-)$ is normal. We now recall two standard constructions in polyhedral geometry.

Definition 2.5. Let $P, Q \subset \mathbb{R}^d$ be (lattice) polytopes. The *Minkowski sum* $P + Q$ is

$$P + Q := \{p + q \in \mathbb{R}^d \mid p \in P,\ q \in Q\}.$$

The *Cayley sum* $P * Q$ is the convex hull of $(P \times \{0\}) \cup (Q \times \{1\})$ in $\mathbb{R}^{d+1}$.

In Section 3 the notion of an edge-unimodular polytope will play a prominent role. Recall that a matrix $M \in \mathbb{Z}^{d \times n}$ is said to be *unimodular* if all $d \times d$ minors are either 0, 1, or -1, a matrix is *totally unimodular* if every square submatrix is unimodular. A polytope P is called *edge-unimodular* if there a unimodular matrix M such that the edges of P are parallel to the columns of M. In Section 3 we employ Corollary 2.7 which is a direct consequence of the following result of Howard [23, 24], see also Danilov and Koshevoy [9].

Theorem 2.6 *(Theorem 4.7 of [24], cf. [23]). Suppose that M is a unimodular matrix and that P and Q are lattice polytopes with edges parallel to the columns of M, that is P and Q are both edge-unimodular with matrix M. Then*

$$P \cap \mathbb{Z}^d + Q \cap \mathbb{Z}^d = (P + Q) \cap \mathbb{Z}^d. \tag{30}$$

From this theorem we immediately obtain the following result which tells us that to show the projective normality of a toric variety X_A it is sufficient to show that the associated polytope $P = \mathrm{conv}(A)$ is edge-unimodular.

Corollary 2.7. *If a polytope P is edge-unimodular, then P is IDP.*

Proof. Suppose P is edge-unimodular and let $Q = (k-1)P$. Since Q is just a dilation of P, thus Q is also edge-unimodular and the prerequisites of Theorem 2.6 are met. Hence,

$$P \cap \mathbb{Z}^d + (k-1)P \cap \mathbb{Z}^d = kP \cap \mathbb{Z}^d.$$

□

To prove Theorem 3.5, our main result in the massless case, we will need the following result by Tsuchiya [41, Theorem 0.4] (see also [21]) where a complete description of IDP Cayley sums is given.

Proposition 2.8 *(Theorem 0.4 of [41]). The Cayley sum $P * Q$ is IDP if and only if P and Q are IDP and also*

$$(a_1 P + a_2 Q) \cap \mathbb{Z}^d = (a_1 P \cap \mathbb{Z}^d) + (a_2 Q \cap \mathbb{Z}^d) \tag{31}$$

for any positive integers a_1, a_2.

An important class of polytopes, which appear in Section 3, are the hypersimplices.

Definition 2.9 *(Hypersimplex).* The hypersimplex $\Delta(d,k) \subset \mathbb{R}^d$ is the polytope

$$\Delta(d,k) = \{(x_1,\ldots,x_d) \mid 0 \le x_1,\ldots,x_d \le 1;\; x_1 + \cdots + x_d = k\}. \tag{32}$$

In Section 3 we will also employ several ideas from matroid theory, our main reference for these notions is the book [34]. Below we give several definitions and a theorem which will be of particular importance.

Given two matroids M_1, M_2 on the same ground set E, we say that M_1 is a *quotient* of M_2 if every circuit of M_2 can be written as a union of circuits in M_1. A pair of matroids $\{M_1, M_2\}$ on the same ground set E form a *flag matroid* if M_1 is a quotient of M_2. In the proof of our main result we will employ the following standard result which tells us that quotients are flipped by duality.

Proposition 2.10 *(Proposition 7.3.1 of [34]). Let M_1, M_2 be two matroids on E, then M_1 is a quotient of M_2 if and only if M_2^* is a quotient of M_1^*.*

Given a matroid M we may define the associated *matroid polytope* P_M to be the convex hull of the indicator vectors of all bases of M. We will also wish to associate a polytope to a flag matroid $\{M_1, M_2\}$.

Definition 2.11. Let $\{M_1, M_2\}$ be a flag matroid, then the *flag matroid polytope* is defined as the Minkowski sum of the constituent matroid polytopes: $P_{M_1} + P_{M_2}$.

3. Normality of Symanzik Polytopes

In this section we prove the main result, namely we show that the polytope associated to entirely massive or entirely massless Feynmann integrals is always IDP, and hence the desirable properties of the associated A-hypergeometric system described in Section 1 hold. Throughout this section $G = (V, E)$ will be a 1PI Feynman graph as described in Section 1.

3.1. Massive Case. Let G be a 1PI Feynman graph with all internal edges massive, i.e. $m_e \neq 0$ for all $e \in E$. We separate the $\mathcal{F}$-polynomial (2) as $\mathcal{F} = \mathcal{F}_m + \mathcal{F}_0$ where $\mathcal{F}_0$ is defined by the two-forests and $\mathcal{F}_m$ is given by $\mathcal{F}_m = \mathcal{U} \cdot \sum m_e^2 x_e$ with $\mathcal{U}$ as in (1). The non-vanishing masses guarantees that every monomial in $\mathcal{F}_0$ will be present in $\mathcal{F}_m$, i.e. writing $\operatorname{span}(F)$ for the k-vector space span of the monomials in a polynomial F over a field k we have $\operatorname{span}(\mathcal{F}_m) \supseteq \operatorname{span}(\mathcal{F}_0)$. To see this, note that every monomial in $\mathcal{F}_0$ can be written on the the form ux_j where u is a monomial in $\mathcal{U}$ and x_j corresponds to one of the edges in the spanning tree defining u. If all masses are non-zero, then every x_j will be in the sum $\sum m_e^2 x_e$ and thus every monomial in $\mathcal{F}_0$ will be in $\mathcal{F}_m$.

This means that the Newton polytope $P_F := \operatorname{Newt}(\mathcal{F})$ of $\mathcal{F}$ satisfies

$$P_F = \operatorname{Newt}(\mathcal{F}_m) = P_U + \Delta_E, \tag{33}$$

where $P_U := \operatorname{Newt}(\mathcal{U})$ and $\Delta_E = \Delta(|E|, 1) = \operatorname{conv}(e_1, \ldots, e_{|E|})$ is the $(|E| - 1)$-dimensional standard simplex in $\mathbb{R}^{|E|}$; note that the final equality in (33) follows from the definition of $\mathcal{F}_m = \mathcal{U} \cdot \sum m_e^2 x_e$. Let $\mathcal{G} = \mathcal{U} + \mathcal{F}$ and let $\widetilde{\Delta}_E = \operatorname{conv}(0, e_1, \ldots, e_{|E|})$ be the standard simplex with 0 added as a vertex, then $P_G := \operatorname{Newt}(\mathcal{G}) = \operatorname{Newt}(\mathcal{U} + \mathcal{F})$ can be expressed as the sum

$$P_G = P_U + \widetilde{\Delta}_E. \tag{34}$$

Our goal is then to prove that the polytope P_G is edge-unimodular.

Theorem 3.1 *(Main Theorem I). Let P_G be the polytope defined in* (34)*; then the polytope P_G is edge-unimodular, and hence is IDP.*

Proof. Note that we can construct a co-graphic matroid from $\mathcal{U}$ by taking the matroid whose bases are the complements of the spanning trees of G; P_U is the matroid polytope of this matroid. By a classical result of Gelfand, Goresky, MacPherson and Serganova [18, Theorem 4.1] the edges of a matroid polytope are parallel to $e_i - e_j$, $i \neq j$, where e_k is the k^{th} standard basis in $\mathbb{R}^{|E|}$. Hence P_U is an edge-unimodular polytope.

The edges of $\widetilde{\Delta}_E$ are clearly either parallel to $e_i - e_j$ or e_i.

The Minkowski sum $P_G = P_U + \widetilde{\Delta}_E$ contains two types of edges: edges parallel to edges of P_U and edges parallel to edges of $\widetilde{\Delta}_E$. This means that P_G has edges in the totally unimodular matrix matrix $(I|A)$ where I is the $(|E| \times |E|)$-dimensional identity matrix and the columns of A consist of vectors which are the columns of some totally unimodular matrix. Hence P_G is edge-unimodular and, by Corollary 2.7, is IDP.

Remark 3.2. Lemma A.1 in the Appendix below shows that the lattice points in P_G are the same as the columns of A_-, (i.e. the exponent vectors of $\mathcal{G}$). Thus P_G being IDP is equivalent to the semi-group $\mathbb{N}A = \mathbb{N}(A_- \times \{1\})$ being normal, see Proposition 2.4 and the surrounding discussion, which also implies that the toric ideal I_A is Cohen-Macaulay by Hochster's theorem.

The Symanzik polynomials $\mathcal{U}$ and $\mathcal{F}$ are not only relevant in the Lee-Pomeransky representation but are also used in other parametric representations of Feynman integrals. As observed in the proof of Theorem 3.1 P_U is a matroid polytope, here we prove a similar result for P_F.

Lemma 3.3. *Let P_F be as in* (33)*. Then P_F is a flag matroid polytope.*

Proof. Let $C(|E|)$ be the cycle graph on $|E|$ vertices, i.e. the graph with $|E|$ vertices connected in a closed chain with $|E|$ edges. Let $M_{C(|E|)}$ be the associated graphic matroid, that is the matroid whose independent sets are given by the forests of $C(|E|)$. Then Δ_E is the matroid polytope of the co-graphic matroid $M^*_{C(|E|)}$. Note that this is a matroid of rank one and whose independent sets are $\mathcal{I} = \{\emptyset, \{1\}, \{2\}, \ldots, \{|E|\}\}$, thus we see that $M^*_{C(|E|)} = U_{1,|E|}$ where $U_{k,n}$ is the uniform matroid of rank k on $\{1, \ldots, n\}$. Let M^*_U be the matroid with matroid polytope P_U, this is a matroid on the same ground set E as $U_{1,|E|}$ but has rank L where L is the number of independent cycles in the underlying Feynman graph.

It is a little easier if we proceed with the dual matroids M_U (the graphical matroid on the underlying Feynman graph) and $U_{|E|-1,|E|}$.

Note that $U_{|E|-1,|E|}$ only contains one cycle: $\{1, \ldots, |E|\}$. Now, since we have assumed that the underlying Feynman graph is 1PI then every element in E will be in some cycle of M_U. Thus the union of the cycles in M_U will be the cycle in $U_{|E|-1,|E|}$. This means that M_U is a quotient of $U_{|E|-1,|E|}$.

We will now employ Proposition 2.10 which tells us that quotients are flipped by duality; in particular Proposition 2.10 implies that $U_{1,|E|}$ is a quotient of M^*_U and thus $\{U_{1,|E|}, M^*_U\}$ is a flag matroid. Since $P_F = P_U + \Delta_E$, where P_U, respectively Δ_E, are the matroid polytopes of M^*_U, respectively $U_{1,|E|}$, and $\{U_{1,|E|}, M^*_U\}$ is a flag matroid, we conclude that P_F is a flag matroid polytope.

From [6, Theorem 3.1] we have that the edges of a flag matroid polytope are contained in the set of edges of a totally unimodular matrix. This gives us the following corollary.

Corollary 3.4. *Let P_F be as in* (33)*. Then the edges of P_F are parallel to the columns of a unimodular matrix.*

3.2. Massless case. If all internal edges of a Feynman graph correspond to massless particles, then the $\mathcal{F}$-polynomial (2) consists only of the sum over spanning 2-forests, $\mathcal{F} = \mathcal{F}_0$, while the $\mathcal{U}$-polynomial (1) is independent of the internal masses. In order for x_e to be included in a term of $\mathcal{U}$ or $\mathcal{F}$, the corresponding edge $e \in E$ must have been removed. Since an edge can only be removed once, this means that x_e can show up at most once in each term of $\mathcal{U}$ or $\mathcal{F}$. In particular this means that the vertices of $\mathrm{Newt}(\mathcal{U})$ and $\mathrm{Newt}(\mathcal{F})$ are vectors with elements in $\{0, 1\}$.

For a Feynman graph with $|E|$ edges and L independent loops, it follows from their definition that $\mathcal{U}$ and $\mathcal{F}$ are homogeneous of degree L and $L + 1$ respectively. This in particular means that their Newton polytopes are contained in hyperplanes:

$$\mathrm{Newt}(\mathcal{U}) \subset \{(y_1, \ldots, y_E) \in \mathbb{R}^{|E|} \mid y_1 + \cdots + y_E = L\}, \tag{35}$$

$$\mathrm{Newt}(\mathcal{F}) \subset \{(y_1, \ldots, y_E) \in \mathbb{R}^{|E|} \mid y_1 + \cdots + y_E = L + 1\}. \tag{36}$$

We noted above that the vertices of the Newton polytopes are vectors built of zeros and ones, this together with the fact the polytopes are contained in hyperplanes yields

$$\mathrm{Newt}(\mathcal{U}) \subseteq \Delta(E, L) \text{ and } \mathrm{Newt}(\mathcal{F}) \subseteq \Delta(E, L + 1),$$

i.e. the Newton polytopes are subsets of hypersimplices (Definition 2.9). Moreover, the fact that $P_U = \mathrm{Newt}(\mathcal{U})$ and $P_{F_0} = \mathrm{Newt}(\mathcal{F}_0)$ are in different parallel hyperplanes (which are isomorphic copies of $\mathbb{R}^{|E|-1}$) means that P_G is their Cayley sum:

$$P_G = P_U * P_{F_0}. \tag{37}$$

For a Feynman graph $G = (V, E)$ with $m_e = 0$ for all edges and with all vertices connected to an off-shell external momenta, i.e. $p_v^2 \neq 0,\ v \in V = V_{\mathrm{ext}}$, we have the following analog of Theorem 3.1.

Theorem 3.5 *(Main Theorem II). Let $G = (V, E)$ be a Feynman graph with $m_e = 0$ for all $e \in E$ and $V_{\mathrm{ext}} = V$, and let $\mathcal{U}$ and $\mathcal{F}_0$ be as above. Then the polytope $P_G = \mathrm{Newt}(\mathcal{U} + \mathcal{F}_0)$ is IDP.*

In light of (37) we will apply Proposition 2.8 to prove that the Cayley sum P_G is IDP, hence proving Theorem 3.5. To employ Proposition 2.8 we need to show three things:

- (i) P_U is edge-unimodular (with respect to the unimodular matrix M) and hence IDP. As already discussed, this is clear since P_U is a matroid polytope (see the beginning of the proof of Theorem 3.1).
- (ii) P_{F_0} is edge-unimodular (with respect to same unimodular matrix M as in **(i)**) and hence IDP, this is considered in Lemma 3.6.
- (iii) That equation (31) holds for the pair P_U and P_{F_0}, this is considered in Lemma 3.7 (keeping in mind P_U and P_{F_0} are both edge-unimodular with the same M).

We now consider **(ii)** above. For each subgraph $\mathbf{g} \subset G = (V, E)$ we associate the 0/1 vector in $\mathbb{R}^{|E|}$ indexed by the edges removed from G to get $\mathbf{g}$, this association is clearly bijective. Given a 0/1 vector w in $\mathbb{R}^{|E|}$ we will write $\mathbf{g}_w$ to denote the corresponding subgraph of G obtained by removing the edges corresponding to entries in w with coordinate one.

Lemma 3.6. *Let F_0 be the set of all spanning two-forests where we view the elements in F_0 as 0/1 vectors in $\mathbb{R}^{|E|}$, i.e. F_0 is the the set of exponent vectors of monomials appearing in $\mathcal{F}_0$, the part of $\mathcal{F}$ in (2) consisting only of the sum over spanning 2-forests. Then F_0 is a set of bases of a matroid. Further the column matrix of the edges of the polytope $P_{F_0} = \mathrm{conv}(F_0)$ forms a totally unimodular matrix.*

Proof. Recall that a finite non-empty set $B \subset \mathbb{Z}^n_{\geq 0}$ is a *base* of a matroid if the following two properties hold:

(B1) all $u \in B$ have the same norm,
(B2) if $u, v \in B$ with $u_i > v_i$, then there exists $j \in \{1, \ldots, n\}$ with $u_j < v_j$ such that $u - e_i + e_j \in B$, where e_ℓ denotes the ℓ^{th} standard basis vector.

We now show these two properties hold for the set of exponent vectors of $\mathcal{F}_0$; for a vector $u \in \mathbb{Z}^n_{\geq 0}$ we will use the norm $|u| = u_1 + \cdots + u_n$.

(B1) The polynomial $\mathcal{F}_0$ is homogeneous of degree $L + 1$, where L is the number of independent cycles in G, so every $u \in F_0$ satisfies $|u| = L + 1$.
(B2) Assume u and v are two different elements in F_0 such that $u_i > v_i$ for some i. Then the graph $\mathbf{g}_{u-e_i}$ corresponding to the 0/1 vector $u - e_i$ can be one of two types of graphs: (a) a spanning tree or (b) a graph with two components, one a tree and the other containing one and only one cycle.
  (a) By assumption $u_j < v_j$ for some j, since $\mathbf{g}_{u-e_i}$ is a spanning tree we know that $\mathbf{g}_{u-e_i+e_j}$ is a spanning two-forest, i.e. $u - e_i + e_j \in F_0$.
  (b) For contradiction, assume that for all j such that $u_j < v_j$ we have $u - e_i + e_j \notin F_0$. This assumption means that for any edge j we cut in the graph $\mathbf{g}_{u-e_i}$ corresponding to the vector $u - e_i$, the cycle in $\mathbf{g}_{u-e_i}$ will stay intact. Let's do all these cuts; then the graph $\mathbf{g}_{u-e_i+\sum e_j}$ will still contain the cycle. The resulting graph contains the edge i and all the cuts from u and v, since the edge i is in the graph $\mathbf{g}_v$ corresponding to v, this means that the resulting graph is a subgraph of $\mathbf{g}_v$. But by assumption $\mathbf{g}_v$ is a spanning two-forest and thus can not contain any cycles. We have a contradiction.

Applying [18, Theorem 4.1] gives us that the column matrix of the edges of P_{F_0} forms a totally unimodular matrix and in particular are parallel to $e_j - e_i$. □

Lemma 3.7. *Let P and Q both be edge-unimodular lattice polytopes with edges parallel to the columns of the same unimodular matrix M. Then P and Q satisfy* (31).

Proof. This follows directly from Theorem 2.6 since edge directions are invariant under scaling. In particular P and Q have the same edge directions as $a_1 P$ and $a_2 Q$. □

Proof of Theorem 3.5. As discussed in **(i)** above P_U is edge-unimodular via [18, Theorem 4.1] since it is a matroid polytope. By Lemma 3.6 P_{F_0} is also edge-unimodular (again via [18, Theorem 4.1] since it is a matroid polytope). Further we saw in the proof of Lemma 3.6 that the edges of P_{F_0} are parallel to $e_j - e_i$, $i \neq j$, and saw in the proof of Theorem 3.1 that the edges of P_U are also parallel to $e_j - e_i$, $i \neq j$. Hence P_U and P_{F_0} are both edge-unimodular lattice polytopes with edges parallel to the columns of the same unimodular matrix. It follows by Lemma 3.7 that (31) is satisfied for P_U and P_{F_0}. Thus Proposition 2.8 applies and $P_G = P_U * P_{F_0}$ is IDP.

Remark 3.8. Since P_U and P_{F_0} are matroid polytopes they have no interior lattice points and additionally they lay in parallel hyperplanes; hence the Cayley sum $P_G = P_U * P_{F_0}$ also has no interior lattice points and $P_G \cap \mathbb{Z}^{|E|}$ consists only of the vertices of P_G. This means that, if the columns of the matrix A_- are the exponent vectors of the polynomial $\mathcal{G} = \mathcal{U} + \mathcal{F}_0$, then the semi-group $\mathbb{N}A = \mathbb{N}(A_- \times \{1\})$ is normal, and the associated toric ideal I_A is Cohen-Macaulay.

Acknowledgments. We would like to thank Georgios Papathanasiou and Volker Schomerus for many helpful discussions, F.T. especially acknowledge G. Papathanasiou's supervision resulting in this project. We would also like to thank Uli Walther for many helpful correspondences, including sharing with us his proof of Lemma A.1 below, and for allowing us to include it here. Additionally, we would like to thank the anonymous referee for their very helpful comments on an earlier draft.

Funding Open Access funding enabled and organized by Projekt DEAL. Uli Walther is supported in part by NSF grant DMS-2100288 and by Simons Foundation Collaboration Grant for Mathematicians #580839.

Declarations

Conflict of interest We declare no conflict of interest.

Appendix A: A Lemma on Lattice Points

Author: Uli Walther Department of Mathematics, Purdue University. E-mail: walther@purdue.edu

In this section we will consider $G = (V, E)$ as any Feynman graph, not necessarily a 1PI graph, and let E_m denote the set of all edges e with $m_e \neq 0$. In order to rule out complications from trivialities we assume that G has at least one edge that is not a loop. In other words, we assume that the rank of the associated co-graphic matroid is greater than one.

Lemma A.1. *Let $G = (V, E)$ be any Feynman graph and let $E_m \subset E$ be the set of all edges with non-zero mass, $m_e \neq 0$. Let $\mathcal{U}$ be as in (1), with $P_U = \mathrm{Newt}(\mathcal{U})$ and let Δ_{E_m} be the simplex in $\mathbb{R}^{|E_m|}$ given by the convex hull of the set of standard basis vectors $\{e_j \mid j \in E_m\}$ with $\widetilde{\Delta}_{E_m}$ being the convex hull of this simplex along with the vector $0 \in \mathbb{R}^{|E_m|}$. The lattice points contained in the polytope $P = P_U + \widetilde{\Delta}_{E_m}$ are exactly those of the form $v + v'$ where v is a vertex of P_U and v' is a vertex of $\widetilde{\Delta}_{E_m}$.*

Proof. Let M_U^* denote the co-graphic matroid of the graph G and P_U its matroid polytope. The lemma clearly holds if $|E| = 1$, and more generally in the case where E is the union of a basis for M_U^* with a set of loops, since then M_U^* has exactly one basis and so P_U is a point and the sum $P_U + \widetilde{\Delta}_{E_m}$ is a shifted standard simplex. Let w be a point of $P_U + \widetilde{\Delta}_{E_m}$. Then w can be written as a real linear combination

$$w = \sum c_i p_i \tag{38}$$

where the real numbers $c_i \geq 0$ with $|c| = \sum c_i = 1$ and where each p_i is a vertex of the polytope $P_U + \widetilde{\Delta}_{E_m}$. Let $r := \mathrm{rank}(M_U^*)$. Note that, for the vertex p_i in $\mathbb{R}^{|E_m|}$ the entry-wise sum $|p_i|$ equals either r or $r+1$. It follows that $|w| \in \{r, r+1\}$. Now assume in addition that w a lattice point; we must then have $|w| \in \{r, r+1\}$. Moreover, in either case, since r and $r+1$ are consecutive integers, the linear combination $\sum c_i p_i$ can only non-trivially involve such p_i with $|w| = |p_i|$.

Let $\mathcal{M}_B$ be the set of basis of a matroid $\mathcal{M}$ on ground set E with $v_B \in \mathbb{Z}^{|E|}$ denoting the indicator vector of a base $B \in \mathcal{M}_B$; results of White [43, Theorems 1 and 2] tell us that the points $(1, a)$ in $\mathbb{Z} \times \mathbb{Z}^{|E|}$ inside the positive cone spanned by all pairs $(1, v_B)$, are precisely the vectors $(1, v_B)$ for $B \in \mathcal{M}_B$. In our case this result tells us that if $|w| = r$ (in which case each p_i with nonzero c_i must have $|p_i| = r$ and be the indicator vector of a basis for M_U^* then w is a vertex of P_U , and so $w = w + 0 \in P_U + \widetilde{\Delta}_{E_m}$ is as stipulated in the lemma. We thus assume from now on that $|w| = r+1$, so $w \in P_U + \widetilde{\Delta}_{E_m}$.

We consider first the massive case $E_m = E$. Both $P_E = P_U$ and $\widetilde{\Delta}_{E_m}$ are contained in the unit cube, so any lattice point w of $P_U + \widetilde{\Delta}_{E_m}$ has coordinate value $x_e(w)$ in the set $\{0, 1, 2\}$, for any $e \in E$. If $x_e(w) = 0$ then all nontrivial terms in (38) must also satisfy $x_e(p_i) = 0$. Since the set of exponent vectors in $\mathcal{U}$ with vanishing e-coordinate is made of the indicator vectors of the bases for the submatroid of bases of M_U^* that avoid e (the cographic matroid to the graph derived from G by contracting e), it follows by induction on $|E|$ that in this case w is as stipulated in the lemma.

We can therefore assume that there is no $e \in E$ with $x_e(w) = 0$ and so $|w| \geq |E| \geq r$. On the other hand, we know that $|w| = r+1$, and so $|E| \in \{r-1, r\}$. In the latter case, M_U^* is Boolean where the lemma is straightforward (a *Boolean* matroid is one whose only base is the ground set). So we are reduced to checking the case $|E| = r+1$ which forces $w = (1, \ldots, 1)$. In the massive case $E_m = E$, choose any basis B for M_U^*, necessarily of size r. Its indicator vector is the difference $w - e_f$ for the edge $\{f\} := E - B$ and thus $w = (w - e_f) + e_f \in P_U + \widetilde{\Delta}_{E_m}$ is a sum of vertices as required.

In the non-massive case, E_m is a proper subset of E. The previous arguments above show that we are reduced to investigating $w = (1, \ldots, 1)$, and $|E| \in \{r, r+1\}$. The Boolean case being trivial, it suffices to show that if $|E| = r+1$ then $w = (1, \ldots, 1)$ is either not in $P_U + \widetilde{\Delta}_{E_m}$ at all, or equal to the sum of a basis indicator vector of M_U^* with a suitable e_f with $f \in E_m$. If the latter fails, none of the bases for M_U^* (all of which are of size $r = |E| - 1$) are the complement in E of an element of E_m. In other words, every element of E_m is contained in each basis. In that case, M_U^* is the matroid sum of the Boolean matroid on E_m (with unique basis E_m) with the co-graphic matroid $M_{U_o}^*$, of the graph G_o, on the ground set $E - E_m$ where G_o is the graph derived from G by deleting the edges of E_m. The matroid basis polytope of M_U^* is that of $M_{U_o}^*$ shifted by $\sum_{f \in E_m} e_f$. In other words, we have reduced the problem to the massless case $E_m = \emptyset$. Then, however, $|w| = r+1$ implies that w cannot be in $P_U + \widetilde{\Delta}_{E_m}$.

References

1. Adolphson, A.: Hypergeometric functions and rings generated by monomials. Duke Math. J. **73**(2), 269–290 (1994)
2. Berkesch, C., Forsgård, J., Passare, M.: Euler-Mellin integrals and A-hypergeometric functions. Mich. Math. J. **63**(1), 101–123 (2014)
3. Bloch, S., Esnault, H., Kreimer, D.: On motives associated to graph polynomials. Comm. Math. Phys. **267**(1), 181–225 (2006)
4. Bogner, C., Weinzierl, S.: Feynman graph polynomials. Int. J. Mod. Phys. A **25**, 2585–2618 (2010)
5. Bönisch, K., Fischbach, F., Klemm, A., Nega, C., Safari, R.: Analytic structure of all loop banana integrals. JHEP **05**, 066 (2021)
6. Borovik, A.V., Gelfand, I.M., Vince, A., White, N.: The lattice of flats and its underlying flag matroid polytope. Ann. Comb. **1**(1), 17–26 (1997)
7. Cox, D., Little, J., O'Shea, D.: Ideals, varieties, and algorithms: an introduction to computational algebraic geometry and commutative algebra. Springer Science & Business Media (2013)

8. Cox, D.A, Haase, C., Hibi, T., H., Akihiro: Integer decomposition property of dilated polytopes. Electron. J. Combinat., P4–28 (2014)
9. Danilov, V.I., Koshevoy, G.A.: Discrete convexity and unimodularity-i. Adv. Math. **189**(2), 301–324 (2004)
10. de la Cruz, L.: Feynman integrals as A-hypergeometric functions. JHEP **12**, 123 (2019)
11. Denham, G., Schulze, M., Walther, U.: Matroid connectivity and singularities of configuration hypersurfaces. Lett. Math. Phys. **111**(1), Paper No. 11, 67 (2021)
12. Eisenbud, D.: Commutative Algebra: With a View Toward Algebraic Geometry, vol. 150. Springer Science & Business Media, New York (2013)
13. Feng, T.-F., Chang, C.-H., Chen, J.-B., Zhang, H.-B.: GKZ-hypergeometric systems for Feynman integrals. Nucl. Phys. B **953**, 114952 (2020)
14. Folland, G.B.: Quantum field theory, Mathematical Surveys and Monographs, vol. 149. American Mathematical Society, Providence, RI, A tourist guide for mathematicians (2008)
15. Gel'fand, I.M., Kapranov, M.M., Zelevinsky, A.V.: Generalized Euler integrals and A-hypergeometric functions. Adv. Math. **84**(2), 255–271 (1990)
16. Gel'fand, I.M., Zelevinsky, A.V., Kapranov, M.M.: Hypergeometric functions and toral manifolds. Funct. Anal. Appl. **23**(2), 94–106 (1989)
17. Gel'fand, I.M., Zelevinsky, A.V., Kapranov, M.M.: Correction to the paper: "Hypergeometric functions and toric varietie" [Funktsional. Anal. i Prilozhen. **23** (1989), no. 2, 12–26; MR1011353 (90m:22025)], Funktsional. Anal. i Prilozhen. **27** (1993), no. 4, 91
18. Gelfand, I.M., Goresky, R.M., MacPherson, R.D., Serganova, V.V.: Combinatorial geometries, convex polyhedra, and schubert cells. Adv. Math. **63**(3), 301–316 (1987)
19. Gelfand, I.M., Kapranov, M., Zelevinsky, A.: Discriminants, Resultants, and Multidimensional Determinants. Springer Science & Business Media, New York (2008)
20. Grayson, D.R., Stillman, M.E.: Macaulay2, a software system for research in algebraic geometry. Available at http://www.math.uiuc.edu/Macaulay2
21. Haase, C., Hofmann, J.: Convex-normal (pairs of) polytopes. Canad. Math. Bull. **60**(3), 510–521 (2017)
22. Hochster, M.: Rings of invariants of tori, Cohen-Macaulay rings generated by monomials, and polytopes. Ann. Math. **96**(2), 318–337 (1972)
23. Howard, B.: Edge unimodular polytopes in mini-Workshop: Projective Normality of Smooth Toric Varieties, vol. 4: Abstracts from the mini-workshop held August 12–18, 2007, Organized by Christian Haase, Takayuki Hibi and Diane Maclagan. Oberwolfach Reports. **4**(3), 2283–2319 (2007)
24. Howard, B.: Matroids and geometric invariant theory of torus actions on flag spaces. J. Algebra **312**(1), 527–541 (2007)
25. Huber, B., Thomas, R.R.: Computing Gröbner Fans of Toric Ideals. Exp. Math. **9**(3), 321–331 (2000)
26. Jensen, A.N.: Gfan, a software system for Gröbner fans and tropical varieties, Available at http://home.imf.au.dk/jensen/software/gfan/gfan.html
27. Kalmykov, M., Bytev, V., Kniehl, B.A, Sven-Olaf Moch, Bennie F.L. Ward, and Scott A. Yost: Hypergeometric Functions and Feynman Diagrams, Antidifferentiation and the Calculation of Feynman Amplitudes, 12 (2020)
28. Kashiwara, M., Kawai, T.: Holonomic systems of linear differential equations and Feynman integrals. Publ. Res. Inst. Math. Sci. **12**, 131–140 (1976)
29. Klausen, R.P.: Hypergeometric series representations of Feynman integrals by GKZ hypergeometric systems. JHEP **04**, 121 (2020)
30. Klemm, A., Nega, C., Safari, R.: The l-loop Banana amplitude from GKZ systems and relative Calabi-Yau periods. JHEP **04**, 088 (2020)
31. Roman, N., Lee, A.A.: Pomeransky. Critical points and number of master integrals, JHEP **11**, 165 (2013)
32. Matusevich, L.F., Miller, E., Walther, U.: Homological methods for hypergeometric families. J. Amer. Math. Soc. **18**(4), 919–941 (2005)
33. Mateusz Michałek and Bernd Sturmfels, Invitation to nonlinear algebra, vol. 211, American Mathematical Soc., 2021
34. Oxley, J.: Matroid theory, Oxford Graduate Texts in Mathematics, vol. 21, 2nd edn. Oxford University Press, Oxford (2011)
35. Patterson, E.: On the singular structure of graph hypersurfaces. Commun. Number Theory Phys. **4**(4), 659–708 (2010)
36. Michael, E.: Peskin and Daniel V. Schroeder, An Introduction to quantum field theory, Addison-Wesley, Reading, USA (1995)
37. Saito, M.: Logarithm-free A-hypergeometric series. Duke Math. J. **115**(1), 53–73 (2002)
38. Saito, M., Sturmfels, B., Takayama, N.: Gröbner deformations of hypergeometric differential equations, vol. 6. Springer Science & Business Media (2013)
39. Stanley, R.P.: Combinatorics and commutative algebra, vol. 41. Springer Science & Business Media (2007)

40. Sturmfels, Bernd: Grobner bases and convex polytopes, vol. 8, American Mathematical Soc., 1996
41. Tsuchiya, Akiyoshi: Cayley sums and minkowski sums of 2-convex-normal lattice polytopes, (2019)
42. Weinberg, S.: The Quantum theory of fields, vol. 1. Cambridge University Press, Foundations (2005)
43. White, N.L.: The basis monomial ring of a matroid. Adv. Math. **24**(2), 292–297 (1977)

Paper III

Landau Singularities from Whitney Stratifications
Martin Helmer, Georgios Papathanasiou and **Felix Tellander**
Submitted to *Physical Review Letters*, [2402.14787]

Landau Singularities from Whitney Stratifications

Martin Helmer, [1,*] Georgios Papathanasiou, [2,3,†] and Felix Tellander [3,‡]

[1] Department of Mathematics, North Carolina State University, Raleigh, USA
[2] Department of Mathematics, City, University of London, Northampton Square, EC1V 0HB, London, UK
[3] Deutsches Elektronen-Synchrotron DESY, Notkestr. 85, 22607 Hamburg, Germany.

(Dated: February 23, 2024)

We demonstrate that the complete and non-redundant set of Landau singularities of Feynman integrals may be explicitly obtained from the Whitney stratification of an algebraic map. As a proof of concept, we leverage recent theoretical and algorithmic advances in their computation, as well as their software implementation, in order to determine this set for several nontrivial examples of two-loop integrals. Interestingly, different strata of the Whitney stratification describe not only the singularities of a given integral, but also those of integrals obtained from kinematic limits, e.g. by setting some of its masses or momenta to zero.

I. INTRODUCTION

At the heart of both cross-section calculations at the Large Hadron Collider and gravitational wave physics lie the evaluation of *Feynman integrals.* These integrals are multivalued meromorphic functions of the kinematic variables they depend on, and understanding their analytic structure has been an ongoing quest for theoretical physicists since the late 50's [1].

Key information on the analytic structure of Feynman integrals is provided by the values of the kinematic variables for which these become singular, this study was initiated in the pioneering work of Landau [2]. A virtue of these *Landau singularities*, is that knowing them in advance may significantly aid the evaluation of the integrals, for example with the canonical differential equations approach [3]: They may constrain or even fully predict [4] the analytic building blocks or (symbol) *letters* [5] of this approach, thereby turning the determination of the differential equations from a symbolic, to a much simpler numerical problem. Thanks to their utility, also in other aspects of Feynman integration [6], the analysis of Landau singularities is currently experiencing a revival with ever-increasing momentum, see for example [4, 7–14].

A mathematically robust definition of what a Landau singularity is has been provided by Pham [15] as his *Landau variety*; roughly speaking it is characterized by the critical values of a projection map from the variety describing the integrand in terms of all integration and kinematic variables, to the space of just the kinematic variables. Its direct calculation from this definition has proven quite challenging, and much of the recent effort has focused on developing alternative methods that more simply compute varieties that either contain it [7, 8], or are contained in it [4, 13, 14]. In other words, these methods may in general either provide spurious candidates or miss certain Landau singularities entirely, and it is not known when these phenomena do not occur beyond certain special classes of integrals.

In this work, we demonstrate that the rigorous definition of Landau singularities *can* be used to obtain their complete set, and nothing but their complete set, in a practical manner. To this end, we apply recent theoretical and algorithmic advances on the computation of Whitney stratifications [16, 17], which enter this definition. In particular, we leverage their implementation in the `WhitneyStratifications` 2.03 package for the Macaulay2 [18] scientific computation software, available at http://martin-helmer.com/Software/WhitStrat/index.html [19], in order to compute the Landau singularities of several nontrivial two-loop integrals, such as the two-mass hard slashed box and the parachute. While this computational route is currently not as efficient as that of other specialized software for sub- or supersets of Landau singularities [8, 13, 14], it provides a proof of concept that paves the way for their fast and accurate determination in the future.

II. FEYNMAN INTEGRALS AND THEIR SINGULARITIES

In this article we consider one-particle irreducible Feynman graphs $G := (E, V)$ with set of edges and vertices E and V, respectively, and loop number $L = n - |V| + 1$, where we abbreviate $n := |E|$. The vertex set V has the disjoint partition $V = V_{\text{ext}} \sqcup V_{\text{int}}$ where each vertex $v \in V_{\text{ext}}$ is assigned an external incoming 4-dimensional momenta $p_v \in \mathbb{R}^{1,3}$, and each internal edge e is assigned a mass parameter m_e. Using dimensional regularization with $D := 4 - 2\epsilon$ and the *Lee-Pomeransky representation* [20] we assign the following integral to G:

$$\mathcal{I} = \int_{\mathbb{R}^n_+} \left(\prod_{i=1}^{n} \frac{x_i^{\nu_i}\, dx_i}{x_i \Gamma(\nu_i)} \right) \frac{1}{\mathcal{G}^{D/2}}, \qquad \mathcal{G} = \mathcal{U} + \mathcal{F}, \qquad (1)$$

where the ν_i are propagator powers and $\mathcal{U}$, respectively $\mathcal{F}$, are the first and second *Symanzik polynomials.* These are homogeneous polynomials of degree L and $L+1$ in the

* mhelmer@ncsu.edu
† georgios.papathanasiou@desy.de
‡ felix@tellander.se

x_i, respectively, and may be easily obtained from graph-theoretic data, see e.g. [21]. The polynomial coefficients of $\mathcal{U}$ are just numbers, whereas those of $\mathcal{F}$ depend on the kinematic variables p_v, m_e, and are not necessarily algebraically independent.

The study of singularities of Feynman integrals was initially formulated in terms of conditions for their contour of integration to become trapped between colliding poles of the integrand. These conditions are known as the Landau equations [2], which in the representation (1) above read,

$$\mathcal{G}_h = 0 \text{ and } x_i \frac{\partial \mathcal{G}_h}{\partial x_i} = 0 \; \forall \; i = 0, 1, \ldots, n, \qquad (2)$$

where $\mathcal{G}_h := \mathcal{U}x_0 + \mathcal{F}$ is the *homogenized* Lee-Pomeransky polynomial.

Due to their generically nonlinear nature, directly solving the above equations in an efficient and systematic manner remains a challenge. When the polynomials $\mathcal{U}$ and $\mathcal{F}$ are taken to have generic coefficients, then Landau singularities are alternatively captured by the *principal A-determinant* [22], see also [9]. This is a polynomial in the kinematic variables, which vanishes whenever the equations (2) have a solution.

Despite the algorithmic character of principal A-determinant calculations, an issue that arises when specialising the polynomial coefficients back to their Feynman integral values, is that certain factors of the principal A-determinant may vanish identically. Given the unphysical conclusion this would lead to, that the Feynman integral is singular for all values of the kinematic variables, one may be tempted to define its Landau singularities by simply removing these vanishing factors. However this definition is incomplete, as it has been definitely shown to miss singularities e.g. in the case of the parachute integral [12]. An empirical refinement of this definition, based on sequential limits of the generic polynomial coefficients, has also been proposed and tested in many one- and some two-loop integrals in [4], yet more extensive vetting and/or a proof would be desirable. Another closely related refinement of the principal A-determinant, known as the *principal Landau determinant* (PLD), has also been recently defined and implemented in the Julia package `PLD.jl` [13, 14]. Unfortunately, this too appears to miss singularities in certain cases.

A different approach to singularities of integrals is provided by the homological study of integrals depending on parameters. In this setting Pham's definition of the Landau variety provides a set describing when the topology of $x_0 \cdots x_n \mathcal{G}_h = 0$ changes. This naturally probes deeper than just considerations of singularities of this variety. An upper bound of the Landau variety is provided by the polynomial reduction described by Brown [7] and is also implemented in `HyperInt` [8]. A simple sufficient measure for changes in topology is given by the Euler characteristic, which provides a way of reducing this superset closer to the Landau variety. In the case where the Landau variety is equal to the zero set of the principal A-determinant it is a corollary of either [23, Theorem 1.1] or [24, Theorem 13] that this superset can be reduced to the Landau variety by only keeping the components where the Euler characteristic of $x_0 \cdots x_n \mathcal{G}_h = 0$ changes from its generic value. In the general case these results, as well as the result of [25, Corollary 37] relating the number of master integrals to this Euler characteristic, support such an approach to reduce the superset produced by `HyperInt` to the Landau variety, but we are unaware of any known results which guarantee the correctness of such reductions.

The Landau variety is defined in Section IV, Definition 1, in an algebraic form suitable for direct calculations. In order to do so we require the theory of Whitney stratification, which we introduce in the next section.

III. WHITNEY STRATIFICATION BACKGROUND

Let k be a field, for us this will always be either the real or complex numbers. In the discussion that follows it will be convenient to employ the following notation for the *algebraic variety* defined by polynomials $g_1, \ldots, g_r$ in a polynomial ring $k[x_1, \ldots, x_n]$:

$$\mathbf{V}(g_1, \ldots, g_r) := \{x \in k^n \mid g_1(x) = \cdots = g_r(x) = 0\}.$$

Consider an algebraic variety X of dimension d. We say a flag $X_\bullet$ of varieties $X_0 \subset \cdots \subset X_d = X$ is a *Whitney stratification* of X if, for all i, $X_i - X_{i-1}$ is a smooth manifold such that *Whitney's condition B* holds for all pairs M, N, where M is a connected component of $X_i - X_{i-1}$ and N is a connected component of $X_j - X_{j-1}$. Such connected components are called *strata*. A pair of strata, M, N with $\overline{M} \subset \overline{N}$, satisfy Whitney's condition B at a point $x \in M$ with respect to N if: for every sequence $\{p_n\} \subset M$ and every sequence $\{q_n\} \subset N$, with $\lim p_n = \lim q_n = x$, we have $s \subset T$ where s is the limit of secant lines between p_n, q_n and T is the limit of tangent plans to N at q_n. We say the pair M, N satisfies condition B if condition B holds, with respect to N, at all points $x \in M$. This is illustrated in Figures 1 and 2 below.

Note that a Whitney stratification of a variety is not unique, however it was shown in [26, Chapter V–VI] that when X is any complex algebraic (or analytic) variety there exists a **unique** *minimal (or coarsest) Whitney stratification*, such that all other Whitney stratifications are obtained by adding strata inside the strata of the minimal one, see also [27, pg. 736–737].

Consider an algebraic map $f : X \to Y$ between varieties X and Y. A *Whitney stratification* of the map f is a pair $(X_\bullet, Y_\bullet)$ where $X_\bullet$ is a Whitney stratification of X, $Y_\bullet$ is a Whitney stratification of Y and for each strata M of X there is a strata N of Y with $f(M) \subset N$ such that the map $f|_M : M \to N$ is a *submersion*, i.e. the differential $df|_M$ is surjective. It follows from the existence of the minimal Whitney stratification of a variety and, e.g. the

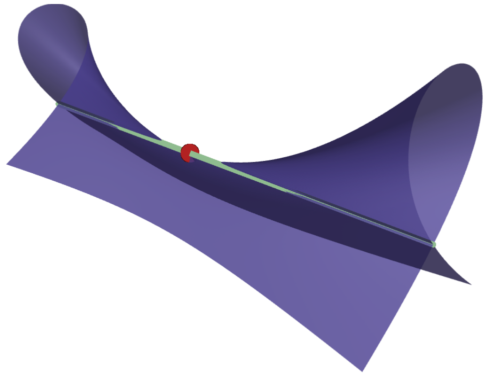

FIG. 1: The Whitney stratification of the *Whitney cusp*, $X = \mathbf{V}(x^2 + z^3 - y^2z^2) \subset \mathbb{R}^3$, is given by $X \supset \mathbf{V}(x, z) \supset \{(0, 0, 0)\}$.

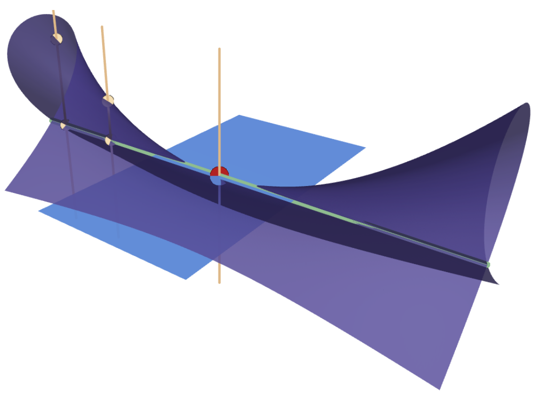

FIG. 2: Two sequences of points, one on the y-axis and one along the top of the surface, both approaching the origin. The limiting secant line is the z-axis, while the limiting tangent plane is the (x, y)-plane, meaning condition B fails at $(0, 0, 0)$ for the y-axis relative to the rest of the surface. Hence, the origin must be placed in a separate strata from the other points on the y-axis.

algorithm of [17, §2], that there exists a unique minimal or coarsest stratification of a map as well. Given the defining equations of varieties X, Y and of a map f between them, the stratification $(X_\bullet, Y_\bullet)$ may be obtained explicitly using the algorithm of [16, 17] as implemented in the `WhitneyStratifications` Macaulay2 package.

When the map f is proper then we have, by *Thom's First Isotopy Lemma* [28, Proposition 11.1], that the topology of the fiber $f^{-1}(q)$ is constant over **all** points $q \in N$ for any strata N of Y.

Example 1 (Topology of Parameterized Cubic) Consider the planar cubic curve in $\mathbb{R}^2$ defined by the parametric polynomial

$$f_z(x, y) = (y - 1)^2 - (x - z)x^2 \tag{3}$$

in variables x, y with parameter z. For parameter values $z < 0$ this is a nodal cubic, with one closed loop, while for $z = 0$ it is a cusp, and it is a smooth curve with two connected components (over the reals) for positive z, see Figure 3. We may use the stratification of the projection map onto the parameter space to detect this change in topology. In particular, if we treat x, y, z as variables, set $X = \mathbf{V}((y - 1)^2 - (x - z)x^2) \subset \mathbb{R}^3$, and consider the projection $\pi : X \to Y = \mathbb{R}$ given by $(x, y, z) \mapsto z$ we may compute a stratification $(X_\bullet, Y_\bullet)$ of π using methods of [17]. The stratification of $Y = \mathbb{R}$ is given by:

$$\mathbf{V}(z) \subset Y = \mathbb{R}.$$

Hence we see that in particular the topology of the curve changes at $z = 0$, dividing $\mathbb{R} - 0$ into two connected components, the positive and negative real axis [29].

This example was used in [14, Example 3.9] to illustrate that the principal Landau determinant, as defined in [14, Definition 3.4], fails to capture the change in topology of this curve (and the corresponding change in Euler characteristic); the authors of [14] also give larger examples arising from actual Feynman integrals where the Principal Landau discriminant fails to capture all topological changes which lead to a singular Feynman integral, see [14, §3.5].

IV. WHITNEY STRATIFICATION OF MAPS AND THE LANDAU VARIETY

Consider a Feynman integral specified by a polynomial $\mathcal{G}_h$ in the ring $\mathbb{C}[z][x] := \mathbb{C}[z_1, \dots, z_m][x_0, \dots, x_n]$, which is homogeneous in x, where the z_i are parameters (e.g. masses, momenta) and the x_i are variables. For a fixed vector of constants z the resulting polynomial G_h is homogeneous and defines a (projective) variety in the complex projective space $\mathbb{P}^n$. We make no assumptions on the independence of the parameters, and in particular allow there to be algebraic relations between them. We then seek to describe the *Landau variety*, which is locus in the parameter space $\mathbb{C}^m$ where the Feynman integral is singular; the following definition is (a minor rephrasing of) that of Pham [15, §IV.5] for Feynman integrals in Lee-Pomeransky form:

Definition 1 (Landau variety). *Consider a Feynman integral in Lee-Pomeransky form and let $\mathcal{G}_h$ be the x-homogeneous polynomial defining it. Set $X = \mathbf{V}(x_0 \cdots x_n \mathcal{G}_h) \subset \mathbb{P}^n_x \times \mathbb{C}^m_z$ and consider the projection map $\pi : X \to \mathbb{C}^m_z$, then the Landau variety is given by the variety Y_{m-1} appearing in the unique minimal Whitney stratification $(X_\bullet, Y_\bullet)$ of the map π.*

Note that the map π in Definition 1 is proper by construction, since the fibers are projective varieties (which are always compact), hence Thom's isotopy lemma always holds for the strata in the map stratification.

Regarding computation, the Whitney stratifications produced by the `WhitneyStatifications` package have been found to be minimal in all tested cases, however

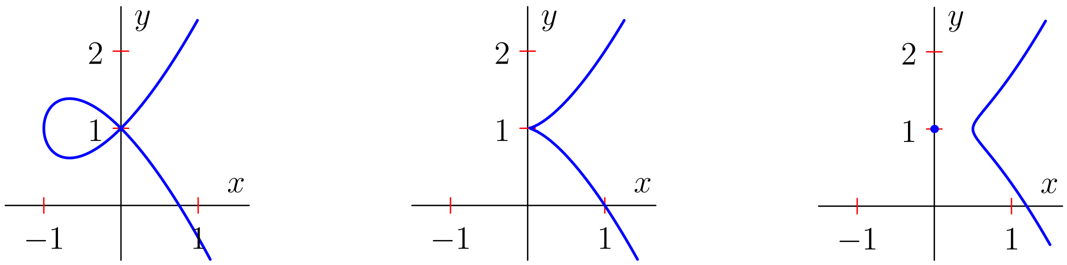

(a) Setting $z = -1$ gives a nodal cubic with one loop.

(b) Setting $z = 0$ gives a cusp cubic.

(c) Setting $z = 1/2$ gives a curve with two connected components.

FIG. 3: Plots of the curve defined by (3) for different parameter values z; the topology of the curve changes at $z = 0$. While the curve in (c) is smooth and has two connected components (of different dimensions) in $\mathbb{R}^2$ it is connected and singular, with singularity at $(0, 1)$, in $\mathbb{C}^2$.

there is currently no theoretical guarantee that this will always be the case. The minimality of a computed stratification may be checked using the results of [27, page 751–752] and standard computational tools, e.g. the `SegreClasses` Macaulay2 package [30].

It is also interesting to note that the lower dimensional strata in the stratification of $\pi : X \to \mathbb{C}^m_z$ as in Definition 1 tell us which singular parameter values lead to further topological changes. Hence, in particular, we also obtain the Landau variety for integrals corresponding to kinematic limits which arise from taking parameter values on the original Landau variety, e.g. if we take parameter values in Y_{m-1} which correspond to a kinematic limit, then the Landau variety of this kinematic limit is given by Y_{m-2}, and so on.

Hence, more broadly speaking, the stratification in Definition 1 precisely describes all regions of the parameter space such that within each regions any choices of parameters yield a variety X in $\mathbb{P}^n$ with constant topology (note we slightly abuse notation here and use X to refer to both the variety in $\mathbb{P}^n \times \mathbb{C}^m$, where we treat x, z as variables, and the variety in $\mathbb{P}^n$ arising from the same equation for a fixed choice of parameter values z).

It is shown in [25, Corollary 37] that the number of master integrals is given by the Euler characteristic $|n + 1 - \chi(\mathbf{V}(x_0 x_1 \cdots x_n \mathcal{G}_h))|$. Since we have that the topology is constant for parameter values outside the Landau variety (this follows from Thom's Isotopy Lemma since it is the codimension 1 part of of a stratification of the projection map), then the Euler characteristic is constant as well, and hence the number of master integrals is fixed for these parameter choices. Note that in fact our stratification gives us yet more information than this, in particular when combined with the Euler characteristic computation we may identify **all** possible numbers of master integrals for all choices of parameters, even ones that yield a singularity.

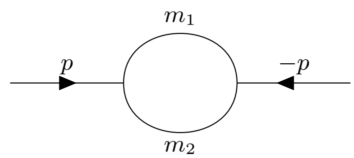

FIG. 4: The singularity structure of the one-loop bubble is classical and well-known. We show that the Landau variety not only reproduces these results but that the full Whitney stratification provides the singularities of kinematic limits.

V. EXAMPLE COMPUTATIONS

We demonstrate that the Landau variety, Definition 1, can explicitly be calculated and how the result compares to other approaches. Interestingly, often the full Whitney stratification of the map is not needed but it is enough to calculate the stratification of the map imposing only that the successive differences of elements in each of the flags $X_\bullet, Y_\bullet$ are smooth, which can be done by computing consecutive singular loci [31]. The latter is not guaranteed to provide all singularities, but the correctness has been verified a posteriori for the cases considered.

A. One-loop bubble

We begin be showing how the full Whitney stratification for the generic one-loop bubble, Figure 4, not only provides the Landau variety but also the singularities in kinematic limits. Let $\mathcal{G}_h$ be the homogenized Lee-Pomeransky polynomial for the bubble graph: $\mathcal{G}_h = x_0(x_1 + x_2) + (m_1^2 + m_2^2 - p^2)x_1 x_2 + m_1^2 x_1^2 + m_2^2 x_2^2$. We have the variety $X = \mathbf{V}(x_0 x_1 x_2 \mathcal{G}_h) \subset \mathbb{P}^2 \times \mathbb{C}^3$; also let $Y = \mathbb{C}^3$ be the space of kinematics. Calculating the (minimal) Whitney stratification $(X_\bullet, Y_\bullet)$ of the corresponding projection map $\pi : X \to \mathbb{C}^3$ gives the following

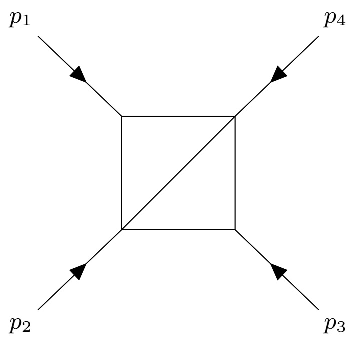

FIG. 5: The slashed box is one of the simplest graphs where different approaches to calculating Landau singularities do not coincide. This is discussed in Section V B.

expression for $Y_\bullet$,

$$\begin{aligned}
Y_3 =& Y = \mathbb{C}^3, \\
Y_2 =& \mathbf{V}(m_1^2) \cup \mathbf{V}(m_2^2) \cup \mathbf{V}(p^2) \\
& \cup \mathbf{V}(p^4 + m_1^4 + m_2^4 - 2p^2 m_1^2 - 2p^2 m_2^2 - 2m_1^2 m_2^2), \\
Y_1 =& \mathbf{V}(p^2,\, m_1^2 - m_2^2) \cup \mathbf{V}(m_2^2 - p^2,\, m_1^2) \cup \mathbf{V}(m_2^2,\, m_1^2 - p^2) \\
& \cup \mathbf{V}(p^2,\, m_1^2) \cup \mathbf{V}(p^2,\, m_2^2) \cup \mathbf{V}(m_2^2,\, m_1^2), \\
Y_0 =& \mathbf{V}(p^2,\, m_1^2,\, m_2^2).
\end{aligned}$$

Per Definition 1, the components of codimension one, Y_2, constitutes the Landau variety. As already mentioned, the lower dimensional strata correspond to the Landau variety at certain limits. In the limit $m_1 \to 0$, the Landau variety is read of from the components in Y_1 containing a single m_1^2: $\mathbf{V}(m_2^2 - p^2,\, m_1^2)$, $\mathbf{V}(p^2, m_1^2)$ and $\mathbf{V}(m_2^2, m_1^2)$. This means that the Landau variety in this limit is $\mathbf{V}(m_2^2 - p^2) \cup \mathbf{V}(p^2) \cup \mathbf{V}(m_2^2)$.

In this example this is exactly the same as substituting $m_1^2 = 0$ in the original Landau variety, but unlike the stratification the latter is not always guaranteed to work.

We also remark that special kinematic configurations can also be specified in the codomain of the `mapStratify` command, e.g. the Gram determinant constraint for a six-point process may be specified as the space of kinematics Y and the resulting Whitney stratification will only provide strata satisfying this constraint.

The Landau variety gives information of the full analytic structure of the meromorphic function defined by the integral and not the singularities in the physical region. However, the methods in [17] are capable of calculating Whitney stratifications of real semi-algebraic sets, potentially allowing direct access to the physical singularities as well; we leave this fascinating exploration to a future work.

B. Slashed box

As a first simple two-loop example, we consider the slashed box in Figure 5 with all internal edges massless and the external legs satisfying $p_1^2 = 0 = p_3^2$ and $p_2^2 \neq 0$, $p_4^2 \neq 0$. This is a kinematic setup relevant for the two-loop correction of of certain QCD processes [32]. The setup for the calculating the Landau variety is $X = \mathbf{V}(x_0 \cdots x_5 \mathcal{G}_h) \subset \mathbb{P}^5 \times \mathbb{C}^4$, with $Y = \mathbb{C}^4$. Calculating the Whitney stratification $(X_\bullet, Y_\bullet)$ of the corresponding projection map $\pi : X \to \mathbb{C}^4$ gives the following expression for the Landau variety

$$\begin{aligned}
Y_3 =& \mathbf{V}(p_2^2) \cup \mathbf{V}(p_4^2) \cup \mathbf{V}(s) \cup \mathbf{V}(t) \\
& \cup \mathbf{V}(p_2^2 - s) \cup \mathbf{V}(p_2^2 - t) \cup \mathbf{V}(p_4^2 - s) \cup \mathbf{V}(p_4^2 - t) \\
& \cup \mathbf{V}(p_2^2 + p_4^2 - s - t) \cup \mathbf{V}(p_2^2 p_4^2 - st)
\end{aligned}$$

Which is the same as obtained with both `HyperInt` and the principal Landau determinant.

More interesting is the slashed box with the setup $p_1^2 = 0 = p_2^2$ and $p_3^2 \neq 0$, $p_4^2 \neq 0$. The Landau variety now consists of the 9 components

$$\begin{aligned}
Y_3 =& \mathbf{V}(p_3^2) \cup \mathbf{V}(s) \cup \mathbf{V}(st + t^2 - tp_3^2 - tp_4^2 + p_3^2 p_4^2) \\
& \cup \mathbf{V}(t - p_4^2) \cup \mathbf{V}(s^2 - 2sp_3^2 + p_3^4 - 2sp_4^2 - 2p_3^2 p_4^2 + p_4^4) \\
& \cup \mathbf{V}(t - p_3^2) \cup \mathbf{V}(t) \cup \mathbf{V}(p_4^2) \cup \mathbf{V}(p_4^2 - s - t).
\end{aligned}$$

which coincide with the result from `HyperInt`, meanwhile, the principal Landau determinant contains 8 of these components, in particular it is missing $p_4^2 - s - t = 0$. That this component is significant can be further strengthened: the Euler characteristic $\chi(\mathbf{V}(x_0 \cdots x_5 \mathcal{G}_h))$ changes for kinematics on this component and it is a letter in the symbol alphabet for the double box topology studied in [32].

We remark that another way of obtaining all 9 components is the limiting procedure from [4, §3.4] used on the “proper” principal A-determinant [33]. That is, using the monomial support for the slashed box but with all coefficients treated as generic and then applying the limit where the coefficients becomes the physical ones.

C. Parachute graph

In [12], Berghoff and Panzer showed that the integrand geometry $\{\mathcal{U} = 0\} \cup \{\mathcal{F} = 0\} \cup \{x_i = 0,\, i = 1, \ldots, 4\}$ of the parachute graph (Figure 6) has a special non-normal intersection requiring the sequential blow-up of the projective point $[x_1 : x_2]$ and $x_1 + x_2 = 0$ to resolve the geometry. The discriminant of this new hypersurface is (see [12, Eq. (6.15)])

$$p_3^2(m_4^2 - p_2^2)(m_3^2 - p_1^2) + (m_3^2 - m_4^2 - p_1^2 + p_2^2)(m_3^2 p_2^2 - m_4^2 p_1^2) \quad (4)$$

which is not captured by either direct principal A-determinant calculation nor the principal Landau determinant [14, Eq. (3.18)]. However, it is an output from `HyperInt` and the Euler characteristic of the hypersurface complement drops from the generic value 19 to the value 18 on it, so it should indeed be a part of the Landau variety. We note that the method of blow-ups to resolve non-transverse intersections is an equivalent alternative

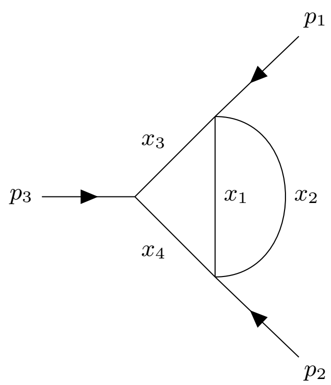

FIG. 6: The full singularity structure of the parachute graph was first uncovered by Berghoff and Panzer in [12]. For restricted kinematics we use Whitney stratifications to find the full Landau variety, including components missed by other methods.

method to calculate the Whitney stratification, in the latter cases non-transverse intersections are resolved by imposing the B condition (see Section III).

Stratifying the map $\pi : \mathbb{P}^4 \times \mathbb{C}^7 \to \mathbb{C}^7$ is at the current stage of the implementation too taxing. Restricting the kinematics to $\{m_1^2 = 1, m_2^2 = 0, m_3^2 = 0, m_4^2 = 2, p_1^2 = -1, p_2^2 = 0\}$ keeping only p_3^2 free, the discriminant (4) reduces to $p_3^2 - 1$. Direct integration in `HyperInt` confirms that this is a letter of the integral [34]. At this reduced kinematic point, calculation of the PLD provides three singularities, $\{p_3^2,\ p_3^2+2,\ p_3^2-2\}$ while the Whitney stratification gives five:

$$Y_0 = \mathbf{V}(p_3^2) \cup \mathbf{V}(p_3^2+2) \cup \mathbf{V}(p_3^2-2) \cup \mathbf{V}(p_3^2+1) \cup \mathbf{V}(p_3^2-1).$$

In particular it gives the discriminant (4) at this kinematic point.

VI. CONCLUSIONS AND OUTLOOKS

In this letter we use the Whitney stratification of maps to calculate the Landau variety as defined by Pham. This not only yields the complete set of singularities for the integral at hand but also the singularities for integrals arising as kinematic limits. As the stratification is a taxing computation, the examples in this letter are restricted to two-loop graphs, however, the methods are fully rigorous and in general applicable to any loop order and kinematic set-up. Even more, this method is agnostic to the fact that these are Feynman integrals and can be applied to calculate singularities of any parameterized integral of Euler type, that is, every integral with rational integrand.

In particular, since the Whitney stratification gives the full Landau variety, we are able to calculate the singularities that the naive principal A-determinant or the principal Landau determinant misses.

That discriminant based methods miss certain singularities provokes the obvious question: is anything special about these singularities, both from a physical and mathematical perspective? In forthcoming work we will expand on this by strengthen the connection between stratified maps, blow-ups and Euler characteristics.

Finally we note that the current implementation of the map stratification algorithms is general purpose, being applicable to any algebraic map between any two varieties, and does not take any special advantage of the highly structured nature of the input in the Feynman integral context. Hence, there is hope for substantial performance improvements if more specialized implementations are developed.

ACKNOWLEDGMENTS

MH and FT would like to thank the Isaac Newton Institute for Mathematical Sciences, Cambridge, for support and hospitality during the program "New equivariant methods in algebraic and differential geometry" where work on this paper was undertaken. This visit was supported by EPSRC grant no EP/R014604/1.

MH was supported by the Air Force Office of Scientific Research (AFOSR) under award number FA9550-22-1-0462, managed by Dr. Frederick Leve, and would like to gratefully acknowledge this support.

The authors would also like to thank Rigers Aliaj, Saiei Matsubara-Heo, Erik Panzer and Simon Telen for helpful discussions during the preparation of this letter.

[1] R. J. Eden, P. V. Landshoff, D. I. Olive, and J. C. Polkinghorne, *The analytic S-matrix* (Cambridge Univ. Press, Cambridge, 1966).

[2] L. D. Landau, On analytic properties of vertex parts in quantum field theory, Nucl. Phys. **13**, 181 (1959).

[3] J. M. Henn, Multiloop integrals in dimensional regularization made simple, Phys. Rev. Lett. **110**, 251601 (2013), arXiv:1304.1806 [hep-th].

[4] C. Dlapa, M. Helmer, G. Papathanasiou, and F. Tellander, Symbol alphabets from the Landau singular locus, JHEP **10**, 161, arXiv:2304.02629 [hep-th].

[5] A. B. Goncharov, M. Spradlin, C. Vergu, and A. Volovich, Classical Polylogarithms for Amplitudes and Wilson Loops, Phys.Rev.Lett. **105**, 151605 (2010), arXiv:1006.5703 [hep-th].

[6] E. Gardi, F. Herzog, S. Jones, Y. Ma, and J. Schlenk, The on-shell expansion: from Landau equations to the Newton polytope, JHEP **07**, 197, arXiv:2211.14845 [hep-th].

[7] F. C. S. Brown, On the periods of some Feynman inte-

grals, (2009), arXiv:0910.0114 [math.AG].
[8] E. Panzer, Algorithms for the symbolic integration of hyperlogarithms with applications to Feynman integrals, Comput. Phys. Commun. **188**, 148 (2015), arXiv:1403.3385 [hep-th].
[9] R. P. Klausen, Kinematic singularities of Feynman integrals and principal A-determinants, JHEP **02**, 004, arXiv:2109.07584 [hep-th].
[10] H. S. Hannesdottir, A. J. McLeod, M. D. Schwartz, and C. Vergu, Constraints on sequential discontinuities from the geometry of on-shell spaces, JHEP **07**, 236, arXiv:2211.07633 [hep-th].
[11] S. Mizera and S. Telen, Landau discriminants, JHEP **08**, 200, arXiv:2109.08036 [math-ph].
[12] M. Berghoff and E. Panzer, Hierarchies in relative Picard-Lefschetz theory, (2022), arXiv:2212.06661 [math-ph].
[13] C. Fevola, S. Mizera, and S. Telen, Landau Singularities Revisited, (2023), arXiv:2311.14669 [hep-th].
[14] C. Fevola, S. Mizera, and S. Telen, Principal Landau Determinants, (2023), arXiv:2311.16219 [math-ph].
[15] F. Pham, *Singularities of integrals*, Universitext (Springer, London; EDP Sciences, Les Ulis, 2011).
[16] M. Helmer and V. Nanda, Conormal spaces and Whitney stratifications, Found. Comput. Math. **23**, 1745 (2023), arXiv:2106.14555 [math.AG].
[17] M. Helmer and V. Nanda, Effective Whitney Stratification of Real Algebraic varieties, (2023), arXiv:2307.05427 [math.AG].
[18] D. R. Grayson and M. E. Stillman, Macaulay2, a software system for research in algebraic geometry, Available at `http://www.math.uiuc.edu/Macaulay2`.
[19] The relevant function is `mapStratify`, whose documentation in the current version of the `WhitneyStratifications` package is available here: `http://martin-helmer.com/Software/WhitStrat/_map__Stratify.html`.
[20] R. N. Lee and A. A. Pomeransky, Critical points and number of master integrals, JHEP **11**, 165, arXiv:1308.6676 [hep-ph].
[21] S. Weinzierl, *Feynman Integrals* (2022) arXiv:2201.03593 [hep-th].
[22] I. M. Gel'fand, M. Kapranov, and A. Zelevinskĭ, *Discriminants, resultants, and multidimensional determinants* (Springer Science & Business Media, 2008).
[23] A. Esterov, The discriminant of a system of equations, Adv. Math. **245**, 534 (2013), arXiv:1110.4060 [math.AG].
[24] C. Améndola, N. Bliss, I. Burke, C. R. Gibbons, M. Helmer, S. Hoşten, E. D. Nash, J. I. Rodriguez, and D. Smolkin, The maximum likelihood degree of toric varieties, J. Symb. Comput. **92**, 222 (2019), arXiv:1703.02251 [math.AG].
[25] T. Bitoun, C. Bogner, R. P. Klausen, and E. Panzer, Feynman integral relations from parametric annihilators, Lett. Math. Phys. **109**, 497 (2019), arXiv:1712.09215 [hep-th].
[26] B. Teissier, Variétés polaires. II. Multiplicités polaires, sections planes, et conditions de Whitney, in *Algebraic geometry (La Rábida, 1981)*, Lecture Notes in Math., Vol. 961 (Springer, Berlin, 1982) pp. 314–491.
[27] A. G. Flores and B. Teissier, Local polar varieties in the geometric study of singularities, Ann. Fac. Sci. Toulouse Math. (6) **27**, 679 (2018).
[28] J. Mather, Notes on topological stability, Bull. Amer. Math. Soc. **49**, 475 (2012).
[29] Note the the projection map from the affine variety X to $\mathbb{R}$ is not proper, hence rigorously speaking, we actually compactify X by considering its projective closure $\overline{X} = \mathbf{V}(x^2z\,w - x^3 + y^2w - 2\,y\,w^2 + w^3)$ in $\mathbb{P}^2\times\mathbb{C}$, where w, x, y are the coordinates on $\mathbb{P}^2$, and deduce the above result form the computation of the stratification of this induced projection $\overline{X}\to\mathbb{C}$.
[30] C. Harris and M. Helmer, Segre class computation and practical applications, Math. Comp. **89**, 465–491 (2019), arXiv:1806.07408 [math.AG].
[31] This faster, but potentially incomplete, version of the stratification can be found using an option in the `mapStratify` function, see the documentation for more details: `http://martin-helmer.com/Software/WhitStrat/_map__Stratify.html`.
[32] J. M. Henn, K. Melnikov, and V. A. Smirnov, Two-loop planar master integrals for the production of off-shell vector bosons in hadron collisions, JHEP **05**, 090, arXiv:1402.7078 [hep-ph].
[33] In this calculation we use Gale duality to fix six coefficients to one, we do also add the constraint that the coefficients corresponding to p_3^2 are the same. This goes beyond what is strictly allowed, but as the correct limit is obtained from this object, it is also obtained from the full principal A-determinant.
[34] We thank Erik Panzer for confirming this.

Paper IV

Tropical Feynman integration in the Minkowski regime
Michael Borinsky, Henrik J. Munch and **Felix Tellander**
Comput. Phys. Commun., **292** (2023) 108874, [2302.08955]

Computer Physics Communications 292 (2023) 108874

Contents lists available at ScienceDirect

Computer Physics Communications

journal homepage: www.elsevier.com/locate/cpc

Computer Programs in Physics

Tropical Feynman integration in the Minkowski regime ☆,☆☆

Michael Borinsky [a,*], Henrik J. Munch [b], Felix Tellander [c]

[a] Institute for Theoretical Studies, ETH Zürich, 8092 Zürich, Switzerland
[b] Dipartimento di Fisica e Astronomia, Università degli Studi di Padova, 35131 Padova, Italy
[c] Deutsches Elektronen-Synchrotron DESY, Notkestr. 85, 22607 Hamburg, Germany

ARTICLE INFO

Article history:
Received 1 March 2023
Received in revised form 5 June 2023
Accepted 27 July 2023
Available online 9 August 2023

Dataset link: https://github.com/michibo/feyntrop

Keywords:
Feynman integrals
Monte Carlo integration
Tropical geometry
Epsilon-expansion
Contour deformation
Causal i-epsilon prescription

ABSTRACT

We present a new computer program, `feyntrop`, which uses the tropical geometric approach to evaluate Feynman integrals numerically. In order to apply this approach in the physical regime, we introduce a new parametric representation of Feynman integrals that implements the causal $i\varepsilon$ prescription concretely while retaining projective invariance. `feyntrop` can efficiently evaluate dimensionally regulated, quasi-finite Feynman integrals, with not too exceptional kinematics in the physical regime, with a relatively large number of propagators and with arbitrarily many kinematic scales. We give a systematic classification of all relevant kinematic regimes, review the necessary mathematical details of the tropical Monte Carlo approach, give fast algorithms to evaluate (deformed) Feynman integrands, describe the usage of `feyntrop` and discuss many explicit examples of evaluated Feynman integrals.

Program summary
Program title: `feyntrop`.
CPC Library link to program files: https://doi.org/10.17632/k6r62hgdvd.1
Developer's repository link: https://github.com/michibo/feyntrop.
Licensing provisions: MIT License.
Programming language: The tropical Monte Carlo code is written in `C++`. The high-level interface is written in `python`.
Supplementary material: The repository includes installation and usage instructions (`README.md`), a jupyter notebook tutorial (`tutorial_2L_3pt.ipynb`), the collection of examples presented in section 6 (see the folder `/examples`), and a test suite to ensure a successful installation (see the folder `/tests`).
Nature of problem: Sufficiently fast numerical integration of (dimensionally regularized) Feynman integrals (also in the Minkowski regime of phase space).
Solution method: Tropical Monte Carlo integration of a manifestly $i\varepsilon$-free parametric representation of Feynman integrals.
Additional comments: The program `feyntrop` is based on previous code available at https://github.com/michibo/tropical-feynman-quadrature, which was published as a proof-of-concept with, Michael Borinsky, 'Tropical Monte Carlo quadrature for Feynman integrals', *Ann. Inst. Henri Poincaré Comb. Phys. Interact. (in press)* [1]. This previous code did not have features which are required for phenomenological studies in high-energy physics. In particular, it only allowed for phase space points in the Euclidean regime, and only computed the leading term in the ϵ expansion.
Restrictions: The Feynman integral must be quasi-finite and the momentum configuration must be sufficiently generic. Numerators of Feynman integrals are not implemented.

☆ The review of this paper was arranged by Prof. Z. Was.
☆☆ This paper and its associated computer program are available via the Computer Physics Communications homepage on ScienceDirect (http://www.sciencedirect.com/science/journal/00104655).
* Corresponding author.
E-mail address: michael.borinsky@eth-its.ethz.ch (M. Borinsky).

https://doi.org/10.1016/j.cpc.2023.108874

References

Eigen3 [2]. The xoshiro256+ pseudo-random-number generator [3]. python [4]. pybind11 [5]. sympy [6].

Contents

1. Introduction

Feynman integrals are a key tool in quantum field theory. They are necessary to produce accurate predictions from given theoretical input such as a Lagrangian. Applications are, for instance, the computations of virtual contributions to scattering cross-sections for particle physics phenomenology [7], corrections to the magnetic moment of the muon or the half-life of positronium [8], critical exponents in statistical field theory [9] and corrections to the Newton potential due to general relativity [10]. An entirely mathematical application of Feynman integrals is the certification of cohomology classes in moduli spaces of curves or of graphs [11].

In this paper, we introduce feyntrop,[1] a new tool to evaluate Feynman integrals numerically. In contrast to existing tools, feyntrop can efficiently evaluate Feynman integrals with a relatively large number of propagators and with an arbitrary number of scales. Moreover, feyntrop can deal with Feynman integrals in the *physical* Minkowski regime and automatically takes care of the usually intricate contour deformation procedure. The spacetime dimension is completely arbitrary and integrals that are expanded in a dimensional regulator can be evaluated. The main restriction of feyntrop is that it cannot deal with Feynman integrals having subdivergences, that means the input Feynman integrals are required to be *quasi-finite*. Moreover, feyntrop is not designed to integrate Feynman integrals at certain highly exceptional kinematic points. Outside the Euclidean regime, the external kinematics are required to be sufficiently *generic*. It is worthwhile mentioning though that such highly exceptional kinematic points seem quite rare and feyntrop performs surprisingly well in these circumstances—in spite of the lack of mathematical guarantees for functioning. In fact, we were not able to find a quasi-finite integral with exceptional kinematics for which the integration with feyntrop fails. We only observed significantly decreased rates of convergence in such cases.

The mathematical theory of Feynman integrals has advanced rapidly in the last decades. Corner stone mathematical developments for Feynman integrals were, for instance, the systematic exploitation of their unitarity constraints (see, e.g., [12,13]), the systematic solution of their integration-by-parts identities (see, e.g., [14,15]), the application of modern algebraic geometric and number theoretic tools for

[1] feyntrop can be downloaded from https://github.com/michibo/feyntrop.

the benefit of their evaluation (see, e.g., [16–18]) and the systematic understanding of the differential equations which they fulfill (see, e.g., [19,20]).

Primarily, these theoretical developments were aimed at facilitating the *analytic* evaluation of Feynman integrals. All known analytic evaluation methods are inherently limited to a specific class of sufficiently simple diagrams. Especially for high-accuracy collider physics phenomenology, such analytic methods are often not sufficient to satisfy the demand for Feynman integral computations at higher loop order, which frequently involve complicated kinematics with many scales. Even if an analytic expression for a given Feynman integral is available, it is usually a highly non-trivial task to perform the necessary analytic continuation into the physical kinematic regime. On a different tack, computations of corrections to the Newton potential in the post-Newtonian expansion of general relativity [10] require the evaluation of large amounts of Feynman diagrams in three dimensional Euclidean space. As analytic evaluation is often more difficult in odd-dimensional spacetime, tropical Feynman integration is a promising candidate to fulfill the high demand for large loop order Feynman integrals in this field.

For this reason, numerical methods for the evaluation of Feynman integrals seem unavoidable once a certain threshold in precision has to be overcome. In this paper, we will use *tropical sampling* that was introduced in [1] to evaluate Feynman integrals numerically. This numerical integration technique is faster than traditional methods because the known (tropical) geometric structures of Feynman integrals are employed for the benefit of their numerical evaluation. For instance, general Euclidean Feynman integrals with up to 17 loops and 34 propagators can be evaluated using basic hardware with the proof-of-concept implementation that was distributed by the first author with [1]. The code of `feyntrop` is based on this implementation. The relevant mathematical structure is the *tropical geometry* of Feynman integrals in the parametric representation [21,1]. This tropical geometry itself is a simplification of the intricate *algebraic geometry* Feynman integrals display (see, e.g., [22]). Tropical Feynman integration was already used, for instance, in [23] to estimate the ϕ^4 theory β function up to loop order 11. Some ideas from [1] were already implemented in the `FIESTA` package [24]. Tropical sampling was extended to toric varieties with applications to Bayesian statistics [25]. Moreover, the tropical approach was recently applied to study infrared divergences of Feynman integrals in the Minkowski regime [26].

The tropical approach to Feynman integrals falls in line with the increasing number of fruitful applications of tools from convex geometry in the context of quantum field theory. These include, for example, the discovery of polytopes in amplitudes (see, e.g. [27,28]). Further, Feynman integrals can be seen as generalized Mellin-transformations [29–31]. As such they are solutions to GKZ-type differential equation systems [32]. Tropical and convex geometric tools are central to this analytic approach towards Feynman integrals (see, e.g., [33–37]).

Tropical Feynman integration is closely related to the *sector decomposition* approach [38–40], which applies to completely general algebraic integrals. State of the art implementations of sector decompositions are, for instance, `pySecDec` [41] and `FIESTA` [24]. Other numerical methods that are tailored specifically to Feynman integrals are, for instance, difference equations [15], unitarity methods [42], the Mellin-Barnes representation [43] and loop-tree duality [44,45]. With respect to potential applications to collider phenomenology, the latter three have the advantage of being inherently adapted to Minkowski spacetime kinematics. A newer technique is the systematic semi-numerical evaluation of Feynman integrals using differential equations [46,47], which is implemented, for instance, in `AMFlow` [48], `DiffExp` [49] and `SeaSyde` [50]. A similar semi-numerical approach was put forward in [51]. This technique can evaluate Feynman integrals quickly in the physical regime with high accuracy. A caveat is that it relies on the algebraic solution of the usually intricate integration-by-parts system associated to the respective Feynman integral and (usually) on analytic boundary values for the differential equations (see [48,52] for an exception where the boundary values are computed exclusively from algebraic input). We expect `feyntrop`, which does not rely on any analytic or algebraic input, to be useful for computing boundary values as input for such methods.

`feyntrop` uses the *parametric representation* of Feynman integrals for the numerical evaluation, which we briefly review in Section 2.1. This numerical evaluation has quite different characters in separate *kinematic regimes*. We propose a new classification of such kinematic regimes in Section 2.2 which, in addition to the usual Euclidean and Minkowski regimes, includes the intermediate *pseudo-Euclidean* regime. The original tropical Feynman integration implementation from [1] was limited to the Euclidean regime. Here, we achieve the extension of this approach to non-Euclidean regimes.

In the Minkowski regime, parametric Feynman integrands can have a complicated pole structure inside the integration domain. For the numerical integration an explicit *deformation* of the integration contour, which respects the desired causality properties, is needed. The use of explicit contour deformation prescriptions for numerics was pioneered in [42] and was later applied in the sector decomposition framework [53]. (Recently, a momentum space based approach for the solution of the deformation problem was put forward [54].) In Section 2.3, we propose an explicit deformation prescription which, in its basic form, was employed in [55] in the context of cohomological properties of Feynman integrals. This deformation prescription has the inherent advantage of retaining the projective symmetry of the parametric Feynman integrand. We provide explicit formulas for the Jacobian and thereby propose a new *deformed parametric representation* of the Feynman integral.

It is often desirable to evaluate a Feynman integral using dimensional regularization by adding a formal expansion parameter to the spacetime dimension, e.g. $D = D_0 - 2\epsilon$, where D_0 is a fixed number and we wish to evaluate the Laurent or Taylor expansion of the integral in ϵ. We will explain how `feyntrop` deals with such dimensionally regularized Feynman integrals in Section 2.4. Moreover, we will discuss one of the major limitations of `feyntrop` in this section: In its present form `feyntrop` can only integrate Feynman integrals that are *quasi-finite*. That means, input Feynman integrals are allowed to have an overall divergence, but no subdivergences. Further analytic continuation prescriptions (along the lines of [29,30,56]) would be needed to deal with such subdivergences and we postpone the implementation of such prescriptions into `feyntrop` to a future publication. For now, the user of the program is responsible to render all input integrals quasi-finite; for instance by projecting them to a quasi-finite basis [56]. Note, however, that within our approach, the base dimension D_0 is completely arbitrary and can even be a non-integer value if desired. The applicability in the case $D_0 = 3$ makes `feyntrop` a promising tool for the computation of post-Newtonian corrections to the gravitational potential [57].

In Sections 3.1 and 3.2, we will review the necessary ingredients for the tropical Monte Carlo approach from [1]: The concepts of the *tropical approximation* and *tropical sampling*. In Section 3.3, we review the (tropical) geometry of parametric Feynman integrands and the particular shape that the Symanzik polynomials' Newton polytopes exhibit. We will put special focus on the *generalized permutahedron* property of the second Symanzik $\mathcal{F}$ polynomial. At particularly exceptional kinematic points, this property of the $\mathcal{F}$ polynomial can be lost. In these cases the integration with `feyntrop` might fail. We discuss this limitation in detail in Section 3.3. The overall tropical sampling algorithm is summarized in Section 3.4.

In Section 4.2, we summarize the necessary steps for the efficient evaluation of (deformed) parametric Feynman integrands. The key step is to express the entire integrand in terms of explicit matrix expressions. Our method is more efficient than the naive expansion of the Symanzik polynomials, as fast linear algebra routines can be used for the evaluation of such matrix expressions.

The structure, installation and usage of the program `feyntrop` is described in Section 5. To illustrate its capabilities we give multiple detailed examples of evaluated Feynman integrals in Section 6. In Section 7, we conclude and give pointers for further developments of the general tropical Feynman integration method and the program `feyntrop`.

2. Feynman integrals

2.1. Momentum and parametric representations

Let G be a one-particle irreducible Feynman graph with edge set E and vertex set V. Each edge $e \in E$ comes with a mass m_e and an edge weight ν_e. Each vertex $v \in V$ comes with an incoming spacetime momentum p_v. Vertices without incoming momentum, i.e. where $p_v = 0$, are internal. Let $\mathcal{E}$ by the incidence matrix of G which is formed by choosing an arbitrary orientation for the edges and setting $\mathcal{E}_{v,e} = \pm 1$ if e points to/from v and $\mathcal{E}_{v,e} = 0$ if e is not incident to v. The Feynman integral associated to G reads

$$\mathcal{I} = \int \prod_{e\in E} \frac{\mathrm{d}^D q_e}{i\pi^{D/2}} \left(\frac{-1}{q_e^2 - m_e^2 + i\varepsilon} \right)^{\nu_e} \prod_{v \in V\setminus\{v_0\}} i\pi^{D/2} \delta^{(D)} \left(p_v + \sum_{e\in E} \mathcal{E}_{v,e} q_e \right), \tag{1}$$

where we integrate over all D-dimensional spacetime momenta q_e and we extracted the δ function that accounts for overall momentum conservation by removing the vertex $v_0 \in V$. We compute the squared length $q_e^2 = (q_e^0)^2 - (q_e^1)^2 - (q_e^2)^2 - \dots$ using the mostly-minus signature Minkowski metric.

To evaluate $\mathcal{I}$ numerically, we will use the equivalent parametric representation (see, e.g., [58])

$$\mathcal{I} = \Gamma(\omega) \int_{\mathbb{P}_+^E} \phi \quad \text{with} \quad \phi = \left(\prod_{e\in E} \frac{x_e^{\nu_e}}{\Gamma(\nu_e)} \right) \frac{1}{\mathcal{U}(\boldsymbol{x})^{D/2}} \left(\frac{1}{\mathcal{V}(\boldsymbol{x}) - i\varepsilon \sum_{e\in E} x_e} \right)^{\omega} \Omega\,. \tag{2}$$

We integrate over the *positive projective simplex* $\mathbb{P}_+^E = \{\boldsymbol{x} = [x_0, \dots, x_{|E|-1}] \in \mathbb{RP}^{E-1} : x_e > 0\}$ with respect to its canonical volume form

$$\Omega = \sum_{e=0}^{|E|-1} (-1)^{|E|-e-1} \frac{\mathrm{d}x_0}{x_0} \wedge \dots \wedge \widehat{\frac{\mathrm{d}x_e}{x_e}} \wedge \dots \wedge \frac{\mathrm{d}x_{|E|-1}}{x_{|E|-1}}\,. \tag{3}$$

Note that in the scope of this article we make the unusual choice to start the indexing with 0 for the benefit of a seamless notational transition to our computer implementation. So, the edge and vertex sets are always assumed to be given by $E = \{0, 1, \dots, |E|-1\}$ and $V = \{0, 1, \dots, |V|-1\}$.

The *superficial degree of divergence* of the graph G is given by $\omega = \sum_{e\in E} \nu_e - DL/2$, where $L = |E| - |V| + 1$ is the number of loops of G.

We use $\mathcal{V}(\boldsymbol{x}) = \mathcal{F}(\boldsymbol{x})/\mathcal{U}(\boldsymbol{x})$ as a shorthand for the quotient of the two *Symanzik polynomials* that can be defined using the *reduced graph Laplacian* $\mathcal{L}(\boldsymbol{x})$, a $(|V|-1) \times (|V|-1)$ matrix given element-wise by $\mathcal{L}(\boldsymbol{x})_{u,v} = \sum_{e\in E} \mathcal{E}_{u,e}\mathcal{E}_{v,e}/x_e$ for all $u, v \in V \setminus \{v_0\}$. We have the identities

$$\mathcal{U}(\boldsymbol{x}) = \det \mathcal{L}(\boldsymbol{x}) \left(\prod_{e\in E} x_e \right), \qquad \mathcal{F}(\boldsymbol{x}) = \mathcal{U}(\boldsymbol{x}) \left(- \sum_{u,v \in V\setminus\{v_0\}} \mathcal{P}^{u,v}\, \mathcal{L}^{-1}(\boldsymbol{x})_{u,v} + \sum_{e\in E} m_e^2 x_e \right), \tag{4}$$

where $\mathcal{P}^{u,v} = p_u \cdot p_v$ with the scalar product being computed using the Minkowski metric.

Combinatorial Symanzik polynomials We also have the combinatorial formulas for $\mathcal{U}$ and $\mathcal{F}$

$$\mathcal{U}(\boldsymbol{x}) = \sum_T \prod_{e\notin T} x_e\,, \qquad \mathcal{F}(\boldsymbol{x}) = -\sum_F p(F)^2 \prod_{e\notin F} x_e + \mathcal{U}(\boldsymbol{x}) \sum_{e\in E} m_e^2 x_e\,, \tag{5}$$

where we sum over all spanning trees T and all spanning two-forests F of G, and $p(F)^2$ is the Minkowski squared momentum running between the two-forest components. From this formulation it can be seen that $\mathcal{U}$ and $\mathcal{F}$ are homogeneous polynomials of degree L and $L+1$ respectively. Hence, $\mathcal{V}$ is a homogeneous rational function of degree 1.

We will give fast algorithms to evaluate $\mathcal{U}(\boldsymbol{x})$ and $\mathcal{F}(\boldsymbol{x})$ in Section 4.2.

2.2. Kinematic regimes

By Poincaré invariance, the value of the Feynman integral (1) only depends on the $|V| \times |V|$ Gram matrix $\mathcal{P}^{u,v} = p_u \cdot p_v$ and not on the explicit form of the vectors p_v. In fact, it is even irrelevant in which ambient dimension the vectors p_v are defined. The following characterization of the different *kinematic regimes* that we propose will therefore only take the input of a symmetric $|V| \times |V|$ matrix $\mathcal{P}$ with vanishing row and column sums (i.e. the momentum conservation conditions $\sum_{v\in V} p_u \cdot p_v = \sum_{v\in V} \mathcal{P}^{u,v} = 0$ for all $u \in V$), without requiring any explicit knowledge of the p_v vectors. In fact, we will not even require that there are any vectors p_v for which $\mathcal{P}^{u,v} = p_u \cdot p_v$.

Euclidean regime We say a given Feynman integral computation problem is in the *Euclidean regime* if the matrix $\mathcal{P}$ is negative semi-definite. In this regime, $\mathcal{F}(\boldsymbol{x}) \geq 0$ for all $\boldsymbol{x} \in \mathbb{P}_+^E$. We call this the Euclidean regime, because the integral (1) is equivalent to an analogous Feynman integral where scalar products are computed with the Euclidean all-minus metric. To see this, note that as $-\mathcal{P}$ is positive semi-definite, there is a $|V| \times |V|$ matrix $\mathcal{Q}$ such that $\mathcal{P} = -\mathcal{Q}^T \mathcal{Q}$. We can think of the column vectors $\widetilde{p}_1, \ldots, \widetilde{p}_{|V|}$ of $\mathcal{Q}$ as an auxiliary set of incoming momentum vectors. Elements of $\mathcal{P}$ can be interpreted as Euclidean, all-minus metric, scalar products of the $\widetilde{p}_v$-vectors: $\mathcal{P}^{u,v} = -\widetilde{p}_u^T \widetilde{p}_v = -\sum_{w \in V} \mathcal{Q}^{w,u} \mathcal{Q}^{w,v}$. Translating this back to (1) means that we can change the signature of the scalar products to the all-minus metric if we replace the external momenta with the $\widetilde{p}_v$ vectors which are defined in an auxiliary space $\mathbb{R}^{|V|}$. We emphasize that this way of relating Euclidean and Minkowski space integrals is inherently different from the typical *Wick rotation* procedure and that the $\widetilde{p}_v$-vectors will in general be different from the original p_v vectors.

Pseudo-Euclidean regime In fact, $\mathcal{F}(\boldsymbol{x}) \geq 0$ for all $\boldsymbol{x} \in \mathbb{P}_+^E$ in a larger kinematic regime, where $\mathcal{P}$ is not necessarily negative semi-definite. If for each subset $V' \subset V$ of the vertices the inequality

$$\left(\sum_{v \in V'} p_v\right)^2 = \sum_{u,v \in V'} p_u \cdot p_v = \sum_{u,v \in V'} \mathcal{P}^{u,v} \leq 0 \tag{6}$$

is respected, then we are in the *pseudo-Euclidean* regime. The first two equalities in (6) are only included as mnemonic devices; knowledge of $\mathcal{P}$ is sufficient to check the inequalities. Equivalently, we can require the element sums of all *principle minor matrices* of the $\mathcal{P}$ matrix to be ≤ 0.

By (5) and (6), the coefficients of $\mathcal{F}$ are non-negative in the pseudo-Euclidean regime. Our choice of normalization factors ensures that (1) and (2) are real positive in this case.

We remark that there is a commonly used alternative definition of a kinematic regime which, on first sight, is similar to the condition above. This alternative definition requires the inequalities $p_u \cdot p_v \leq 0$ to be fulfilled for all $u, v \in V$ (see, e.g., [59, Sec. 2.5]). This is more restrictive than our condition in (6). In fact, it is too restrictive for our purposes, as not even entirely *Euclidean Feynman integrals* can generally be described in this regime. The reason for this is that not all negative semi-definite matrices $\mathcal{P}$ fulfill this more restrictive condition.

In our case, the Euclidean regime is contained in the pseudo-Euclidean regime. To verify this, we have to make sure that a negative semi-definite $\mathcal{P}$ fulfills the conditions in (6). Such a $\mathcal{P}$ can be represented with an appropriate set of $\widetilde{p}_v$ vectors as above: $\mathcal{P}^{u,v} = -\widetilde{p}_u^T \widetilde{p}_v$. For each $V' \subset V$ we get the principle minor element sum

$$\sum_{u,v \in V'} \mathcal{P}^{u,v} = -\sum_{u,v \in V'} \widetilde{p}_u^T \widetilde{p}_v = -\left(\sum_{v \in V'} \widetilde{p}_v\right)^T \left(\sum_{v \in V'} \widetilde{p}_v\right) \leq 0\,. \tag{7}$$

Minkowski regime If we are not in the pseudo-Euclidean regime (and thereby also not in the Euclidean regime), then we are in the *Minkowski regime*.

Generic and exceptional kinematics Without any resort to the explicit incoming momentum vectors p_v, we call a vertex v *internal* if $\mathcal{P}^{u,v} = 0$ for all $u \in V$ and *external* otherwise. Let $V^{\text{ext}} \subset V$ be the set of external vertices. Complementary to the classification above, we say that our kinematics are *generic* if for each *proper* subset $V' \subsetneq V^{\text{ext}}$ of the external vertices of G and for each non-empty subset $E' \subset E$ of the edges of G we have

$$\left(\sum_{v \in V'} p_v\right)^2 = \sum_{u,v \in V'} p_u \cdot p_v = \sum_{u,v \in V'} \mathcal{P}^{u,v} \neq \sum_{e \in E'} m_e^2\,. \tag{8}$$

For example, the kinematics are always generic in the pseudo-Euclidean regime if $m_e > 0$ for all $e \in E$ or if $\sum_{u,v \in V'} \mathcal{P}^{u,v} < 0$ for all $V' \subsetneq V^{\text{ext}}$. Note that generic kinematics also exclude *on-shell external momenta*, i.e. cases where $p_v^2 = \mathcal{P}^{v,v} = 0$ for some $v \in V^{\text{ext}}$ as long as not all $m_e > 0$, for then there exists at least one edge $e \in E$ such that $p_v^2 = 0 = m_e^2$, thus violating (8). Genericity, for instance, guarantees that there will be no cancellation between the momentum and the mass part of the $\mathcal{F}$-polynomial as defined in (5).

Kinematic configurations that are not generic are called *exceptional*.

As above, only the statements on $\mathcal{P}^{u,v}$ are sufficient for the classification. The other equalities are added to enable a seamless comparison to the literature.

The discussed kinematic regimes and their respective overlaps are illustrated in Fig. 1. In contrast to what the figure might suggest, the exceptional kinematics only cover a space that is of lower dimension than the one of the generic regime. The Minkowski regime is not explicitly shown as it covers the whole area that is not pseudo-Euclidean. Note that Minkowski, pseudo-Euclidean and Euclidean kinematics can be exceptional.

`feyntrop` detects the relevant kinematic regime using the conditions discussed above.

2.3. Contour deformation

In the pseudo-Euclidean (and thereby also in the Euclidean) regime, $\mathcal{F}(\boldsymbol{x})$ stays positive and the integral (2) cannot have any simple poles inside the integration domain.

In the Minkowski regime however, simple propagator poles of the integrand (1) and simple poles associated to zeros of $\mathcal{F}$ in (2) are avoided using the causal $i\varepsilon$ prescription (see, e.g., [60]). This prescription tells us to which side of the pole the integration contour needs to be deformed. When evaluating integrals such as (1) numerically, we have to find an *explicit* choice for such an integration

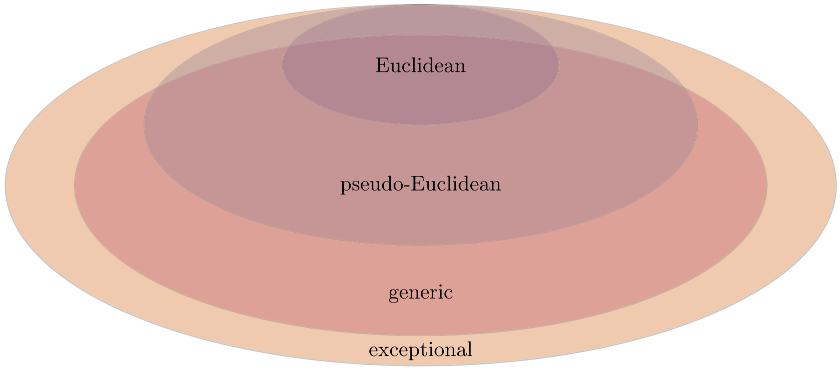

Fig. 1. Partition of kinematics into different regimes.

contour. Finding such an explicit contour deformation, which also has decent numerical stability properties, is a surprisingly complicated task. Explicit contour deformations for numerical evaluation were pioneered by Soper [42] and later refined [53,61]. This original type of contour deformation has the caveat that the projective symmetry of the integral (2) is lost as these deformations are inherently non-projective and usually formulated in affine charts, i.e. 'gauge fixed' formulations of (2). Experience, e.g. from [1], shows that the projective symmetry of (2) is a treasured good that should not be given up lightly.

To retain projective symmetry we will hence use a different deformation than established numerical integration tools. We will use the embedding $\iota_\lambda : \mathbb{P}_+^E \hookrightarrow \mathbb{CP}^{|E|-1}$ (recall that $\mathbb{P}_+^E$ is a subset of $\mathbb{RP}^{|E|-1}$) of the projective simplex into $|E|-1$ complex dimensional projective space given by

$$\iota_\lambda : x_e \mapsto x_e \exp\left(-i\lambda \frac{\partial \mathcal{V}}{\partial x_e}(\boldsymbol{x})\right). \tag{9}$$

This deformation prescription was proposed in [55, eq. (43)] in the context of the cohomological viewpoint on Feynman integrals (see also [62, Sec. 4.3]). As $\mathcal{U}$ and $\mathcal{F}$ are homogeneous polynomials of degree L and $L+1$ respectively and $\mathcal{V}(\boldsymbol{x}) = \mathcal{F}(\boldsymbol{x})/\mathcal{U}(\boldsymbol{x})$, the partial derivative $\frac{\partial \mathcal{V}}{\partial x_e}$ is a rational function in $\boldsymbol{x}$ of homogeneous degree 0, so ι_λ indeed respects projective equivalence.

We want to deform the integration contour $\mathbb{P}_+^E$ of (2) into $\iota_\lambda(\mathbb{P}_+^E) \subset \mathbb{CP}^{|E|-1}$. The deformation ι_λ does not change the boundary of $\mathbb{P}_+^E$ as each boundary face of $\mathbb{P}_+^E$ is characterized by at least one vanishing homogeneous coordinate $x_e = 0$. So, $\iota_\lambda(\partial\mathbb{P}_+^E) = \partial\mathbb{P}_+^E$. By Cauchy's theorem, we can deform the contour as long as we do not hit any poles of the integrand ϕ. Supposing that λ is small enough such that no poles of ϕ are hit by the deformation, we have

$$\mathcal{I} = \Gamma(\omega) \int_{\iota_\lambda(\mathbb{P}_+^E)} \phi = \Gamma(\omega) \int_{\mathbb{P}_+^E} \iota_\lambda^* \phi\,, \tag{10}$$

where $\iota_\lambda^*\phi$ denotes the *pullback* of the differential form ϕ. A computation on forms reveals that $\iota_\lambda^*\,\Omega = \det(\mathcal{J}_\lambda(\boldsymbol{x}))\,\Omega$, where the Jacobian $\mathcal{J}_\lambda(\boldsymbol{x})$ is the $|E| \times |E|$ matrix given element-wise by

$$\mathcal{J}_\lambda(\boldsymbol{x})^{e,h} = \delta_{e,h} - i\lambda x_e \frac{\partial^2 \mathcal{V}}{\partial x_e \partial x_h}(\boldsymbol{x}) \text{ for all } e, h \in E\,. \tag{11}$$

Thus, we arrive at the desired *deformed parametric Feynman integral* by making (10) explicit,

$$\mathcal{I} = \Gamma(\omega) \int_{\mathbb{P}_+^E} \iota_\lambda^* \phi = \Gamma(\omega) \int_{\mathbb{P}_+^E} \left(\prod_{e\in E} \frac{X_e^{\nu_e}}{\Gamma(\nu_e)}\right) \frac{\det \mathcal{J}_\lambda(\boldsymbol{x})}{\mathcal{U}(\boldsymbol{X})^{D/2} \cdot \mathcal{V}(\boldsymbol{X})^{\omega}}\,\Omega\,, \tag{12}$$

where $\boldsymbol{X} = \iota_\lambda(\boldsymbol{x})$, that means $\boldsymbol{X} = (X_0, \ldots, X_{|E|-1})$ and $X_e = x_e \exp\left(-i\lambda \frac{\partial \mathcal{V}}{\partial x_e}(\boldsymbol{x})\right)$ for all $e \in E$.

Although the prescription (9) was proposed before in a more formal context, the deformed formulation of the parametric Feynman integral (12) with the explicit Jacobian factor given by (11) appears not to have been considered previously in the literature.

In Section 4.2, we provide fast algorithms and formulas to evaluate $\frac{\partial \mathcal{V}}{\partial x_e}(\boldsymbol{x})$ and X_e.

Landau singularities In the formulation (12), the $i\varepsilon$ prescription is taken care of by the deformation of the rational function $\mathcal{V}$. To see this, consider the Taylor expansion of $\mathcal{V}(\boldsymbol{X})$ in λ,

$$\mathcal{V}(\boldsymbol{X}) = \mathcal{V}(\boldsymbol{x}) - i\lambda \sum_{e\in E} x_e \left(\frac{\partial \mathcal{V}}{\partial x_e}(\boldsymbol{x})\right)^2 + \mathcal{O}(\lambda^2)\,. \tag{13}$$

The $i\varepsilon$ prescription in (2) is ensured if the imaginary part of $\mathcal{V}(\boldsymbol{X})$ is strictly negative for *sufficiently small* λ. This is the case for all $\boldsymbol{x} \in \mathbb{P}_+^E$ as long as there are no solutions of the *Landau equations*

$$0 = x_e \frac{\partial \mathcal{V}}{\partial x_e}(\boldsymbol{x}) \quad \text{for each} \quad e \in E\,, \quad \text{for any} \quad \boldsymbol{x} \in \mathbb{P}_+^E\,, \tag{14}$$

whose solutions are the *Landau singularities*. We will assume that our Feynman integral is always free of Landau singularities.

Even though we require that λ is *small enough*, we can give it, in contrast to the ε in (2), an explicit *finite* value. Hence, eq. (12) is finally an explicit form of the original Feynman integral (1) that is going to serve as input for the tropical numerical integration algorithm.

2.4. Dimensional regularization and ϵ expansions

So far, we did not make any restrictions on the finiteness properties of the integrals (1), (2) and (12). We say a Feynman integral is *quasi-finite* if the integral in the parametric representation (2) (or equivalently (12)) is finite. Only the integral needs to be finite. The Γ function prefactor is allowed to give divergent contributions. Note that this is more permissive than requiring that (1) is finite, which is already divergent, e.g., for the 1-loop bubble in $D=4$ with unit edge weights.

In this paper, we will restrict our attention to such quasi-finite Feynman integrals. If an integral is not quasi-finite, it can be expanded as a linear combination of quasi-finite integrals [29,30,56].

Quasi-finiteness allows *overall* divergences due to the $\Gamma(\omega)$ factor that becomes singular if ω is an integer ≤ 0. Such divergences are easily taken care of by using dimensional regularization. As usual we will perturb the dimension by ϵ in the sense that

$$D = D_0 - 2\epsilon\,, \tag{15}$$

where D_0 is a fixed number and ϵ is an expansion parameter.[2] Analogously, we define $\omega_0 = \sum_{e\in E} \nu_e - D_0 L/2$. Using this notation, we may make the ϵ dependence in (12) explicit and expand,

$$\mathcal{I} = \Gamma(\omega_0 + \epsilon L) \sum_{k=0}^{\infty} \frac{\epsilon^k}{k!} \int_{\mathbb{P}_+^E} \left(\prod_{e\in E} \frac{X_e^{\nu_e}}{\Gamma(\nu_e)} \right) \frac{\det \mathcal{J}_\lambda(\boldsymbol{x})}{\mathcal{U}(\boldsymbol{X})^{D_0/2} \cdot \mathcal{V}(\boldsymbol{X})^{\omega_0}} \log^k \left(\frac{\mathcal{U}(\boldsymbol{X})}{\mathcal{V}(\boldsymbol{X})^L} \right) \Omega\,. \tag{16}$$

If the $k=0$ integral is finite, all higher orders in ϵ are also finite as the $\log^k$ factors cannot spoil the integrability. The Γ factor can be expanded in ϵ using $\Gamma(z+1) = z\Gamma(z)$ and the expansion

$$\log\Gamma(1-\epsilon) = \gamma_E \epsilon + \sum_{n=2}^{\infty} \frac{\zeta(n)}{n} \epsilon^n\,, \tag{17}$$

with Euler's γ_E and Riemann's ζ function.

Together, eqs. (16) and (17) give us an explicit formulation of the ϵ expansion of the Feynman integral (1) in the quasi-finite case. In the remainder of this article we will explain how to evaluate the expansion coefficients in (16) using the tropical sampling approach.

3. Tropical geometry

3.1. Tropical approximation

We will use the tropical sampling approach which was put forward in [1] to evaluate the deformed parametric Feynman integrals in (12) and (16). Here we briefly review the basic concepts.

For any homogeneous polynomial in $|E|$ variables $p(\boldsymbol{x}) = \sum_{k\in\mathrm{supp}(p)} a_k \prod_{e=0}^{|E|-1} x_e^{k_e}$, the support $\mathrm{supp}(p)$ is the set of multi-indices for which p has a non-zero coefficient a_k. For any such polynomial p, we define the *tropical approximation* p^{tr} as

$$p^{\mathrm{tr}}(\boldsymbol{x}) = \max_{k\in\mathrm{supp}(p)} \prod_{e=0}^{|E|-1} x_e^{k_e}\,. \tag{18}$$

If, for example, $p(\boldsymbol{x}) = x_0^2 x_1 - 2x_0x_1x_2 + 5ix_2^3$, then $p^{\mathrm{tr}}(\boldsymbol{x}) = \max\{x_0^2x_1, x_0x_1x_2, x_2^3\}$. Note that the tropical approximation forgets about the explicit value of the coefficients; it only depends on the fact that a specific coefficient is zero or non-zero. This way, the tropical approximation only depends on the set $\mathrm{supp}(p) \subset \mathbb{Z}_{\geq 0}^{|E|}$. In fact, it only depends on the shape of the *convex hull* of $\mathrm{supp}(p)$, which is the *Newton polytope* of p. For this reason, p^{tr} is nothing but a function avatar of this polytope. Indeed, we can write $p^{\mathrm{tr}}(\boldsymbol{x})$ as follows,

$$p^{\mathrm{tr}}(\boldsymbol{x}) = \exp\left(\max_{\mathbf{v}\in\mathbf{N}[p]} \mathbf{v}^T\mathbf{y} \right), \tag{19}$$

where $\mathbf{y} = (y_0, \ldots, y_{|E|-1})$ with $y_e = \log x_e$, $\mathbf{v}^T\mathbf{y} = \sum_{e\in E} v_e y_e$ and we maximize over the Newton polytope $\mathbf{N}[p]$ of p. The exponent above is the *tropicalization* $\mathrm{Trop}[p]$ of p over $\mathbb{C}$ with trivial valuation. It plays a central role in tropical geometry (see, e.g., [63]). For us, the key property of the tropical approximation is that it may be used to put upper and lower bounds on a polynomial:

Theorem 3.1 *([1, Theorem 8]). For a homogeneous $p \in \mathbb{C}[x_0, \ldots, x_{|E|-1}]$ that is completely non-vanishing on $\mathbb{P}_+^E$ there exist constants $C_1, C_2 > 0$ such that*

$$C_1 \leq \frac{|p(\boldsymbol{x})|}{p^{\mathrm{tr}}(\boldsymbol{x})} \leq C_2 \quad \textit{for all} \quad \boldsymbol{x} \in \mathbb{P}_+^E\,. \tag{20}$$

[2] Note that the causal $i\varepsilon$ and the regularization/expansion parameter ϵ are (unfortunately) usually referred to with the same Greek letter. We will follow this tradition, but use different versions of the letter for the respective meanings consistently.

A polynomial p is *completely non-vanishing* on $\mathbb{P}_+^E$ if it does not vanish in the interior of $\mathbb{P}_+^E$ and if another technical condition is fulfilled (see [29, Definition 1] for a precise definition).

The $\mathcal{U}$ polynomial is always completely non-vanishing on $\mathbb{P}_+^E$ and in the pseudo-Euclidean regime also $\mathcal{F}$ is completely non-vanishing on $\mathbb{P}_+^E$. We define the associated tropical approximations $\mathcal{U}^{\text{tr}}$, $\mathcal{F}^{\text{tr}}$ and $\mathcal{V}^{\text{tr}} = \mathcal{F}^{\text{tr}}/\mathcal{U}^{\text{tr}}$.

Our key assumption for the integration of Feynman integrals in the Minkowski regime is that the approximation property can also be applied to the deformed Symanzik polynomials.

Assumption 3.2. There are λ dependent constants $C_1(\lambda), C_2(\lambda) > 0$ such that for small $\lambda > 0$,

$$C_1(\lambda) \leq \left| \left(\frac{\mathcal{U}^{\text{tr}}(\boldsymbol{x})}{\mathcal{U}(\boldsymbol{X})}\right)^{D_0/2} \left(\frac{\mathcal{V}^{\text{tr}}(\boldsymbol{x})}{\mathcal{V}(\boldsymbol{X})}\right)^{\omega_0} \right| \leq C_2(\lambda) \quad \text{for all} \quad \boldsymbol{x} \in \mathbb{P}_+^E, \tag{21}$$

where we recall that $\boldsymbol{X} = (X_1, \ldots, X_{|E|})$ and $X_e = x_e \exp\left(-i\lambda \frac{\partial \mathcal{V}}{\partial x_e}(\boldsymbol{x})\right)$.

In the pseudo-Euclidean regime the assumption is fulfilled, as we are allowed to set $\lambda = 0$ and use the established approximation property from [1] on $\mathcal{U}$ and $\mathcal{F}$. In the Minkowski regime, Assumption 3.2 can only be fulfilled if there are no Landau singularities, i.e. solutions to (14). After extensive numerical testing we conjecture that Assumption 3.2 is fulfilled if there are no Landau singularities. It would be very interesting to give a concise set of conditions for the validity of Assumption 3.2 and how it interplays with such singularities. We leave this to future research.

Another highly promising research question is to find a value for λ such that the constants $C_1(\lambda)$ and $C_2(\lambda)$ tighten the bounds as much as possible. Finding such an optimal value for λ would result in the first entirely *canonical* deformation prescription which does not depend on free parameters.

3.2. Tropical sampling

Intuitively, Assumption 3.2 tells us that the integrands in (12) and (16) are, except for phase factors, reasonably approximated by the tropical approximation of the undeformed integrand. To evaluate the integrals (16) with *tropical sampling*, as in [1, Sec. 7.2], we define the probability distribution

$$\mu^{\text{tr}} = \frac{1}{I^{\text{tr}}} \frac{\prod_{e \in E} x_e^{\nu_e}}{\mathcal{U}^{\text{tr}}(\boldsymbol{x})^{D_0/2}\, \mathcal{V}^{\text{tr}}(\boldsymbol{x})^{\omega_0}}\, \Omega\,, \tag{22}$$

where I^{tr} is a normalization factor, which is chosen such that $\int_{\mathbb{P}_+^E} \mu^{\text{tr}} = 1$. As of Assumption 3.2 and the requirement that the integrals in (16) shall be finite, the factor I^{tr} must also be finite. If $\omega_0 = 0$, this normalization factor is equal to the associated *Hepp bound* of the graph G [21]. Because $\mu^{\text{tr}} > 0$ for all $\boldsymbol{x} \in \mathbb{P}_+^E$, μ^{tr} gives rise to a proper probability distribution on this domain.

Using the definition of μ^{tr} to rewrite (16) results in

$$\begin{aligned} \mathcal{I} &= \frac{\Gamma(\omega_0 + \epsilon L)}{\prod_{e \in E} \Gamma(\nu_e)} \sum_{k=0}^{\infty} \frac{\epsilon^k}{k!} \mathcal{I}_k, \quad \text{with} \\ \mathcal{I}_k &= I^{\text{tr}} \int_{\mathbb{P}_+^E} \frac{\left(\prod_{e \in E} (X_e/x_e)^{\nu_e}\right) \det \mathcal{J}_\lambda(\boldsymbol{x})}{\left(\mathcal{U}(\boldsymbol{X})/\mathcal{U}^{\text{tr}}(\boldsymbol{x})\right)^{D_0/2} \cdot \left(\mathcal{V}(\boldsymbol{X})/\mathcal{V}^{\text{tr}}(\boldsymbol{x})\right)^{\omega_0}} \log^k\left(\frac{\mathcal{U}(\boldsymbol{X})}{\mathcal{V}(\boldsymbol{X})^L}\right) \mu^{\text{tr}}. \end{aligned} \tag{23}$$

We will evaluate the integrals above by sampling from the probability distribution μ^{tr}.

In [1], two different methods to generate samples from μ^{tr} were introduced. The first method [1, Sec. 5], which does not take the explicit structure of $\mathcal{U}$ and $\mathcal{F}$ into account, requires the computation of a triangulation of the refined normal fans of the Newton polytopes of $\mathcal{U}$ and $\mathcal{F}$. Once such a triangulation is computed, arbitrarily many samples from μ^{tr} can be generated with little computational effort. Unfortunately, obtaining such a triangulation is a highly computationally demanding process.

The second method [1, Sec. 6] to generate samples from the probability distribution μ^{tr} makes use of a particular property of the Newton polytopes of $\mathcal{U}$ and $\mathcal{F}$ which allows to bypass the costly triangulation step. This second method additionally has the advantage that it is relatively straightforward to implement. This faster method of sampling from μ^{tr} relies on the Newton polytopes of $\mathcal{U}$ and $\mathcal{F}$ being *generalized permutahedra*.

For the program `feyntrop` we will make use of this second method. Our tropical sampling algorithm to produce samples from μ^{tr} is essentially equivalent to the one published with [1].

3.3. Base polytopes and generalized permutahedra

A fantastic property of generalized permutahedra is that they come with a *canonical normal fan* which greatly facilitates the sampling of μ^{tr}, see [1, Theorem 27 and Algorithm 4]. Here, we briefly explain the necessary notions. As a start, we define a more general class of polytopes first and discuss restrictions later.

Base polytopes Consider a function $z : \mathbf{2}^E \to \mathbb{R}$ that assigns a number to each subset of E, the edge set of our Feynman graph G. In the following we often identify a subset of E with a subgraph of G and use the respective terms interchangeably. So, z assigns a number to each subgraph of G. We define $\mathbf{P}[z]$ to be the subset of $\mathbb{R}^{|E|}$ that consists of all points $(a_0, \ldots, a_{|E|-1}) \in \mathbb{R}^{|E|}$ which fulfill $\sum_{e \in E} a_e = z(E)$ and the $2^{|E|} - 1$ inequalities

$$\sum_{e\in\gamma} a_e \geq z(\gamma) \quad \text{for all} \quad \gamma \subsetneq E\,. \tag{24}$$

Clearly, these inequalities describe a convex bounded domain, i.e. a *polytope*. This polytope $\mathbf{P}[z]$ associated to an arbitrary function $z: \mathbf{2}^E \to \mathbb{R}$ is called the *base polytope*.

Generalized permutahedra The following is a special case of a theorem by Aguiar and Ardila who realized that numerous seemingly different structures from combinatorics can be understood using the same object: The *generalized permutahedron* which was initially defined by Postnikov [64].

Theorem 3.3 *([65, Theorem 12.3] and the references therein). The polytope* $\mathbf{P}[z]$ *is a* generalized permutahedron *if and only if the function z is* supermodular. *That means, z fulfills the inequalities*

$$z(\gamma) + z(\delta) \leq z(\gamma \cup \delta) + z(\gamma \cap \delta) \text{ for all pairs of subgraphs } \gamma, \delta \subset E\,. \tag{25}$$

Because other properties of generalized permutahedra are not of central interest in this paper, we will take Theorem 3.3 as our definition of these special polytopes. Important for us is that for many kinematic situations the Newton polytopes of the Symanzik polynomials are of this type.

Let L_γ denote the number of loops of the subgraph γ, then we have the following theorem due to Schultka [31]:

Theorem 3.4. *The Newton polytope* $\mathbf{N}[\mathcal{U}]$ *of* $\mathcal{U}$ *is equal to the base polytope* $\mathbf{P}[z_\mathcal{U}]$ *with* $z_\mathcal{U}$ *being the function* $z_\mathcal{U}(\gamma) = L_\gamma$. *Moreover,* $z_\mathcal{U}$ *is supermodular. Hence, by Theorem 3.3,* $\mathbf{N}[\mathcal{U}]$ *is a generalized permutahedron.*

Proof. See [31, Sec. 4] and the references therein. In [21], it was observed that $\mathbf{N}[\mathcal{U}]$ is a *matroid polytope*, which by [65, Sec. 14] also proves the statement. □

Because $\mathbf{N}[\mathcal{U}]$ is a generalized permutahedron, we also say that $\mathcal{U}$ has the generalized permutahedron property.

Generalized permutahedron property of the $\mathcal{F}$ *polynomial* For the second Symanzik $\mathcal{F}$ polynomial the situation is more tricky. We need the notion of *mass-momentum spanning* subgraphs which was defined by Brown [22] (see also [31, Sec. 4] for an interesting relationship to the concept of *s-irreducibility* [66] or [67] where related results were obtained or [68] for relations to the $R^\star$ operation). We use the following slightly generalized version of Brown's definition (see also [1, Sec. 7.2]): We call a subgraph $\gamma \subset E$ mass-momentum spanning if the second Symanzik polynomial of the cograph G/γ vanishes identically $\mathcal{F}_{G/\gamma} = 0$.

Theorem 3.5. *In the Euclidean regime with generic kinematics, the Newton polytope* $\mathbf{N}[\mathcal{F}]$ *is a generalized permutahedron. It is equal to the base polytope* $\mathbf{P}[z_\mathcal{F}]$ *with the function* $z_\mathcal{F}$ *defined for all subgraphs* γ *by* $z_\mathcal{F}(\gamma) = L_\gamma + 1$ *if* γ *is mass-momentum spanning and* $z_\mathcal{F}(\gamma) = L_\gamma$ *otherwise. Consequently, this function* $z_\mathcal{F}: \mathbf{2}^E \to \mathbb{R}$ *is supermodular, i.e. it fulfills (25).*

Proof. This has also been proven in [31, Sec. 4]. The proof relies on a special infrared factorization property of $\mathcal{F}$ that was discovered by Brown [22, Theorem 2.7]. □

We explicitly state the following generalization of Theorem 3.5:

Theorem 3.6. *Theorem 3.5 holds in all regimes if the kinematics are generic.*

Proof. The $\mathcal{F}$ polynomial has the same monomials (with different coefficients) as in the Euclidean regime with generic kinematics. To verify this, note that the conditions for generic kinematics prevent cancellations between the mass and momentum part of the $\mathcal{F}$ polynomial as given in eq. (5). So, the respective Newton polytopes coincide. □

There is also the following further generalization of Theorem 3.5 to Euclidean but exceptional kinematics. This generalization is very plausible (see [22, Example 2.5]), but it is a technical challenge to prove it. We will not attempt to include a proof here for the sake of brevity. So, we state this generalization as a conjecture:

Conjecture 3.7. *Theorem 3.5 holds in the Euclidean regime for all (also exceptional) kinematics.*

We emphasize that $\mathbf{N}[\mathcal{F}]$ is generally *not* a generalized permutahedron outside of the Euclidean regime. This was observed in [31, Remark 4.16] (see also [69, Sec. 4.2], [70, Sec. 2.2.3] or [1, Remark 35]). Explicit counter examples are encountered while computing the massless on-shell boxes depicted in Fig. 2. The $\mathcal{F}$ polynomials of the completely massless box with only on-shell external momenta, the massless box with one off-shell momentum and the massless box with two adjacent off-shell momenta (depicted in Figs. 2a, 2b and 2c) do not fulfill the generalized permutahedron property. On the other hand, the $\mathcal{F}$ polynomial does fulfill the generalized permutahedron property for the massless box with two or more off-shell legs such that two off-shell legs are on opposite sides (as depicted in Fig. 2d).

Therefore, we have to make concessions in the Minkowski regime with exceptional kinematics.

An observation of Arkani-Hamed, Hillman, Mizera is helpful (see [26, eq. (8)] and the discussion around it): the facet presentation of $\mathbf{N}[\mathcal{F}]$ given in Theorem 3.5 turns out to hold in a quite broad range of kinematic regimes, even if $\mathbf{N}[\mathcal{F}]$ is not a generalized permutahedron.

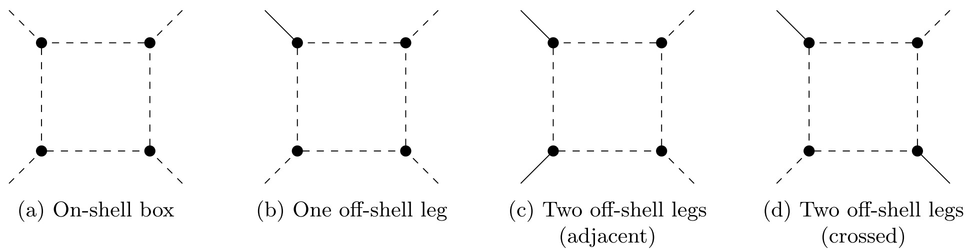

Fig. 2. Massless box with different external legs on- or off-shell. On-shell ($p^2 = 0$) legs are drawn as dashed lines and off-shell ($p^2 \neq 0$) legs with solid lines. Internal propagators are massless.

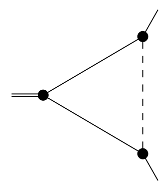

Fig. 3. Triangle Feynman graph relevant in QED. The two solid propagators have mass m and the solid legs have incoming squared momentum m^2. The dashed propagator is massless and the doubled leg has incoming squared momentum Q^2.

Observation 3.8. The Newton polytope of $\mathcal{F}$ is often equal to the base polytope $\mathbf{P}[z_\mathcal{F}]$ with the function $z_\mathcal{F}$ defined as in Theorem 3.5.

This is significant since `feyntrop` uses the polytope $\mathbf{P}[z_\mathcal{F}]$ internally as a substitute for $\mathbf{N}[\mathcal{F}]$ as the former is easier to handle and faster to compute than the latter.

For instance, all massless boxes depicted in Fig. 2 have the property that the Newton polytopes of their $\mathcal{F}$ polynomial are base polytopes described by the respective $z_\mathcal{F}$ functions, i.e. $\mathbf{N}[\mathcal{F}] = \mathbf{P}[z_\mathcal{F}]$. In the first three cases (Figs. 2a, 2b, 2c) the $z_\mathcal{F}$ function does not fulfill the inequalities (25). For the graph in Fig. 2d these inequalities are fulfilled and the associated Newton polytope $\mathbf{N}[\mathcal{F}] = \mathbf{P}[z_\mathcal{F}]$ is a generalized permutahedron.

It would be very beneficial to have precise conditions for when $\mathbf{P}[z_\mathcal{F}]$ indeed is equal to $\mathbf{N}[\mathcal{F}]$, we leave this for a future project. Empirically, we have observed that it is valid for quite a wide range of exceptional kinematics. We know, however, that this condition is not fulfilled for arbitrary exceptional kinematics [71]. An explicit counter example[3] is depicted in Fig. 3. For this triangle graph with the indicated exceptional kinematic configuration, the polytope $\mathbf{N}[\mathcal{F}]$ is different from $\mathbf{P}[z_\mathcal{F}]$. We find that $\mathcal{F}(\boldsymbol{x}) = m^2(x_1^2 + x_2^2) + (2m^2 - Q^2)x_1x_2$ which implies that $\mathbf{N}[\mathcal{F}]$ is a one-dimensional polytope. On the other hand, $\mathbf{P}[z_\mathcal{F}]$ can be shown to be a two-dimensional polytope. In $D = 4$, the Feynman integral associated to Fig. 3 is infrared divergent and therefore not quasi-finite. In $D = 6$, `feyntrop` can evaluate the integral without problems. Nonetheless, we expect there to be more complicated Feynman graphs with similarly exceptional external kinematics, that are quasi-finite, but which cannot be evaluated using `feyntrop`. We did not, however, manage to find such a graph.

Even if $\mathbf{N}[\mathcal{F}] \neq \mathbf{P}[z_\mathcal{F}]$, the Newton polytope $\mathbf{N}[\mathcal{F}]$ is *bounded* by the base polytope $\mathbf{P}[z_\mathcal{F}]$. The reason for this is that $\mathcal{F}$ can only lose monomials if we make the kinematics less generic.

Theorem 3.9. *We have* $\mathbf{N}[\mathcal{F}] \subset \mathbf{P}[z_\mathcal{F}]$.

Efficient check of the generalized permutahedron property of a base polytope Naively, it is quite hard to check if the base polytope $\mathbf{P}[z]$ associated to a given function $z : \mathbf{2}^E \to \mathbb{R}$ is a generalized permutahedron. There are of the order $2^{2|E|}$ many inequalities to be checked for (25). A more efficient way is to only check the following inequalities

$$z(\gamma \cup \{e\}) + z(\gamma \cup \{h\}) \leq z(\gamma) + z(\gamma \cup \{e, h\}) \tag{26}$$

for all subgraphs $\gamma \subset E$ and edges $e, h \in E \setminus \gamma$. The inequalities (26) imply the ones in (25). For (26) less than $|E|^2 2^{|E|}$ inequalities need to be checked. So, (26) is a more efficient version of (25).

3.4. Generalized permutahedral tropical sampling

`feyntrop` uses a slightly adapted version of the generalized permutahedron tropical sampling algorithm from [1, Sec. 6.1 and Sec. 7.2] to sample from the distribution given by μ^{tr} in eq. (22).

The algorithm involves a preprocessing and a sampling step.

Preprocessing The first algorithmic task to prepare for the sampling from μ^{tr} is to check in which regime the kinematic data are located. The kinematic data are provided via the matrix $\mathcal{P}^{u,v}$ as it was defined in Section 2.1 and via a list of masses m_e for each edge $e \in E$. If the symmetric $|V| \times |V|$ matrix $\mathcal{P}^{u,v}$ is negative semi-definite (which is easy to check using matrix diagonalization), then we are in

[3] We thank Erik Panzer for sharing this (counter) example with us.

Table 1
Table of the necessity of a deformation (def.) and the fulfillment of the generalized permutahedron property of $\mathcal{F}$ (GP) in each kinematic regime.

	Euclidean	Pseudo-Euclidean	Minkowski
Generic	no def. / always GP	no def. / always GP	def. / always GP
Exceptional	no def. / always GP	no def. / not always GP	def. / not always GP

the Euclidean regime. Similarly we check if the defining (in)equalities for the other kinematic regimes given in Section 2.2 are fulfilled or not. Depending on the kinematic regime, we need to use a contour deformation for the integration or not. Further, if the kinematics are Euclidean or generic, we know that the generalized permutahedron property of $\mathcal{F}$ is fulfilled (also thanks to the unproven Conjecture 3.7). Table 1 summarizes this dependence of the algorithm on the kinematic regime.

If we find that we are at an exceptional and non-Euclidean kinematic point, $\mathbf{N}[\mathcal{F}]$ might not be a generalized permutahedron and it might not even be equal to $\mathbf{P}[z_{\mathcal{F}}]$. In this case, the program prints a message warning the user that the integration might not work. The program then continues under the assumption that $\mathbf{N}[\mathcal{F}] = \mathbf{P}[z_{\mathcal{F}}]$. In any other case, $\mathbf{N}[\mathcal{F}]$ is a generalized permutahedron and equal to $\mathbf{P}[z_{\mathcal{F}}]$. Hence, the tropical sampling algorithm is guaranteed to give a convergent Monte Carlo integration method by [1, Sec. 6.1].

The next task is to compute the loop number L_γ and check if γ is mass-momentum spanning (by asking if $\mathcal{F}_{G/\gamma} = 0$) for each subgraph $\gamma \subset E$. Using these data, we can compute the values of $z_{\mathcal{U}}(\gamma)$ and $z_{\mathcal{F}}(\gamma)$ for all subgraphs $\gamma \subset E$ using the respective formulas from Theorems 3.4 and 3.5.

If we are at an exceptional and non-Euclidean kinematic point, we check the inequalities (26) for the $z_{\mathcal{F}}$ function. If they are all fulfilled, then $\mathbf{P}[z_{\mathcal{F}}]$ is a generalized permutahedron and we get further indication that the tropical integration step will be successful. The program prints a corresponding message in this case. Also assuming that Assumption 3.2 is fulfilled, we can compute all integrals in (23) efficiently.

Note that even in the pseudo-Euclidean and the Minkowski regimes with exceptional kinematics, the integration is often successful. For instance, we can integrate all Feynman graphs depicted in Fig. 2 regardless of the fulfillment of the generalized permutahedron property. In fact, we did not find a quasi-finite example where the algorithm fails (even though the convergence rate is quite bad for examples in highly exceptional kinematic regimes). We emphasize, however, that the user should check the convergence of the result separately when integrating at a manifestly exceptional and non-Euclidean kinematic point. For instance, by running the program repeatedly with different numbers of sample points or by slightly perturbing the kinematic point. Recall that for generic kinematics $\mathbf{N}[\mathcal{F}]$ is always a generalized permutahedron by Theorem 3.6 and the integration is guaranteed to work if the finiteness assumptions are fulfilled.

The next computational step is to compute the *generalized degree of divergence* (see [1, Sec. 7.2]) for each subgraph $\gamma \subset E$. It is defined by

$$\omega(\gamma) = \sum_{e\in\gamma} \nu_e - DL_\gamma/2 - \omega\delta_\gamma^{\text{m.m.}}, \tag{27}$$

where L_γ is the loop number of the subgraph γ and $\delta_\gamma^{\text{m.m.}} = 1$ if γ is mass-momentum spanning and 0 otherwise. The prefactor ω of $\delta_\gamma^{\text{m.m.}}$ is the usual superficial degree of divergence of the overall graph G as it was defined in Section 2.1, $\omega = \sum_{e\in E} \nu_e - DL/2$.

If $\omega(\gamma) \le 0$ for any proper subgraph γ, then we discovered a subdivergence. This means that all integrals (16) are divergent. Tropical sampling is not possible in this case and the program prints an error message and terminates. An additional analytic continuation step from (16) to a set of quasi-finite integrals (see Section 2.4) would resolve this problem. Translating a divergent integral into a linear combination of quasi-finite integrals is always possible, but we will leave the implementation of this step into `feyntrop` to a future research project.

If we have $\omega(\gamma) > 0$ for all $\gamma \subset E$, we can proceed to the key preparatory step for generalized permutahedral tropical sampling: We use $\omega(\gamma)$ to compute the following auxiliary subgraph function $J(\gamma)$, which is *recursively* defined by setting $J(\emptyset) = 1$, agreeing that $\omega(\emptyset) = 1$ and

$$J(\gamma) = \sum_{e\in\gamma} \frac{J(\gamma \setminus e)}{\omega(\gamma \setminus e)} \text{ for all } \gamma \subset E\,, \tag{28}$$

where $\gamma \setminus e$ is the subgraph γ with the edge e removed. The terminal element of this recursion is the subgraph that contains all edges E of G. We find that $J(E) = I^{\text{tr}}$, where I^{tr} is the normalization factor in (22) and (23) (see [1, Proposition 29] for a proof and details).

In the end of the preprocessing step we compile a table with the information $L_\gamma, \delta_\gamma^{\text{m.m.}}, \omega(\gamma)$ and $J(\gamma)$ for each subgraph $\gamma \subset E$ and store it in the memory of the computer.

Sampling step The sampling step of the algorithm repeats the following simple algorithm to generate samples $\boldsymbol{x} \in \mathbb{P}_+^E$ that are distributed according to the probability density (22). It is completely described in Algorithm 1. The runtime of our implementation of the algorithm grows roughly quadratically with $|E|$, but a linear runtime is achievable. The validity of the algorithm was proven in a more general setup in [1, Proposition 31]. The additional computation of the values of $\mathcal{U}^{\text{tr}}(\boldsymbol{x})$ and $\mathcal{V}^{\text{tr}}(\boldsymbol{x})$ is an application of an optimization algorithm by Fujishige and Tomizawa [72] (see also [1, Lemma 26]).

The key step of the sampling algorithm is to interpret the recursion (28) as a probability distribution for a given subgraph over its edges. That means, for a given $\gamma \subset E$ we define $p_e^\gamma = \frac{1}{J(\gamma)}\frac{J(\gamma\setminus e)}{\omega(\gamma\setminus e)}$. Obviously, $p_e^\gamma \ge 0$ and by (28) we have $\sum_{e\in\gamma} p_e^\gamma = 1$. So, for each $\gamma \subset E$, p_e^γ gives a proper probability distribution on the edges of the subgraph γ.

Algorithm 1 Generating a sample distributed as μ^{tr} from (22).

Initialize the variables $\gamma = E$ and $\kappa, U = 1$.
while $\gamma \neq \emptyset$ **do**
  Pick a random edge $e \in \gamma$ with probability $p_e^\gamma = \frac{1}{J(\gamma)} \frac{J(\gamma \setminus e)}{\omega(\gamma \setminus e)}$.
  Set $x_e = \kappa$.
  If γ is mass-momentum spanning but $\gamma \setminus e$ is not, set $V = x_e$.
  If $L_{\gamma \setminus e} < L_\gamma$, multiply U with x_e and store the result in U, i.e. set $U \leftarrow x_e \cdot U$.
  Remove the edge e from γ, i.e. set $\gamma \leftarrow \gamma \setminus e$.
  Pick a uniformly distributed random number $\xi \in [0, 1]$.
  Multiply κ with $\xi^{1/\omega(\gamma)}$ and store the result in κ, i.e. set $\kappa \leftarrow \kappa \xi^{1/\omega(\gamma)}$.
end while
Return $\boldsymbol{x} = [x_0, \ldots, x_{|E|-1}] \in \mathbb{P}_+^E$, $\mathcal{U}^{\mathrm{tr}}(\boldsymbol{x}) = U$ and $\mathcal{V}^{\mathrm{tr}}(\boldsymbol{x}) = V$.

The algorithm can also be interpreted as iteratively *cutting* edges of the graph G: We start with $\gamma = E$ and pick a random edge with probability p_e^γ. This edge is *cut* and removed from γ. We continue with the newly obtained graph and repeat this cutting process until all edges are removed. In the course of this, Algorithm 1 computes appropriate random values for the coordinates $\boldsymbol{x} \in \mathbb{P}_+^E$.

4. Numerical integration

4.1. Monte Carlo integration

We now have all the necessary tools at hand to evaluate the integrals in (23) using Monte Carlo integration. In this section, we briefly review this procedure. The integrals in (23) are of the form

$$I_f = \int\limits_{\mathbb{P}_+^E} f(\boldsymbol{x}) \mu^{\mathrm{tr}}, \tag{29}$$

where, thanks to the tropical approximation property, $f(\boldsymbol{x})$ is a function that is at most log-singular inside, or on the boundary of, $\mathbb{P}_+^E$. To evaluate such an integral, we first use the tropical sampling Algorithm 1 to randomly sample N points $\boldsymbol{x}^{(1)}, \ldots, \boldsymbol{x}^{(N)} \in \mathbb{P}_+^E$ that are distributed according to the tropical probability measure μ^{tr}. By the central limit theorem and as $f(\boldsymbol{x})$ is square-integrable,

$$I_f \approx I_f^{(N)} \qquad \text{where} \qquad I_f^{(N)} = \frac{1}{N} \sum_{i=1}^{N} f(\boldsymbol{x}^{(i)}) \,. \tag{30}$$

For sufficiently large N, the expected error of this approximation of the integral I_f is

$$\sigma_f = \sqrt{\frac{I_{f^2} - I_f^2}{N}} \qquad \text{where} \qquad I_{f^2} = \int\limits_{\mathbb{P}_+^E} f(\boldsymbol{x})^2 \mu^{\mathrm{tr}}, \tag{31}$$

which itself can be estimated (as long as $f(\boldsymbol{x})^2$ is square-integrable) by

$$\sigma_f \approx \sigma_f^{(N)} \qquad \text{where} \qquad \sigma_f^{(N)} = \sqrt{\frac{1}{N-1}\left(I_{f^2}^{(N)} - \left(I_f^{(N)}\right)^2\right)} \text{ and } I_{f^2}^{(N)} = \frac{1}{N} \sum_{i=1}^{N} f(\boldsymbol{x}^{(i)})^2 \,. \tag{32}$$

To evaluate the estimator $I_f^{(N)}$ and the expected error $\sigma_f^{(N)}$ it is necessary to evaluate $f(\boldsymbol{x})$ for N different values of $\boldsymbol{x}$. As the random points $\boldsymbol{x}^{(1)}, \ldots, \boldsymbol{x}^{(N)} \in \mathbb{P}_+^E$ can be obtained quite quickly using Algorithm 1, this evaluation becomes a bottleneck. In the next section, we describe a fast method to perform this evaluation, which is implemented in `feyntrop` to efficiently obtain Monte Carlo estimates and error terms for the integrals in (23).

4.2. Fast evaluation of (deformed) Feynman integrands

To evaluate the integrals in (23) using a Monte Carlo approach we do not only have to be able to sample from the distribution μ^{tr}, but we also need to rapidly evaluate the remaining integrand (denoted as $f(\boldsymbol{x})$ in the last section). Explicitly for the numerical evaluation of (23), we have to be able to compute $X_e = x_e \exp\left(-i\lambda \frac{\partial \mathcal{V}}{\partial x_e}(\boldsymbol{x})\right)$ as well as $\mathcal{U}(\boldsymbol{X})$, $\mathcal{V}(\boldsymbol{X})$ and $\det \mathcal{J}_\lambda(\boldsymbol{x})$ for any $\boldsymbol{x} \in \mathbb{P}_+^E$.

Evaluation of the $\mathcal{U}$ and $\mathcal{F}$ polynomials Surprisingly, the explicit polynomial expression for $\mathcal{U}$ and $\mathcal{F}$ from eq. (5) are *harder* to evaluate than the matrix and determinant expression (4) if the underlying graph exceeds a certain complexity. The reason for this is that the number of monomials in (5) increases exponentially with the loop number (see, e.g., [73] for the asymptotic growth rate of the number of spanning tress in a regular graph), while the size of the matrices in (4) only increases linearly. Standard linear algebra algorithms as the Cholesky or LU decompositions [74] provide polynomial time algorithms to compute the inverse and determinant of $\mathcal{L}(\boldsymbol{x})$ and therefore values of $\mathcal{U}(\boldsymbol{x})$ and $\mathcal{F}(\boldsymbol{x})$ (see, e.g., [1, Sec. 7.1]). In fact, the linear algebra problems on *graph Laplacian* matrices that need to be solved to compute $\mathcal{U}(\boldsymbol{x})$ and $\mathcal{F}(\boldsymbol{x})$ fall into a class of problems for which *nearly linear time* algorithms are available [75].

Explicit formulas for the $\mathcal{V}$ derivatives We need explicit formulas for the derivatives of $\mathcal{V}$. These formulas provide fast evaluation methods for $\boldsymbol{X}$ and the Jacobian $\mathcal{J}_\lambda(\boldsymbol{x})$.

Consider the $(|V|-1)\times(|V|-1)$ matrix $\mathcal{M}(\boldsymbol{x}) = \mathcal{L}^{-1}(\boldsymbol{x})\,\mathcal{P}\,\mathcal{L}^{-1}(\boldsymbol{x})$ with $\mathcal{L}(\boldsymbol{x})$ and $\mathcal{P}$ as defined in Section 2.1. For edges e and h that connect the vertices u_e, v_e and u_h, v_h respectively, we define

$$\begin{aligned}\mathcal{A}(\boldsymbol{x})_{e,h} &= \frac{1}{x_e x_h}\left(\mathcal{M}(\boldsymbol{x})_{u_e,u_h} + \mathcal{M}(\boldsymbol{x})_{v_e,v_h} - \mathcal{M}(\boldsymbol{x})_{u_e,v_h} - \mathcal{M}(\boldsymbol{x})_{v_e,u_h}\right)\\ \mathcal{B}(\boldsymbol{x})_{e,h} &= \frac{1}{x_e x_h}\left(\mathcal{L}^{-1}(\boldsymbol{x})_{u_e,u_h} + \mathcal{L}^{-1}(\boldsymbol{x})_{v_e,v_h} - \mathcal{L}^{-1}(\boldsymbol{x})_{u_e,v_h} - \mathcal{L}^{-1}(\boldsymbol{x})_{v_e,u_h}\right),\end{aligned} \tag{33}$$

where we agree that $\mathcal{L}^{-1}(\boldsymbol{x})_{u,v} = \mathcal{M}(\boldsymbol{x})_{u,v} = 0$ if any of u or v is equal to v_0, the arbitrary vertex that was removed in the initial expression of the Feynman integral (1). It follows from (4) and the matrix differentiation rule $\frac{\partial}{\partial x_e}\mathcal{L}^{-1}(\boldsymbol{x})_{u,v} = \left(-\mathcal{L}^{-1}(\boldsymbol{x})\frac{\partial \mathcal{L}}{\partial x_e}(\boldsymbol{x})\mathcal{L}^{-1}(\boldsymbol{x})\right)_{u,v}$ that

$$\frac{\partial \mathcal{V}}{\partial x_e}(\boldsymbol{x}) = -\mathcal{A}(\boldsymbol{x})_{e,e} + m_e^2\,, \qquad \frac{\partial^2 \mathcal{V}}{\partial x_e \partial x_h}(\boldsymbol{x}) = 2\delta_{e,h}\frac{\mathcal{A}(\boldsymbol{x})_{e,e}}{x_e} - 2(\mathcal{A}(\boldsymbol{x}) \circ \mathcal{B}(\boldsymbol{x}))_{e,h}\,, \tag{34}$$

where we use the *Hadamard* or *element-wise matrix product*, $(\mathcal{A}(\boldsymbol{x}) \circ \mathcal{B}(\boldsymbol{x}))_{e,h} = \mathcal{A}(\boldsymbol{x})_{e,h} \cdot \mathcal{B}(\boldsymbol{x})_{e,h}$.

Computation of the relevant factors in the integrands of (23) We summarize the necessary steps to compute all the factors in the deformed and ϵ-expanded tropical Feynman integral representation (23).

1. Compute the graph Laplacian $\mathcal{L}(\boldsymbol{x})$ as defined in Section 2.1.
2. Compute the inverse $\mathcal{L}^{-1}(\boldsymbol{x})$ (e.g. by Cholesky decomposing $\mathcal{L}(\boldsymbol{x})$).
3. Use this to evaluate the derivatives of $\mathcal{V}(\boldsymbol{x})$ via the formulas in (33) and (34).
4. Compute the values of the deformed $\boldsymbol{X}$ parameters: $X_e = x_e \exp\left(-i\lambda \frac{\partial \mathcal{V}}{\partial x_e}(\boldsymbol{x})\right)$.
5. Compute the Jacobian $\mathcal{J}_\lambda(\boldsymbol{x})$ using the formula in (11).
6. Evaluate $\det \mathcal{J}_\lambda(\boldsymbol{x})$ (e.g. by using a LU decomposition of $\mathcal{J}_\lambda(\boldsymbol{x})$).
7. Compute the deformed graph Laplacian $\mathcal{L}(\boldsymbol{X})$.
8. Compute $\mathcal{L}^{-1}(\boldsymbol{X})$ and $\det \mathcal{L}(\boldsymbol{X})$ (e.g. by using a LU decomposition of $\mathcal{L}(\boldsymbol{X})$ as a Cholesky decomposition is not possible, because $\mathcal{L}(\boldsymbol{X})$ is not a hermitian matrix in contrast to $\mathcal{L}(\boldsymbol{x})$).
9. Use the formulas (4) to obtain values for $\mathcal{U}(\boldsymbol{X})$, $\mathcal{F}(\boldsymbol{X})$ and $\mathcal{V}(\boldsymbol{X}) = \mathcal{F}(\boldsymbol{X})/\mathcal{U}(\boldsymbol{X})$.

The computation obviously simplifies if we set $\lambda = 0$, in which case we have $\boldsymbol{X} = \boldsymbol{x}$. We are allowed to set $\lambda = 0$ if we do not need the contour deformation. This is the case, for instance, in the Euclidean or the pseudo-Euclidean regimes. In our implementation we check if we are in these regimes and adjust the evaluation of the integrand accordingly.

5. The program `feyntrop`

We have implemented the contour-deformed tropical integration algorithm, which we discussed in the previous sections, in a `C++` module named `feyntrop`. This module is an upgrade to previous code developed by the first author in [1].

`feyntrop` was checked against `AMFlow` [48] and `pySecDec` [41] for roughly 15 different diagrams with 1-3 loops and 2-5 legs at varying kinematics points, in both the Euclidean and Minkowski regimes, finding agreement in all cases within the given uncertainty bounds. In the Euclidean regime, the original algorithm was checked against numerous analytic computations that were obtained at high loop order using conformal four-point integral and graphical function techniques [76].

Note that our prefactor convention, which we fixed in eqs. (1) and (2), differs from the one in `AMFlow` and `pySecDec` by a factor of $(-1)^{|\nu|}$, where $|\nu| = \sum_{e=0}^{|E|-1}\nu_e$. In comparison to `FIESTA` [24], our convention differs by a factor of $(-1)^{|\nu|}\exp(-L\gamma_E\epsilon)$.

5.1. Installation

The source code of `feyntrop` is available in the repository https://github.com/michibo/feyntrop on `github`. It can be downloaded and built by running the following sequence of commands

```
git clone --recursive https://github.com/michibo/feyntrop.git
cd feyntrop
make
```

in a `Linux` environment. `feyntrop` is interfaced with `python` [4] via the library `pybind11` [5][4]. Additionally, it uses the optimized linear algebra routines from the `Eigen3` package [2], the `OpenMP C++` module [77] for the parallelization of the Monte Carlo sampling step and the `xoshiro256+` pseudo random number generator [3].

[4] Note added in proof: Due to compatibility issues on some hardware, the newest version of `feyntrop` available and described at https://github.com/michibo/feyntrop does not make use of `pybind11` anymore. This new version also provides a low-level command-line interface that works without any dependency on `python`. This interface enables the easy use of `feyntrop` in high-performance computing environments.

feyntrop can be loaded in a python environment by importing the file py_feyntrop.py, located in the top directory of the package. To ensure that feyntrop was built correctly, one may execute the python file /tests/test_suite.py. This script compares the output of feyntrop against pre-computed values. To do so, it will locally compute six examples with 1-2 loops and 2-5 legs, some in the Euclidean and others in the Minkowski regime.

The file py_feyntrop.py includes additional functionality for the python interface serving three purposes. Firstly, it simplifies the specification of vertices and edges of a Feynman diagram in comparison to the C++ interface of feyntrop. Secondly, it allows for self-chosen momentum variables given by a set of replacement rules, instead of having to manually specify the full scalar product matrix $\mathcal{P}^{u,v}$ from (4). Lastly, the output of the ϵ expansion can be printed in a readable format. To do so, the py_feyntrop.py program uses the sympy [6] library.

As already indicated in Section 2.1, we employ zero-indexing throughout. This means that edges and vertices are labeled as $\{0, 1, \ldots\}$. This facilitates seamless interoperability with the programming language features of python.

5.2. Basic usage of feyntrop

In this section, we will illustrate the basic workflow of feyntrop with an example. The code for this example can be executed and inspected with jupyter [78] by calling

```
jupyter notebook tutorial_2L_3pt.ipynb
```

within the top directory of the feyntrop package.

We will integrate the following 2-loop 3-point graph in $D = 2 - 2\epsilon$ dimensional spacetime:

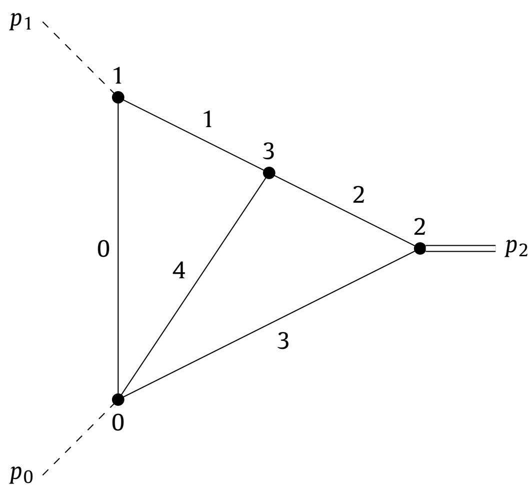

The dashed lines denote on-shell, massless particles with momenta p_0 and p_1 such that $p_0^2 = p_1^2 = 0$. The solid, internal lines each have mass m. The double line is associated to some off-shell momentum $p_2^2 \neq 0$. For the convenience of the reader, both vertices and edges are labeled explicitly in this example. feyntrop requires us to label the external vertices (as defined in Section 2.2) *before* the internal vertices. In the current example, the vertices are $V = V^{\text{ext}} \sqcup V^{\text{int}} = \{0, 1, 2\} \sqcup \{3\}$.

The momentum space Feynman integral representation (1) with unit edge weights reads

$$\mathcal{I} = \pi^{-2+2\epsilon} \int \frac{\mathrm{d}^{2-2\epsilon} k_0 \, \mathrm{d}^{2-2\epsilon} k_1}{\left(q_0^2 - m^2 + i\varepsilon\right)\left(q_1^2 - m^2 + i\varepsilon\right)\left(q_2^2 - m^2 + i\varepsilon\right)\left(q_3^2 - m^2 + i\varepsilon\right)\left(q_4^2 - m^2 + i\varepsilon\right)} \,, \tag{35}$$

where we integrated out the δ functions in eq. (1) by requiring that $q_0 = k_0$, $q_1 = k_0 + p_1$, $q_2 = k_0 + k_1 + p_1$, $q_3 = p_0 - k_0 - k_1$ and $q_4 = k_1$. We choose the phase space point

$$m^2 = 0.2 \,, \quad p_0^2 = p_1^2 = 0 \,, \quad p_2^2 = 1 \,, \tag{36}$$

which is in the Minkowski regime because $p_2^2 > 0$ - see Section 2.2. To begin this calculation, first open a python script or a jupyter notebook and import py_feyntrop:

```
from py_feyntrop import *
```

Here we are assuming that feyntrop.so and py_feyntrop.py are both in the working directory.

To define the graph, we provide a list of edges with edge weights ν_e and squared masses m_e^2:

$$\big((u_0, v_0)\,,\, \nu_0\,,\, m_0^2\big)\,,\, \ldots\,,\, \big((u_{|E|-1}, v_{|E|-1})\,,\, \nu_{|E|-1}\,,\, m_{|E|-1}^2\big)\,. \tag{37}$$

The notation (u_e, v_e) denotes an edge e incident to the vertices u_e and v_e. We therefore write

```
edges = [((0,1), 1, 'mm'), ((1,3), 1, 'mm'), ((2,3), 1, 'mm'),
         ((2,0), 1, 'mm'), ((0,3), 1, 'mm')]
```

138

in the code to input the graph which is depicted above. The ordering of vertices (u_e, v_e) in an edge is insignificant. Here we set $\nu_e = 1$ for all e. The chosen symbol for m^2 is `mm`, which will be replaced by its value 0.2 later on. It is also allowed to input numerical values for masses already in the `edges` list, for instance by replacing the first element of the list by `((0,1), 1, '0.2')`.

Next we fix the momentum variables. Recall that the external vertices are required to be labeled $\{0, 1, \ldots, |V^{\text{ext}}| - 1\}$, so the external momenta are $p_0, \ldots, p_{|V^{\text{ext}}|-1}$. Moreover, the last momentum is inferred automatically by `feyntrop` using momentum conservation, leaving $p_0, \ldots, p_{|V^{\text{ext}}|-2}$ to be fixed by the user. A momentum configuration is then specified by the collection of scalar products,

$$p_u \cdot p_v \text{ for all } 0 \le u \le v \le |V^{\text{ext}}| - 2\,. \tag{38}$$

In the code, we must provide replacement rules for these scalar products in terms of some variables of choice. For the example at hand, $|V^{\text{ext}}| = 3$, so we must provide replacement rules for p_0^2, p_1^2 and $p_0 \cdot p_1$. In the syntax of `feyntrop` we thus write

```
replacement_rules = [(sp[0,0], '0'), (sp[1,1], '0'), (sp[0,1], 'pp2/2')]
```

where `sp[u,v]` stands for $p_u \cdot p_v$, the **s**calar **p**roduct of p_u and p_v. We have immediately set $p_0^2 = p_1^2 = 0$ and also defined a variable `pp2` which stands for p_2^2, as, by momentum conservation,

$$p_2^2 = 2 p_0 \cdot p_1\,. \tag{39}$$

Eventually, we fix numerical values for the two auxiliary variables `pp2` and `mm`. This is done via

```
phase_space_point = [('mm', 0.2), ('pp2', 1)]
```

which fixes $m^2 = 0.2$ and $p_2^2 = 1$. It is possible to obtain the $\mathcal{P}^{u,v}$ matrix (as defined in Section 2.1) and a list of all the propagator masses, which are computed from the previously provided data, by

```
P_uv_matrix, m_sqr_list = prepare_kinematic_data(edges, replacement_rules,
                                                  phase_space_point)
```

The final pieces of data that need to be provided are

```
D0 = 2
eps_order = 5
Lambda = 7.6
N = int(1e7)
```

`D0` is the integer part of the spacetime dimension $D = D_0 - 2\epsilon$. We expand up to, but not including, `eps_order`. `Lambda` denotes the deformation parameter from (9). `N` is the number of Monte Carlo sampling points.

Tropical Monte Carlo integration of the Feynman integral, with the kinematic configuration chosen above, is now performed by running the command

```
trop_res, Itr =  tropical_integration(
                    N,
                    D0,
                    Lambda,
                    eps_order,
                    edges,
                    replacement_rules,
                    phase_space_point)
```

If the program runs correctly (i.e. no error is printed), `trop_res` will contain the ϵ-expansion (16) *without* the prefactor $\Gamma(\omega)/(\Gamma(\nu_1)\cdots\Gamma(\nu_{|E|})) = \Gamma(2\epsilon + 3)$. `Itr` is the value of the normalization factor in (22). Running this code on a laptop, we get, after a couple of seconds, the output

```
Prefactor: gamma(2*eps + 3).
(Effective) kinematic regime: Minkowski (generic).
Generalized permutahedron property: fulfilled.
Analytic continuation: activated. Lambda = 7.6
Started integrating using 8 threads and N = 1e+07 points.
Finished in 6.00369 seconds = 0.00166769 hours.

-- eps^0: [-46.59  +/- 0.13]  +  i * [ 87.19  +/- 0.12]
-- eps^1: [-274.46 +/- 0.55]  +  i * [111.26  +/- 0.55]
-- eps^2: [-435.06 +/- 1.30]  +  i * [-174.47 +/- 1.33]
-- eps^3: [-191.72 +/- 2.15]  +  i * [-494.69 +/- 2.14]
-- eps^4: [219.15  +/- 2.68]  +  i * [-431.96 +/- 2.67]
```

These printed values for the ϵ expansion are contained in the list `trop_res` in the following format:

$$\left[\left((\mathrm{re}_0,\sigma_0^{\mathrm{re}}),(\mathrm{im}_0,\sigma_0^{\mathrm{im}})\right),\ldots,\left((\mathrm{re}_4,\sigma_4^{\mathrm{re}}),(\mathrm{im}_4,\sigma_4^{\mathrm{im}})\right)\right],$$

where $\mathrm{re}_0 \pm \sigma_0^{\mathrm{re}}$ is the real part of the 0th order term, and so forth.

The ϵ-expansion, with prefactor included, can finally be output via

```
eps_expansion(trop_res, edges, D0)
```

giving

```
174.3842115*i - 93.17486662 + eps*(-720.8731714 + 544.3677186*i) +
eps**2*(-2115.45025 + 496.490128*i) + eps**3*(-3571.990969 - 677.5254794*i) +
eps**4*(-3872.475723 - 2726.965026*i) + O(eps**5)
```

If the `tropical_integration` command fails, for instance because a subdivergence of the input graph is detected, it prints an error message. The command also prints a warning if the kinematic point is too exceptional and convergence cannot be guaranteed due to the $\mathcal{F}$ polynomial lacking the generalized permutahedron property (see Section 3.3).

5.3. Deformation parameter

The uncertainties on the integrated result may greatly vary with the value of the deformation parameter λ from (9) (what was called `Lambda` above). Moreover, the optimal value of λ might change depending on the phase space point. It is up to the user to pick a suitable value by trial and error, for instance by integrating several times with a low number of sampling points N. In Section 6, this method is used to evaluate multiple examples of Feynman integrals in the Minkowski regime. Typical values for the parameter λ can be found there. It would be beneficial to automate this procedure, possibly by minimizing the sampling variance with respect to λ, for instance by solving $\partial_\lambda \sigma_f = 0$ with σ_f defined in (31), or by tightening the bounds in Assumption 3.2 (see the discussion after this assumption). We leave the exploration of such ideas to future research.

Note that λ has mass dimension $1/\mathrm{mass}^2$. Heuristically, this implies that the value of λ should be of order $\mathcal{O}(1/\Lambda^2)$, where Λ is the maximum physical scale in the given computation.

6. Examples of Feynman integral evaluations

In this section, we use `feyntrop` to numerically evaluate certain Feynman integrals of interest. The first two examples, 6.1 and 6.2, show that `feyntrop` is capable of computing Feynman integrals at high loop-orders involving many kinematic scales. The four examples that follow, 6.4, 6.3, 6.6 and 6.5, demonstrate that `feyntrop` is capable of computing phenomenologically relevant diagrams. The final example, 6.7, is an invitation to study conformal integrals with our code, as they are important for, e.g., $\mathcal{N}=4$ SYM and the cosmological bootstrap.

We have chosen phase space points which are not close to thresholds to insure good numerical convergence, and expand up to and including ϵ^{2L} in all but up the last example.

Each of the following examples can be computed with `feyntrop` using 10^8 sampling points within a few minutes on a consumer laptop with 16 GBs of RAM. To crosscheck, we used the same machine to evaluate the examples using both `AMFlow`[5] and `pySecDec`. All computations agreed within the indicated error bounds. Our computations using `AMFlow` and `pySecDec` did not always terminate. Particularly for the Examples 6.1 and 6.6, neither software finished due to memory constraints of 16 GB on our test laptop. After the initial version of this article became available, Vitaly Magerya informed us that he was able to reproduce also Example 6.6 and verify our numbers using `pySecDec` with an only slightly more powerful computer. He also found indication that Example 6.1 is reproducible using a new version of `pySecDec` that was made available three months after the initial version of the present article was posted [83].

We emphasize that these additional computations using `AMFlow` and `pySecDec` should be seen as a crosscheck and not a benchmark comparison. A comparison of `feyntrop` and `AMFlow` is difficult as the former directly integrates via Monte Carlo while the latter integrates via differential equations. To integrate a Feynman integral using `AMFlow` an IBP system needs to be solved. Finding this solution is a memory constrained problem and a 16 GB laptop is not appropriate to systematically perform computations within this approach. If the IBP system is solved, `AMFlow` provides the evaluated integral at an accuracy which is almost unachievable using a Monte Carlo approach. The comparison to `pySecDec` is similarly flawed as it can also deal with inherently divergent integrals. To do so it has to check for divergences in each sector which takes time. Moreover, it can deal with completely general algebraic integrals, whereas `feyntrop` completely relies on the inherent mathematical structure of Feynman integrals. We postpone a proper benchmark comparison with the new version of `pySecDec` and updated versions of `AMFlow` to a future research project.

To further highlight the capabilities of `feyntrop`, we computed every example on a high-performance machine, namely a single `AMD EPYC 7H12` 64-core processor using all cores. For each example we use 10^8 sample points to get a relative accuracy of the order of 10^{-2} to 10^{-4}. The output for each example includes the total evaluation time that `feyntrop` needs to compute the respective diagram. This evaluation time includes all steps of the computation. The time needed for the preprocessing step is negligible in comparison to the sampling time as long as the number of edges is relatively small (i.e. $|E| \le 15$). Hence, for such moderate numbers of propagators, the evaluation time is proportional to the number of sample points. The sampling step is completely parallelizable. So, doubling the number of CPUs, halfs the evaluation time. As the evaluation is based on Monte Carlo, increasing the relative accuracy is costly: one additional digit costs a 100-fold increase in CPU-time.

The code for each example can be found on the `github` repository in the folder `examples`.

[5] As `AMFlow` relies on DEQs for Feynman integrals, it is necessary to link it to IBP software. In our examples, we tried the following two options for IBP software: 1) `FIRE` [79] combined with `LiteRed` [80,81], and 2) `Blade` [82].

6.1. A 5-loop 2-point zigzag diagram

We evaluate the following 5-loop 2-point function with all masses different in $D = 3 - 2\epsilon$ dimensions

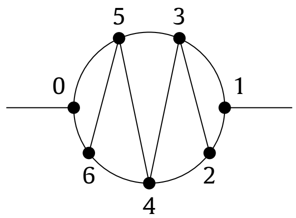

corresponding to the edge set

```
edges = [((0,6), 1, '1') , ((0,5), 1, '2'), ((5,6), 1, '3'),
          ((6,4), 1, '4') , ((5,3), 1, '5'), ((5,4), 1, '6'),
          ((4,3), 1, '7') , ((4,2), 1, '8'), ((3,2), 1, '9'),
          ((3,1), 1, '10'), ((2,1), 1, '11')]
```

Here we already input the chosen values for masses, namely $m_e^2 = e + 1$ for $e = 0, \ldots, 10$.

There is only a single independent external momentum p_0, whose square we set equal to 100 via

```
replacement_rules = [(sp[0,0], 'pp0')]
phase_space_point = [('pp0', 100)]
```

The value $\lambda = 0.02$ turns out to give small errors, which is of order $\mathcal{O}(1/p_0^2)$ in accordance with the comment at the end of the previous section. Using $N = 10^8$ Monte Carlo sampling points, `feyntrop`'s `tropical_integration` command gives

```
Prefactor: gamma(5*eps + 7/2).
(Effective) kinematic regime: Minkowski (generic).
Finished in 9.62 seconds.
-- eps^0: [0.0001976 +/- 0.0000016]  +  i * [0.0001415 +/- 0.0000018]
-- eps^1: [-0.004961 +/- 0.000023 ]  +  i * [-0.000802 +/- 0.000024 ]
-- eps^2: [ 0.04943  +/-  0.00017 ]  +  i * [-0.01552  +/-  0.00017 ]
-- eps^3: [-0.25468  +/-  0.00083 ]  +  i * [ 0.24778  +/-  0.00093 ]
-- eps^4: [ 0.5909   +/-  0.0033  ]  +  i * [ -1.7261  +/-  0.0038  ]
-- eps^5: [  1.048   +/-   0.012  ]  +  i * [  7.410   +/-   0.013  ]
-- eps^6: [ -14.652  +/-   0.037  ]  +  i * [ -20.933  +/-   0.038  ]
-- eps^7: [  65.87   +/-   0.10   ]  +  i * [  35.25   +/-   0.11   ]
-- eps^8: [ -190.90  +/-   0.27   ]  +  i * [  -4.91   +/-   0.26   ]
-- eps^9: [ 393.08   +/-   0.70   ]  +  i * [ -182.56  +/-   0.59   ]
-- eps^10:[ -558.01  +/-   1.64   ]  +  i * [ 685.62   +/-   1.29   ]
```

We have not been able to compute this expansion with `AMFlow` for the sake of verification. The memory constraints of 16 GB were insufficient. `pySecDec` applied to this example exhausted the available memory while building the sector decomposition library on our test laptop, but Vitaly Magerya informed us that he was able to create the integration library on a `32 GB 8-core Intel i7` computer in a couple of hours. We again emphasize that, for a proper benchmark comparison, our `AMFlow` and `pySecDec` code should be put on a machine with more memory. Still, this example illustrates that `feyntrop` can operate at high loop order with little memory, CPU and time resources.

6.2. A 3-loop 4-point envelope diagram

Here, we evaluate a $D = 4 - 2\epsilon$ dimensional, non-planar, 3-loop 4-point, envelope diagram:

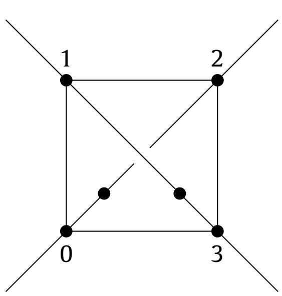

The dots on the crossed lines represent squared propagators, i.e. edge weights equal to 2, rather than vertices. The weighted edge set with corresponding mass variables is thus

141

```
edges = [((0,1), 1, 'mm0'), ((1,2), 1, 'mm1'), ((2,3), 1, 'mm2'),
         ((3,0), 1, 'mm3'), ((0,2), 2, 'mm4'), ((1,3), 2, 'mm5')]
```

Let us define the two-index Mandelstam variables $s_{ij} = (p_i + p_j)^2$, which are put into `feyntrop`'s replacement rules in the form `(sp[i,j], '(sij - ppi - ppj)/2)')` for $0 \leq i < j \leq 2$. The chosen phase space point is

$$p_0^2 = 1.1\,, \quad p_1^2 = 1.2\,, \quad p_2^2 = 1.3\,, \quad s_{01} = 2.1\,, \quad s_{02} = 2.2\,, \quad s_{12} = 2.3\,, \qquad (40)$$
$$m_0^2 = 0.05\,, \quad m_1^2 = 0.06\,, \quad m_2^2 = 0.07\,, \quad m_3^2 = 0.08\,, \quad m_4^2 = 0.09\,, \quad m_5^2 = 0.1\,.$$

With additional settings $\lambda = 1.24$ and $N = 10^8$, we find

```
Prefactor: gamma(3*eps + 2).
(Effective) kinematic regime: Minkowski (generic).
Finished in 5.12 seconds.
-- eps^0: [-10.8335 +/- 0.0084]  +  i * [-12.7145 +/- 0.0083]
-- eps^1: [ 47.971  +/- 0.059 ]  +  i * [-105.057 +/- 0.059 ]
-- eps^2: [ 413.05  +/-  0.23 ]  +  i * [  7.29   +/-  0.23 ]
-- eps^3: [ 372.07  +/-  0.65 ]  +  i * [ 947.82  +/-  0.65 ]
-- eps^4: [-1412.36 +/-  1.45 ]  +  i * [1325.74  +/-  1.45 ]
-- eps^5: [-2726.00 +/-  2.67 ]  +  i * [-1295.36 +/-  2.69 ]
-- eps^6: [ 287.25  +/-  4.28 ]  +  i * [-3982.04 +/-  4.30 ]
```

We verified these numbers using `pySecDec`. The test machine's memory of 16 GBs was exhausted before `AMFlow` could finish the calculation. The examples in [84] indicate that using a computer with more memory might also make this 3-loop diagram accessible using `AMFlow`.

6.3. A 2-loop 4-point μe-scattering diagram

We evaluate a non-planar, 2-loop 4-point diagram appearing in muon-electron scattering [85], which is finite in $D = 6 - 2\epsilon$ dimensions. It was previously evaluated for vanishing electron mass in [86].

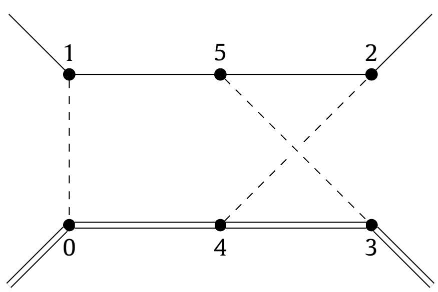

The dashed lines represent photons, the solid lines are electrons with mass m, and the double lines are muons with mass M (which is approximately 200 times larger than m). The edge set is

```
edges = [((0,1), 1, '0'), ((0,4), 1, 'MM'), ((1,5), 1, 'mm'), ((5,2), 1, 'mm'),
         ((5,3), 1, '0'), ((4,3), 1, 'MM'), ((4,2), 1, '0')]
```

where `MM` and `mm` stand for M^2 and m^2 respectively. With a phase space point similar to that of [86, Section 4.1.2]

$$p_0^2 = M^2 = 1\,, \quad p_1^2 = p_2^2 = m^2 = 1/200\,, \quad s_{01} = -1/7\,, \qquad (41)$$
$$s_{12} = -1/3\,, \quad s_{02} = 2M^2 - 2m^2 - s_{01} - s_{12} = 2.49$$

and settings $\lambda = 1.29$, $N = 10^8$, the result becomes

```
Prefactor: gamma(2*eps + 1).
(Effective) kinematic regime: Minkowski (exceptional).
Finished in 6.53 seconds.
-- eps^0: [1.16483 +/- 0.00083]  +  i * [0.24155 +/- 0.00074]
-- eps^1: [5.5387  +/- 0.0086 ]  +  i * [2.2818  +/- 0.0093 ]
-- eps^2: [15.171  +/-  0.058 ]  +  i * [10.079  +/-  0.064 ]
-- eps^3: [ 28.02  +/-  0.32  ]  +  i * [ 28.17  +/-  0.28  ]
-- eps^4: [ 38.20  +/-  1.42  ]  +  i * [ 56.94  +/-  0.85  ]
```

The momentum configuration is exceptional, so we cannot be sure that the generalized permutahedron property holds - see Section 3.3. In spite of that, `feyntrop` gives the correct numbers, which we confirmed using both `AMFlow` and `pySecDec`.

The leading order term differs from [86, eq. (4.20)] by roughly 10% due to our inclusion of the electron mass. We do, however, reproduce the computation in this reference if we set this mass to 0 in the `feyntrop` configuration.

6.4. A QCD-like, 2-loop 5-point diagram

This example is a QCD-like, $D = 6 - 2\epsilon$ dimensional, 2-loop 5-point diagram:

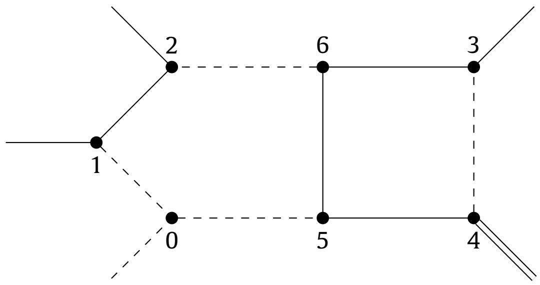

The dashed lines represent gluons, the solid lines are quarks each with mass m, and the double line is some off-shell momentum $p_4^2 \neq 0$ fixed by conservation. The edge data are

```
edges = [((0,1), 1, '0'), ((1,2), 1, 'mm'), ((2,6), 1, '0'), ((6,3), 1, 'mm'),
         ((3,4), 1, '0'), ((4,5), 1, 'mm'), ((5,0), 1, '0'), ((5,6), 1, 'mm')]
```

where mm stands for m^2. Let us choose the phase space point

$$p_0^2 = 0\,, \quad p_1^2 = p_2^2 = p_3^2 = m^2 = 1/2\,, \quad s_{01} = 2.2\,, \quad s_{02} = 2.3\,, \\ s_{03} = 2.4\,, \quad s_{12} = 2.5\,, \quad s_{13} = 2.6\,, \quad s_{23} = 2.7\,, \tag{42}$$

where again $s_{ij} = (p_i + p_j)^2$. Finally, setting $\lambda = 0.28$, $N = 10^8$, we obtain

```
Prefactor: gamma(2*eps + 2).
(Effective) kinematic regime: Minkowski (exceptional).
Finished in 8.20 seconds.
-- eps^0: [0.06480 +/- 0.00078]  +  i * [-0.08150 +/- 0.00098]
-- eps^1: [0.4036  +/- 0.0045 ]  +  i * [ 0.3257  +/- 0.0035 ]
-- eps^2: [-0.7889 +/- 0.0060 ]  +  i * [ 0.957   +/-  0.016 ]
-- eps^3: [-1.373  +/-  0.030 ]  +  i * [ -1.181  +/-  0.034 ]
-- eps^4: [ 1.258  +/-  0.088 ]  +  i * [ -1.205  +/-  0.036 ]
```

The kinematic configuration is again exceptional. Nevertheless, `feyntrop` returns the correct numbers, which we verified with `pySecDec`.[6] We were not able to compute this diagram with `AMFlow` due to our memory constraints. As similarly intricate Feynman integrals can be evaluated with `AMFlow` using more memory (see [84]), these constraints are very likely the only obstruction for a crosscheck with `AMFlow`.

6.5. Diagram contributing to triple Higgs production via gluon fusion

In this example, we evaluate the following diagram contributing to the process[7] $gg \to HHH$ in $D = 4 - 2\epsilon$ dimensions:

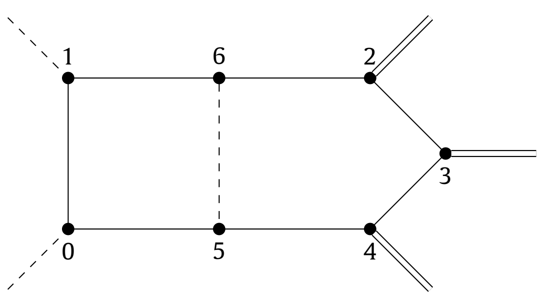

The dashed lines are massless propagators (representing gluons), the single solid lines are propagators containing the top quark mass, and the three external double lines are put on-shell to the Higgs mass. In this case, the list of edges reads

```
edges = [((0,1), 1, 'mm_top'), ((1,6), 1, 'mm_top'), ((5,6), 1, '0'),
         ((6,2), 1, 'mm_top'), ((2,3), 1, 'mm_top'), ((3,4), 1, 'mm_top'),
         ((4,5), 1, 'mm_top'), ((5,0), 1, 'mm_top')]
```

[6] An earlier version of this article wrongly stated that this computation was not verifiable with `pySecDec`. We thank both an anonymous referee and Vitaly Magerya for pointing this out to us.

[7] We thank Babis Anastasiou for suggesting this example.

with `mm_top` being the square of the top quark mass, m_t^2.

Given $s_{ij} := (p_i + p_j)^2$, we employ the following kinematic setup:

$$p_0^2 = p_1^2 = 0\,, \quad p_2^2 = p_3^2 = p_4^2 = m_H^2\,,$$
$$s_{01} = 5m_H^2 - s_{02} - s_{03} - s_{12} - s_{13} - s_{23}\,. \tag{43}$$

The kinematic space is then parameterized by $(s_{02}, s_{03}, s_{12}, s_{13}, s_{23}, m_t^2, m_H^2)$.

Let us evaluate this integral at the phase space point

$$m_t^2 = 1.8995\,, \quad m_H^2 = 1\,, \tag{44}$$
$$s_{02} = -4.4\,, \quad s_{03} = -0.5\,, \quad s_{12} = -0.6\,, \quad s_{13} = -0.7\,, \quad s_{23} = 1.8\,,$$

which lies in the physical region, and has the physically relevant mass ratio $m_t^2/m_H^2 = 1.8995$. The remaining Mandelstam invariants are then fixed by momentum conservation to

$$(s_{01}, s_{04}, s_{14}, s_{24}, s_{34}) = (9.4, -1.5, -5.1, 7.2, 3.4).$$

Setting $\lambda = 0.64$ and $N = 10^8$, we get

```
Prefactor: gamma(2*eps + 4).
(Effective) kinematic regime: Minkowski (generic).
Finished in 8.12 seconds.
-- eps^0: [-0.0114757 +/- 0.0000082]  +  i * [0.0035991 +/- 0.0000068]
-- eps^1: [ 0.003250  +/- 0.000031 ]  +  i * [-0.035808 +/- 0.000041 ]
-- eps^2: [ 0.046575  +/- 0.000098 ]  +  i * [0.016143  +/- 0.000088 ]
-- eps^3: [ -0.01637  +/-  0.00017 ]  +  i * [ 0.03969  +/-  0.00016 ]
-- eps^4: [ -0.02831  +/-  0.00023 ]  +  i * [-0.00823  +/-  0.00024 ]
```

We were unable to evaluate this example in reasonable time with `AMFlow`. Again, adding more memory would likely solve this problem. With `pySecDec` we were able to confirm `feyntrop`'s numbers within 3 hours[8] on a laptop, with relative errors around 10^{-2}. Running `feyntrop` on the same laptop with 10^8 sampling points, we obtain the same numbers within 2.5 minutes and with relative errors of order 10^{-3}.

6.6. A QED-like, 4-loop vacuum diagram

Next we evaluate a QED-like, 4-loop vacuum diagram in $D = 4 - 2\epsilon$ dimensions:

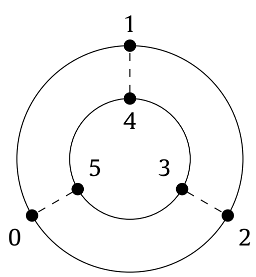

The dashed lines represent photons, and the solid lines are electrons of mass m. No analytic continuation is required in this case since there are no external momenta - the final result should hence be purely real. We specify

```
replacement_rules = []
```

in the code to indicate that all scalar products are zero.

The collection of edges is

```
edges = [((0,1), 1, 'mm'), ((1,2), 1, 'mm'), ((2,0), 1, 'mm'),
          ((0,5), 1, '0' ), ((1,4), 1, '0' ), ((2,3), 1, '0' ),
          ((3,4), 1, 'mm'), ((4,5), 1, 'mm'), ((5,3), 1, 'mm')]
```

where `mm` stands for m^2. Choosing

```
phase_space_point = [('mm', 1)]
```

and setting $\lambda = 0\,,\ N = 10^8$, we then find

[8] Three months after the initial version of this article was posted, a new version of `pySecDec` became available which is, in some cases, up to four times as efficient as the former version [83]. We postpone a systematic comparison of `feyntrop` with this new version to a future research project.

```
Prefactor: gamma(4*eps + 1).
(Effective) kinematic regime: Euclidean (generic).
Finished in 3.58 seconds.
-- eps^0: [3.01913 +/- 0.00047]  +  i * [0.0 +/- 0.0]
-- eps^1: [-7.0679 +/- 0.0021 ]  +  i * [0.0 +/- 0.0]
-- eps^2: [20.5399 +/- 0.0074 ]  +  i * [0.0 +/- 0.0]
-- eps^3: [-27.895 +/-  0.024 ]  +  i * [0.0 +/- 0.0]
-- eps^4: [62.043  +/-  0.074 ]  +  i * [0.0 +/- 0.0]
-- eps^5: [-59.46  +/-  0.23  ]  +  i * [0.0 +/- 0.0]
-- eps^6: [155.27  +/-  0.73  ]  +  i * [0.0 +/- 0.0]
-- eps^7: [-90.81  +/-  2.26  ]  +  i * [0.0 +/- 0.0]
-- eps^8: [403.78  +/-  6.71  ]  +  i * [0.0 +/- 0.0]
```

We were not able to verify this example with AMFlow or pySecDec within our memory constraints. However, Vitaly Magerya informed us that he was able to verify these numbers with pySecDec in under one hour using an only slightly larger computer.

6.7. An elliptic, conformal, 4-point integral

The final example is a 1-loop 4-point conformal integral with edge weights $\nu_{1,\dots,4} = 1/2$ in $D = 2$ dimensions, the result of which was computed in terms of elliptic K functions in [87, Sec. 7.2]:

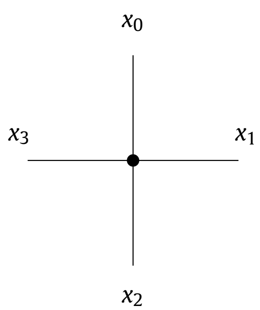

$$= \frac{4}{\sqrt{-p_2^2}} \left[K(z)K(1-\bar{z}) + K(\bar{z})K(1-z) \right] \tag{45}$$

The denominator above differs from [87, eq. (7.6)] because we have used conformal symmetry to send $x_3 \to \infty$, thereby reducing the kinematic space to that of a 3-point integral. After identifying dual momentum variables x_i in terms of ordinary momenta as $p_i = x_i - x_{i+1}$, the conformal cross ratios, with the usual single-valued complex parameterization in terms of z and $\bar{z}$, read

$$z\bar{z} = \frac{p_0^2}{p_2^2}, \quad (1-z)(1-\bar{z}) = \frac{p_1^2}{p_2^2}. \tag{46}$$

In feyntrop we specify the associated 1-loop 3-point momentum space integral as

```
edges = [((0,1), 1/2, '0'), ((1,2), 1/2, '0'), ((2,0), 1/2, '0')]
```

where all internal masses are zero and edge weights are set to 1/2.

We choose a momentum configuration in the Euclidean regime:

$$p_0^2 = -2, \quad p_1^2 = -3, \quad p_2^2 = -5. \tag{47}$$

Although feyntrop can compute integrals with rational edge weights in the Minkowski regime, it is most natural to study conformal integrals in the Euclidean regime.

With $\lambda = 0$ and $N = 10^8$, we then obtain

```
(Effective) kinematic regime: Euclidean (generic).
Finished in 1.34 seconds.
-- eps^0: [9.97192 +/- 0.00027]  +  i * [0.0 +/- 0.0]
```

The result agrees with the analytic expression (45). This example also illustrates the high efficiency of feyntrop in the Euclidean regime where very high accuracies can be obtained quickly.

7. Conclusions and outlook

With this article we introduced feyntrop, a general tool to numerically evaluate quasi-finite Feynman integrals in the physical regime with sufficiently general kinematics. To do so, we gave a detailed classification of different kinematic regimes that are relevant for numerical integration. Moreover, we presented a completely projective integral expression for concretely $i\varepsilon$-deformed Feynman integrals and their dimensionally regularized expansions. We used tropical sampling for the numerical integration, which we briefly reviewed, and we discussed the relevant issues on facet presentations of the Newton polytopes of Symanzik polynomials in detail. To be able to perform the numerical integration efficiently, we gave formulas and algorithms for the fast evaluation of Feynman integrals. To give a concise usage manual for feyntrop and to illustrate its capabilities, we gave numerous, detailed examples of evaluated Feynman integrals.

The most important restrictions of `feyntrop` are 1) it is not capable of dealing with Feynman integrals that have subdivergences (i.e. non-quasi-finite integrals) and 2) it is not capable of dealing with certain highly exceptional kinematic configurations.

The first restriction can be lifted by implementing an analytic continuation of the integrand in the spirit of [29,30,56] into `feyntrop`. Naively, preprocessing input integrals with such a procedure increases the number of Feynman integrals and thereby also the necessary computer time immensely. However, this proliferation of terms comes from the expansion of the derivatives of the $\mathcal{U}$ and $\mathcal{F}$ polynomials as numerators. This expansion can be avoided, because also the derivatives of $\mathcal{U}$ and $\mathcal{F}$ (mostly) have the generalized permutahedron property, and because we have fast algorithms to evaluate such derivatives. For instance, we derived a fast algorithm to evaluate the first and second derivatives of $\mathcal{F}$ in Section 4.2. We postpone the elaboration and implementation of this approach to future work.

A promising approach to lift the second restriction is to try to understand the general shape of the $\mathcal{F}$ polynomial's Newton polytope. Outside of the Euclidean and generic kinematic regimes, this polytope is not always a generalized permutahedron. In these exceptional kinematic situations, it can have new facets that cannot be explained by known facet presentations. It might be possible to explain these new facets with the help of the Coleman–Norton picture of infrared divergences [88] (see, e.g., [89] where explicit per-diagram factorization of Feynman integrals was observed in a position space based framework). An alternative approach to fix the issue is to implement the tropical sampling approach that requires a full triangulation of the respective Newton polytopes (see [1, Sec. 5]).

Besides this there are numerous, desirable, gradual improvements of `feyntrop` that we also postpone to future works. The most important such improvement would be to use the algorithm in conjunction with a *quasi-Monte Carlo* approach. The runtime to obtain the value of an integral up to accuracy δ currently scales as δ^{-2}, as is standard for a Monte Carlo method. Changing to a quasi-Monte Carlo based procedure would improve this scaling to δ^{-1}.

Another improvement would be to find an entirely *canonical* deformation prescription. Currently, our deformation still relies on an external parameter that has to be fine-tuned to the respective integral. A canonical deformation prescription that does not depend on a free parameter would lift the burden of this fine-tuning from the user and would likely also produce better rates of convergence.

A more technical update of `feyntrop` would involve an implementation of the tropical sampling algorithm on GPUs or on distributed cluster systems. The current implementation of `feyntrop` is parallelized and can make use of all cores of a single computer. Running `feyntrop` on multiple computers in parallel is not implemented, but there are no technical obstacles to write such an implementation, which we postpone to a future research project.

Declaration of competing interest

The authors declare that they have no known competing financial interests or personal relationships that could have appeared to influence the work reported in this paper.

Data availability

The code is submitted as a tar.gz file and is made available at https://github.com/michibo/feyntrop.

Acknowledgements

We thank Nima Arkani-Hamed, Aaron Hillman, Sebastian Mizera and Erik Panzer for helpful exchanges on facet presentations of Newton polytopes of Symanzik polynomials, Pierpaolo Mastrolia for stimulating discussions on applications to phenomenology, Yan-Qing Ma for helpful comments on the manuscript and Vitaly Magerya for comments and independently verifying our numbers in Example 6.6 using `pySecDec`. FT thanks Georgios Papathanasiou for continued support. HJM and FT thank the Institute for Theoretical Studies at the ETH Zürich for hosting the workshop 'Tropical and Convex Geometry and Feynman integrals' in August 2022, which was beneficial for the completion of this work. All authors thank the Institute for Advanced Studies, Princeton US, for hospitality during a stay in May 2023 where parts of this work were completed. MB was supported by Dr. Max Rössler, the Walter Haefner Foundation and the ETH Zürich Foundation. Some of our calculations were carried out on the ETH Euler cluster.

References

[1] M. Borinsky, Ann. Inst. Henri Poincaré Comb. Phys. Interact. (2023), https://doi.org/10.4171/AIHPD/158, in press, arXiv:2008.12310.
[2] G. Guennebaud, B. Jacob, et al., Eigen v3, http://eigen.tuxfamily.org, 2010.
[3] D. Blackman, S. Vigna, ACM Trans. Math. Softw. 47 (2021) 36, 32.
[4] G. Van Rossum, F.L. Drake, Python 3 Reference Manual, CreateSpace, Scotts Valley, CA, 2009.
[5] W. Jakob, J. Rhinelander, D. Moldovan, pybind11 – seamless operability between C++11 and python, https://github.com/pybind/pybind11, 2017.
[6] A. Meurer, C.P. Smith, M. Paprocki, O. Čertík, S.B. Kirpichev, M. Rocklin, et al., PeerJ Comput. Sci. 3 (2017) e103.
[7] G. Heinrich, Phys. Rep. 922 (2021) 1, arXiv:2009.00516.
[8] S.G. Karshenboim, Phys. Rep. 422 (2005) 1, arXiv:hep-ph/0509010.
[9] J. Zinn-Justin, Quantum Field Theory and Critical Phenomena, vol. 171, Oxford University Press, 2021.
[10] J.F. Donoghue, Phys. Rev. D 50 (1994) 3874, arXiv:gr-qc/9405057.
[11] F. Brown, SIGMA 17 (2021) 103, arXiv:2101.04419.
[12] Z. Bern, L.J. Dixon, D.C. Dunbar, D.A. Kosower, Nucl. Phys. B 425 (1994) 217, arXiv:hep-ph/9403226.
[13] Z. Bern, L.J. Dixon, D.A. Kosower, Phys. Rev. D 73 (2006) 065013, arXiv:hep-ph/0507005.
[14] K.G. Chetyrkin, F.V. Tkachov, Nucl. Phys. B 192 (1981) 159.
[15] S. Laporta, Int. J. Mod. Phys. A 15 (2000) 5087, arXiv:hep-ph/0102033.
[16] S. Bloch, H. Esnault, D. Kreimer, Commun. Math. Phys. 267 (2006) 181, arXiv:math/0510011.
[17] F. Brown, Commun. Math. Phys. 287 (2009) 925, arXiv:0804.1660.
[18] E. Panzer, Comput. Phys. Commun. 188 (2015) 148, arXiv:1403.3385.
[19] E. Remiddi, Nuovo Cimento A 110 (1997) 1435, arXiv:hep-th/9711188.
[20] J.M. Henn, Phys. Rev. Lett. 110 (2013) 251601, arXiv:1304.1806.
[21] E. Panzer, Ann. Inst. Henri Poincaré Comb. Phys. Interact. 10 (2023) 31, arXiv:1908.09820.
[22] F. Brown, Commun. Number Theory Phys. 11 (2017) 453, arXiv:1512.06409.

[23] G.V. Dunne, M. Meynig, Phys. Rev. D 105 (2022) 025019, arXiv:2111.15554.
[24] A.V. Smirnov, N.D. Shapurov, L.I. Vysotsky, Comput. Phys. Commun. 277 (2022) 108386, arXiv:2110.11660.
[25] M. Borinsky, A.-L. Sattelberger, B. Sturmfels, S. Telen, SIAM J. Appl. Algebra Geom. (2022), https://doi.org/10.1137/22M1490569, in press, arXiv:2204.06414.
[26] N. Arkani-Hamed, A. Hillman, S. Mizera, Phys. Rev. D 105 (2022) 125013, arXiv:2202.12296.
[27] N. Arkani-Hamed, J. Trnka, J. High Energy Phys. 10 (2014) 030, arXiv:1312.2007.
[28] N. Arkani-Hamed, Y. Bai, T. Lam, J. High Energy Phys. 11 (2017) 039, arXiv:1703.04541.
[29] L. Nilsson, M. Passare, J. Geom. Anal. 23 (2013) 24.
[30] C. Berkesch, J. Forsgård, M. Passare, Mich. Math. J. 63 (2014) 101.
[31] K. Schultka, Toric geometry and regularization of Feynman integrals, arXiv:1806.01086.
[32] I.M. Gel'fand, M.M. Kapranov, A.V. Zelevinsky, Adv. Math. 84 (1990) 255.
[33] L. de la Cruz, J. High Energy Phys. 12 (2019) 123, arXiv:1907.00507.
[34] R.P. Klausen, J. High Energy Phys. 04 (2020) 121, arXiv:1910.08651.
[35] A. Klemm, C. Nega, R. Safari, J. High Energy Phys. 04 (2020) 088, arXiv:1912.06201.
[36] V. Chestnov, F. Gasparotto, M.K. Mandal, P. Mastrolia, S.J. Matsubara-Heo, H.J. Munch, et al., J. High Energy Phys. 09 (2022) 187, arXiv:2204.12983.
[37] F. Tellander, M. Helmer, Commun. Math. Phys. 399 (2023) 1021, arXiv:2108.01410.
[38] T. Binoth, G. Heinrich, Nucl. Phys. B 585 (2000) 741, arXiv:hep-ph/0004013.
[39] C. Bogner, S. Weinzierl, Comput. Phys. Commun. 178 (2008) 596, arXiv:0709.4092.
[40] T. Kaneko, T. Ueda, Comput. Phys. Commun. 181 (2010) 1352, arXiv:0908.2897.
[41] S. Borowka, G. Heinrich, S. Jahn, S.P. Jones, M. Kerner, J. Schlenk, et al., Comput. Phys. Commun. 222 (2018) 313, arXiv:1703.09692.
[42] D.E. Soper, Phys. Rev. D 62 (2000) 014009, arXiv:hep-ph/9910292.
[43] C. Anastasiou, A. Daleo, J. High Energy Phys. 10 (2006) 031, arXiv:hep-ph/0511176.
[44] S. Catani, T. Gleisberg, F. Krauss, G. Rodrigo, J.-C. Winter, J. High Energy Phys. 09 (2008) 065, arXiv:0804.3170.
[45] Z. Capatti, V. Hirschi, D. Kermanschah, B. Ruijl, Phys. Rev. Lett. 123 (2019) 151602, arXiv:1906.06138.
[46] X. Liu, Y.-Q. Ma, C.-Y. Wang, Phys. Lett. B 779 (2018) 353, arXiv:1711.09572.
[47] M.K. Mandal, X. Zhao, J. High Energy Phys. 03 (2019) 190, arXiv:1812.03060.
[48] X. Liu, Y.-Q. Ma, Comput. Phys. Commun. 283 (2023) 108565, arXiv:2201.11669.
[49] M. Hidding, Comput. Phys. Commun. 269 (2021) 108125, arXiv:2006.05510.
[50] T. Armadillo, R. Bonciani, S. Devoto, N. Rana, A. Vicini, Comput. Phys. Commun. 282 (2023) 108545, arXiv:2205.03345.
[51] I. Dubovyk, A. Freitas, J. Gluza, K. Grzanka, M. Hidding, J. Usovitsch, Phys. Rev. D 106 (2022) L111301, arXiv:2201.02576.
[52] Z.-F. Liu, Y.-Q. Ma, Phys. Rev. Lett. 129 (2022) 222001, arXiv:2201.11637.
[53] T. Binoth, J.P. Guillet, G. Heinrich, E. Pilon, C. Schubert, J. High Energy Phys. 10 (2005) 015, arXiv:hep-ph/0504267.
[54] R. Pittau, B. Webber, Eur. Phys. J. C 82 (2022) 55, arXiv:2110.12885.
[55] S. Mizera, S. Telen, J. High Energy Phys. 08 (2022) 200, arXiv:2109.08036.
[56] A. von Manteuffel, E. Panzer, R.M. Schabinger, J. High Energy Phys. 02 (2015) 120, arXiv:1411.7392.
[57] B. Kol, M. Smolkin, Class. Quantum Gravity 25 (2008) 145011, arXiv:0712.4116.
[58] N. Nakanishi, Graph Theory and Feynman Integrals, Gordon and Breach, 1971.
[59] S. Weinzierl, Feynman Integrals, Springer, Cham, 2022, arXiv:2201.03593.
[60] R.J. Eden, P.V. Landshoff, D.I. Olive, J.C. Polkinghorne, The Analytic S-Matrix, Cambridge University Press, 1966.
[61] Z. Nagy, D.E. Soper, Phys. Rev. D 74 (2006) 093006, arXiv:hep-ph/0610028.
[62] H.S. Hannesdottir, S. Mizera, What Is the iε for the S-Matrix?, Springer, 2023, arXiv:2204.02988.
[63] D. Maclagan, B. Sturmfels, Introduction to Tropical Geometry, Graduate Studies in Mathematics, vol. 161, American Mathematical Society, Providence, RI, 2015.
[64] A. Postnikov, Int. Math. Res. Not. (2009) 1026.
[65] M. Aguiar, F. Ardila, Hopf monoids and generalized permutahedra, arXiv:1709.07504.
[66] K.G. Chetyrkin, V.A. Smirnov, Theor. Math. Phys. 56 (1983) 770.
[67] E. Speer, Ann. IHP, Phys. Théor. 23 (1975) 1.
[68] R. Beekveldt, M. Borinsky, F. Herzog, J. High Energy Phys. 07 (2020) 061, arXiv:2003.04301.
[69] V.A. Smirnov, Analytic Tools for Feynman Integrals, Springer Tracts in Modern Physics, vol. 250, Springer, Heidelberg, 2012.
[70] E. Panzer, Feynman integrals and hyperlogarithms, Ph.D. thesis, Humboldt U, 2015, arXiv:1506.07243.
[71] A. Hillman, S. Mizera, E. Panzer, Personal communication, January–February 2023.
[72] S. Fujishige, N. Tomizawa, J. Oper. Res. Soc. Jpn. 26 (1983) 309.
[73] B.D. McKay, Eur. J. Comb. 4 (1983) 149.
[74] R.A. Horn, C.R. Johnson, Matrix Analysis, second ed., Cambridge University Press, Cambridge, 2013.
[75] D.A. Spielman, S.-H. Teng, SIAM J. Matrix Anal. Appl. 35 (2014) 835, arXiv:cs/0607105.
[76] M. Borinsky, O. Schnetz, J. High Energy Phys. 08 (2022) 291, arXiv:2206.10460.
[77] R. Chandra, L. Dagum, D. Kohr, R. Menon, D. Maydan, J. McDonald, Parallel Programming in OpenMP, Morgan Kaufmann, 2001.
[78] T. Kluyver, B. Ragan-Kelley, F. Pérez, B. Granger, M. Bussonnier, J. Frederic, et al., in: F. Loizides, B. Schmidt (Eds.), Positioning and Power in Academic Publishing: Players, Agents and Agendas, IOS Press, 2016, pp. 87–90.
[79] A.V. Smirnov, F.S. Chuharev, Comput. Phys. Commun. 247 (2020) 106877, arXiv:1901.07808.
[80] R.N. Lee, Presenting LiteRed: a tool for the Loop InTEgrals REDuction, arXiv:1212.2685.
[81] R.N. Lee, J. Phys. Conf. Ser. 523 (2014) 012059, arXiv:1310.1145.
[82] X. Guan, X. Liu, Y.-Q. Ma, W.-H. Wu, https://gitlab.com/multiloop-pku/blade/. (Accessed 17 May 2023).
[83] G. Heinrich, S.P. Jones, M. Kerner, V. Magerya, A. Olsson, J. Schlenk, Numerical scattering amplitudes with pySecDec, arXiv:2305.19768.
[84] X. Liu, Y.-Q. Ma, Phys. Rev. D 105 (2022) L051503, arXiv:2107.01864.
[85] A. Broggio, et al., J. High Energy Phys. 01 (2023) 112, arXiv:2212.06481.
[86] S. Di Vita, S. Laporta, P. Mastrolia, A. Primo, U. Schubert, J. High Energy Phys. 09 (2018) 016, arXiv:1806.08241.
[87] L. Corcoran, F. Loebbert, J. Miczajka, J. High Energy Phys. 04 (2022) 131, arXiv:2112.06928.
[88] S. Coleman, R.E. Norton, Nuovo Cimento 38 (1965) 438.
[89] M. Borinsky, Z. Capatti, E. Laenen, A. Salas-Bernárdez, J. High Energy Phys. 01 (2023) 172, arXiv:2210.05532.

Paper V

Tropical Feynman integration in the physical region
Michael Borinsky, Henrik J. Munch and **Felix Tellander**
PoS **EPS-HEP2023** (2024) 499, [2310.19890]

PROCEEDINGS OF SCIENCE
DESY-23-168

Tropical Feynman integration in the physical region

Michael Borinsky,[a] **Henrik J. Munch**[b] **and Felix Tellander**[c,*]

[a] *Institute for Theoretical Studies, ETH Zürich, 8092 Zürich, Switzerland*
[b] *Dipartimento di Fisica e Astronomia, Università degli Studi di Padova, 35131 Padova, Italy*
[c] *Deutsches Elektronen-Synchrotron DESY, Notkestr. 85, 22607 Hamburg, Germany*
E-mail: michael.borinsky@eth-its.ethz.ch, henrikjessen.munch@studenti.unipd.it, felix@tellander.se

The software `feyntrop` for direct numerical evaluation of Feynman integrals is presented. We focus on the underlying combinatorics and polytopal geometries facilitating these methods. Especially matroids, generalized permutohedra and normality are discussed in detail.

The European Physical Society Conference on High Energy Physics (EPS-HEP2023)
21-25 August 2023
Hamburg, Germany

[*] Speaker

https://pos.sissa.it/

1. Introduction

The evaluation and understanding of Feynman integrals play an important role in many areas of modern physics, for example in particle accelerator phenomenology [1], gravitational wave physics [2, 3], calculations of the magnetic moment of the muon [4] and critical exponents in statistical field theory [5]. Many modern numerical methods uses the canonical differential equation approach [6], see e.g. `AMFlow` [7], `DiffExp` [8] and `SeaSyde` [9]. Deriving the canonical differential equation is a potential bottleneck in these calculations which can be sidestepped using direct integration. Analytic integration can be performed in `HyperInt` [10] while numerical Monte Carlo techniques are for example implemented in `pySecDec` [11]. The program `feyntrop` [12] is of the latter type and integrates dimensionally regulated quasi-finite integrals numerically using Monte Carlo methods. The relevant sectors of integration are not determined using sector decomposition but relies on special properties of the Newton polytope of the integrand. If these polytopes are *generalized permutohedra*, the decomposition into relevant sectors is greatly simplified. Integrable singularities of the integrand are regulated with the *tropical approximation* [13] which also makes the integrand bounded from both above and below. For details on the tropical approximation, see [12, 14].

The program `feyntrop` has recently been used in [15] to numerically verify the canonical differential equation result for a four-point three-loop process with one massive leg. It has also been used in [16] to calculate Feynman integrals in ϕ^4-theory to 13 loops and beyond. The tropical way of thinking also sheds light on infrared singularities [17] and how to calculate entire amplitudes directly without using Feynman integrals at all [18].

2. Feynman Integrals and Generalized Hypergeometry

Feynman integrals have many different equivalent representations, each with its own advantages and disadvantages. Consider one-particle irreducible Feynman graphs $G := (E, V)$ with the number of cycles (loops) given by $L = |E|-|V|+1$. The vertex set V has the disjoint partition $V = V_{\text{ext}} \bigsqcup V_{\text{int}}$ where each $u \in V_{\text{ext}}$ is assigned an external incoming momenta $p_u \in \mathbb{R}^{1,D-1}$. Each edge $e \in E$ is assigned a non-negative mass m_e.

For the purpose of direct numerical evaluation in `feyntrop` the following projective representation is used:

$$\mathcal{I} = \Gamma(\omega) \int_{\mathbb{P}^E_+} \phi \quad \text{with} \quad \phi = \left(\prod_{e \in E} \frac{x_e^{\nu_e}}{\Gamma(\nu_e)} \right) \frac{1}{\mathcal{U}(\boldsymbol{x})^{D/2}} \left(\frac{1}{\mathcal{V}(\boldsymbol{x}) - i\varepsilon \sum_{e\in E} x_e} \right)^{\omega} \Omega \,. \tag{1}$$

Where the integration domain is over the *projective simplex* $\mathbb{P}^E_+ = \{\boldsymbol{x} = [x_1 : \cdots : x_{|E|}] \in \mathbb{RP}^{E-1} : x_e > 0\}$ with respect to its canonical Kronecker form

$$\Omega = \sum_{e=1}^{|E|} (-1)^{|E|-e} \frac{dx_1}{x_1} \wedge \cdots \wedge \widehat{\frac{dx_e}{x_e}} \wedge \cdots \wedge \frac{dx_{|E|}}{x_{|E|}} \,. \tag{2}$$

The *superficial degree of divergence* of the graph G are given by $\omega = \sum_{e\in E} \nu_e - DL/2$. We write $\mathcal{V}(\boldsymbol{x}) = \mathcal{F}(\boldsymbol{x})/\mathcal{U}(\boldsymbol{x})$ as a shorthand for the quotient of the two *Symanzik polynomials* that is defined from the underlying graph G by

$$\mathcal{U}(\boldsymbol{x}) := \sum_T \prod_{e \notin T} x_e\,, \qquad \mathcal{F}(\boldsymbol{x}) := \mathcal{F}_0 + \mathcal{F}_m = -\sum_F p(F)^2 \prod_{e \notin F} x_e + \mathcal{U}(\boldsymbol{x}) \sum_{e \in E} m_e^2 x_e\,, \tag{3}$$

where we sum over all spanning trees T and all spanning two-forests F of G, and $p(F)^2$ is the squared momentum running between the two-forest components. By this definition, $\mathcal{U}$ and $\mathcal{F}$ are homogeneous of degree L, resp. $L+1$, and hence $\mathcal{V}$ is a homogeneous rational function of degree 1.

2.1 Contour deformation

In order to define the integral on the correct analytic branch we need to implement Feynman's causal $i\varepsilon$ prescription. This is done using a finite contour deformation respecting the projective invariance [19].

The deformation is given by the embedding $\iota_\lambda : \mathbb{P}_+^E \hookrightarrow \mathbb{CP}^{|E|-1}$:

$$\iota_\lambda : x_e \mapsto X_e := x_e \exp\left(-i\lambda \frac{\partial \mathcal{V}}{\partial x_e}(\boldsymbol{x})\right). \tag{4}$$

Since the boundary is characterized by $x_e = 0$, ι_λ does not change the boundary. Using Cauchy's theorem, the integral is independent of ι_λ as long as the deformation does not cross any poles of ϕ. Set

$$\mathcal{I} = \Gamma(\omega) \int_{\iota_\lambda(\mathbb{P}_+^E)} \phi = \Gamma(\omega) \int_{\mathbb{P}_+^E} \iota_\lambda^* \phi \tag{5}$$

where $\iota_\lambda^*\phi$ is the pull-back, it can be written with the Jacobian $\iota_\lambda^*\Omega = \det(\mathcal{J}_\lambda(\boldsymbol{x}))\Omega$ where

$$\mathcal{J}_\lambda(\boldsymbol{x})^{e,h} = \delta_{e,h} - i\lambda x_e \frac{\partial^2 \mathcal{V}}{\partial x_e \partial x_h}(\boldsymbol{x}) \text{ for all } e, h \in E. \tag{6}$$

The deformed Feynman integral can thus be written as

$$\mathcal{I} = \Gamma(\omega) \int_{\mathbb{P}_+^E} \iota_\lambda^* \phi = \Gamma(\omega) \int_{\mathbb{P}_+^E} \left(\prod_{e \in E} \frac{X_e^{\nu_e}}{\Gamma(\nu_e)}\right) \frac{\det \mathcal{J}_\lambda(\boldsymbol{x})}{\mathcal{U}(\boldsymbol{X})^{D/2} \cdot \mathcal{V}(\boldsymbol{X})^{\omega}}\, \Omega \tag{7}$$

where $\boldsymbol{X} = \iota_\lambda(\boldsymbol{x})$.

2.2 Generalized hypergeometry

Another useful representation is due to Lee and Pomeransky [20]:

$$\mathcal{I} = \frac{\Gamma(D/2)}{\Gamma(D/2-\omega)} \int_0^\infty \left(\prod_{e \in E} \frac{x_e^{\nu_e} dx_e}{x_e \Gamma(\nu_e)}\right) \frac{1}{\mathcal{G}^{D/2}} \qquad \text{where} \qquad \mathcal{G} = \mathcal{U} + \mathcal{F}. \tag{8}$$

In this form, it is a generalized hypergeometric integral (Mellin transform) [21, 22] of the type studied by Passare and collaborators [23, 24]. This means that it satisfies a generalized hypergeometric system of partial differential equations in the sense of Gel'fand, Graev, Kapranov and Zelevinskiĭ (GGKZ, commonly shortened to GKZ) [25–29].

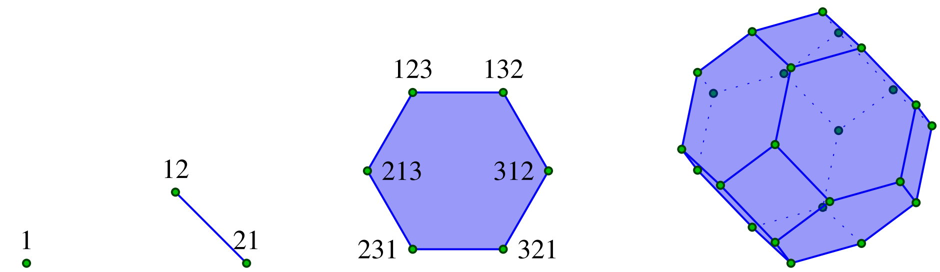

Figure 1: The first four permutohedra where it is easily seen from the explicit vertex coordinates (permutations) that all edges are parallel to $\mathbf{e}_i - \mathbf{e}_j$ for $i \neq j$.

Using multi-index notation we may write the Lee-Pomeransky polynomial as $\mathcal{G} = \sum_{i=1}^{r} c_i x^{\alpha_i}$ with $c_i \neq 0$ and $\alpha_i \in \mathbb{Z}_{\geq 0}^{|E|}$ for all $i = 1, \ldots, r$. We define the two matrices

$$A := \{1\} \times A_- = \begin{pmatrix} 1 & 1 & \cdots & 1, \\ \alpha_1 & \alpha_2 & \cdots & \alpha_r \end{pmatrix} \in \mathbb{Z}_{\geq 0}^{(|E|+1)\times r}, \text{ and} \tag{9}$$

$$\beta := \begin{pmatrix} -D/2, & -\nu_1 & , \ldots & , -\nu_{|E|} \end{pmatrix}^T \in \mathbb{C}^{|E|+1}, \tag{10}$$

from which we construct the GKZ hypergeometric system $H_A(\beta)$ as the sum of two ideals:

$$I_A := \left\langle \partial^u - \partial^v \mid u, v \in \mathbb{Z}_{\geq 0}^r \text{ s.t. } Au = Av \right\rangle, \quad \text{and} \tag{11}$$

$$Z_A(\beta) := \left\langle \Theta_i(c, \partial) \mid \Theta = A \cdot \begin{pmatrix} c_1\partial_1 \\ \vdots \\ c_r\partial_r \end{pmatrix} - \beta \right\rangle. \tag{12}$$

The ideal I_A is actually an ideal in the *commutative* polynomial ring $\mathbb{Q}[\partial_1, \cdots, \partial_r]$, and as such has a finite generating set $I_A = \langle h_1, \ldots h_\ell \rangle$ with $h_i \in \mathbb{Q}[\partial_1, \cdots, \partial_r]$. This ideal I_A is a *toric ideal* and it gives the defining equations of the projective *toric variety*

$$X_A = \{z \in \mathbb{P}^{r-1} \mid h_1(z) = \cdots = h_\ell(z) = 0\}$$

associated to the matrix A, see e.g. [30], [31, II, Chapter 5].

3. Generalized Permutohedra

The classical *perumtohedron* is a polytopal model of permutations, see Fig. 1. For n elements the permutohedron P_n is the $(n-1)$-dimensional polytope in $\mathbb{R}^n$ with vertices $(\sigma(1), \ldots, \sigma(n))$ where σ runs over all permutations of $[n] := \{1, 2, \ldots, n\}$. Every point in P_n satisfy $\sum_i x_i = n(n+1)/2$, meaning that P_n lies in a hyperplane and hence $\dim(P_n) = n - 1$. Note that every edge in P_n is parallel to $\mathbf{e}_i - \mathbf{e}_j$ for some $i \neq j$ where $\mathbf{e}_i$ denote the standard basis of $\mathbb{R}^n$.

In the theory of GKZ, the permutohedron appears as a *secondary polytope* $\Sigma(A)$, where A denotes the vertices of the triangular prism $Q = \Delta^1 \times \Delta^{n-1}$. The vertices (or equivalently, the top-dimensional normal cones) of $\Sigma(A)$ correspond to regular triangularizations of Q and also to

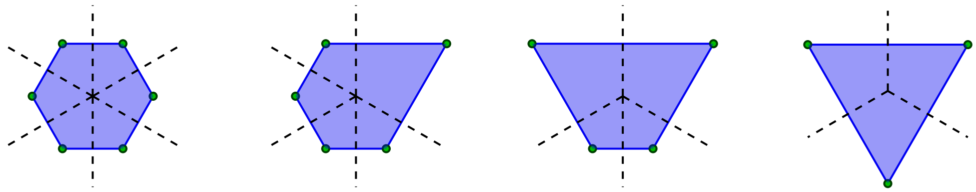

Figure 2: A permutohedron and the three deformations of it into generalized permutohedra, keeping the edge directions parallel to $\mathbf{e}_i - \mathbf{e}_j$ for $i \neq j$.

regions of convergence of series solutions to the generalized hypergeometric system defined by A [31].

As remarked above, the permutohedron has the property that all edges are parallel to $\mathbf{e}_i - \mathbf{e}_j$, this is the defining property of a *generalized permutohedra* (GP) [32] (cf. Fig. 2) but can also be strengthened to define the *matroid polytope* [33, 34].

Definition 3.1 (Generalized permutohedron)**.** A polytope P is said to be a *generalized permutohedron* if all its edges are parallel to $\mathbf{e}_i - \mathbf{e}_j$ for some $i \neq j$.

Definition 3.2 (Matroid polytope)**.** A polytope P is said to be a *matroid polytope* if all its vertices lie in a hypersimplex and all edges are equal to $\mathbf{e}_i - \mathbf{e}_j$ for some $i \neq j$.

We remark that a matroid polytope is bijective to its associated matroid and that every matroid polytope is a generalized permutohedra. The geometry of toric varieties are closely connected to matroids [33, 34]:

Theorem 3.3 ([34, Lemma 1.4])**.** *The torus orbit of a point $p \in \mathbf{Gr}(k, n)$ is isomorphic to the toric variety defined by the matroid polytope of the representable matroid defined by the columns of the matrix of Steifel coordinates of p.*

Another important property that is more on the algebraic side is that of *normality*.

Definition 3.4. The semigroup $\mathbb{N}A$ is said to be *normal* if $\mathbb{N}A = \mathbb{Z}A \cap \mathbb{R}_+A$.

Normality is satisfied by all closed torus orbits in a Grassmannian [35]:

Corollary 3.5. *The closure of any torus orbit in a Grassmannian is projectively normal in its Plücker embedding.*

The importance of normality in the study of Feynman integrals comes in that it guarantees that characteristic variety and dimension of the solution space of the generalized hypergeometric system $H_A(\beta)$ are independent of the parameters β of the integral (that is, space-time dimension and propagator powers). Normality is in general stronger than this, what is actually of interest is that the toric ideal defined by A should be *Cohen-Macaulay* [29, 36], by a theorem of Hochster [37], normality implies the Cohen-Macaulay property.

Normality is connected to the GP property according to following theorem (cf. [38, Fig. 5]).

Theorem 3.6. *If P is a generalized permutohedron and $A = \mathbb{Z}^n \cap P$, then A is normal.*

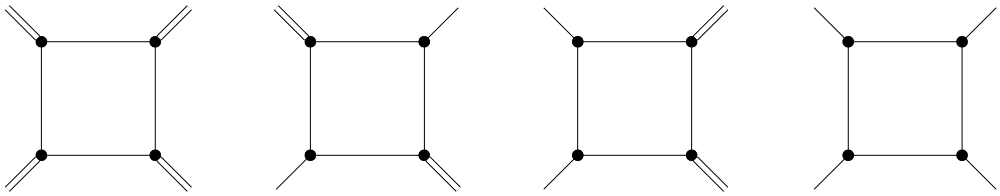

Figure 3: Box diagrams with all internal masses equal to zero and some external legs being off-shell ($p^2 \neq 0$, denoted by double lines) and some on-shell ($p^2 = 0$).

Example 3.7. We consider four different kinematic setups for the one-loop box integral with all internal masses equal to zero, see Fig. 3.

The A-matrix for the off-shell box is

$$A = \begin{pmatrix} 1 & 1 & 1 & 1 & 0 & 0 & 0 & 0 & 0 & 0 \\ 1 & 0 & 0 & 0 & 1 & 1 & 1 & 0 & 0 & 0 \\ 0 & 1 & 0 & 0 & 1 & 0 & 0 & 1 & 1 & 0 \\ 0 & 0 & 1 & 0 & 0 & 1 & 0 & 1 & 0 & 1 \\ 0 & 0 & 0 & 1 & 0 & 0 & 1 & 0 & 1 & 1 \end{pmatrix} \tag{13}$$

which is precisely the vertices of the second hypersimplex $\Delta(2,5)$ and the toric variety $X_A = \mathbf{V}(I_A)$ is a Veronese-like embedding of $\mathbb{P}^4$. This variety is isomorphic to the orbit closure of a generic point in the Grassmannian $\mathbf{Gr}(2,5)$ under the natural mapping of $(\mathbb{C}^*)^5$. Also note that $\text{conv}(A)$ is the basis polytope of the uniform matroid $U_{2,5}$. From this we know that $\mathbb{N}A$ is normal (hence I_A is Cohen-Macaulay) and $\text{conv}(A)$ is a generalized permutohedron.

The three-mass box and two-mass easy, Fig. 3b, correspond to sub matroid strata and thus normality and the GP property follows directly.

However, the two-mass hard (Fig. 3c), one-mass and on-shell box (Fig. 3d) do not correspond to any matroid strata. This means that $\text{conv}(A)$ is not a matroid polytope so neither normality nor the GP property follows directly. From the results in [38, Corollary 5.6] it follows that $\mathbb{N}A$ is normal, however, $\text{conv}(A)$ is not a GP.

Below we summarize some of the known results for GP and normality, we always use $A = \{1\} \times \text{Supp}(\mathcal{G})$ with $\mathcal{G} = \mathcal{U} + \mathcal{F}$ and $\mathbf{N}[f] = \text{conv}(\text{Supp}(f))$ as the Newton polytope of f.

- $\mathbf{N}[\mathcal{U}]$ is a matroid polytope, thus always a GP.
- For $m_e \neq 0$ for all $e \in E$, then $\mathbf{N}[\mathcal{F}] = \mathbf{N}[\mathcal{U}] + \Delta(1, |E|)$ and thus always a GP. Moreover, if no cancellation between $\mathcal{F}_0$ and $\mathcal{F}_m$ occurs, then A is normal [39].
- If no cancellation between $\mathcal{F}_0$ and $\mathcal{F}_m$ occurs, $p(V')^2 \neq 0$ for all $V' \subset V_{\text{ext}}$ and every internal vertex is connected to an external vertex via a massive path, then $\mathbf{N}[\mathcal{F}]$ is a GP and A is normal [40] cf. [38].
- When $m_e = 0$ for all $e \in E$ and $V = V_{\text{ext}}$, then $\mathbf{N}[\mathcal{F}]$ is a matroid polytope and thus GP and A is normal [39].

- When $m_e = 0$ for all $e \in E$ and $p(V')^2 \neq 0$ for all $V' \subset V_{\text{ext}}$, then $\mathbf{N}[\mathcal{F}]$ is a matroid polytope and thus GP and A is normal [40] cf. [38].

4. The program `feyntrop`

The program `feyntrop` is available at

https://github.com/michibo/feyntrop

It is a `C++` program with `Python` and `JSON` interface. It uses the contour deformation from section 2.1 and the sampling relies on the generalized permutohedron property, section 3.

Example 4.1 ([12, Section 6.5]). The following 5-point process with three massive external legs and a massive loop

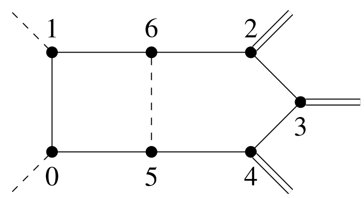

can be evaluated to percent precision to five orders in the dimensional regulator ϵ on a laptop in two seconds.

References

[1] G. Heinrich, *Collider physics at the precision frontier*, Phys. Rept. **922** (2021) 1–69, [2009.00516].

[2] Z. Bern, C. Cheung, R. Roiban, C.-H. Shen, M. P. Solon and M. Zeng, *Scattering Amplitudes and the Conservative Hamiltonian for Binary Systems at Third Post-Minkowskian Order*, Phys. Rev. Lett. **122** (2019) 201603, [1901.04424].

[3] C. Dlapa, G. Kälin, Z. Liu, J. Neef and R. A. Porto, *Radiation Reaction and Gravitational Waves at Fourth Post-Minkowskian Order*, Phys. Rev. Lett. **130** (2023) 101401, [2210.05541].

[4] S. G. Karshenboim, *Precision physics of simple atoms: QED tests, nuclear structure and fundamental constants*, Phys. Rept. **422** (2005) 1–63, [hep-ph/0509010].

[5] J. Zinn-Justin, *Quantum field theory and critical phenomena*, vol. 171. Oxford University Press, 2021.

[6] J. M. Henn, *Multiloop integrals in dimensional regularization made simple*, Phys. Rev. Lett. **110** (2013) 251601, [1304.1806].

[7] X. Liu and Y.-Q. Ma, *AMFlow: A Mathematica package for Feynman integrals computation via auxiliary mass flow*, Comput. Phys. Commun. **283** (2023) 108565, [2201.11669].

[8] M. Hidding, *DiffExp, a Mathematica package for computing Feynman integrals in terms of one-dimensional series expansions*, Comput. Phys. Commun. **269** (2021) 108125, [2006.05510].

[9] T. Armadillo, R. Bonciani, S. Devoto, N. Rana and A. Vicini, *Evaluation of Feynman integrals with arbitrary complex masses via series expansions*, Comput. Phys. Commun. **282** (2023) 108545, [2205.03345].

[10] E. Panzer, *Algorithms for the symbolic integration of hyperlogarithms with applications to Feynman integrals*, Comput. Phys. Commun. **188** (2015) 148–166, [1403.3385].

[11] S. Borowka, G. Heinrich, S. Jahn, S. P. Jones, M. Kerner, J. Schlenk et al., *pySecDec: a toolbox for the numerical evaluation of multi-scale integrals*, Comput. Phys. Commun. **222** (2018) 313–326, [1703.09692].

[12] M. Borinsky, H. J. Munch and F. Tellander, *Tropical Feynman integration in the Minkowski regime*, Comput. Phys. Commun. **292** (2023) 108874, [2302.08955].

[13] E. Panzer, *Hepp's bound for Feynman graphs and matroids*, Ann. Inst. Henri Poincaré D **10** (8, 2023) 31–119, [1908.09820].

[14] M. Borinsky, *Tropical Monte Carlo quadrature for Feynman integrals*, Ann. Inst. Henri Poincaré Comb. Phys. Interact. (8, 2023) , [2008.12310].

[15] J. M. Henn, J. Lim and W. J. Torres Bobadilla, *First look at the evaluation of three-loop non-planar Feynman diagrams for Higgs plus jet production*, JHEP **05** (2023) 026, [2302.12776].

[16] P.-H. Balduf, *Statistics of Feynman amplitudes in ϕ^4-theory*, 2305.13506.

[17] N. Arkani-Hamed, A. Hillman and S. Mizera, *Feynman polytopes and the tropical geometry of UV and IR divergences*, Phys. Rev. D **105** (2022) 125013, [2202.12296].

[18] N. Arkani-Hamed, H. Frost, G. Salvatori, P.-G. Plamondon and H. Thomas, *All Loop Scattering as a Counting Problem*, 2309.15913.

[19] H. S. Hannesdottir and S. Mizera, *What is the $i\varepsilon$ for the S-matrix?* SpringerBriefs in Physics. Springer, 1, 2023, 10.1007/978-3-031-18258-7.

[20] R. N. Lee and A. A. Pomeransky, *Critical points and number of master integrals*, JHEP **11** (2013) 165, [1308.6676].

[21] L. de la Cruz, *Feynman integrals as A-hypergeometric functions*, JHEP **12** (2019) 123, [1907.00507].

[22] R. P. Klausen, *Hypergeometric Series Representations of Feynman Integrals by GKZ Hypergeometric Systems*, JHEP **04** (2020) 121, [1910.08651].

[23] L. Nilsson and M. Passare, *Mellin transforms of multivariate rational functions*, *J. Geom. Anal.* **23** (2013) 24–46.

[24] C. Berkesch, J. Forsgård and M. Passare, *Euler-Mellin integrals and A-hypergeometric functions*, *Michigan Math. J.* **63** (2014) 101–123.

[25] I. M. Gel'fand, *General theory of hypergeometric functions*, *Dokl. Akad. Nauk SSSR* **288** (1986) 14–18.

[26] I. M. Gel'fand, M. I. Graev and A. V. Zelevinskiĭ, *Holonomic systems of equations and series of hypergeometric type*, *Dokl. Akad. Nauk SSSR* **295** (1987) 14–19.

[27] I. M. Gel'fand, A. V. Zelevinskiĭ and M. M. Kapranov, *Hypergeometric functions and toric varieties*, *Funktsional. Anal. i Prilozhen.* **23** (1989) 12–26.

[28] I. M. Gel'fand, M. M. Kapranov and A. V. Zelevinskiĭ, *Generalized Euler integrals and A-hypergeometric functions*, *Adv. Math.* **84** (1990) 255–271.

[29] I. M. Gel'fand, M. M. Kapranov and A. V. Zelevinskiĭ, *A correction to the paper "hypergeometric functions and toric varieties"*, *Funct. Anal. Appl.* **27** (1993) 295–295.

[30] D. Eisenbud and B. Sturmfels, *Binomial ideals*, *Duke Math. J.* **84** (1996) 1–45.

[31] I. M. Gel'fand, M. Kapranov and A. Zelevinskĭ, *Discriminants, resultants, and multidimensional determinants*. Springer Science & Business Media, 2008.

[32] A. Postnikov, *Permutohedra, associahedra, and beyond*, *Int. Math. Res. Not.* (2009) 1026–1106.

[33] I. M. Gel'fand and V. V. Serganova, *Combinatorial geometries and the strata of a torus on homogeneous compact manifolds*, *Uspekhi Mat. Nauk* **42** (1987) 107–134, 287.

[34] I. M. Gel'fand, R. M. Goresky, R. D. MacPherson and V. V. Serganova, *Combinatorial geometries, convex polyhedra, and Schubert cells*, *Adv. in Math.* **63** (1987) 301–316.

[35] N. L. White, *The basis monomial ring of a matroid*, *Adv. in Math.* **24** (1977) 292–297.

[36] A. Adolphson, *Hypergeometric functions and rings generated by monomials*, *Duke Math. J.* **73** (1994) 269–290.

[37] M. Hochster, *Rings of invariants of tori, Cohen-Macaulay rings generated by monomials, and polytopes*, *Ann. of Math. (2)* **96** (1972) 318–337.

[38] C. Dlapa, M. Helmer, G. Papathanasiou and F. Tellander, *Symbol Alphabets from the Landau Singular Locus*, *JHEP* **10** (2023) 161, [2304.02629].

[39] F. Tellander and M. Helmer, *Cohen-Macaulay Property of Feynman Integrals*, *Commun. Math. Phys.* **399** (2022) 1021–1037, [2108.01410].

[40] U. Walther, *On Feynman graphs, matroids, and GKZ-systems*, *Lett. Math. Phys.* **112** (2022) 120, [2206.05378].

Ich versichere, dass dieses gebundene Exemplar der Dissertation und das in elektronischer Form eingereichte Dissertationsexemplar (über den Docata-Upload) und das bei der Fakultät (zuständiges Studienbüro bzw. Promotionsbüro Physik) zur Archiverung eingereichte gedruckte gebundene Exemplar der Dissertationsschrift identisch sind.

Ort, Datum

Vorname und Nachtname, Unterschrift